frontiers | Research Topics

Advances in research on aging in female infertility and pathologic pregnancy

Edited by
Bin Liu, Gendie Lash, Fengxiang Wei
and Priyadarshini Pantham

Published in
Frontiers in Physiology
Frontiers in Endocrinology
Frontiers in Medicine

ISSN 1664-8714
ISBN 978-2-8325-4798-4
DOI 10.3389/978-2-8325-4798-4

About Frontiers

Frontiers is more than just an open access publisher of scholarly articles: it is a pioneering approach to the world of academia, radically improving the way scholarly research is managed. The grand vision of Frontiers is a world where all people have an equal opportunity to seek, share and generate knowledge. Frontiers provides immediate and permanent online open access to all its publications, but this alone is not enough to realize our grand goals.

Frontiers journal series

The Frontiers journal series is a multi-tier and interdisciplinary set of open-access, online journals, promising a paradigm shift from the current review, selection and dissemination processes in academic publishing. All Frontiers journals are driven by researchers for researchers; therefore, they constitute a service to the scholarly community. At the same time, the *Frontiers journal series* operates on a revolutionary invention, the tiered publishing system, initially addressing specific communities of scholars, and gradually climbing up to broader public understanding, thus serving the interests of the lay society, too.

Dedication to quality

Each Frontiers article is a landmark of the highest quality, thanks to genuinely collaborative interactions between authors and review editors, who include some of the world's best academicians. Research must be certified by peers before entering a stream of knowledge that may eventually reach the public - and shape society; therefore, Frontiers only applies the most rigorous and unbiased reviews. Frontiers revolutionizes research publishing by freely delivering the most outstanding research, evaluated with no bias from both the academic and social point of view. By applying the most advanced information technologies, Frontiers is catapulting scholarly publishing into a new generation.

What are Frontiers Research Topics?

Frontiers Research Topics are very popular trademarks of the *Frontiers journals series*: they are collections of at least ten articles, all centered on a particular subject. With their unique mix of varied contributions from Original Research to Review Articles, Frontiers Research Topics unify the most influential researchers, the latest key findings and historical advances in a hot research area.

Find out more on how to host your own Frontiers Research Topic or contribute to one as an author by contacting the Frontiers editorial office: frontiersin.org/about/contact

Advances in research on aging in female infertility and pathologic pregnancy

Topic editors

Bin Liu — Baoan Women's and Children's Hospital, China

Gendie Lash — Guangzhou Medical University, China

Fengxiang Wei — Shenzhen Longgang District Maternal and Child Health Care Hospital, China

Priyadarshini Pantham — University of California, San Diego, United States

Citation

Liu, B., Lash, G., Wei, F., Pantham, P., eds. (2024). *Advances in research on aging in female infertility and pathologic pregnancy*. Lausanne: Frontiers Media SA.

doi: 10.3389/978-2-8325-4798-4

Table of contents

frontiers | Frontiers in Physiology

TYPE Editorial
PUBLISHED 19 April 2024
DOI 10.3389/fphys.2024.1413425

OPEN ACCESS

EDITED AND REVIEWED BY
Trish Berger,
University of California, Davis, United States

*CORRESPONDENCE
Bin Liu,
gz12liubin@163.com

RECEIVED 07 April 2024
ACCEPTED 11 April 2024
PUBLISHED 19 April 2024

CITATION
Liu B, Lash G, Wei F and Pantham P (2024), Editorial: Advances in research on aging in female infertility and pathologic pregnancy. *Front. Physiol.* 15:1413425.
doi: 10.3389/fphys.2024.1413425

Editorial: Advances in research on aging in female infertility and pathologic pregnancy

Bin Liu[1]*, Gendie Lash[2], Fengxiang Wei[3] and Priyadarshini Pantham[4]

[1]Maternal and Child Health Research Institute, Shenzhen Baoan Women's and Children's Hospital, Shenzhen, Guangdong, China, [2]Division of Uterine Vascular Biology, Guangzhou Institute of Pediatrics, Guangzhou Women and Children's Medical Center, Guangzhou Medical University, Guangzhou, China, [3]Genetics Laboratory, Longgang District Maternity and Child Healthcare Hospital of Shenzhen City, Shenzhen, Guangdong, China, [4]Department of Obstetrics, Gynecology, and Reproductive Sciences, University of California, San Diego, La Jolla, CA, United States

KEYWORDS

advanced age, female infertility, pathological pregnancy, ovarian diseases, peripheral index

Editorial on the Research Topic
Advances in research on aging in female infertility and pathologic pregnancy

Older women of childbearing age have increased risks of infertility and pregnancy complications. These impose greater challenges to woman's reproductive health because of the global shift in population structure toward older age groups. Female reproductive health includes normal ovarian and endometrial function, successful fertilization and embryo implantation, and fetal growth. Various environmental and physiological factors contribute to declined fertility and pathological pregnancy in females. Researchers have conducted a large amount of functional and multiple-omics studies in reproductive tissues and organs in respect of various reproductive health issues including endometritis, polycystic ovarian syndrome (PCOS), recurrent miscarriage, preeclampsia, preterm birth, and various age-associated reproductive disorders. However, the mechanisms of these disorders remain largely unknown, and the methods of diagnosis and treatment of related diseases needs be significantly improved.

In this Research Topic, we aimed to collect manuscripts that would contribute to our understanding of age-associated reproductive disorders and their effects on infertility.

This Research Topic contains 12 manuscripts covering both original articles and reviews. The collected articles highlight the importance of ovarian aging in female infertility and pathological pregnancy. Zhang et al. reviewed recent developments in the mechanisms underlying primordial follicle activation and their clinical applications for improving the pregnancy rate for premature ovarian failure patients (POF). In this review, the authors focused on several signaling pathways between oocytes and granulosa cells and two waves of primordial follicle activation, which is determined by PI3K signaling in the oocytes and mTOR signaling in pre-granulosa cells, respectively. Finally, they introduced the application of *in vitro* activation (IVA) of primordial follicles for POF patients. In addition, Hu et al. discussed the latest *in vitro* techniques for fertility preservation of patients with cancer and POF, mainly on ovarian organ function reconstruction, including *in vitro* culture of oocytes, female germ cell induction from pluripotent stem cells *in vitro*, artificial

ovary construction, and construction of ovarian-related organoids. Tang et al. summarized the roles of macrophages both in normal ovarian function and in the process of ovarian senescence, especially macrophage polarization, and inflammation and fibrosis within the aging ovary. In a mouse model of PCOS, Shah et al. found that quercetin can reverse the molecular, functional and morphological abnormalities brought up by letrozole, particularly the improvement of reproduction in PCOS. The authors thought that this flavonoid molecule may act as a promising medicine for human PCOS. Low response to controlled ovarian stimulation is a crucial concern in poor responders to ovarian stimulation and patients with poor-quality embryos who are undergoing assisted reproductive technology. Takeuchi et al. developed an original protocol using medroxyprogesterone acetate and high-dose gonadotropin, and found that it increased the number of collected MII oocytes, 2PN zygotes, blastocysts with high quality, and live birth rates in both poor responders to ovarian stimulation and those with poor-quality embryos.

Pathological pregnancy is a major concern for mothers of advanced age. Wang et al. reviewed the basic function of exosome lncRNA and its roles in endometrial tolerance, embryo implantation, and immune tolerance at the maternal-fetal interface. Moreover, its associations with preeclampsia, gestational diabetes mellitus, and recurrent pregnancy loss were discussed. Diagnoses of pathological pregnancy was also involved in this Research Topic. Zhang et al. used a combination of uterocervical angle (UCA) and cervical length (CL) in early and mid-pregnancy and achieved a higher probability to predict preterm birth than CL or UCA alone. Meanwhile, Ripani et al. studied the side effects of CFTR modulators on the child of a successful pregnancy in one 30-year-old Italian with cystic fibrosis (CF, F508del/R334W) and observed no significant side effects in this child.

Aging-related risk factors of female infertility and pathological pregnancy is another area address in this Research Topic. Liu et al. analyzed the long-term trend of uterine fibroid burden in Chinese women from 1990 to 2019 and found that the age-standardized rates were all on the ascending trend, with the greatest increase in the age-standardized mortality rate (53% of annual increase). They concluded that uterine fibroids are still the most common benign gynecological tumors in women, and more work on social health prevention and control should be applied. Yong et al. found that age-related CPT1B decline may explain decreased metabolic function in placenta, and therefore may be related to pregnancy complications in women with advanced age, particularly in those who are overweight. In addition to uterine fibroids and obesity, there is an increasing number of patients experiencing infertility due to chronic salpingitis after various of infections. Zhang et al. found that extracellular vesicles derived from human umbilical cord mesenchymal stem cells can relieve salpingitis by promoting M1-to-M2 transformation of macrophages in a mouse model. Urinary incontinence (UI) is linked to obesity and childbirth in aged women. Hong et al. retrospectively analyzed the NHANES data and found that total muscle-to-fat ratio showed a negative association with UI, and this association might be mediated by the peripheral index lymphocyte count.

We hope this Research Topic will be useful for researchers and clinicians alike to help further studies. More functional and population studies on aging in female infertility and pathological pregnancy are warranted.

Author contributions

BL: Conceptualization, Supervision, Writing–original draft, Writing–review and editing. GL: Conceptualization, Data curation, Writing–review and editing. FW: Data curation, Formal Analysis, Writing–review and editing. PP: Data curation, Formal Analysis, Validation, Writing–review and editing.

Funding

The author(s) declare that no financial support was received for the research, authorship, and/or publication of this article.

Conflict of interest

The authors declare that the research was conducted in the absence of any commercial or financial relationships that could be construed as a potential conflict of interest.

Publisher's note

frontiers | Frontiers in Physiology

TYPE Original Research
PUBLISHED 16 February 2023
DOI 10.3389/fphys.2023.1131701

OPEN ACCESS

EDITED BY
Bin Liu,
Independent researcher, Shenzhen, China

REVIEWED BY
Vincent Yeung,
Harvard University, United States
Huan Li,
Shenzhen Hospital, Peking University, China

*CORRESPONDENCE
David Y. B. Deng,
dengyub@mail.sysu.edu.cn
Wuguo Deng,
dengwg@sysucc.org.cn
Tian Li,
litian@sysush.com

†These authors contributed equally to this work and share first authorship.

SPECIALTY SECTION
This article was submitted to Reproductive and Mating Physiology, a section of the journal Frontiers in Physiology

RECEIVED 26 December 2022
ACCEPTED 06 February 2023
PUBLISHED 16 February 2023

CITATION
Zhang C, Liao W, Li W, Li M, Xu X, Sun H, Xue Y, Liu L, Qiu J, Zhang C, Zhang X, Ye J, Du J, Deng DYB, Deng W and Li T (2023), Human umbilical cord mesenchymal stem cells derived extracellular vesicles alleviate salpingitis by promoting M1–to–M2 transformation. *Front. Physiol.* 14:1131701. doi: 10.3389/fphys.2023.1131701

Human umbilical cord mesenchymal stem cells derived extracellular vesicles alleviate salpingitis by promoting M1–to–M2 transformation

Changlin Zhang[1†], Wei Liao[1†], Weizhao Li[1†], Mengxiong Li[1], Xiaoyu Xu[1], Haohui Sun[2], Yaohua Xue[3], Lixiang Liu[1], Jiehong Qiu[1], Chi Zhang[1], Xunzhi Zhang[4], Juntong Ye[1], Jingran Du[1], David Y. B. Deng[1*], Wuguo Deng[2*] and Tian Li[1*]

[1]Pelvic Floor Disorders Center, Scientific Research Center, Department of Gynecology, The Seventh Affiliated Hospital of Sun Yat-sen University, Shenzhen, China, [2]Sun Yat-Sen University Cancer Center, State Key Laboratory of Oncology in South China, Collaborative Innovation Center of Cancer Medicine, Guangzhou, China, [3]Department of Clinical Laboratory, Dermatology Hospital, Southern Medical University, Guangzhou, China, [4]College of Life Sciences and Oceanography, Shenzhen University, Shenzhen, China

Background: With an increasing number of patients experiencing infertility due to chronic salpingitis after *Chlamydia trachomatis* (CT) infection, there is an unmet need for tissue repair or regeneration therapies. Treatment with human umbilical cord mesenchymal stem cell-derived extracellular vesicles (hucMSC-EV) provides an attractive cell-free therapeutic approach.

Methods: In this study, we investigated the alleviating effect of hucMSC-EV on tubal inflammatory infertility caused by CT using *in vivo* animal experiments. Furthermore, we examined the effect of hucMSC-EV on inducing macrophage polarization to explore the molecular mechanism.

Results: Our results showed that tubal inflammatory infertility caused by *Chlamydia* infection was significantly alleviated in the hucMSC-EV treatment group compared with the control group. Further mechanistic experiments showed that the application of hucMSC-EV induced macrophage polarization from the M1 to the M2 type *via* the NF-κB signaling pathway, improved the local inflammatory microenvironment of fallopian tubes and inhibited tube inflammation.

Conclusion: We conclude that this approach represents a promising cell-free avenue to ameliorate infertility due to chronic salpingitis.

KEYWORDS

chronic salpingitis, macrophage polarization, NF-κB signaling pathway, mesenchymal stem cell (MSC), extracellular vesicles

Abbreviations: CT, *Chlamydia trachomatis*; MSCs, Mesenchymal stem cells; MSC-EV, Mesenchymal stem cells-derived extracellular vesicles; MSC-CM, Mesenchymal stem cells-conditional medium; hucMSC-EV, human umbilical cord mesenchymal stem cell-derived extracellular vesicles; WHO, World Health Organization; MST1, Mammalian sterile 20-like kinase 1

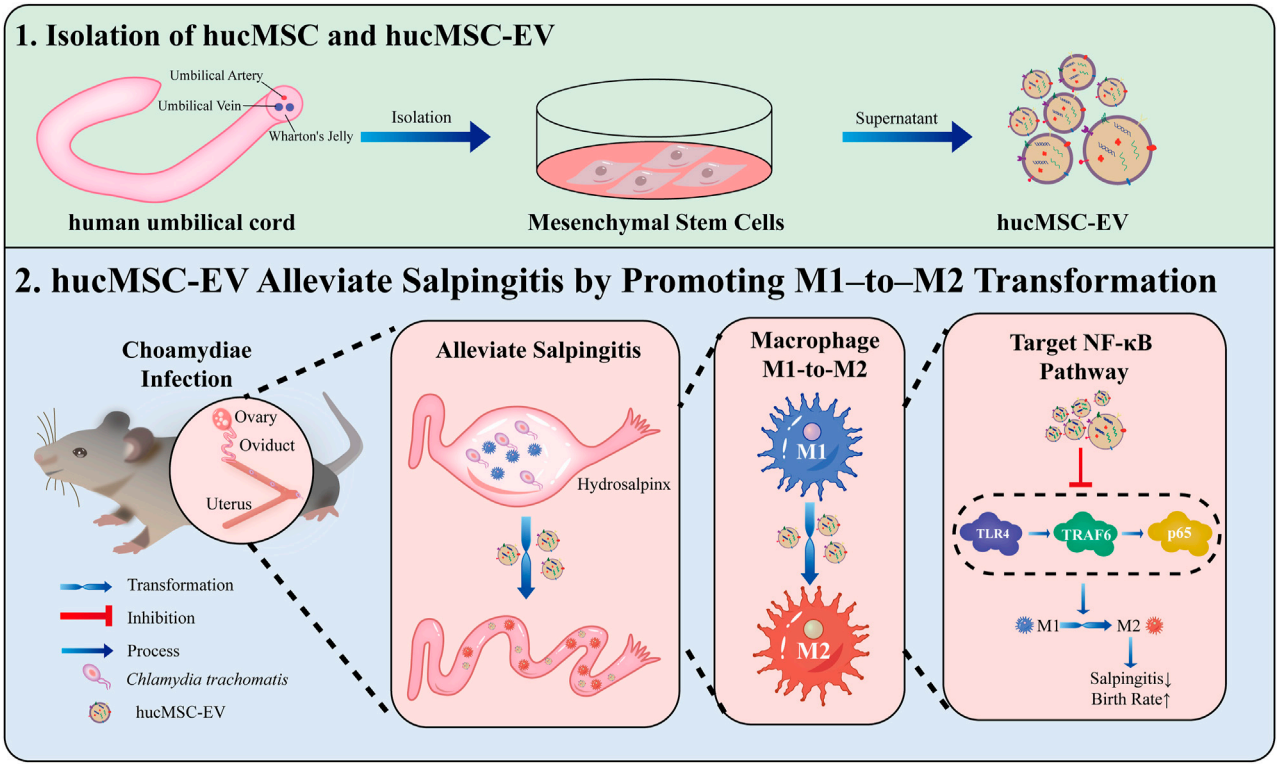

GRAPHICAL ABSTRACT

1 Introduction

Having a healthy and happy baby is vital to the wellbeing of millions of families; however, ~15% of couples worldwide (~50 million couples) experience infertility (Tsevat et al., 2017). In 2013, the World Health Organization (WHO) estimated that 25% of couples in developing countries could not meet their fertility needs, with female infertility accounting for ~50% of infertility cases (Newman et al., 2015). Tubal factor (fallopian tubes) infertility accounts for ~10%–30% of female infertility (Tsevat et al., 2017).

Chlamydia trachomatis (CT) infection is the main cause of fallopian tube obstruction and infertility, responsible for ~43% of cases (Ruijin Shao et al., 2012). The infection persists in many patients who received treatment, causing pathological damage and ultimately leading to fibrosis and scar formation, damage to the normal function of fallopian tubes, and, in serious cases, fallopian tube obstruction and infertility (Haggerty et al., 2010).

The mechanism of fallopian tube injury caused by CT infection remains unclear and may be related to ontogenetic factors, cytokine activation, immune escape, and co-infection (Brunham, 2022). The formation of fallopian tube scars is not only due to the destruction of the fallopian tube epithelial cells by CT but also due to the accumulation of inflammatory cells, release of cytokines, and activation of the complement system in the immune microenvironment (Murthy et al., 2018). Macrophages play a crucial role in the occurrence and development of inflammatory diseases and are classified into two main types: M1, generated by classical activation, and M2, generated by selective activation (Shapouri-Moghaddam et al., 2018; Galipeau, 2021; Pouyanfard et al., 2021).

Mesenchymal stem cells (MSCs) are adult stem cells derived from mesoderm with high self-renewal ability and multidirectional differentiation potential (Dominici et al., 2006; Andrzejewska et al., 2019).

At present, MSCs are rarely used in the treatment of tubal factor infertility, especially tubal infertility. Tubal infertility is closely related to inflammatory adhesions (Ling et al., 2022). The formation of inflammatory adhesions is a mechanism that protects the body against external stimuli (Medzhitov, 2008). It can limit inflammation, which is conducive to the repair of tissue damage (Cooke, 2019; Yuan et al., 2021; Li-Tao Shao et al., 2022); however, under certain conditions, it can cause adhesion and infertility (Hafner, 2015). MSCs exert their functions through the paracrine pathway. *In vitro* and *in vivo* studies have confirmed that the culture supernatant of MSCs can inhibit the abnormal activation of T cells after co-culture *in vitro* (Negi and Griffin, 2020; Markov et al., 2021). Injections of the culture supernatant of MSCs into a mouse model of renal injury effectively reduced the area of injured tissue (Erpicum et al., 2017). This suggests that factors in the culture supernatant of MSCs exert functions similar to those of MSCs themselves.

Treatments based on umbilical cord derived mesenchymal stem cells (MSCs) have shown some promising achievements (V Yeung et al., 2019). Our previous study showed that MSCs transplantation can markedly reduce inflammation in salpingitis caused by CT infection (Liao et al., 2019). However, their potential

tumorigenicity (Webber et al., 2015), low perfusion, low retention and other limitations are still controversial, which limit the clinical application of MSCs. In contrast, hucMSC-EV exhibit a similar function to their source cells and are expected to overcome these limitations. EV are tiny vesicles (40–100 nm in diameter) secreted out of cells by membrane fusion (Pegtel and Gould, 2019). EV contain active substances, such as nucleic acids and proteins, which are transferred to target tissues to perform their functions (Simons and Raposo, 2009; Pluchino and Smith, 2019). MSC-extracellular vesicles (MSC-EV) participate in tissue-damage repair (Yin et al., 2019; Vincent Yeung et al., 2022), immune regulation (Harrell et al., 2019; Farhat et al., 2022), and reshaping of the immune microenvironment (Seo et al., 2019). In addition, compared with MSC treatment, exosome components are relatively simple, and their structural characteristics enable them to reach the target tissues with high efficiency, likely avoiding the risk of long-term abnormal differentiation and tumor formation caused by stem-cell transplantation in the host (Vizoso et al., 2017; Ning et al., 2018).

Our previous study showed that MSC transplantation can markedly reduce inflammation in salpingitis caused by CT infection (Liao et al., 2019). The role of MSCs in the repair and reconstruction of inflammatory adhesions may be related to the regulation of different inflammatory environments and inflammatory cells (Shi et al., 2018). *In vitro* studies have confirmed that MSCs can promote the transformation of macrophages into the M2 type through the paracrine pathway, suggesting that MSC-induced M2 macrophages are important components in the treatment of oviduct inflammatory injury (Liao et al., 2019). Based on the results of our previous *in vivo* and *in vitro* studies and literature reports, we propose the following hypothesis: MSCs regulate macrophage polarization to the M2 type by secreting extracellular vesicles and change the level of cytokines secreted by macrophages, reducing local inflammatory responses in the oviduct and promoting tissue-damage repair.

The aim of this study was to use hucMSC-EV to treat CT salpingitis and explore the relationship between hucMSC-EV and macrophage polarization *in vitro* and *in vivo*, as well as the regulation of cytokine levels secreted by macrophages, to provide new ideas for the treatment of salpingitis caused by CT infection.

2 Methods

2.1 *In vitro* experiments

We collected fresh umbilical cords from full-term, cesarean section puerperae. The puerperae had tested negative for gestational diabetes mellitus, infection, fever, and autoimmune or other diseases. The acquisition of the human umbilical cords (hucs) was approved by the Ethics Committee of the Seventh Affiliated Hospital, Sun Yat-sen University (KY-2022-007-01). The puerperae were fully informed and consented.

The fresh umbilical cords were processed in a biosafety cabinet within 6 h. First, the cords were rinsed twice with 1×PBS containing 100 U/mL penicillin and 100 mg/mL streptomycin (BL505A; Biosharp, Hefei, China). Arteries, veins, blood vessels, and epithelial cells were removed under aseptic conditions to obtain Wharton's jelly, which was cut into 1 mm^3 pieces and placed at the bottom of T25 culture flasks. The flasks were incubated at 37°C with 5% CO_2 for 30 min. Next, 1.5 mL DMEM/F12 medium containing 15% FBS (164210; Procell, Wuhan, China), 100 U/mL penicillin, and 100 mg/mL streptomycin was added to fully soak the pieces. The flasks were placed in a 37°C incubator with 5% CO_2, and the medium was gently replaced every 3 days. Approximately 10 days later, fibroblast-like MSCs were observed around the umbilical cord pieces. The umbilical cord pieces were removed, and the cells were marked as passage zero.

To investigate the capacity of the isolated MSCs to adhere to plastic in standard culture conditions, we used an inverted phase-contrast microscope (ECLIPSE C1; Nikon, Japan). MSCs were identified using flow-cytometric analysis (FACSCalibur™; Becton Dickinson) to detect cell surface markers (CD19, CD34, CD45, CD73, CD90, CD105, and HLA-DR). When 90%–100% confluency was reached, we used trypsin to prepare cell suspensions at a concentration of 1 × 10^6 cells/mL. Cells were incubated with antibodies on ice under dark conditions for 30 min. Cells were washed thrice with 1 × PBS to remove the uncombined antibodies and analyzed using a flow cytometer within 1 h.

2.2 Differentiation of HucMSCs

To evaluate differentiation capacity, MSCs were cultured with osteogenic (PD-003; Procell, Wuhan, China) or adipogenic media (PD-004; Procell, Wuhan, China) according to protocols. The medium was replaced with a fresh differentiation medium every 3 days. After 3 weeks, the medium was removed, and the cells were washed thrice with 1 × PBS, fixed with 4% neutral formalin for 15 min, and washed thrice with 1 × PBS. The osteogenic and adipogenic cells were stained with alizarin red S (ARS) and oil red O, respectively, for 30 min at 22–25°C and washed thrice with PBS, and observed under a microscope.

2.3 Extraction of hucMSC-EV

We used ultracentrifugation to collect extracellular vesicles from the culture supernatant of hucMSCs (3rd–5th passage cells). When cell density reached 70%–80%, we removed the medium, washed the cells thrice with 1×PBS, and added serum-free DMEM/F12 for 48 h to exclude the influence of EV from fetal blood serum. We collected the culture supernatant and collected EV immediately or froze them at −80°C. The culture supernatant was centrifuged at 10 000 × *g* for 45 min at 4°C to remove unwanted cells and cell debris. To obtain higher-purity EV, the collected supernatant was filtered through a 0.22-μm filter (SLGP033RB-0.22; Merck Millipore, United States) and ultracentrifuged (JXN-30; Beckman, United States) at 108 000 × *g* for 70 min at 4°C (Optima L-90K; Beckman, United States). The supernatant was discarded, and the pellet was resuspended in 1×Dulbecco's phosphate-buffered saline (DPBS) to remove unwanted proteins. The samples were ultracentrifuged at 108 000 × *g* for 70 min at 4°C and resuspended in 200 μL of 1×DPBS to obtain high-density, pure EV.

2.4 Identification of hucMSC-EV

2.4.1 Electron microscopy

Twenty microliters of extracellular vesicles suspension were transferred onto a copper grid with a carbon film for 3–5 min. A 2% phosphotungstic acid solution was added to the copper grid. After 1–2 min to allow for staining, excess liquid was blotted using filter paper, and the grid was left to dry at room temperature. The cuprum grids were observed under TEM (HT7800; HITACHI, Japan), and images were captured.

2.4.2 Western blot

The adherent cells were scraped off the dish using trypsin or a plastic cell scraper, and the cell pellet was collected after centrifugation. To acquire cell lysates, RIPA buffer (P0013B; Beyotime, Shanghai, China) was added to the cell pellet on ice. After 30 min, the cell lysate was centrifuged at 4°C for 10 min to remove the dissolved pellet. A BCA kit (P0012; Beyotime, Shanghai, China) was used to quantify protein. After adding the appropriate loading buffer, each cell lysate was boiled at 100°C for 10 min. A 10% SDS-PAGE was prepared using a PAGE gel fast preparation kit (PG112; EpiZyme, Shanghai), and equal amounts of protein were loaded into the wells, along with a molecular weight marker (26616; Thermo Fisher, United States). The gel was run for 50 min at 150 V. Proteins were transferred to PVDF membranes (IPVH00010; Merck Millipore, United Statesa) and blocked for 1 h in 5% skim milk (LP0033B; Oxoid, United Kingdom) at room temperature. The membranes were incubated overnight at 4°C with primary antibodies from Proteintech (Rosemont, IL, United States) against CD81 (27855-1-AP, rabbit; 1:1000), Tsg101 (28283-1-AP, rabbit; 1:2000), calnexin (10427-2-AP, rabbit; 1:20000), P65 (10745-1-AP, rabbit; 1:1000), TLR4 (19811-1-AP, rabbit; 1:1000), glyceraldehyde-3-phosphate dehydrogenase (GAPDH, 10494-1-AP, rabbit; 1:1000), and tumor necrosis factor receptor-associated factor 6 (TRAF6) (#67591, rabbit; 1:1000) (Cell Signaling Technology, Beverly, MA, United States). The membranes were washed thrice with PBST (10 min per wash), re-probed with HRP-conjugated Affinipure Goat Anti-Rabbit IgG (SA00001-2; 1:10,000, Proteintech) at room temperature for 1 h, and washed thrice with PBST (10 min per wash). The membranes were covered with chemiluminescent HRP substrate (WBKLS0100; Merck Millipore, United States), and images were acquired using a ChemiDoc Touch Imaging System (1708370; Bio-Rad, United States). The gray value of the target protein bands was quantified using ImageJ 1.53k software, using GAPDH for normalization.

2.4.3 Nanoparticle Tracking Analysis

To measure the particle size of purified hucMSC-EV, we chose Nanoparticle Tracking Analysis using NanoSight (NS300; Malvern, United Kingdom). The hucMSC-EV suspension (20 μL) was diluted to 1 mL using 1×DPBS, and the diluent was pumped into the NanoSight device avoiding air bubbles.

2.5 Animal experiments

2.5.1 Establishment and treatment of the murine chronic salpingitis model

Four-week-old male and female C3H mice were obtained from VITAL RIVER (Beijing, China) and housed in an SPF barrier system in appropriate facilities (certificate number: SYXK [Guang-dong] 2015-0102), seeing the attached Supplementary Figure S1 for the flow chart of the experiment. All animal experiments were conducted according to the regulations of the Institutional Animal Care and Use Committee at Sun Yat-sen University Cancer Center (Certificate Number: KY-2022-007-01).

The 24 female C3H mice were subcutaneously injected with 2.5 mg of medroxyprogesterone at days 3 and 7. After 1 week, the female mice were transvaginally injected with 1×10^7 inclusion-forming units MoPn *chlamydia* (ATCC VR-123TM; United States). To prevent *chlamydia* flow out of the vagina, the mice were hung upside down for 1 min after injection.

After 2 weeks, the female mice were randomly divided into three groups—hucMSC-EV, DPBS, and DMEM—of eight mice. The mice in the hucMSC-EV group were transvaginally injected with 25 μL of 100 μg/mL hucMSC-EV three times every 3 days.

After 2 weeks, three mice from each group were randomly selected to be sacrificed. The enterocoelia were exposed to observe the fallopian tubes and acquire images. The fallopian tubes were dissected in a 4% paraformaldehyde solution or liquid nitrogen for subsequent detection. To test the fertilization capacity of female mice, the remaining five female mice of each group were cohoused with two male mice in a cage for 2 weeks. When the vaginal plug was observed, the female mouse was considered fertilized; feeding continued for 7 days to determine the presence of embryos in the uterus, whereby, female mice were marked as pregnant.

2.5.2 Histology and immunofluorescence

Fresh fallopian tubes were fixed in 4% paraformaldehyde (BL539A; Biosharp, Hefei) for >24 h, and then was dehydrated, paraffin-embedded, and cut into 4-μm-thick sections, The sections were deparaffinized, rehydrated using Xylene and alcohol gradients, and stained with Hematoxylin and Eosin (H&E). The stained sections were dehydrated and sealed with neutral gum. Observation, image acquisition, and analysis were performed under a microscope.

We used immunofluorescence to identify macrophages in the fallopian tubes. The slides were deparaffinized, rehydrated, and immersed in EDTA antigen retrieval buffer (pH 8.0). After blocking with serum, the slides were incubated with CD206 primary antibody (GB13438, Rabbit; Servicebio; 1:500), followed by CY3-conjugated Affinipure Goat Anti-Rabbit IgG secondary antibody (GB21303; Servicebio; 1:300). DAPI was used for nuclear staining. The slides were coverslipped using an antifade mounting medium. Images were obtained using fluorescent microscopy (ECLIPSE C1; Nikon, Japan).

2.6 RAW264.7 macrophage uptake of membrane components

RAW264.7 (Donated by Professor Deng Wuguo from Sun Yat-Sen University Cancer Center) cells were To verify that macrophage RAW264.7 cells could uptake membrane components of the hucMSC culture supernatant, the PKH67 Green Fluorescent Cell Linker Mini Kit (MINI67-1KT; Sigma, Germany) was used. Twenty microliters of PKH67 solution were mixed with 10 mL of hucMSC culture supernatant. RAW264.7 cells were plated in 6-well culture dishes; when 70%–80% confluency was reached, the cells were washed thrice with 1×PBS. For nuclear staining, DAPI (C0065-10; Solarbio, Beijing) was added to the wells for 10 min at room temperature. After washing thrice with 1×PBS, the PKH67 working solution was added; the plates were incubated at 37 °C and 5% CO_2 for 1 h. After washing thrice with 1×PBS, observation and image collection were performed using fluorescent microscopy.

2.7 Cell culture

The mouse RAW264.7 macrophages were cultured in DMEM (Gibco, United States) with 10% FBS, 100 U/mL penicillin, and 100 mg/mL streptomycin and maintained under standard culture conditions.

2.8 RAW264.7 macrophages uptake hucMSC-EV

We used live-cell imaging to verify hucMSC-EV uptake by RAW264.7 macrophages. First, a working solution was prepared by mixing 100 μg hucMSC-EV, 0.1 mL Alexa Fluor 488 dye, and 10 mmol sodium carbonate in 1 mL 1×PBS, followed by incubation with RAW264.7 cells. Images were obtained at 3 h using confocal microscopy (FV300; Olympus, Japan).

CellTracker™ Red CMTPX Dye (C34552, ThermoFisher, United States) can enter and stay in live cells, and can emit 602 nm light excitated by 577 nm excitating light. Incubated EV with CellTracker™ Red CMTPX Dye for 30 min at 37°C, and centrifuged the EV to remove the uncombined CellTracker™ working solution. Added the labeled EV into RAW264.7 cells and took images with inverted fluorescence microscope (DMi8, Leica, Germany). If RAW264.7 cells could uptake exosoems, we can see red light in RAW264.7 cells.

2.9 Quantitative PCR

RAW264.7 cells (1×10^6) were seeded in 6-well dishes. When 40% confluency was reached, the medium was replaced with complete DMEM (containing 10% FBS, 100 U/mL penicillin, and 100 mg/mL streptomycin), and, for the LPS group, 100 ng/mL LPS. After 8 h, the medium was replaced with fresh complete DMEM, in which 20 μL DMEM or DPBS or 1 mg/mL hucMSC-EV solution was added. Cells were collected after 12 h. Total RNA was extracted using a RaPure Total RNA Micro Kit (R4012-02; Magen, Shanghai) according to standard protocols. cDNA (from 1 μg mRNA) was generated using the Fast All-in-One RT Kit (RT001; ES Science, Shanghai). mRNA expression was assessed using quantitative (qRT)–PCR with SYBR qPCR Mix (Q311; Vazyme, Nanjing) in Bio-Rad CFX996 and analyzed using the Bio-Rad manager software (Bio-Rad, Hercules, CA, United States) normalized to GAPDH. Results were calculated using the $2^{-\Delta\Delta CT}$ method. cDNA was then amplified *via* PCR using the primer sequences listed in Supplementary Table S1.

2.10 ELISA

We used an ELISA kit to measure the levels of TNF-α, IL-1β, and IL-10 (KE10002, KE10003, KE10008; Proteintech, United States of America) in the culture supernatant. The experimental method follows that described for qRT-PCR. After adding hucMSC-EV for 48 h, the culture supernatant was collected. Following centrifugation at 500 × *g* for 5 min, the culture supernatant was stored at −20°C. The microplate strips were removed, and the microwells were placed in the strip holder. One hundred microliters of each sample were added to the appropriate wells, and the plate was incubated for 2 h at 37°C in a humid environment. After washing the wells 4 times with 1 × Wash Buffer, 100 μL of 1 × antibody detection solution was added, followed by incubation for 1 h at 37°C in a humid environment. After washing, 100 μL of 1 × HRP-conjugated antibody was added to each well, followed by incubation for 40 min at 37°C in a humid environment. After washing, 100 μL of TMB substrate solution was added to each well, followed by incubation for 15 min at 37°C in the dark. Stop solution (100 μL) was added, and absorbance at 450 nm was read immediately on a microplate reader. (BioTek, Synergy H1M) Cytokine concentrations were calculated according to the standard curve.

2.11 Statistical analysis

Data were processed using SPSS 20.0 statistical software (IBM, Armonk, NY, United States). The data are shown as the mean ± standard deviation from at least three independent experiments. Comparisons among multiple groups were performed using one-way analysis of variance (ANOVA) and Tukey's test. Data between two groups were compared using the unpaired t-test or Kruskal–Wallis test. Statistical significance was set at $p < .05$.

3 Results

3.1 Extraction and identification of HucMSCs

The high quality of the extracted hucMSCs was identified based on three properties: adherence capacity, differentiation ability, and presence of surface markers, according to the criteria proposed by the mesenchymal and tissue stem cell Committee of the International Society for Cellular Therapy. As shown in Figure 1A, MSCs climbed outward from the central umbilical cord block and could adhere to the wall for growth. Osteogenic and adipogenic experiments verified the differentiation potential of the cells. After a 3-week induction and culture in an osteogenic differentiation medium, MSCs successfully differentiated into

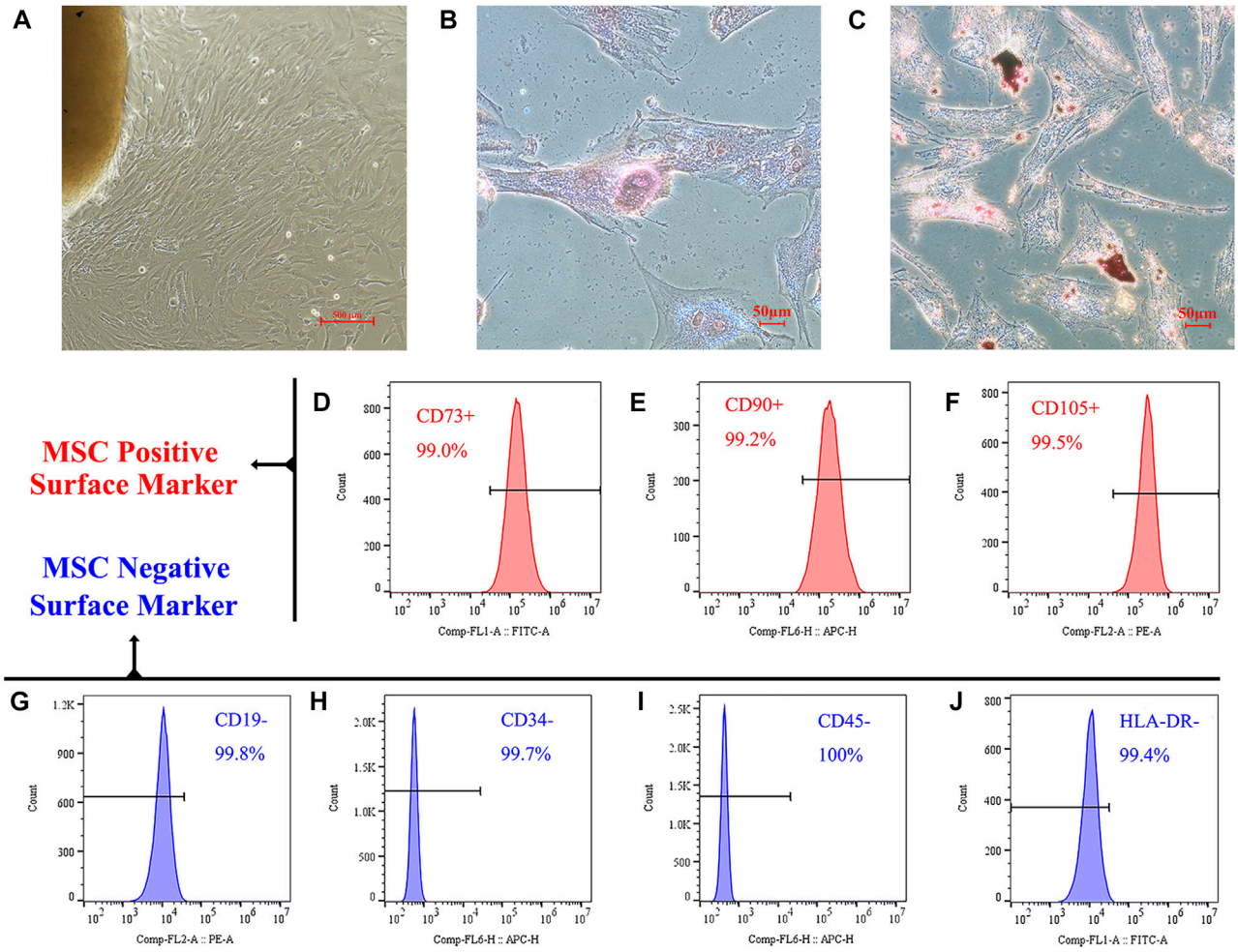

FIGURE 1
Identification of hucMSCs. **(A)** HucMSCs were isolated and purified through their physical adherence to the plastic cell culture plate. **(B)** Alizarin red S staining demonstrated that mineralized nodules were formed in the hucMSCs 3 weeks after osteogenic induction. **(C)** Oil-red-O staining showed lipid-rich vacuole formation in the mouse BM-MSCs after 3 weeks of adipogenic induction. **(D–F)** Flow cytometry analysis showed that these cells were positive for MSC markers CD73 **(D)**, CD90 **(E)**, and CD105 **(F)**. **(G–J)** Cells were negative for B cell marker CD19 **(G)**, endothelial cell marker CD34 **(H)**, pan-leukocyte marker CD45 **(I)**, and stimulated immune cell marker HLA-DR **(J)**.

osteoblasts (Figure 1B); calcium deposition could be observed using ARS staining. After a 3-week induction and culture with an adipogenic differentiation medium, MSCs successfully differentiated into adipocytes (Figure 1C). Using oil red O staining, red lipid droplets in the cells were observed.

We further verified that our isolated and cultured cells were MSCs using flow cytometry. As shown in Figures 1D–F, the positive markers, CD73, CD90, and CD105, on the surface of MSCs were expressed in >99% of the cells. Figures 1G–J shows that the expression rate of MSC negative markers and exclusion proteins, CD19, CD34, CD45, and HLA-DR, on the cell surface was <1%.

3.2 Identification of hucMSC-derived EV

To evaluate whether the extracted EV conformed to international standards, we separated and extracted extracellular vesicles using ultracentrifugation. Figures 2A–D showed size distribution and schematic illustration of hucMSC-EV measured from NanoSight and then we observed isolated structures using projection electron microscopy. The results are shown in Figure 2E. We observed a double concave disc-shaped vesicle structure with a diameter of ~100 nm. Using NTA, the peak particle size of extracellular vesicles was estimated at 142 nm; particle size was within the 40–100 nm range and complied with international standards (Figure 2C). Further verification using western blotting (WB) showed that the extracellular vesicle structure expressed the membrane protein CD81 and intracellular protein TSG101 but not calnexin (located in the endoplasmic reticulum). In contrast, hucMSCs expressed TSG101 and calnexin, and the expression of CD81 was substantially lower than that of the extracted MSC extracellular vesicle structure (Figure 2F). Therefore, we successfully extracted hucMSC-EV that conformed to international standards.

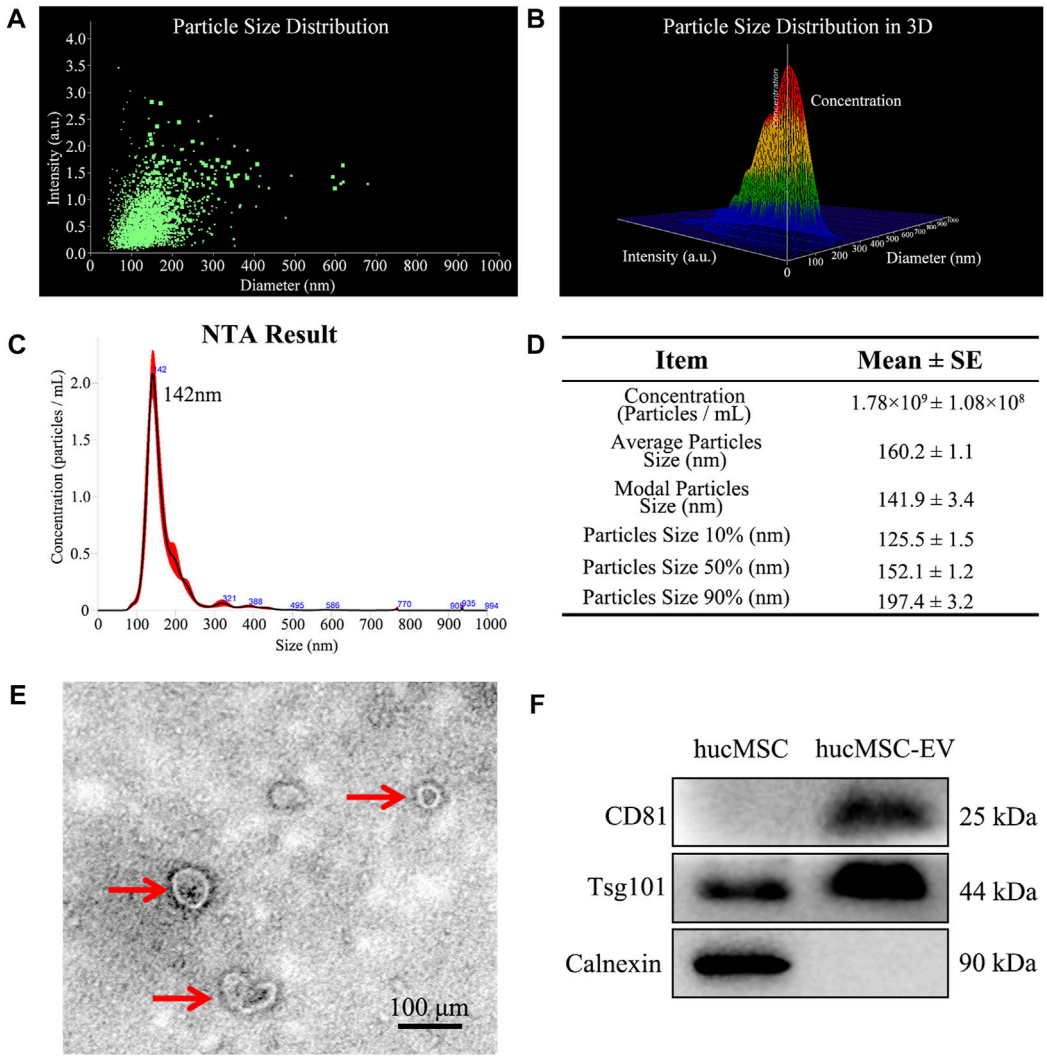

FIGURE 2
Identification of hucMSC-EV. **(A, B)** Size distribution and schematic illustration of hucMSC-EV measured from NanoSight. **(C)** NanoSight measure of the particle diameter of hucMSC-EV. **(D)** A table for particle concentration, average particle size and modal particle size. **(E)** Transmission electron micrographs of hucMSC-EV. **(F)** Western blotting identified the positive exosome protein markers CD81 and Tsg101 and negative exosome protein marker Calnexin.

3.3 hucMSC-EV alleviated tubal factor infertility caused by CT infection and increased the pregnancy rate of nude mice

We successfully induced a mouse model of tubal inflammatory infertility caused by CT infection. To verify that hucMSC-EV can alleviate salpingitis and improve the pregnancy rate in pathogenic animals, mice were first divided into hucMSC-EV, DPBS, and DMEM groups, as shown in Figures 3A–F. After hucMSC-EV treatment, local hyperemia and the inflammatory hydrosalpinx in the mouse oviduct and uterus were considerably reduced compared with those in the control group. In contrast, local hyperemia and hydrosalpinx were observed in the DPBS and DMEM groups. H&E tissue staining showed that the structure of oviduct villi in the hucMSC-EV group was complete, while the villi structure in the DPBS and DMEM groups almost disappeared, with evident tissue expansion due to ponding (Figure 3G–L). The above results showed that hucMSC-EV can significantly improve reproductive tract congestion and the inflammatory response in pathogenic mice.

In the next experiment, we examined whether the pregnancy rate in these mice could be improved. As shown in Figures 3M, N, all five mice in the hucMSC-EV group were pregnant, compared with none in the DPBS group and one in the DMEM group. The above results further verified that the application of hucMSC-EV could significantly improve the reproductive tract congestion and inflammatory response of pathogenic mice, thereby improving the pregnancy rate.

To further explore the molecular mechanism and signaling pathway of hucMSC-EV in alleviating the inflammatory response in pathogenic mice, we detected the proteins p65 and TLR4 related to the inflammatory signaling pathway. We prepared protein samples and carried out WB analysis using oviduct tissues from

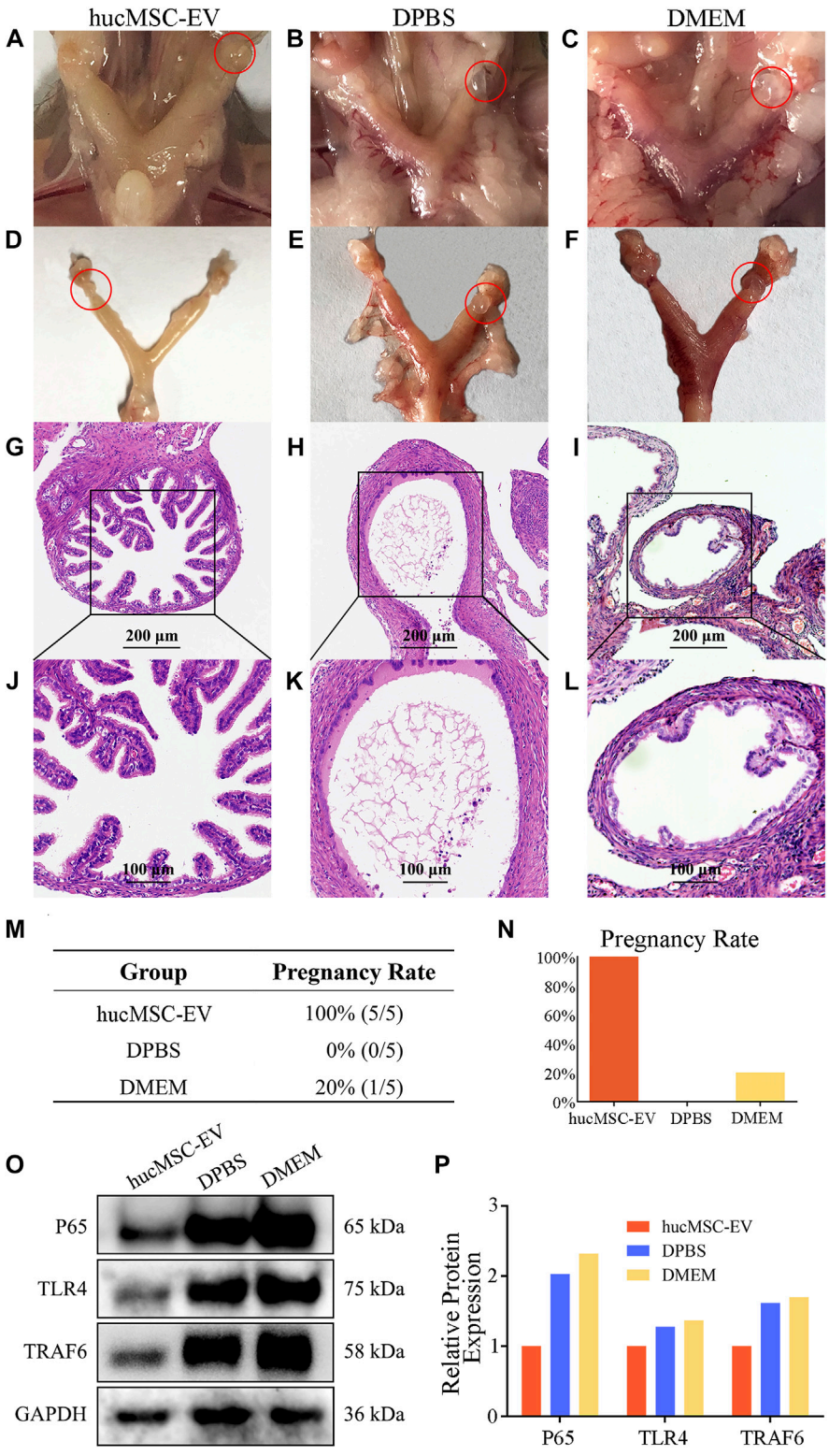

FIGURE 3
The therapeutic effect of hucMSCs on a murine model of chronic salpingitis and molecular mechanism. **(A–L)** Representative photographs and H&E microphotographs of mice fallopian tubes in the murine chronic salpingitis model. **(M, N)** The pregnancy rate table and graph of each group. **(O, P)** Representative western blots of P65 and TLR4 in the mice fallopian tubes from each group **(O)** and the relative protein expression **(P)**; band intensities were normalized against the corresponding GAPDH.

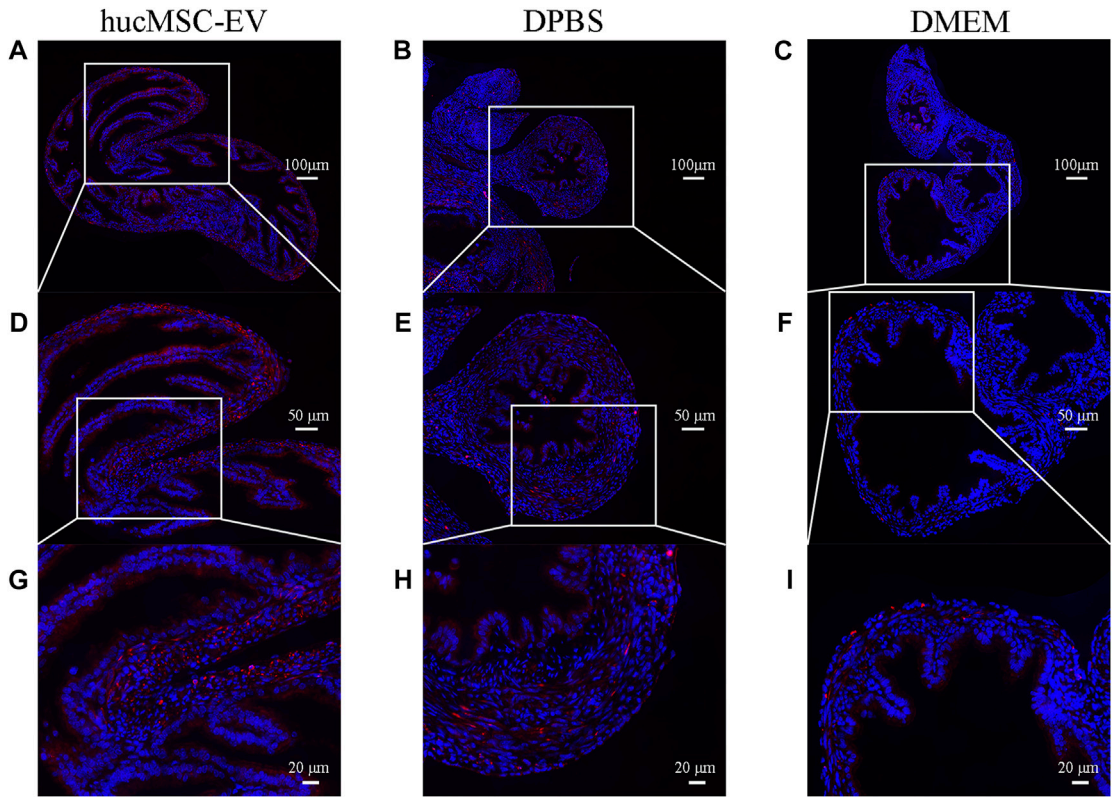

FIGURE 4
Immunofluorescence of CD206 showing M2 macrophages in the murine fallopian tubes in each experimental group **(A-I)**. Immunofluorescence of CD206 (red) showing M2 macrophages in the murine fallopian tubes in hucMSC-EV group **(A, D, G)**, DPBS group **(B, E, H)**, and DMEM group **(C, F, I)**.

the three mice groups (Figures 3O, P). The expression levels of p65 and TLR4 in the hucMSC-EV group were significantly lower than those in the DPBS and DMEM groups. These results suggest that p65 and TLR4 may play an important role in the hucMSC-EV-mediated alleviation of oviduct inflammation.

3.4 hucMSC-EV induced macrophage polarization from M1 to M2

To explore whether hucMSC-EV play a crucial role in tubal factor infertility by regulating macrophage polarization, we labeled CD206 with immunofluorescence to show the distribution of M2 macrophages in tubal tissue. The results revealed (Figure 4) that the number of M2 macrophages in the hucMSC-EV group was considerably higher than that in the DPBS and DMEM groups, suggesting that hucMSC-EV may inhibit the oviduct inflammatory response caused by *chlamydia* infection by inducing macrophage polarization from the M1 to M2 type.

3.5 Macrophages ingest membrane components of HucMSC culture supernatant and hucMSC-EV *in vitro*

How do hucMSC-EV induce macrophages to polarize from M1 cells to M2 cells to alleviate salpingitis? To further explore the molecular mechanism of the macrophage program, we conducted the following experiments. As shown in Figures 5A–C, we first labeled membrane components in the hucMSC culture supernatant using PKH67 (green fluorescence) and nuclei using DAPI (blue fluorescence). After fusion, we found that the green fluorescence signal (model component) surrounded the blue nuclei, indicating that macrophage RAW264.7 cells can swallow membrane components in the hucMSC culture supernatant.

Additionally, we used CellTracker™ Red CMTPX Dye to label EV. Fluorescent microscopy showed that the red signal coincided with macrophages, verifying that macrophages could phagocytose EV (Figures 5D,E).

Next, we explored whether hucMSC-EV could reverse the M1-type macrophages to the M2 type.

We first treated macrophages separately with LPS and hucMSC-EV and detected the surface marker proteins of M1 and M2 macrophages using RT-PCR to verify the role of hucMSC-EV. As shown in Figures 5F–H, after treatment with 100 ng/ml of LPS, the transcription level of iNOS in M1 macrophages increased significantly, while that of CD206 in M2 macrophages decreased significantly. When hucMSC-EV and LPS were present simultaneously, the transcription level of iNOS in M1 macrophages was not significantly different from that in the untreated group, while the transcription level of CD206 in M2 macrophages was significantly different from that in the other three groups. LPS and hucMSC-EV had no significant effect on the expression of macrophage general marker F4/80.

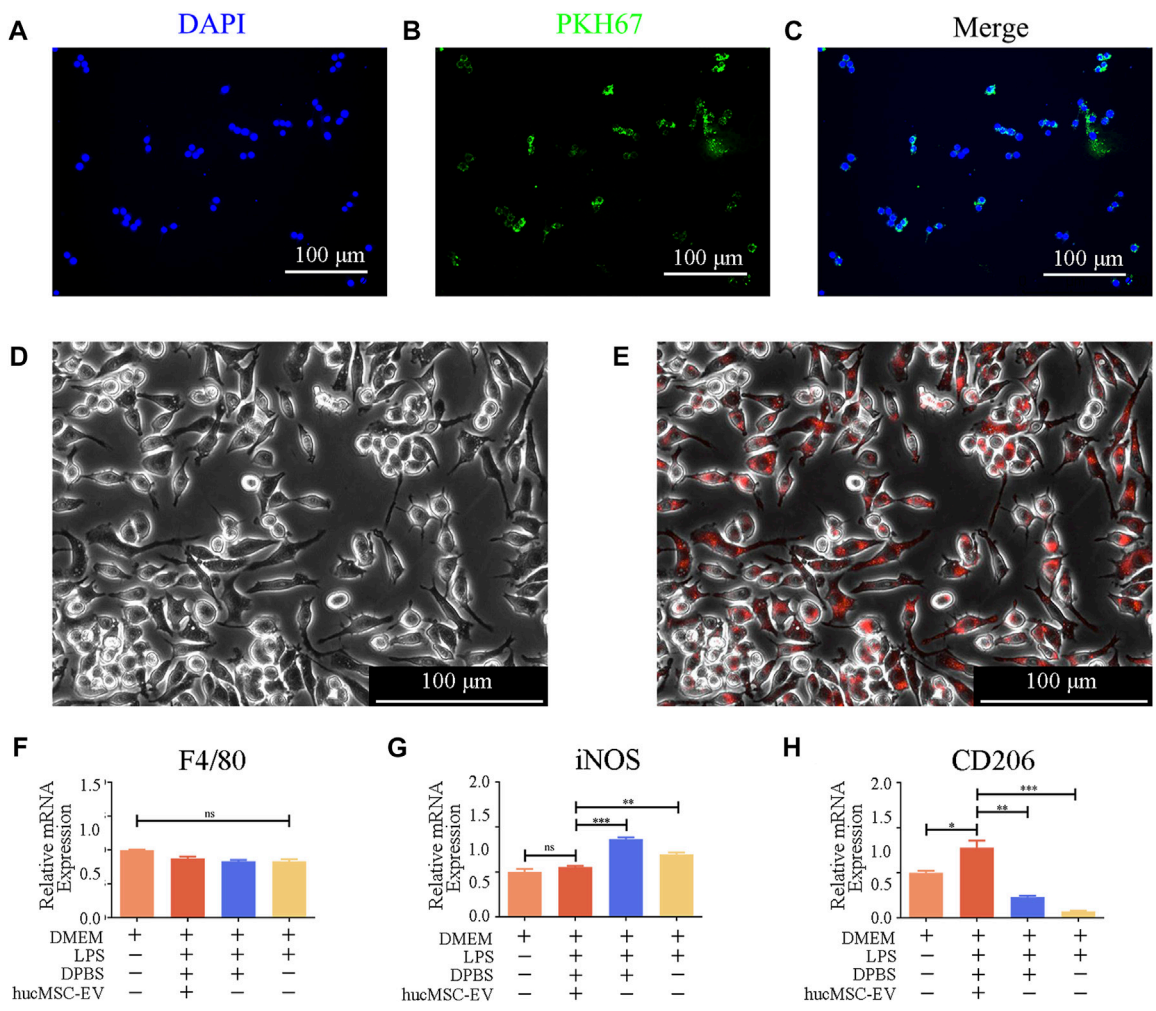

FIGURE 5
hucMSC-EV uptake by mouse RAW264.7 macrophages and hucMSC-EV-mediated polarization of RAW264.7 cells. **(A–C)** Immunofluorescence image showing the uptake of membrane components of hucMSC culture supernatant by RAW264.7 cells. **(D, E)** Immunofluorescence image indicating RAW264.7 cell uptake of hucMSC-EV. **(F–H)** Gene expression profiles of macrophage subtype markers in RAW264.7 cells in each group (n = 3). Data are expressed as the mean ± SD. Statistical significance was determined using one-way ANOVA followed by an unpaired t-test or Kruskal–Wallis test. *p < .05, **p < .01, ***p < .001.

The above results indicate that hucMSC-EV can reverse LPS-induced macrophage transformation and promote the conversion of M1-type to M2-type macrophages.

3.6 hucMSC-EV reverse p65 and TRAF6 expression in LPS-induced macrophages and promote IL-10 transcription

To further explore the molecular mechanism by which hucMSC-EV induce macrophage polarization, we treated macrophages with hucMSC-EV and LPS in vitro cell experiments and verified the expression of p65 and TRAF6 proteins using WB. As shown in Figures 6A,B, LPS significantly upregulated the expression levels of p65 and TRAF6, while simultaneous treatment of macrophages with LPS and hucMSC-EV did not result in significant increases in the expression levels of p65 and TRAF6. These results indicate that hucMSC-EV can reverse these processes through the p65/TRAF6 pathway.

M1 macrophages usually secrete proinflammatory cytokines and IL-1β, while M2 macrophages usually secrete anti-inflammatory cytokine IL-10. Could hucMSCs promote the expression of anti-inflammatory cytokine IL-10? The results show (Figures 6C–H) that LPS treatment significantly increased macrophage TNF-α and IL-1β mRNA transcription and secretion levels, whereas treatment with hucMSC-EV downregulated the transcription and expression levels of both factors. Furthermore, LPS significantly reduced the mRNA transcription and secretion level of IL-10 in macrophages, while hucMSC-EV significantly upregulated the transcription and expression level of IL-10. The above results show that hucMSC-EV can reverse the expression of p65 and TRAF6 proteins in macrophages induced by LPS and promote the transcription and secretion of IL-10.

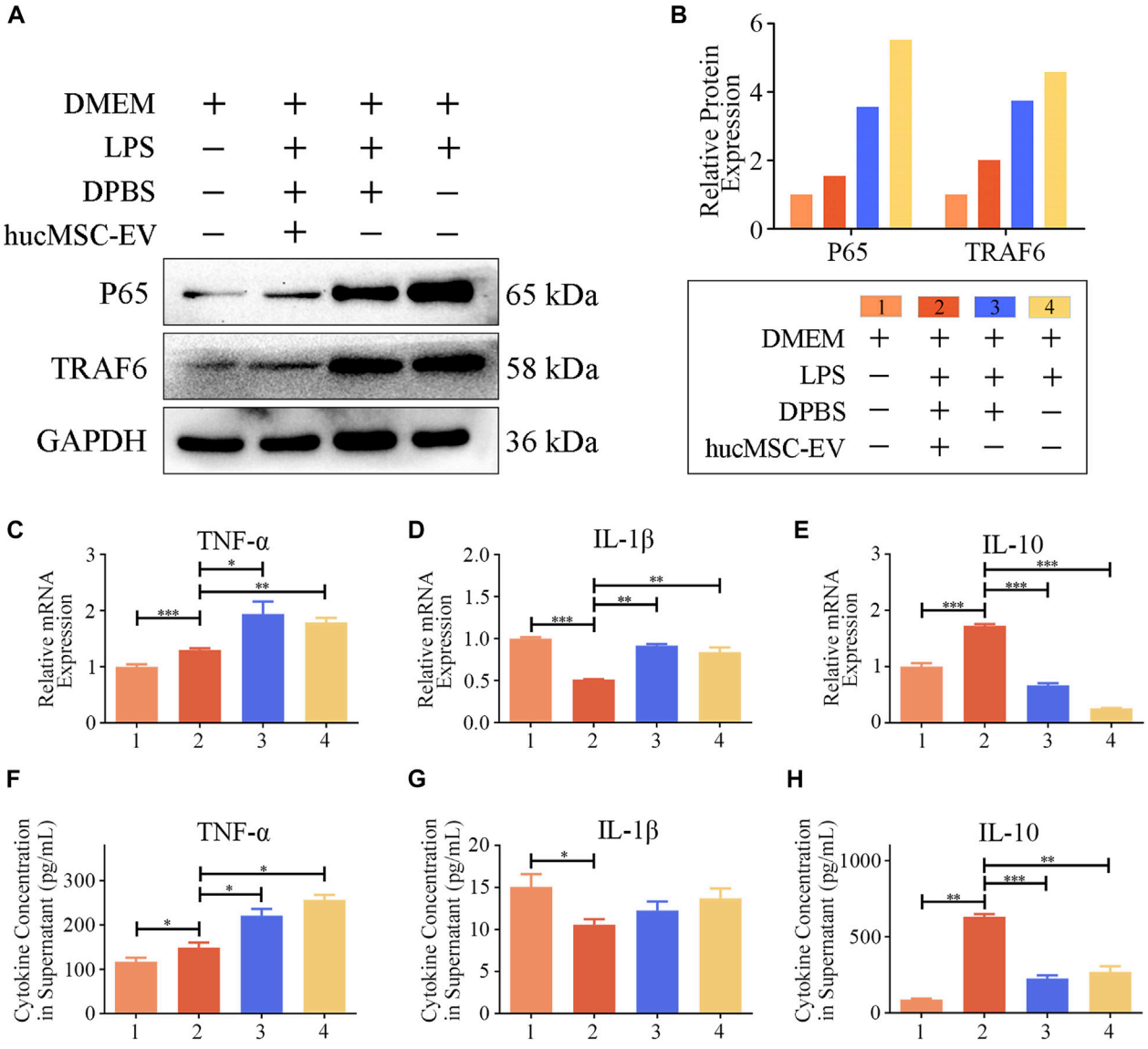

FIGURE 6
hucMSC-EV regulate p65, TRAF6, and cytokine transcription and expression. **(A, B)** Representative western blots of p65 and TRAF6 in RAW264.7 cells from each group **(A)** and the relative protein expression **(B)**; band intensities were normalized against the corresponding GAPDH. **(C–E)** mRNA expression levels of cytokine genes in RAW264.7 cells treated with LPS for 8 h and hucMSC-EV for 12 h (n = 3). **(F–H)** Concentration of cytokines TNF-α **(F)**, IL-1β **(G)**, and IL-10 **(H)** in the culture supernatant of RAW264.7 cells treated with LPS for 8 h and hucMSC-EV for 48 h (n = 4). Data are expressed as the mean ± SD. Statistical significance was determined using one-way ANOVA followed by an unpaired t-test or Kruskal–Wallis test. *p < .05, **p < .01, ***p < .001.

4 Discussion

WHO has predicted that infertility will become the third major disease in the 21st century (Mascarenhas et al., 2012). The most common cause of infertility is salpingitis caused by CT, with up to 70% of patients being asymptomatic (Yonke et al., 2022); lack of appropriate treatment in undiagnosed cases can lead to infertility (Hafner, 2015). Here, we demonstrated the functional significance of hucMSC-derived EV in infertility caused by CT-induced salpingitis *in vitro* and *in vivo* and the possible mechanisms of hucMSC-EV. hucMSC-EV reduced the congestion and inflammation in fallopian tubes caused by the CT infection and increased the pregnancy rate of nude mice. Regarding the molecular mechanism, we found that hucMSC-EV, through the NF-κB signaling pathway, can induce macrophages to transform from the M1 to the M2 type and inhibit tubal factor infertility (Figure 7). These results lay a solid foundation for the future clinical applications of EV to inhibit CT inflammatory infertility.

EV can be obtained from a variety of specimens, including cell culture supernatants and various body fluids, such as blood and urine (Logozzi et al., 2020). MSC-derived EV play an increasingly important role in intracellular communication and tissue repair (Joo et al., 2020; Lin et al., 2022). Compared with living cells, their clinical application may offer significant advantages because they may

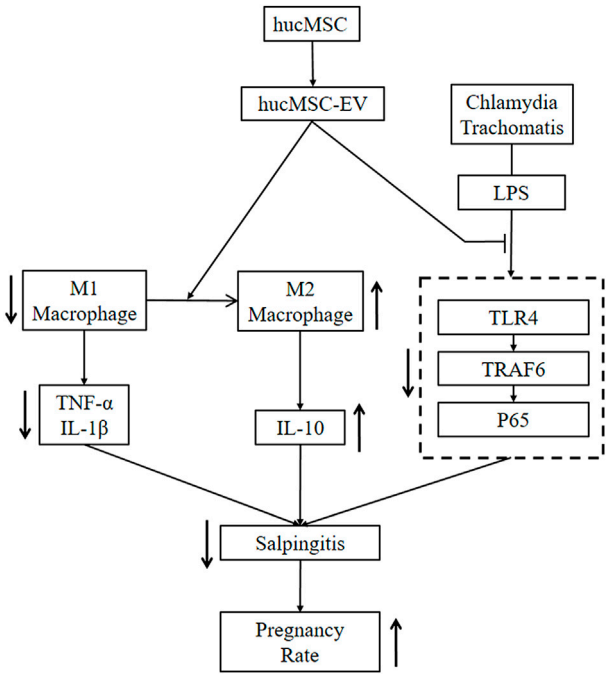

FIGURE 7
hucMSC-EV treat salpingitis by promoting macrophage polarization from M1 to M2 and inhibiting the TLR4 signaling pathway. hucMSC-EV downregulated M1 macrophages and cytokines TNF-α and IL-1β and upregulated M2 macrophages and cytokine IL-10. hucMSC-EV downregulated the TLR4, TRAF6, and p65 proteins to treat salpingitis and upregulated the pregnancy rate.

reduce adverse side effects after application, as well as infusion toxicity, uncontrolled cell growth, and possible tumor formation (Liang et al., 2014; Qiu et al., 2019; Weng et al., 2021).

The use of hucMSC-EV has shown beneficial effects in a variety of diseases, such as lung disease (Willis et al., 2020; Willis et al., 2021), oxygen-Induced multi-organ disease (Fernandez-Gonzalez et al., 2021), preeclamptic lung Injury (Taglauer et al., 2022), various detrimental sequalae of hyperoxia exposure (Reis et al., 2021), cornea disease (McKay et al., 2021), hepatic fibrosis (Rong et al., 2019), *etc.* In rat calvarial defects, miR-196a (Qin et al., 2016), miR-27a, and miR-206 (Lai et al., 2022) positively regulate the expression of osteogenic genes and osteoblast differentiation to stimulate bone formation (Liu et al., 2018). In a mouse model of Alzheimer's disease, miR-21 and miR-181c effectively reduced amyloid-β accumulation and increased synaptic protein expression and miR-21 levels in the brains of APP/PS1 mice (Cui et al., 2018). EV inhibited the hypoxic activation of STAT3 signaling and upregulation of miR-204 and miR-17 in a mouse model of suppressed pulmonary hypertension (Lee et al., 2012). Inhibition of the IL-6-related signaling pathway by miR-455-3p in a mouse model of acute liver injury suppressed monocyte/macrophage overactivation and reduced injury (Shao M et al., 2020). In a rat model of acute kidney injury, the renal injury was suppressed by improving oxidative stress and apoptosis, and cell proliferation was promoted by activation of ERK1/2 *in vivo* and *in vitro* (Ullah et al., 2020). Inhibition of myofibroblast formation and TGF by miR-21, miR-23a, miR-125b, and miR-145 in a mouse model of skin disease- β 2, TGF- β R2 and Smad2 pathways, thereby inhibiting α-SMA expression and decreasing collagen I deposition (Hu et al., 2020). EV act on TRAF1-mediated macrophage polarization, thereby treating severe steroid-resistant asthma. Treatment of cerebral ischemic injury with miR-542-3p prevented ischemia-induced glial inflammatory response by inhibiting TLR4 (Cai et al., 2021). Many studies have also explored the use of hucMSC-EV or their secretomes to treat COVID-19 infection with promising results (Meng et al., 2020; Sengupta et al., 2020; Tang et al., 2020; Hashemian et al., 2021).

At present, MSCs are rarely used in the treatment of tubal factor infertility. Our previous study showed that MSC transplantation can significantly reduce the degree of inflammation in salpingitis caused by CT infection (Liao et al., 2019). In this study, we demonstrate that hucMSC-EV can reduce salpinx congestion and inflammatory reactions caused by CT infection and improve the pregnancy rate of nude mice. Therefore, we speculate that the role of MSCs in the repair and reconstruction of inflammatory adhesions may be related to the immunoregulatory effects of MSCs under different inflammatory environments and on other inflammatory cells.

Some studies have confirmed that MSCs can promote the transformation of M1 macrophages to the M2 type through the paracrine pathway (Xin et al., 2020; Li et al., 2022; Teng et al., 2022; Zhang et al., 2022), suggesting that M2-type macrophages are important in the MSC-mediated treatment of salpingitis. Based on previous studies, we used CT intravaginal inoculation to generate a mouse model of salpingitis. hucMSC-EV were used to treat CT salpingitis, and the therapeutic effects were evaluated. We found that membrane components in the supernatant of hucMSCs could be engulfed by M1 macrophages, inducing M2-type polarization. Furthermore, the number of M2 macrophages in the hucMSC-EV group was substantially higher than that in the other groups, suggesting that hucMSC-EV can inhibit tubal inflammation caused by chlamydial infection by inducing macrophage polarization from the M1 to M2 type. However, the molecular mechanism by which hucMSC-EV induce macrophage polarization remains unknown.

NF-κB is a major transcription factor with a key role in the immune response (Xu et al., 2019; Barnabei et al., 2021; Luo et al., 2022). Strict regulation of the NF-κB signaling pathway is essential for maintaining immune homeostasis (Mitchell and Carmody, 2018; Yu et al., 2020). Uncontrolled hyperactivation of this pathway may lead to excessive inflammation and ultimately to various pathological conditions (Taniguchi and Karin, 2018).

NF-κB acts *via* two signaling pathways: a typical pathway that mediates inflammatory responses (Barnabei et al., 2021) and an atypical pathway that participates in the differentiation and maturation of immune cells (Hayden and Ghosh, 2011) and secondary lymphoid organogenesis (Hahn et al., 2016; Sun, 2017). Inhibition of NF-κB activation can promote immunosuppression in inflammation and tumors (Li et al., 2020); in contrast, stimulation of NF-κB activation promotes immunity and activates $CD8^+$ T cell cytotoxicity (Yatim et al., 2015). In patients with multiple sclerosis, related gene alterations

led to the enhancement of the NF-κB signaling pathway, enhancing the inflammatory response (Leibowitz and Yan, 2016). The degradation of NF that induces autophagy κ B-rela cells, restoring NF κ After B activity, tumor-associated macrophages can be seen to polarize toward M2 (Qian M et al., 2020; Korbecki et al., 2021; Zhang et al., 2022).

Inhibition of the nuclear translocation of NF-κB leads to decreased transcriptional activity (Yu et al., 2020); when its phosphorylation is inhibited, the inflammatory response is suppressed (Baldwin, 2012). Valsartan is the latest generation of angiotensin II receptor antagonists, which can reduce NF-κB nuclear translocation, decrease its expression, inhibit NF-κB-related inflammatory pathways, and reduce the expression of the inflammatory end products COX-2 and IL-1 (Dandona et al., 2003; Sun et al., 2018). In addition, inhibition of the NF-κB p65 signaling pathway can inhibit TNF-α-induced expression of inflammatory mediators (Deng et al., 2010). The LPS-induced NF-κB signaling pathway can be selectively regulated to inhibit the expression of proinflammatory genes, thereby inhibiting the inflammatory response (Gao et al., 2022). In addition, Mammalian sterile 20-like kinase 1 (MST1) attenuates NF-κB-dependent inflammatory gene expression by phosphorylating HOIP and, thus, functions as a negative regulatory mechanism, promoting the regression of inflammation and preventing unnecessary tissue damage (In Young Lee et al., 2019).

To further explore the molecular mechanism and signaling pathways of hucMSC-EV in reducing inflammation in pathogenic mice, we detected the proteins p65 and TLR4, associated with the inflammatory signaling pathway. The results show that the protein expression levels of p65 and TLR4 were significantly downregulated in hucMSC-EV, suggesting that p65 and TLR4 may play an important role in the hucMSC-EV-mediated treatment of salpingitis. Subsequently, we found that hucMSC-EV can reverse the expression of p65 and TRAF6 proteins in LPS-induced macrophages and promote the transcription and secretion of IL-10; therefore, hucMSC-EV can regulate the NF-κB signaling pathway and induce macrophage-polarization from M1 to M2, improving the local inflammatory microenvironment of fallopian tubes.

Although we found that hucMSC-EV can downregulate the NF-κB inflammatory signaling pathway, contributing to the reduction of inflammation, several factors remain unknown: 1) identification of the upstream molecules in the TLR4 signaling pathway; 2) secretions comprise several substances, including RNA, proteins, and other biological molecules, with yet unresolved roles. In this regard, future investigations using chip technology and bioinformatics may be useful; 3) the potential anti-inflammatory effects and synergistic actions of substances in the culture supernatant of hucMSCs, such as growth factors and other types of cell vesicles, require investigation; 4) in addition, application of hucMSC-EV to studies of infertility caused by other factors, such as endometritis caused by CT (Yang et al., 2021), remains open. The above issues remain the direction and goal of our future studies, and our efforts will be toward designing appropriate experiments.

5 Conclusion

CT infection can cause chronic salpingitis and infertility. hucMSC-EV can induce macrophage polarization from the M1 to M2 type through the NF-κB signaling pathway, thus improving the local inflammatory microenvironment of the fallopian tube, treating chronic salpingitis caused by CT infection, and ultimately improving the reproductive outcome. Thus, hucMSC-EV can be a promising, cell-free method to treat infertility due to chronic salpingitis.

Data availability statement

The original contributions presented in the study are included in the article/Supplementary Material, further inquiries can be directed to the corresponding authors.

Ethics statement

The studies involving human participants were reviewed and approved by Ethics Committee of the Seventh Affiliated Hospital, Sun Yat-sen University. The patients/participants provided their written informed consent to participate in this study. The animal study was reviewed and approved by Ethics Committee of the Seventh Affiliated Hospital, Sun Yat-sen University.

Author contributions

TL: conception, design, supervision, and full responsibility of the study; supervision of manuscript writing. CLZ: conception, design, supervision, manuscript writing, and full responsibility of the study. WEL, WZL: study design and manuscript writing. YX: provided the necessary *Chlamydia trachomatis* for the experiment. HS, JQ, JY, XX: performed the experiments. LL, JD, ML: data supervision. CIZ, XZ: statistical analysis. DD, WD: supervision of manuscript writing. All authors critically reviewed the article and approved the final manuscript.

Funding

This work was supported by funds from the National Natural Science Foundation of China (82002899, 82172883, 82001498), the Guangdong Basic and Applied Basic Research Foundation (2019A1515110085, 2022A1515012444), and the Open Funds of State Key Laboratory of Oncology in South China (HN 2021-05).

Acknowledgments

We thank all the participants recruited for this study and our colleagues from the Department of Gynecology, The Seventh Affiliated Hospital of Sun Yat-sen University, Shenzhen, China.

Conflict of interest

The authors declare that the research was conducted in the absence of any commercial or financial relationships that could be construed as a potential conflict of interest.

Publisher's note

All claims expressed in this article are solely those of the authors and do not necessarily represent those of their affiliated organizations, or those of the publisher, the editors and the reviewers. Any product that may be evaluated in this article, or claim that may be made by its manufacturer, is not guaranteed or endorsed by the publisher.

Supplementary material

The Supplementary Material for this article can be found online at: https://www.frontiersin.org/articles/10.3389/fphys.2023.1131701/full#supplementary-material

References

Andrzejewska, A., Lukomska, B., and Janowski, M. (2019). Concise Review: Mesenchymal stem cells: From roots to boost. *Stem Cells Dayt. Ohio)* 37 (7), 855–864. doi:10.1002/stem.3016

Baldwin, A. S. (2012). Regulation of cell death and autophagy by IKK and NF-?b: Critical mechanisms in immune function and cancer. *Immunol. Rev.* 246 (1), 327–345. doi:10.1111/j.1600-065X.2012.01095.x

Barnabei, L., Laplantine, E., Mbongo, W., Rieux-Laucat, F., and Weil, R. (2021). NF-KB: At the borders of autoimmunity and inflammation. *Front. Immunol.* 12, 716469. doi:10.3389/fimmu.2021.716469

Brunham, R. C. (2022). Problems with understanding Chlamydia trachomatis immunology. *J. Infect. Dis.* 225 (11), 2043–2049. doi:10.1093/infdis/jiab610

Cai, G., Cai, G., Zhou, H., Zhuang, Z., Liu, K., Pei, S., et al. (2021). Mesenchymal stem cell-derived exosome MiR-542-3p suppresses inflammation and prevents cerebral infarction. *Stem Cell. Res. Ther.* 12 (1), 2. doi:10.1186/s13287-020-02030-w

Cooke, J. P. (2019). Inflammation and its role in regeneration and repair. *Circulation Res.* 124 (8), 1166–1168. doi:10.1161/CIRCRESAHA.118.314669

Cui, G.-H., Wu, J., Mou, F.-F., Xie, W.-H., Wang, F.-B., Wang, Q.-L., et al. (2018). Exosomes derived from hypoxia-preconditioned mesenchymal stromal cells ameliorate cognitive decline by rescuing synaptic dysfunction and regulating inflammatory responses in APP/PS1 mice. *FASEB J. Official Publ. Fed. Am. Soc. Exp. Biol.* 32 (2), 654–668. doi:10.1096/fj.201700600R

Dandona, P., Kumar, V., Aljada, A., Ghanim, H., Syed, T., and Hofmayer, D. (2003). Angiotensin II receptor blocker valsartan suppresses reactive oxygen species generation in leukocytes, nuclear factor-kappa B, in mononuclear cells of normal subjects: Evidence of an antiinflammatory action. *J. Clin. Endocrinol. Metabolism* 88 (9). doi:10.1210/jc.2002-021836

Deng, N., Ye, Y., Wang, W., and Li, L. (2010). Dishevelled interacts with P65 and acts as a repressor of NF-KB-Mediated transcription. *Cell. Res.* 20 (10), 1117–1127. doi:10.1038/cr.2010.108

Dominici, M., Le Blanc, K., Mueller, I., Slaper-Cortenbach, I., Marini, F., Krause, D., et al. (2006). Minimal criteria for defining multipotent mesenchymal stromal cells. The international society for cellular Therapy position statement. *Cytotherapy* 8 (4), 315–317. doi:10.1080/14653240600855905

Erpicum, P., Rowart, P., Poma, L., Krzesinski, J.-M., Detry, O., and Jouret, F. (2017). Administration of mesenchymal stromal cells before renal ischemia/reperfusion attenuates kidney injury and may modulate renal lipid metabolism in rats. *Sci. Rep.* 7 (1), 8687. doi:10.1038/s41598-017-08726-z

Farhat, W., Yeung, V., Kahale, F., Parekh, M., Cortinas, J., Chen, L., et al. (2022). Doxorubicin-loaded extracellular vesicles enhance tumor cell death in retinoblastoma. *Bioeng. (Basel, Switz.* 9 (11), 671. doi:10.3390/bioengineering9110671

Fernandez-Gonzalez, A., Willis, G. R., Yeung, V., Reis, M., Liu, X., Mitsialis, S. A., et al. (2021). Therapeutic effects of mesenchymal stromal cell-derived small extracellular vesicles in oxygen-induced multi-organ disease: A developmental perspective. *Front. Cell. Dev. Biol.* 9, 647025. doi:10.3389/fcell.2021.647025

Galipeau, J. (2021). Macrophages at the nexus of mesenchymal stromal cell potency: The emerging role of chemokine cooperativity. *Stem Cells Dayt. Ohio)* 39 (9), 1145–1154. doi:10.1002/stem.3380

Gao, Y., Xu, Z., Li, X., Liu, Z., Li, W., Kang, Y., et al. (2022). Resibufogenin, one of bufadienolides in toad venom, suppresses LPS-induced inflammation via inhibiting NF-?b and AP-1 pathways. *Int. Immunopharmacol.* 113, 109312. doi:10.1016/j.intimp.2022.109312

Hafner, L. M. (2015). Pathogenesis of fallopian tube damage caused by Chlamydia trachomatis infections. *Contraception* 92 (2), 108–115. doi:10.1016/j.contraception.2015.01.004

Haggerty, C. L., Gottlieb, S. L., Taylor, B. D., Low, N., Xu, F., and Ness, R. B. (2010). Risk of sequelae after Chlamydia trachomatis genital infection in women. *J. Infect. Dis.* 201 (2), S134–S155. doi:10.1086/652395

Hahn, M., Macht, A., Waisman, A., and Hövelmeyer, N. (2016). NF-KB-Inducing kinase is essential for B-cell maintenance in mice. *Eur. J. Immunol.* 46 (3), 732–741. doi:10.1002/eji.201546081

Harrell, C. R., Jovicic, N., Djonov, V., Arsenijevic, N., and Volarevic, V. (2019). Mesenchymal stem cell-derived exosomes and other extracellular vesicles as new remedies in the Therapy of inflammatory diseases. *Cells* 8 (12), 1605. doi:10.3390/cells8121605

Hashemian, S.-M. R., Aliannejad, R., Zarrabi, M., Soleimani, M., Vosough, M., Hosseini, S.-E., et al. (2021). Mesenchymal stem cells derived from perinatal tissues for treatment of critically ill COVID-19-induced ards patients: A case series. *Stem Cell. Res. Ther.* 12, 91. doi:10.1186/s13287-021-02165-4

Hayden, M. S., and Ghosh, S. (2011). NF-KB in immunobiology. *Cell. Res.* 21 (2), 223–244. doi:10.1038/cr.2011.13

Hu, J., Chen, Y., Huang, Y., and Su, Y. (2020). Human umbilical cord mesenchymal stem cell-derived exosomes suppress dermal fibroblasts-myofibroblats transition via inhibiting the TGF-ß1/smad 2/3 signaling pathway. *Exp. Mol. Pathology* 115, 104468. doi:10.1016/j.yexmp.2020.104468

Joo, H. S., Suh, J. H., Lee, H. J., Bang, E. S., and Lee, J. M. (2020). Current knowledge and future perspectives on mesenchymal stem cell-derived exosomes as a new therapeutic agent. *Int. J. Mol. Sci.* 21 (3), E727. doi:10.3390/ijms21030727

Korbecki, J., Simińska, D., Gąssowska-Dobrowolska, M., Listos, J., Gutowska, I., Chlubek, D., et al. (2021). Chronic and cycling hypoxia: Drivers of cancer chronic inflammation through HIF-1 and NF-?b activation: A Review of the molecular mechanisms. *Int. J. Mol. Sci.* 22 (19), 10701. doi:10.3390/ijms221910701

Lai, G., Zhao, R., Zhuang, W., Hou, Z., Yang, Z., He, P., et al. (2022). BMSC-derived exosomal MiR-27a-3p and MiR-196b-5p regulate bone remodeling in ovariectomized rats. *PeerJ* 10, e13744. doi:10.7717/peerj.13744

Lee, C., Mitsialis, S. A., Aslam, M., Vitali, S. H., Vergadi, E., Konstantinou, G., et al. (2012). Exosomes mediate the cytoprotective action of mesenchymal stromal cells on hypoxia-induced pulmonary hypertension. *Circulation* 126 (22), 2601–2611. doi:10.1161/CIRCULATIONAHA.112.114173

Lee, I. Y., Lim, J. M., Cho, H., Kim, E., Kim, Y., Oh, H.-K., et al. (2019). MST1 negatively regulates TNFα-induced NF-?b signaling through modulating LUBAC activity. *Mol. Cell.* 73 (6), 1138–1149. e6, March 21. doi:10.1016/j.molcel.2019.01.022

Leibowitz, S. M., and Yan, J. (2016). NF-KB pathways in the pathogenesis of multiple sclerosis and the therapeutic implications. *Front. Mol. Neurosci.* 9, 84. doi:10.3389/fnmol.2016.00084

Li, L., Yu, R., Cai, T., Chen, Z., Lan, M., Zou, T., et al. (2020). Effects of immune cells and cytokines on inflammation and immunosuppression in the tumor microenvironment. *Int. Immunopharmacol.* 88, 106939. doi:10.1016/j.intimp.2020.106939

Li, P., Lv, S., Jiang, W., Si, L., Liao, B., Zhao, G., et al. (2022). Exosomes derived from umbilical cord mesenchymal stem cells protect cartilage and regulate the polarization of macrophages in osteoarthritis. *Ann. Transl. Med.* 10 (18), 976. doi:10.21037/atm-22-3912

Liang, X., Ding, Y., Zhang, Y., Tse, H.-F., and Lian, Q. (2014). Paracrine mechanisms of mesenchymal stem cell-based Therapy: Current status and perspectives. *Cell. Transplant.* 23 (9), 1045–1059. doi:10.3727/096368913X667709

Liao, W., Tang, X., Li, X., and Li, T. (2019). Therapeutic effect of human umbilical cord mesenchymal stem cells on tubal factor infertility using a chronic salpingitis murine model. *Archives Gynecol. Obstetrics* 300 (2), 421–429. doi:10.1007/s00404-019-05209-6

Lin, Z., Wu, Y., Xu, Y., Li, G., Li, Z., and Liu, T. (2022). Mesenchymal stem cell-derived exosomes in cancer Therapy resistance: Recent advances and therapeutic potential. *Mol. Cancer* 21 (1), 179. doi:10.1186/s12943-022-01650-5

Ling, H., Luo, L., Dai, X., and Chen, H. (2022). Fallopian tubal infertility: The result of Chlamydia trachomatis-induced fallopian tubal fibrosis. *Mol. Cell. Biochem.* 477 (1), 205–212. doi:10.1007/s11010-021-04270-7

Liu, M., Sun, Y., and Zhang, Q. (2018). Emerging role of extracellular vesicles in bone remodeling. *J. Dent. Res.* 97 (8), 859–868. doi:10.1177/0022034518764411

Logozzi, M., Mizzoni, D., Di Raimo, R., and Fais, S. (2020). Exosomes: A source for new and old biomarkers in cancer. *Cancers* 12 (9), E2566. doi:10.3390/cancers12092566

Luo, X., Xu, J., Zhao, R., Qin, J., Wang, X., Yan, Y., et al. (2022). The role of inactivated NF-?b in premature ovarian failure. *Am. J. Pathology* 192 (3), 468–483. doi:10.1016/j.ajpath.2021.12.005

Markov, A., Thangavelu, L., Aravindhan, S., Zekiy, A. O., Jarahian, M., Chartrand, M. S., et al. (2021). Mesenchymal stem/stromal cells as a valuable source for the treatment of immune-mediated Disorders. *Stem Cell. Res. Ther.* 12 (1). 192. doi:10.1186/s13287-021-02265-1

Mascarenhas, M. N., Flaxman, S. R., Boerma, T., Vanderpoel, S., and Stevens, G. A. (2012). National, regional, and global trends in infertility prevalence since 1990: A systematic analysis of 277 Health surveys. *PLoS Med.* 9 (12), e1001356. doi:10.1371/journal.pmed.1001356

McKay, T. B., Yeung, V., Hutcheon, A. E. K., Guo, X., Zieske, J. D., and Ciolino, J. B. (2021). Extracellular vesicles in the cornea: Insights from other tissues. *Anal. Cell. Pathol. Amst.*, 9983900. doi:10.1155/2021/9983900

Medzhitov, R. (2008). Origin and physiological roles of inflammation. *Nature* 454 (7203), 428–435. doi:10.1038/nature07201

Meng, F., Xu, R., Wang, S., Xu, Z., Zhang, C., Li, Y., et al. (2020). Human umbilical cord-derived mesenchymal stem cell Therapy in patients with COVID-19: A phase 1 clinical trial. *Signal Transduct. Target. Ther.* 5, 172. doi:10.1038/s41392-020-00286-5

Mitchell, J. P., and Carmody, R. J. (2018). NF-KB and the transcriptional control of inflammation. *Int. Rev. Cell. Mol. Biol.* 335, 41–84. doi:10.1016/bs.ircmb.2017.07.007

Murthy, A. K., Li, W., and Ramsey, K. H. (2018). Immunopathogenesis of chlamydial infections. *Curr. Top. Microbiol. Immunol.* 412, 183–215. doi:10.1007/82_2016_18

Negi, N., and Griffin, M. D. (2020). Effects of mesenchymal stromal cells on regulatory T cells: Current understanding and clinical relevance. *Stem Cells Dayt. Ohio)* 38 (5), 596–605. doi:10.1002/stem.3151

Newman, L., Rowley, J., Vander Hoorn, S., Wijesooriya, N. S., Unemo, M., Low, N., et al. (2015). Global estimates of the prevalence and incidence of four curable sexually transmitted infections in 2012 based on systematic Review and global reporting. *PLoS ONE* 10 (12), e0143304. doi:10.1371/journal.pone.0143304

Ning, Y., Cui, Y., Li, X., Cao, X., Chen, A., Xu, C., et al. (2018). Co-culture of ovarian cancer stem-like cells with macrophages induced SKOV3 cells stemness via IL-8/STAT3 signaling. *Biomed. Pharmacother. = Biomedecine Pharmacother.* 103, 262–271. doi:10.1016/j.biopha.2018.04.022

Pegtel, D. M., and Gould, S. J. (2019). Exosomes, *Annu. Rev. Biochem.* 88 (1), 487–514. doi:10.1146/annurev-biochem-013118-111902

Pluchino, S., and Smith, J. A. (2019). Explicating exosomes: Reclassifying the rising stars of intercellular communication. *Cell.* 177 (2), 225–227. doi:10.1016/j.cell.2019.03.020

Pouyanfard, S., Meshgin, N., Cruz, L. S., Diggle, K., Hashemi, H., Pham, T. V., et al. (2021). Human induced pluripotent stem cell-derived macrophages ameliorate liver fibrosis. *Stem Cells Dayt. Ohio)* 39 (12), 1701–1717. doi:10.1002/stem.3449

Qian, M., Wang, S., Guo, X., Wang, J., Zhang, Z., Qiu, W., et al. (2020). Hypoxic glioma-derived exosomes deliver MicroRNA-1246 to induce M2 macrophage polarization by targeting TERF2IP via the STAT3 and NF-?b pathways. *Oncogene* 39 (2). doi:10.1038/s41388-019-0996-y

Qin, Y., Wang, L., Gao, Z., Chen, G., and Zhang, C. (2016). Bone marrow stromal/stem cell-derived extracellular vesicles regulate osteoblast activity and differentiation *in vitro* and promote bone regeneration *in vivo*. *Sci. Rep.* 6, 21961. doi:10.1038/srep21961

Qiu, G., Zheng, G., Ge, M., Wang, J., Huang, R., Shu, Q., et al. (2019). Functional proteins of mesenchymal stem cell-derived extracellular vesicles. *Stem Cell. Res. Ther.* 10 (1), 359. doi:10.1186/s13287-019-1484-6

Reis, M., Willis, G. R., Fernandez-Gonzalez, A., Yeung, V., Taglauer, E., Magaletta, M., et al. (2021). Mesenchymal stromal cell-derived extracellular vesicles Restore thymic architecture and T cell function disrupted by neonatal hyperoxia. *Front. Immunol.* 12, 640595. doi:10.3389/fimmu.2021.640595

Rong, X., Liu, J., Yao, X., Jiang, T., Wang, Y., and Xie, F. (2019). Human bone marrow mesenchymal stem cells-derived exosomes alleviate liver fibrosis through the wnt/β-catenin pathway. *Stem Cell. Res. Ther.* 10 (1), 98. doi:10.1186/s13287-019-1204-2

Sengupta, V., Sengupta, S., Lazo, A., Woods, P., Nolan, A., and Bremer, N. (2020). Exosomes derived from bone marrow mesenchymal stem cells as treatment for severe COVID-19. *Stem Cells Dev.* 29 (12), 747–754. doi:10.1089/scd.2020.0080

Seo, Y., Kim, H.-S., and Hong, I.-S. (2019). Stem cell-derived extracellular vesicles as immunomodulatory therapeutics. *Stem Cells Int.* 2019, 5126156. doi:10.1155/2019/5126156

Shao, L.-T., Luo, L., Qiu, J.-H., and Deng, D. Y. B. (2022). PTH (1-34) enhances the therapeutic effect of bone marrow mesenchymal stem cell-derived exosomes by inhibiting proinflammatory cytokines expression on OA chondrocyte repair *in vitro*. *Arthritis Res. Ther.* 24 (1), 96. doi:10.1186/s13075-022-02778-x

Shao, M., Xu, Q., Wu, Z., Chen, Y., Shu, Y., Cao, X., et al. 2020. Exosomes derived from human umbilical cord mesenchymal stem cells ameliorate IL-6-induced acute liver injury through MiR-455-3p. *Stem Cell. Res. Ther.* 11 (1). doi:10.1186/s13287-020-1550-0

Shao, R., Wang, X., Wang, W., Stener-Victorin, E., Mallard, C., Brännström, M., et al. (2012). From mice to women and back again: Causalities and clues for chlamydia-induced tubal ectopic pregnancy. *Fertil. Steril.* 98 (5), 1175–1185. doi:10.1016/j.fertnstert.2012.07.1113

Shapouri-Moghaddam, A., Mohammadian, S., Vazini, H., Taghadosi, M., Esmaeili, S.-A., Mardani, F., et al. (2018). Macrophage plasticity, polarization, and function in Health and disease. *J. Cell. Physiology* 233 (9), 6425–6440. doi:10.1002/jcp.26429

Shi, Y., Wang, Y., Li, Q., Liu, K., Hou, J., Shao, C., et al. (2018). Immunoregulatory mechanisms of mesenchymal stem and stromal cells in inflammatory diseases. *Nat. Rev. Nephrol.* 14 (8), 493–507. doi:10.1038/s41581-018-0023-5

Simons, M., and Raposo, G. (2009). Exosomes – vesicular carriers for intercellular communication. *Curr. Opin. Cell. Biol.* 21 (4), 575–581. doi:10.1016/j.ceb.2009.03.007

Sun, S.-C. (2017). The non-canonical NF-?b pathway in immunity and inflammation. *Nat. Rev. Immunol.* 17 (9), 545–558. doi:10.1038/nri.2017.52

Sun, X., Luan, Q., and Qiu, S. (2018). Valsartan prevents glycerol-induced acute kidney injury in male albino rats by downregulating TLR4 and NF-?b expression. *Int. J. Biol. Macromol.* 119, 565–571. doi:10.1016/j.ijbiomac.2018.07.149

Taglauer, E. S., Fernandez-Gonzalez, A., Willis, G. R., Reis, M., Yeung, V., Liu, X., et al. (2022). Antenatal mesenchymal stromal cell extracellular vesicle Therapy prevents preeclamptic lung injury in mice. *Am. J. Respir. Cell. Mol. Biol.* 66 (1), 86–95. doi:10.1165/rcmb.2021-0307OC

Tang, L., Jiang, Y., Zhu, M., Chen, L., Zhou, X., Zhou, C., et al. (2020). Clinical study using mesenchymal stem cells for the treatment of patients with severe COVID-19. *Front. Med.* 14 (5), 664–673. doi:10.1007/s11684-020-0810-9

Taniguchi, K., and Karin, M. (2018). NF-KB, inflammation, immunity and cancer: Coming of age. *Nat. Rev. Immunol.* 18 (5), 309–324. doi:10.1038/nri.2017.142

Teng, L., Maqsood, M., Zhu, M., Zhou, Y., Kang, M., Zhou, J., et al. (2022). Exosomes derived from human umbilical cord mesenchymal stem cells accelerate diabetic wound healing via promoting M2 macrophage polarization, angiogenesis, and collagen deposition. *Int. J. Mol. Sci.* 23 (18), 10421. doi:10.3390/ijms231810421

Tsevat, D. G., Wiesenfeld, H. C., Parks, C., and Peipert, J. F. (2017). Sexually transmitted diseases and infertility. *Am. J. Obstetrics Gynecol.* 216 (11–9). doi:10.1016/j.ajog.2016.08.008

Ullah, M., Liu, D. D., Rai, S., Razavi, M., Concepcion, W., and Thakor, A. S. (2020). Pulsed focused ultrasound enhances the therapeutic effect of mesenchymal stromal cell-derived extracellular vesicles in acute kidney injury. *Stem Cell. Res. Ther.* 11 (1), 398. doi:10.1186/s13287-020-01922-1

Vizoso, F. J., Eiro, N., Cid, S., Schneider, J., and Perez-Fernandez, R. (2017). Mesenchymal stem cell secretome: Toward cell-free therapeutic strategies in regenerative medicine. *Int. J. Mol. Sci.* 18 (9), E1852. doi:10.3390/ijms18091852

Webber, J., Yeung, V., and Clayton, A. (2015). Extracellular vesicles as modulators of the cancer microenvironment. *Seminars Cell. & Dev. Biol.* 40, 27–34. doi:10.1016/j.semcdb.2015.01.013

Weng, Z., Zhang, B., Wu, C., Yu, F., Han, B., Li, B., et al. (2021). Therapeutic roles of mesenchymal stem cell-derived extracellular vesicles in cancer. *J. Hematol. Oncol.* 14 (1), 136. doi:10.1186/s13045-021-01141-y

Willis, G. R., Fernandez-Gonzalez, A., Reis, M., Yeung, V., Liu, X., Ericsson, M., et al. (2020). Mesenchymal stromal cell-derived small extracellular vesicles Restore lung architecture and improve exercise capacity in a model of neonatal hyperoxia-induced lung injury. *J. Extracell. Vesicles* 9 (1), 1790874. doi:10.1080/20013078.2020.1790874

Willis, G. R., Reis, M., Gheinani, A. H., Fernandez-Gonzalez, A., Taglauer, E. S., Yeung, V., et al. (2021). Extracellular vesicles protect the neonatal lung from hyperoxic injury through the epigenetic and transcriptomic reprogramming of myeloid cells. *Am. J. Respir. Crit. Care Med.* 204 (12), 1418–1432. doi:10.1164/rccm.202102-0329OC

Xin, L., Lin, X., Zhou, F., Li, C., Wang, X., Yu, H., et al. (2020). A scaffold laden with mesenchymal stem cell-derived exosomes for promoting endometrium regeneration and fertility restoration through macrophage immunomodulation. *Acta Biomater.* 113, 252–266. doi:10.1016/j.actbio.2020.06.029

Xu, J.-J., Wang, G., Luo, X., Wang, L.-J., Bao, Y., and Yang, X. (2019). Role of nuclear factor-?b pathway in the transition of mouse secondary follicles to antral follicles. *J. Cell. Physiology* 234 (12), 22565–22580. doi:10.1002/jcp.28822

Yang, C., Lei, L., Collins, J. W. M., Briones, M., Ma, L., Sturdevant, G. L., et al. (2021). Chlamydia evasion of neutrophil host defense results in NLRP3 dependent myeloid-

mediated sterile inflammation through the purinergic P2X7 receptor. *Nat. Commun.* 12 (1), 5454. doi:10.1038/s41467-021-25749-3

Yatim, N., Jusforgues-Saklani, H., Orozco, S., Schulz, O., Barreira da Silva, R., Reis e Sousa, C., et al. (2015). RIPK1 and NF-?b signaling in dying cells determines cross-priming of $CD8^+$ T cells. *Sci. (New York, N.Y.)* 350 (6258), 328–334. doi:10.1126/science.aad0395

Yeung, V., Willis, G. R., and Taglauer, E. (2019). *Stem cell-based Therapy for lung disease*. New York: Springer.

Yeung, Vincent, Zhang, T. C., Yuan, L., Parekh, M., Cortinas, J. A., Delavogia, E., et al. (2022). Extracellular vesicles secreted by corneal myofibroblasts promote corneal epithelial cell migration. *Int. J. Mol. Sci.* 23 (6), 3136. doi:10.3390/ijms23063136

Yin, S., Ji, C., Wu, P., Jin, C., and Qian, H. (2019). Human umbilical cord mesenchymal stem cells and exosomes: Bioactive ways of tissue injury repair. *Am. J. Transl. Res.* 11 (3), 1230–1240.

Yonke, N., Aragón, M., and Phillips, J. K. (2022). Chlamydial and gonococcal infections: Screening, diagnosis, and treatment. *Am. Fam. Physician* 105 (4), 388–396.

Yu, H., Lin, L., Zhang, Z., Zhang, H., and Hu, H. (2020). Targeting NF-?b pathway for the Therapy of diseases: Mechanism and clinical study. *Signal Transduct. Target. Ther.* 5 (1). 209. doi:10.1038/s41392-020-00312-6

Yuan, X., Yuan, W., Ding, L., Shi, M., Luo, L., Wan, Y., et al. (2021). Cell-adaptable dynamic hydrogel reinforced with stem cells improves the functional repair of spinal cord injury by alleviating neuroinflammation. *Biomaterials* 279, 121190. doi:10.1016/j.biomaterials.2021.121190

Zhang, M., Johnson-Stephenson, T. K., Wang, W., Wang, Y., Li, J., Li, L., et al. (2022). Mesenchymal stem cell-derived exosome-educated macrophages alleviate systemic lupus erythematosus by promoting efferocytosis and recruitment of IL-17+ regulatory T cell. *Stem Cell. Res. Ther.* 13 (1), 484. doi:10.1186/s13287-022-03174-7

Zhang, M., Liu, Z. Z., Aoshima, K., Cai, W. L., Sun, H., Xu, T., et al. (2022). CECR2 drives breast cancer metastasis by promoting NF-?b signaling and macrophage-mediated immune suppression. *Sci. Transl. Med.* 14 (630), eabf5473. doi:10.1126/scitranslmed.abf5473

frontiers | Frontiers in Physiology

TYPE Review
PUBLISHED 28 February 2023
DOI 10.3389/fphys.2023.1113684

OPEN ACCESS

EDITED BY
Bin Liu,
Independent Researcher, Shenzhen, China

REVIEWED BY
Shuangbo Kong,
Xiamen University, China
Bunpei Ishizuka,
Rose Ladies Clinic, Japan
Yin-Li Zhang,
Zhejiang University, China

*CORRESPONDENCE
Ziwen Xiao,
xzwe@hotmail.com
Wei Pan,
pw__6602@163.com
Chao Wang,
wangcam@126.com

†These authors have contributed equally to this work

SPECIALTY SECTION
This article was submitted to Reproductive and Mating Physiology, a section of the journal Frontiers in Physiology

RECEIVED 01 December 2022
ACCEPTED 20 February 2023
PUBLISHED 28 February 2023

CITATION
Zhang T, He M, Zhang J, Tong Y, Chen T, Wang C, Pan W and Xiao Z (2023), Mechanisms of primordial follicle activation and new pregnancy opportunity for premature ovarian failure patients.
Front. Physiol. 14:1113684.
doi: 10.3389/fphys.2023.1113684

Mechanisms of primordial follicle activation and new pregnancy opportunity for premature ovarian failure patients

Tuo Zhang [1,2,3,4,5,6‡], Meina He[4,6‡], Jingjing Zhang[2], Yuntong Tong[2], Tengxiang Chen[2,4,5,6], Chao Wang[7]*, Wei Pan[3]* and Ziwen Xiao[1]*

[1]Department of Obstetrics and Gynecology, The Affiliated Hospital of Guizhou Medical University, Guiyang, China, [2]Transformation Engineering Research Center of Chronic Disease Diagnosis and Treatment, Department of Physiology, College of Basic Medicine, Guizhou Medical University, Guiyang, Guizhou, China, [3]Prenatal Diagnosis Center in Guizhou Province, The Affiliated Hospital of Guizhou Medical University, Guiyang, China, [4]College of Basic Medicine, Guizhou Medical University, Guiyang, Guizhou, China, [5]Guizhou Provincial Key Laboratory of Pathogenesis and Drug Research on Common Chronic Diseases, Department of Pathophysiology, School of Basic Medical Sciences, Guizhou Medical University, Guiyang, Guizhou, China, [6]Guizhou Institute of Precision Medicine, Affiliated Hospital of Guizhou Medical University, Guiyang, China, [7]State Key Laboratory of Agrobiotechnology, College of Biological Sciences, China Agricultural University, Beijing, China

Primordial follicles are the starting point of follicular development and the basic functional unit of female reproduction. Primordial follicles are formed around birth, and most of the primordial follicles then enter a dormant state. Since primordial follicles are limited in number and can't be renewed, dormant primordial follicles cannot be reversed once they enter the growing state. Thus, the orderly occurrence of primordial follicles selective activation directly affects the rate of follicle consumption and thus determines the length of female reproductive lifespan. Studies have found that appropriately inhibiting the activation rate of primordial follicles can effectively slow down the rate of follicle consumption, maintain fertility and delay ovarian aging. Based on the known mechanisms of primordial follicle activation, primordial follicle *in vitro* activation (IVA) technique has been clinically developed. IVA can help patients with premature ovarian failure, middle-aged infertile women, or infertile women due to gynecological surgery treatment to solve infertility problems. The study of the mechanism of selective activation of primordial follicles can contribute to the development of more efficient and safe IVA techniques. In this paper, recent mechanisms of primordial follicle activation and its clinical application are reviewed.

KEYWORDS

ovary, follicle, primordial follicle activation, *In vitro* activation, premature ovarian failure

Introduction

Ovary is an important reproductive and endocrine organ for female mammal. The normal ovarian function provides a fundamental guarantee for the body's suitable reproductive life and stable endocrine environment. There are two types of follicles in the adult ovarian follicle pool, one is the growing follicle, and the other is large number of primordial follicles as ovarian reserve. The primordial follicle pool is not renewable, and the

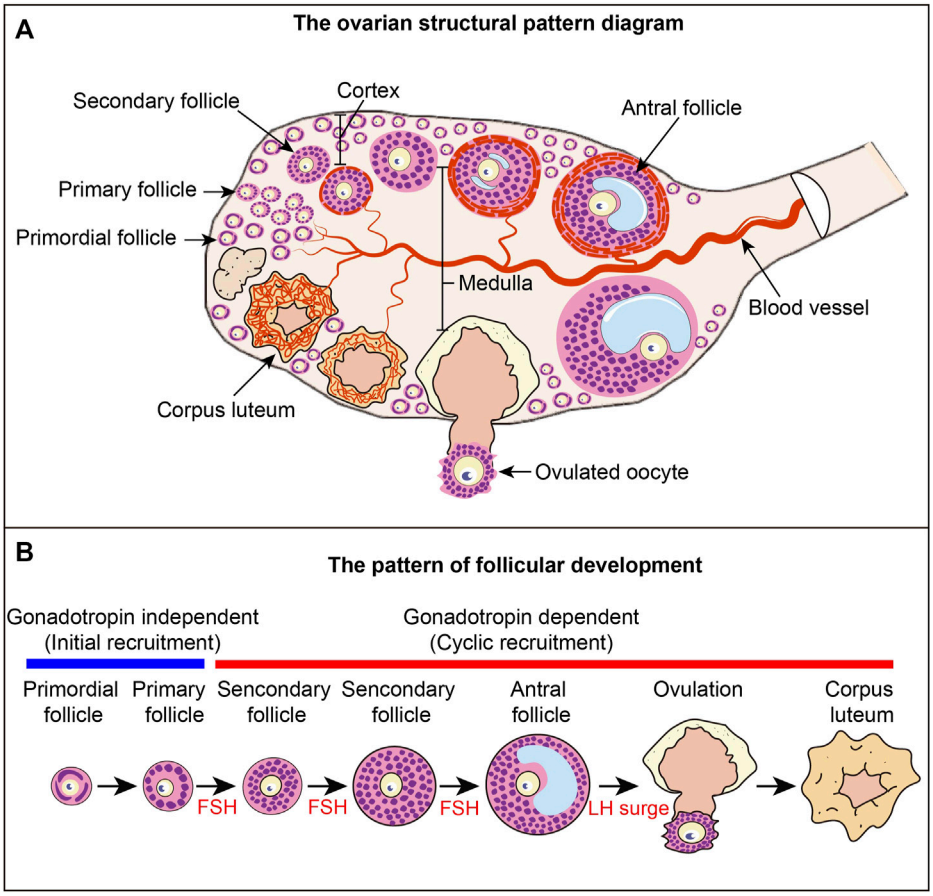

FIGURE 1
Ovarian structure and follicular development pattern diagram **(A)** Ovarian structural pattern diagram. Follicles at different developmental stages constitute the basic structural and functional unit of the ovary. Primordial follicles are mainly distributed in the cortex, and growing follicles are mainly distributed in the medulla. The blood vessels in the ovary provide nutrients to the ovarian tissue and follicles, and the blood vessels around each follicle are relatively independent. **(B)** Follicular development pattern. The development of primordial follicles into primary follicles is independent of gonadotropins, a process called primordial follicle activation, also known as initial recruitment. The process from primary follicle development to ovulation is a gonadotropin-dependent stage. The process of primary follicle development into preantral follicles is called cyclic recruitment and is the FSH response phase. Antral follicles ovulate under the stimulation of the LH surge. After ovulation, the granulosa cells luteinize to form the corpus luteum.

primordial follicle cannot be reversed once it enters the growing state (Zhang et al., 2015; Zhang and Liu, 2015; Kallen et al., 2018). Therefore, the orderly primordial follicle activation plays a decisive role in maintaining the length of female reproductive life (Reddy et al., 2010; Zhao et al., 2021). There are different stages during follicles development included primordial follicle, primary follicle, secondary follicle, antral follicle and preovulatory follicles in the ovary, but most of the follicles are primordial follicles, and these primordial follicles are in a dormant and static state (Pedersen, 1970; Hsueh et al., 2015; Zhang et al., 2015; Monget et al., 2021) (Figure 1). Primordial follicles consist of a single central oocyte surrounded by multiple pre-granulosa cells. Interestingly, the oocytes are arrest in the first meiosis stage and their growth is relatively static, the cell cycle of the pre-granulosa cells is inhibited (Jaffe and Egbert, 2017; Granados-Aparici et al., 2019). This state can be maintained as long as a year in mice, and up to 50 years in humans. These dormant primordial follicles are recruited from the primordial follicle pool and enter the growth follicle stage. This process is named the initial recruitment, also called primordial follicle activation (Lintern-Moore and Moore, 1979). Primordial follicle initial recruitment is different from cyclic recruitment (Kallen et al., 2018). It is generally believed that cyclic recruitment is regulated by gonadotropins, while initial recruitment is not regulated by gonadotropins (McGee and Hsueh, 2000; Bian et al., 2021). Primordial follicle initial recruitment is mainly regulated by the signals in the pre-granulosa cells and oocyte, as well as by conditions such as growth factors and stress in the primordial follicle microenvironment (Bian et al., 2021). After the primordial follicle is activated, the pre-granulosa cells gradually change from flat to wedge-shaped, then cuboidal, and later called granulosa cells. Meanwhile, oocyte diameter increased (Kallen et al., 2018) (Figure 2). When the primordial follicle is activated to enter the growth follicle stage, it enters the irreversible growth and development process, so the activation of the primordial follicle is equivalent to a gate for follicular development (Hirshfield, 1991; Adhikari et al., 2009). In order to maintain a suitable length of reproductive life and the reproductive health of the body, primordial

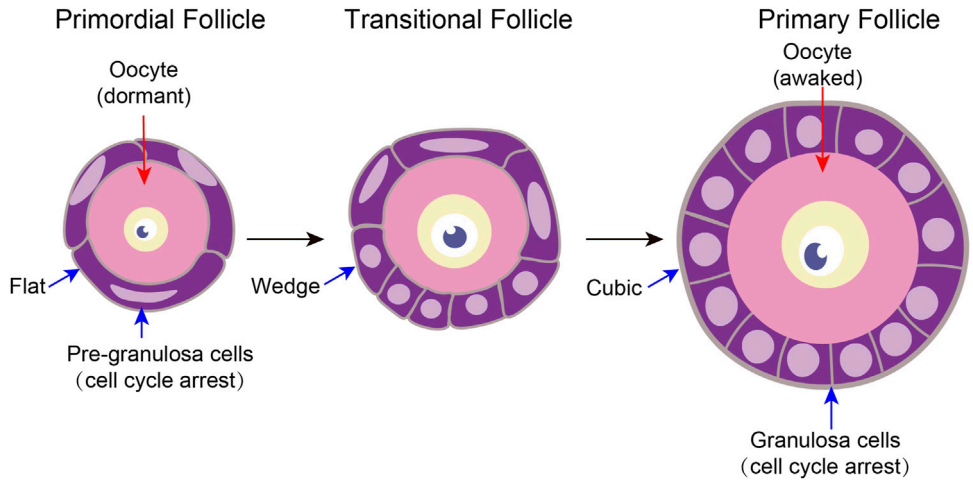

FIGURE 2
Characteristics of tissue structure changes in primordial follicle activation A follicle consists of a single oocyte in the middle and several somatic cells surrounding it. Primitive follicle activation mainly has two characteristics of structural changes. On the one hand, after primordial follicle activation, the pre-granulosa cells slowly changed from flat to wedge-shaped, and then to cubic-shaped. On the other hand, the oocyte diameter increased.

follicles in the ovaries need to be properly activated at the right time (Zhang and Liu, 2015; Chen et al., 2022). The understanding of the mechanisms of primordial follicle activation is still limited. To better grasp the progress of research on primordial follicle activation, we summarize the currently known key networks that regulate the activation of primordial follicles in this review.

Two waves of primordial follicles activation in mouse

Primordial follicles are formed around birth. The primordial follicles in the ovarian medulla are synchronously activated to become the first wave of activated follicles. The dormant primordial follicles in the cortical region of the ovary are gradually activated into a second wave of activated follicles (Hirshfield, 1991; Mork et al., 2012). Primordial follicles are mainly stored in the cortical area, and growing follicles are mainly stored in the medullary area. The developmental dynamics, functions and mechanisms of the two waves of follicles are different (Zheng et al., 2014; Dai et al., 2022). The activation of the first wave primordial follicles in the medulla is regulated by oocytes and has been determined during the formation of primordial follicles in the embryonic stage (Dai et al., 2022). However, the activation of the second wave primordial follicles in the medulla of the adult ovary may be regulated by pre-granulosa cells (Zhang et al., 2014). The first wave of primordial follicle development later contributes to the onset of puberty. The second wave of primordial follicles contributes to the entire reproductive process in adulthood (Zheng et al., 2014). The current understanding of the mechanism of the two waves of primordial follicle activation is limited, and this will be a fundamental scientific topic that needs attention in the development of primordial follicles.

The signal pathway in oocyte

PTEN-PI3K-AKT signaling

Primordial follicles are composed of only two types of cells: oocytes and pre-granulosa cells. The activation of primordial follicles requires the participation of these two types of cells (Zhang et al., 2015). In the process of primordial follicle activation, two signaling pathways, the phosphatidylinositol-3 kinase (PI3K) signaling pathway and the mechanistic target of rapamycin complex (mechanistic target of rapamycin complex 1, mTORC1) signaling pathway play a key role. PI3K signaling in oocytes is required for primordial follicles to maintain dormant state and follicular reserve (Adhikari and Liu, 2009; Adhikari and Liu, 2010; Zhang et al., 2014; Maidarti et al., 2020; Zhao et al., 2021). Phosphatase and tensin homolog (PTEN) negatively regulate intracellular levels of phosphatidylinositol-3,4,5-trisphosphate (PIP3) in cells and functions as a tumor suppressor by negatively regulating protein kinase B (PKB/AKT) signaling pathway (Worby and Dixon, 2014; Yehia et al., 2020). PTEN-PI3K-AKT is a relatively well-studied and clear signaling pathway during primordial follicle activation (Reddy et al., 2005; Liu et al., 2006). PTEN is mainly localized in dormant primordial follicle oocytes, deletion of *Pten* in primordial follicle oocytes will lead to excessive activation of the PI3K signaling pathway in oocytes, leading to premature activation of primordial follicles and ultimately premature ovarian failure (Reddy et al., 2008). Pyruvate dehydrogenase kinase 1 (PDK1) activates AKT through co-binding to PIP3 generated by PI3Ks (Gagliardi et al., 2018). Conditional knockout of *Pdk1* in primordial follicle oocytes results that the majority of primordial follicles are depleted around the onset of sexual maturity. PTEN-PDK1 signaling in oocytes that controls the survival, loss and activation of primordial follicles (Reddy et al., 2009).

TSC1/TSC2-mTOR signaling in oocyte

mTOR is essential for oogenesis, follicular development, maintenance of follicular reserve, and oocyte maturation (Liu et al., 2018; Correia et al., 2020). TSC complex subunit 1 (TSC1) and TSC complex subunit 2 (TSC2) negatively regulates mammalian target of rapamycin complex 1 (mTORC1) signaling. mTOR is a conserved kinase that mediate cellular responses to stresses such as nutrient deprivation, growth factors and DNA damage (Salussolia et al., 2019). Deletion of *Tsc1/2* in primordial follicle oocytes will lead to overactivation of the mTOR signaling pathway in oocytes, which will also lead to the premature activation of primordial follicles and eventually lead to premature ovarian failure (Adhikari et al., 2009). However, primordial follicles are normally activated in the absence of mTOR in primordial follicle oocytes, but subsequent follicle development is arrested, and granulosa cells transform into sertoli-like cells (Guo et al., 2018).

LHX8

LIM homeobox 8 (LHX8) is a member of the LIM homeobox family of proteins (Hobert and Westphal, 2000). In the ovary, LHX8 is specifically expressed in the oocyte nucleus and involved in oogenesis, oocytes differentiation, primordial follicle activation (Choi et al., 2008; Zhao et al., 2022). *Lhx8*-null mice had abnormally increased level of autophagy in oocytes and increased oocyte DNA damage, resulting in massive oocyte loss (Ren et al., 2015; D'Ignazio et al., 2018). Wang's study found that the oocyte-specific transcription factors LHX8, FIGLA and SOHLH1 form a transcriptional regulatory network to regulate oogenesis (Wang et al., 2020b). LHX8 directly regulates *Lin28a* transcription in primordial follicle oocytes to regulate postnatal folliculogenesis (Ren et al., 2015; D'Ignazio et al., 2018).

CDC42

Cell Division Cycle 42 (CDC42) is a small GTPase of the Rho-subfamily, which regulates signaling pathways that control diverse cellular functions including cell morphology, migration, endocytosis and cell cycle progression (Heinrich et al., 2021; Campbell et al., 2022; Wirth et al., 2022). The subcellular localization of CDC42 during primordial follicle activation is interesting. In dormant primordial follicles, CDC42 is specifically expressed in the oocyte cytoplasm. When primordial follicles are activated, the expression of CDC42 on the oocyte membrane is greatly enhanced, the expression of the GTP-active form of CDC42 is enhanced on the oocyte membrane. CDC42 binds to P110-β protein, regulates the activation of PI3K signaling pathway in oocytes, and promotes primordial follicle activation (Yan et al., 2018). In Yan's study, it was found that the expressions of CDC42 and PTEN in primordial follicle oocytes are mutually exclusive, but the specific regulatory relationship between CDC42 and PTEN is not clear, which needs to be explored in future research.

E-cadherin

Cell adhesion is essential for tissue structure and function. The cadherin family members play a key role in cell-cell recognition and adhesion and interact with intracytoplasmic proteins through adaptor proteins (Collins et al., 2017). E-cadherin, a classical cadherin of the cadherin superfamily, is a calcium-dependent cell adhesion molecule that is involved in the establishment and maintenance of epithelial cell morphology during embryogenesis and adulthood (Zaidel-Bar, 2013). E-cadherin is specifically localized to the cytomembrane of oocytes in primordial follicle. E-cadherin in primordial follicle oocytes plays an indispensable role in the maintenance of the primordial follicle pool by facilitating follicular structural stability and regulating NOBOX expression (Yan et al., 2019). The study also demonstrates that oocyte-derived factors are necessary for the maintenance of follicles.

The signal pathway in pre-granulosa cells

TSC1/TSC2-mTOR signaling in pre-granulosa cells

Interestingly, primordial follicles failed to be activated after deletion of *Rptor*, a key member of the mTORC1 complex in pre-granulosa cells, and primordial follicles were hyperactivated after deletion of TSC1/2 (Zhang et al., 2014). Studies using multiple transgenic mouse models reveal that pre-granulosa cells initiate and govern the activation of the second wave of primordial follicles (Zhang et al., 2014; Zhang et al., 2015). Under the stimulation of surrounding factors such as hypoxia, nutritional factors, stress and other factors, mTOR in pre-granulosa cells is upregulated, pre-granulosa cells grow and differentiate into granulosa cells, and they secrete more KIT ligands at the same time (Zhang et al., 2014). KIT ligands bind to KIT receptors on the oocyte membrane and activate the PI3K signaling pathway in the oocyte (Kissel et al., 2000; Nilsson and Skinner, 2004; Hutt et al., 2006; Zhang et al., 2014; Saatcioglu et al., 2016). This enables downstream FOXO3A to be phosphorylated, and FOXO3a is transported out of the nucleus to relieve the inhibition of oocyte growth, thereby enabling primordial follicle activation (Castrillon et al., 2003; Zhang et al., 2014; Ezzati et al., 2015). Other studies have also found that CREB, MAPK, HDAC6, NGF and other molecules can regulate the activation of primordial follicles through the mTOR signaling pathway (He et al., 2017; Zhao et al., 2018; Li et al., 2020; Zhang et al., 2021b; Zhang et al., 2022). These studies further illustrate the important role of the mTOR signaling pathway in the activation of primordial follicles.

FOXL2

Foxl2 forkhead box L2 (FOXL2), a forkhead transcription factor, contains a fork-head DNA-binding domain and it may play a role in ovarian development and function (Benayoun et al., 2011; Georges et al., 2013). Expansion of a polyalanine repeat region and other mutations in FOXL2 are a cause of blepharophimosis syndrome, premature ovarian failure and granulosa cell tumour (De Baere et al., 2002; Nallathambi et al., 2007; Pierini et al., 2020). The formation of primordial follicles in *Foxl2* knockout mice was not affected, but the pre-granulosa cells failed to differentiate and remained flat, resulting

in no growing follicles in the ovary and female mice were sterile (Schmidt et al., 2004). This study also demonstrates that the developmental status of pre-granulosa cells is critical for the activation of primordial follicles and the development of subsequent growing follicles.

SMAD3

SMAD family member 3 (SMAD3) is known to serve as a signaling intermediate for the transforming growth factor beta TGF family (Kawabata et al., 1998) *Smad3* knockout mice are viable. Notably, primordial follicle formation was not affected in *Smad3* knockout mice but delayed the activation of primordial follicles and development of growing follicles, resulted in reduced fertility (Tomic et al., 2002). The transcription factor Smad3 is expressed in the nucleus of pre-granulosa cells. SMAD3 directly regulates the transcription of CCND2 and inhibits the expression of Myc. CCND2 is bound by p27, thereby arresting the cycle of precursor granulosa cells and maintaining the dormant state of primordial follicles. When the level of TGF-β increases, SMAD3 is transported out of the nucleus, p27 dissociates from CCND2 to relieve the inhibition of the pre-granulosa cell cycle and promote the activation of primordial follicles (Granados-Aparici et al., 2019). From the current research, p27 and SMAD3 play key roles in follicle development and oogenesis, and they may regulate primordial follicle activation mainly by affecting the pre-granulosa cell cycle (Rajareddy et al., 2007). However, *p27* and *Smad3* knockout mice were used in the current study, but the precise roles and mechanisms of p27 and SMAD3 in primordial follicle activation cannot be fully elucidated, so further research is needed.

AMH

Anti-mullerian hormone (AMH) is a secreted ligand of the TGF-β superfamily (Pepinsky et al., 1988; Howard et al., 2022). AMH is exclusively produced by granulosa cells of ovarian follicles during the early stages of follicle development (Moolhuijsen and Visser, 2020). AMH plasma levels reflect the continuous non-cyclic growth of small follicles, thereby mirroring the size of the resting primordial follicle pool and thus acting as a useful marker of ovarian reserve (Dewailly et al., 2014). AMH is the best measure of ovarian reserve in different clinical conditions at present. (Teede et al., 2019; Shrikhande et al., 2020; Vatansever et al., 2020). AMH supplementation is able to maintain follicular reserve in some ovarian injury models, such as chemotherapy-induced premature ovarian failure, polycystic ovary syndrome (PCOS) (Sonigo et al., 2019; Hoyos et al., 2020; Ou et al., 2021; Rudnicka et al., 2021).

ESR2

Estrogen and its receptors play an integral role in the periodic recruitment of growing follicles, and estrogen receptor knockout mice lead to infertility in female mice due to abnormal meiosis (Shoham and Schachter, 1996; Liu et al., 2017; Tang et al., 2019). A recent study found that disruption of estrogen receptor β (ESR2) signaling results in increased protein level of AKT and mTOR in both granulosa and oocyte factors and leading to increased activation of primordial follicles (Chakravarthi et al., 2020). This study suggests that estrogen receptors may have no effect on the activation of the first wave of primordial follicles but may regulate the activation of the second wave of primordial follicles. It is also possible that the deletion of the estrogen receptor leads to the development of growth follicles, and the changes in the ovarian microenvironment lead to abnormal activation and loss of primordial follicles.

Wnt ligand secretion mediator

Wingless-type MMTV integration site family (WNT) signaling is an evolutionarily conserved system for cell-cell communication (Liu et al., 2022; Rim et al., 2022). WNT is classified broadly into canonical β-catenin dependent, and non-canonical β-catenin-independent pathways (Clevers and Nusse, 2012; Nusse and Clevers, 2017). The WNT signaling pathway is indispensable for primordial germ cell development, oogenesis, follicle development, and maintenance of follicular reserve (Kocer et al., 2008; Zhou et al., 2012; De Cian et al., 2020; Habara et al., 2021). Among the 19 WNT ligands, the mRNAs for *Wnt4*, *Wnt6* and *Wnt11* were experssed in the pre-granulosa cells during primordial follicle activation. *Wnt2*, *Wnt2b*, *Wnt9a*, *Wnt5b*, *Wnt11* and *Wnt16* was expressed in the oocytes of primordial follicles (Habara et al., 2021). After conditional knockdown of the wntless in pre-granulosa cells, the pre-granulosa cells could not grow and differentiate into cubic granulosa cells, which leads to female infertility (Habara et al., 2021). Wntless in pre-granulosa cells is essential for communication between pre-granulosa cells and oocytes and primordial follicle activation.

Other important molecules and relative signaling pathways

HIPPO

The HIPPO pathway was first discovered in *Drosophila melanogaster*, the pathway name comes from the fact that *Drosophila* overgrew like a hippopotamus after mutations in key molecules of the HIPPO pathway in the head and eyes of *Drosophila*. The HIPPO pathway is highly conserved from *Drosophila* to mammals (Ma et al., 2019; Moya and Halder, 2019). The upstream membrane protein receptors of the Hippo signaling pathway act as receptors for extracellular growth inhibition signals, and once they sense the extracellular growth inhibition signals, they activate a series of kinase cascade phosphorylation reactions that eventually phosphorylate the downstream effectors Yes-associated protein (YAP) and transcriptional coactivator with PDZ-binding motif (TAZ). And cytoskeletal proteins bind to the phosphorylated YAP and TAZ, causing them to remain in the cytoplasm and reduce its cytosolic activity, thus achieving the regulation of regulation of organ size and volume (Huang et al., 2005; Yu et al., 2015; Ma et al., 2019). After ovarian fragmentation promotes actin polymerization, p-YAP levels decrease and promotes

nuclear transfer of YAP. Nuclear localization of YAP further promotes the expression of CCN growth factors and BIRC apoptosis inhibitors, which ultimately promotes follicular overgrowth (Li et al., 2010; Kawamura et al., 2013). The changes in the HIPPO pathway after ovarian fragmentation are a double-edged sword, on the one hand they can lead to follicular overgrowth and premature ovarian failure due to early follicular depletion. On the other hand, this property can be used to promote primordial follicle activation and develop primordial follicle *in vitro* activation techniques to help infertile patients to conceive children.

HDAC6

Histone deacetylase 6 (HDAC6) is a special histone deacetylase with two deacetylation domains and one ubiquitination domain. HDAC6 plays a center role in several processes, including positive regulation of peptidyl-serine phosphorylation, protein deacetylation, protein destabilization, microtubule stability (Olzmann et al., 2007; Wang et al., 2018; Wang et al., 2020a; Osseni et al., 2020; Wang et al., 2022). Our study showed that histone deacetylase HDAC6 was expressed heterogeneously in different primordial follicles. About 3%–4% of primordial follicles in neonatal and adult mouse ovaries had low HDAC6 expression, and 65% of primordial follicles with low HDAC6 expression will be activated. Further studies found that HDAC6 was transiently downregulated during primordial follicle activation, mediating selective activation of mouse primordial follicles by regulating the expression of mTOR (Zhang et al., 2021b). Interestingly, overexpression of *Hdac6* extends fecundity in female mice, longer telomeres and reduced DNA damage may reduce tumorigenesis in *Hdac6* overexpression mice (Zhang et al., 2017). Combined with these studies, we speculate that HDCA6 may regulate primordial follicles to selectively activate primordial follicles, prolong follicular cell telomere length and reduce DNA damage, and ultimately prolong female reproductive lifespan.

SIRT1

NAD-dependent protein deacetylase Sirtuin-1 (SIRT1) has been reported to be involved in the regulation of cellular senescence, aging and organism longevity through the acetylation and deacetylation of these substrates altering their transcriptional and enzymatic activities, as well as protein levels (Yao and Rahman, 2012; Lee et al., 2019; Chen et al., 2020). SIRT1 binds directly to the *Akt1* and *mTOR* promoters to promote their transcription, and increased levels of AKT and mTOR expression promote primordial follicle activation. We conducted a clinical translational potential study and found that short-term SIRT1 agonist treatment activates primordial follicles *in vitro* and these follicles develop normally, both in mice and humans. *In vitro* fertilization experiments in mice showed that the quality of oocytes obtained by this method was normal. These results suggest that SIRT1 may be a key protein regulating primordial follicle activation and has certain clinical value (Zhang et al., 2019). Interestingly, overexpression of *Sirt1* was able to delay ovarian aging, and this effect was the same as that of calorie restriction, Calorie restriction protects fertility in female mice by activating SIRT1 (Long et al., 2019; Zhang et al., 2019).

TGF-β1

TGFB1 transforming growth factor beta 1 (TGF-β1) is a secreted ligand of the TGF-β superfamily. TGF-β binds to various TGF-β receptors leading to recruitment and activation of SMAD family transcription factors that regulate gene expression. The members of TGF-β superfamily, including TGF-β, GDF9, BMP2, BMP4, BMP5, BMP6, BMP7, BMP15, activins and inhibin are expressed by ovarian somatic cells and oocytes in a developmental stage-related manner and function as intraovarian regulators of folliculogenesis (Lee et al., 2001; Hanrahan et al., 2004; Zhao et al., 2016; Vander Ark et al., 2018). Fetal mouse ovary at embryonic stage 18.5 were cultured with the addition of TGF-β ligand for 5–7 days *in vitro* (Wang W. et al., 2014). The results showed that the primordial follicle reserve was reduced and the primordial follicle activation was inhibited. The opposite result was obtained after incubation with SD208, an inhibitor of TGFβ-R1. Further testing found that TGF-β maintained primordial follicle inventory and primordial follicle dormancy by inhibiting the mTOR signaling pathway. In Wang's research, TGF-β only affects the mTOR signaling pathway, and has no effect on the PI3K signaling pathway (Wang Z.-P. et al., 2014). Zhang's research showed that mTOR signaling in precursor granulosa cells initiates and regulates primordial follicle activation, after the mTOR pathway in pre-granulosa cells is activated, PI3K key proteins in oocytes are phosphorylated (Zhang et al., 2014). Combined with the research analysis of Wang's and Zhang's, we speculate that long-term addition of TGF-β may maintain primordial follicle pool and primordial follicle activation by regulating the mTOR signaling pathway in oocytes. Interestingly, the 4-day-old mouse ovaries were cultured with TGF-β for 2 h, and the phosphorylation of S6 which is a key downstream of the mTOR pathway was significantly increased, p-AKT was not changed, and SMAD3 nuclear export in pre-granulosa cells was increased, thereby promoting primordial follicle activation (Granados-Aparici et al., 2019). In our study (data not shown), mTOR and PI3K signaling pathways are significantly inhibited after adding SD208 to cultured 2 dpp ovaries of mice for 2 days. TGF-β plays different roles in different stages of follicular development. Long-term upregulation of TGF-β and short-time upregulation of TGF-β may lead to different or even opposite results for primordial follicle development.

NGF

Neurotrophins are growth factors that promote neuronal and non-neuronal cell survival, proliferation and differentiation (Wang W. et al., 2014; Denk et al., 2017). Nerve growth factor (NGF) is a prototype glycoprotein that belongs to the neurotrophins family. NGF contains two classes of receptors: the high affinity receptor tyrosine kinase A (TrkA) and the low-affinity receptor p75 (Chao and Hempstead, 1995; di Mola et al., 2000). The expression of NGF and its receptors is developmentally regulated during

folliculogenesis in different mice ovary (Chaves et al., 2010). The number of primordial follicles was not changed, but the number of primary and secondary follicles was significantly reduced in *Ngf* knockout mice. In the absence of NGF, primordial follicles cannot be activated. It is worth noting that exogenous addition of NGF has no effect on the activation of primordial follicles (Kerr et al., 2009; Dorfman et al., 2014; Dorfman et al., 2014). After the ovaries are mechanically injured, the expression of NGF in the stroma cells near the injury site increases rapidly, NGF induces selective activation of primordial follicles near the injury site, including near the ovulation site through the mTOR signaling pathway (He et al., 2017). However, how the NGF in the stroma cells induces the activation of nearby primordial follicles, as well as the specific signal transduction and molecular mechanisms are still unclear. This is a scientific issue that needs attention in the future.

EGF

Epidermal growth factor (EGF) encodes a member of the epidermal growth factor superfamily, which acts by binding with high affinity to the cell surface receptor, epidermal growth factor receptor (Schneider and Wolf, 2009). In an *in vitro* ovarian culture model, addition of EGF promotes primordial follicle activation by activating the activity of the PI3K pathway in oocytes, and short-term treatment (30 min) can induce the activation of primordial follicles in humans and mice *in vitro*. EGF is a highly effective drug target for primordial follicle activation *in vitro* (Fujihara et al., 2014; Zhang et al., 2020). EGF is highly expressed in zebrafish ovary and testis, EGFRa is expressed in various organs, including the brain, and EGFRb is mainly expressed in the lung and ovary. It is worth noting that only deletion of EGFRa inhibited primordial follicle activation *in vivo*, whereas primordial follicle activation was not affected by deletion of EGF (Song et al., 2022). This suggests that other growth factors may promote primordial follicle activation through EGFR.

p27

Cyclin-dependent kinase inhibitor 1B (Cdkn1b), also known as p27 or p27Kip1, is a suppressor of cell cycle (Polyak et al., 1994; Chu et al., 2008; Razavipour et al., 2020). The expression of p27 in the ovary during primordial follicle formation and activation is interesting. During primordial follicle formation, p27 is only expressed in the nucleus of somatic cells and not in oocytes. After primordial follicle formation, p27 is expressed in both pre-granulosa cells and oocytes. The expression of p27 is decreased in granulosa cells during primordial follicle activation. In *p27* knockout mice, primordial follicles are formed in advance, and the formed primordial follicles are then activated in advance. In addition, a large number of follicles are atresia and eventually lead to premature ovarian failure. In many studies, it was found that PI3K can regulate the expression of p27, but it is interesting that p27 and PI3K are independent in the process of primordial follicle activation (Rajareddy et al., 2007). However, during chemotherapy, dormant primordial follicles are simultaneously overactivated in the ovary *via* the PI3K/FOXO3a/p27 pathway. Further studies found that in the model of premature ovarian failure induced by cisplatin injection, FOXO3a binds to the promoter of p27 to inhibit its transcription, resulting in excessive activation of primordial follicles. When melatonin and gastrin were injected at the same time, the binding activity of FOXO3a and p27 increased, which promoted the transcription of p27 and saved the over-activation of primitive follicles caused by cisplatin (Jang et al., 2017).

Clinical application of primordial follicle activation *in vitro*

Primordial follicles (about 1,000) remain in the ovaries of patients with premature ovarian failure, but these primordial follicles are dormant, and their development is not regulated by gonadotropins (Nelson, 2009; De Vos et al., 2010). To utilize the primordial follicle resources in the ovarian tissue of POF patients, the dormant primordial follicles in the ovary must first be activated to develop to a stage when they can respond to gonadotropins, and then use assisted reproductive technology to achieve pregnancy (Telfer and Anderson, 2021). Primordial follicle activation *in vitro* (IVA) was recently developed based on the mechanism of primordial follicle activation, which can help patients with premature ovarian failure to achieve fertility (Yin et al., 2016). In addition, IVA can also be used in middle-aged women who are infertile or infertile due to treatment, allowing them to use their own oocytes to carry on offspring (Bertoldo et al., 2018).

The HIPPO signaling pathway determines organ size and is conserved from *drosophila* to mammals (Seo and Kim, 2018; Ma et al., 2019; Wu and Guan, 2021). Following ovarian damage, disruption of the HIPPO pathway accelerates follicle development, including primordial and growing follicles, which results in increased mice ovarian size. Using the feature of HIPPO signaling pathway can promote primordial follicle activation, combined with agonists of the PI3K or mTOR signaling pathway. A method of primordial follicle activation *in vitro* was developed to help patients with premature ovarian failure successfully have healthy babies (Kawamura et al., 2013; Zhai et al., 2016; Fabregues et al., 2018; Grosbois and Demeestere, 2018; Lee and Chang, 2019; De Roo et al., 2020; Devenutto et al., 2020; Hsueh and Kawamura, 2020; Tanaka et al., 2020; Zhang et al., 2021a). At the same time, factors such as long *in vitro* processing time, poor *in vitro* activation efficiency of primordial follicles, and ethical issues have hindered the clinical application of this technology. Several studies are devoted to improving these adverse factors. The combined use of PI3K and mTOR agonists, resveratrol (SIRT1 agonists), and Rac/Cdc42 activator II (CDC42 agonists) can induce mice ovary primordial follicle activation *in vitro*, which greatly shortens the time of *in vitro* activation. These drugs may be a potential new *in vitro* activation target drugs (Sun et al., 2015; Yan et al., 2018; Zhang et al., 2019). Further research found that orthotopic injection of CDC42 agonist into the ovary can promote the activation of primordial follicles in premature ovarian failure mice and induce human ovary primordial follicle activation *in vitro*. This method by inducing activation directly *in vivo* avoids the unknown risks associated with *in vitro* exposure of ovarian tissue (Zhang et al., 2020). Primordial follicle activation *in vitro*, this new assisted reproductive technology, has been developed to provide new fertility hope for patients with premature ovarian failure.

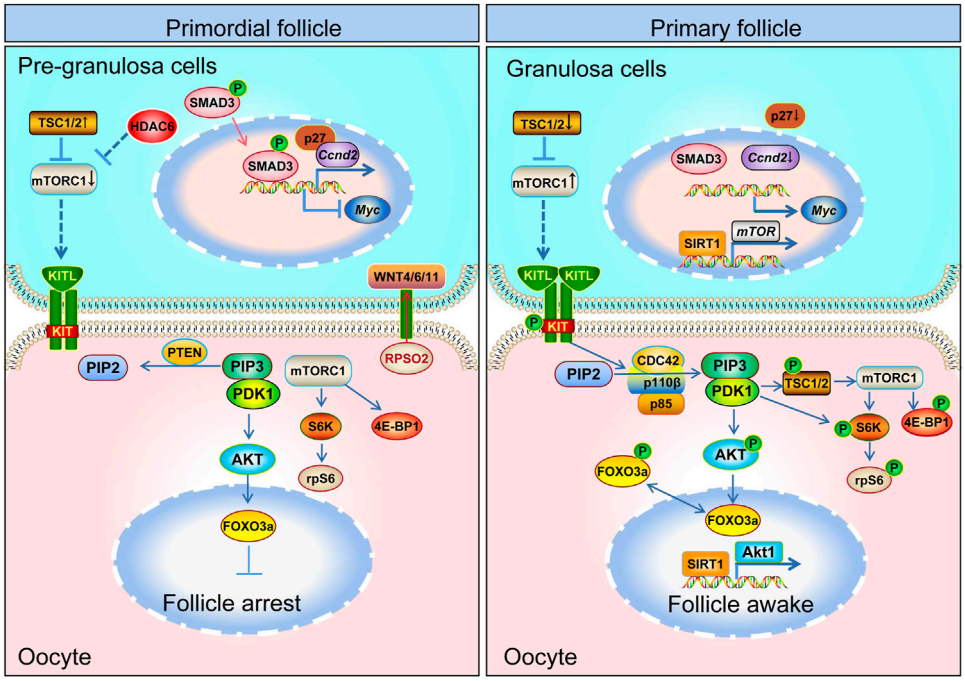

FIGURE 3
Schematic model depicting the mechanisms of primordial follicle activation. Primordial follicle activation is a result of the delicate interaction of pre-granulosa cells and oocytes and the follicular microenvironment. The mTOR and WNT pathways in pre-granulosa cells, the mTOR and PI3K pathway in oocytes, and the communication channel (KITL-KIT) between pre-granulosa cells and oocytes are all necessary for primordial follicle activation. The mTOR signaling pathway in pre-granulosa cells initiates and regulates primordial follicle activation in adult ovary. The mTOR signal in the pre-granulosa cells senses changes in surrounding nutrients, pressure, *etc.*, so that the pre-granulosa cells secrete more KITL. After KITL binds to the receptor on the oocyte membrane, it activates the PI3K signaling pathway in the oocyte, and then promotes the primordial follicle activation.

Conclusion

The rate of primordial follicle activation controls the length of female fertility. The activation of primordial follicles is mutually regulated by various signaling pathways between oocytes and granulosa cells, and is the result of a close interaction between molecules and between cells (Figure 3). The current study shows that the first wave of primordial follicle activation is determined by PI3K signaling in the oocyte and contributes to female puberty. The second wave primordial follicle activation is determined by mTOR signaling in pre-granulosa cells and determines female fertility throughout life. Understanding the mechanism of primordial follicle activation will help us to further analyze the truth of follicle development and promote the progress of *in vitro* activation technology.

Author contributions

MH, TZ, JZ, TY, and TC collected the information. MH and TZ wrote the manuscript. TZ, ZX, CW, and ZX revised the manuscript. All authors read and approved the final manuscript.

Funding

This study is funded by the National Natural Science Foundation of China (32100686 to TZ, 32100913 to MH and 82260291 to TZ), Guizhou Provincial Science and Technology Projects [ZK (2022)346 to MH], Science and Technology Fund Project of Guizhou Provincial Health Commission (gzwkj 2021-299 to TZ, gzwkj 2021-527 to MH), China postdoctoral science foundation (2021M700972 to MH and 2022M710919 to TZ), Doctoral Startup Foundation of Guizhou Medical University [(2020)038 to TZ (2020)039 to MH], the National Natural Science Foundation cultivation project of Guizhou Medical University (20NSP031 to TZ, 20NSP008 to MH), innovation and Entrepreneurship Training Program for College Students in Guizhou Province (S202210660136, S202210660093, 202210660090 202110660058), the Continuous Support Fund for Excellent Scientific Research Platform of Colleges and Universities in Guizhou Province [QJJ (2022) 020 to TC], Guizhou Provincial Natural Science Foundation [No (2021)4029 and (2022)4017].

Acknowledgments

We thank the members of TZ's laboratory for their constructive suggestions in the preparation of the manuscript.

Conflict of interest

The authors declare that the research was conducted in the absence of any commercial or financial relationships that could be construed as a potential conflict of interest.

Publisher's note

References

Adhikari, D., Flohr, G., Gorre, N., Shen, Y., Yang, H., Lundin, E., et al. (2009). Disruption of Tsc2 in oocytes leads to overactivation of the entire pool of primordial follicles. *Mol. Hum. Reprod.* 15, 765–770. doi:10.1093/molehr/gap092

Adhikari, D., and Liu, K. (2009). Molecular mechanisms underlying the activation of mammalian primordial follicles. *Endocr. Rev.* 30 (5), 438–464. doi:10.1210/er.2008-0048

Adhikari, D., and Liu, K. (2010). mTOR signaling in the control of activation of primordial follicles. *Cell cycleGeorget. Tex.)* 9 (9), 1673–1674. doi:10.4161/cc.9.9.11626

Benayoun, B. A., Georges, A. B., L'Hôte, D., Andersson, N., Dipietromaria, A., Todeschini, A. L., et al. (2011). Transcription factor FOXL2 protects granulosa cells from stress and delays cell cycle: Role of its regulation by the SIRT1 deacetylase. *Hum. Mol. Genet.* 20 (9), 1673–1686. doi:10.1093/hmg/ddr042

Bertoldo, M. J., Walters, K. A., Ledger, W. L., Gilchrist, R. B., Mermillod, P., and Locatelli, Y. (2018). *In-vitro* regulation of primordial follicle activation: Challenges for fertility preservation strategies. *Reprod. Biomed. online* 36 (5), 491–499. doi:10.1016/j.rbmo.2018.01.014

Bian, X., Xie, Q., Zhou, Y., Wu, H., Cui, J., Jia, L., et al. (2021). Transcriptional changes of mouse ovary during follicle initial or cyclic recruitment mediated by extra hormone treatment. *Life Sci.* 264, 118654. doi:10.1016/j.lfs.2020.118654

Campbell, B. F., Hercyk, B. S., Williams, A. R., San Miguel, E., Young, H. G., and Das, M. E. (2022). Cdc42 GTPase activating proteins Rga4 and Rga6 coordinate septum synthesis and membrane trafficking at the division plane during cytokinesis. *Traffic* 23, 478–495. doi:10.1111/tra.12864

Castrillon, D. H., Miao, L., Kollipara, R., Horner, J. W., and DePinho, R. A. (2003). Suppression of ovarian follicle activation in mice by the transcription factor Foxo3a. *Science* 301, 215–218. doi:10.1126/science.1086336

Chakravarthi, V. P., Ghosh, S., Roby, K. F., Wolfe, M. W., and Rumi, M. A. K. (2020). A gatekeeping role of ESR2 to maintain the primordial follicle reserve. *Endocrinology* 161, bqaa037. doi:10.1210/endocr/bqaa037

Chao, M. V., and Hempstead, B. L. (1995). p75 and Trk: a two-receptor system. *Trends Neurosci.* 18 (7), 321–326. doi:10.1016/0166-2236(95)93922-k

Chaves, R. N., Alves, A. M. C. V., Duarte, A. B. G., Araújo, V. R., Celestino, J. J. H., Matos, M. H. T., et al. (2010). Nerve growth factor promotes the survival of goat preantral follicles cultured *in vitro*. *Cells Tissues Organs* 192, 272–282. doi:10.1159/000317133

Chen, C., Zhou, M., Ge, Y., and Wang, X. (2020). SIRT1 and aging related signaling pathways. *Mech. Ageing Dev.* 187, 111215. doi:10.1016/j.mad.2020.111215

Chen, Y.-Y., Russo, D. D., Drake, R. S., Duncan, F. E., Shalek, A. K., Goods, B. A., et al. (2022). Single-cell transcriptomics of staged oocytes and somatic cells reveal novel regulators of follicle activation. *Reproduction* 164, 55–70. doi:10.1530/REP-22-0053

Choi, Y., Ballow, D. J., Xin, Y., and Rajkovic, A. (2008). Lim homeobox gene, lhx8, is essential for mouse oocyte differentiation and survival. *Biol. reproduction* 79 (3), 442–449. doi:10.1095/biolreprod.108.069393

Chu, I. M., Hengst, L., and Slingerland, J. M. (2008). The cdk inhibitor p27 in human cancer: Prognostic potential and relevance to anticancer therapy. *Nat. Rev. Cancer* 8 (4), 253–267. doi:10.1038/nrc2347

Clevers, H., and Nusse, R. (2012). Wnt/β-Catenin signaling and disease. *Cell* 149, 1192–1205. doi:10.1016/j.cell.2012.05.012

Collins, C., Denisin, A. K., Pruitt, B. L., and Nelson, W. J. (2017). Changes in E-cadherin rigidity sensing regulate cell adhesion. *Proc. Natl. Acad. Sci.* 114, e5835–e5844. doi:10.1073/pnas.1618676114

Correia, B., Sousa, M. I., and Ramalho-Santos, J. (2020). The mTOR pathway in reproduction: From gonadal function to developmental coordination. *Reproduction* 159, R173–R188. doi:10.1530/REP-19-0057

Dai, Y., Bo, Y., Wang, P., Xu, X., Singh, M., Jia, L., et al. (2022). Asynchronous embryonic germ cell development leads to a heterogeneity of postnatal ovarian follicle activation and may influence the timing of puberty onset in mice. *BMC Biol.* 20, 109. doi:10.1186/s12915-022-01318-y

De Baere, E., Lemercier, B., Christin-Maitre, S., Durval, D., Messiaen, L., Fellous, M., et al. (2002). FOXL2 mutation screening in a large panel of POF patients and XX males. *J. Med. Genet.* 39, e43. doi:10.1136/jmg.39.8.e43

De Cian, M. C., Gregoire, E. P., Le Rolle, M., Lachambre, S., Mondin, M., Bell, S., et al. (2020). R-spondin2 signaling is required for oocyte-driven intercellular communication and follicular growth. *Cell death Differ.* 27 (10), 2856–2871. doi:10.1038/s41418-020-0547-7

De Roo, C., Lierman, S., Tilleman, K., and De Sutter, P. (2020). *In-vitro* fragmentation of ovarian tissue activates primordial follicles through the Hippo pathway. *Hum. Reprod. Open* 2020 (4), hoaa048. doi:10.1093/hropen/hoaa048

De Vos, M., Devroey, P., and Fauser, B. C. (2010). Primary ovarian insufficiency. *Lancet (London, Engl.* 376 (9744), 911–921. doi:10.1016/S0140-6736(10)60355-8

Denk, F., Bennett, D. L., and McMahon, S. B. (2017). Nerve growth factor and pain mechanisms. *Annu. Rev. Neurosci.* 40, 307–325. doi:10.1146/annurev-neuro-072116-031121

Devenutto, L., Quintana, R., and Quintana, T. (2020). *In vitro* activation of ovarian cortex and autologous transplantation: A novel approach to primary ovarian insufficiency and diminished ovarian reserve. *Hum. Reprod. Open* 2020 (4), hoaa046. doi:10.1093/hropen/hoaa046

Dewailly, D., Andersen, C. Y., Balen, A., Broekmans, F., Dilaver, N., Fanchin, R., et al. (2014). The physiology and clinical utility of anti-Mullerian hormone in women. *Hum. Reprod. update* 20 (3), 370–385. doi:10.1093/humupd/dmt062

di Mola, F. F., Friess, H., Zhu, Z. W., Koliopanos, A., Bley, T., Di Sebastiano, P., et al. (2000). Nerve growth factor and Trk high affinity receptor (TrkA) gene expression in inflammatory bowel disease. *Gut* 46 (5), 670–679. doi:10.1136/gut.46.5.670

D'Ignazio, L., Michel, M., Beyer, M., Thompson, K., Forabosco, A., Schlessinger, D., et al. (2018). Lhx8 ablation leads to massive autophagy of mouse oocytes associated with DNA damage. *Biol. Reproduction* 98, 532–542. doi:10.1093/biolre/iox184

Dorfman, M. D., Garcia-Rudaz, C., Alderman, Z., Kerr, B., Lomniczi, A., Dissen, G. A., et al. (2014). Loss of ntrk2/kiss1r signaling in oocytes causes premature ovarian failure. *Endocrinology* 155, 3098–3111. doi:10.1210/en.2014-1111

Ezzati, M. M., Baker, M. D., Saatcioglu, H. D., Aloisio, G. M., Pena, C. G., Nakada, Y., et al. (2015). Regulation of FOXO3 subcellular localization by Kit ligand in the neonatal mouse ovary. *J. Assisted Reproduction Genet.* 32, 1741–1747. doi:10.1007/s10815-015-0589-9

Fabregues, F., Ferreri, J., Calafell, J. M., Moreno, V., Borrás, A., Manau, D., et al. (2018). Pregnancy after drug-free *in vitro* activation of follicles and fresh tissue autotransplantation in primary ovarian insufficiency patient: A case report and literature review. *J. Ovarian Res.* 11, 76. doi:10.1186/s13048-018-0447-3

Fujihara, M., Comizzoli, P., Keefer, C. L., Wildt, D. E., and Songsasen, N. (2014). Epidermal Growth Factor (EGF) Sustains *in vitro* primordial follicle viability by enhancing stromal cell proliferation via MAPK and PI3K Pathways in the prepubertal, but not adult, cat ovary. *Biol. Reproduction* 90 (4), 86. doi:10.1095/biolreprod.113.115089

Gagliardi, P. A., Puliafito, A., and Primo, L. (2018). PDK1: At the crossroad of cancer signaling pathways. *Seminars cancer Biol.* 48, 27–35. doi:10.1016/j.semcancer.2017.04.014

Georges, A., Auguste, A., Bessière, L., Vanet, A., Todeschini, A. L., and Veitia, R. A. (2013). FOXL2: A central transcription factor of the ovary. *J. Mol. Endocrinol.* 52 (1), R17–R33. doi:10.1530/JME-13-0159

Granados-Aparici, S., Hardy, K., Franks, S., Sharum, I. B., Waite, S. L., and Fenwick, M. A. (2019). SMAD3 directly regulates cell cycle genes to maintain arrest in granulosa cells of mouse primordial follicles. *Sci. Rep.* 9, 6513. doi:10.1038/s41598-019-42878-4

Grosbois, J., and Demeestere, I. (2018). Dynamics of PI3K and Hippo signaling pathways during *in vitro* human follicle activation. *Hum. Reprod.* 33, 1705–1714. doi:10.1093/humrep/dey250

Guo, J., Zhang, T., Guo, Y., Sun, T., Li, H., Zhang, X., et al. (2018). Oocyte stage-specific effects of MTOR determine granulosa cell fate and oocyte quality in mice. *Proc. Natl. Acad. Sci.* 115, e5326–e5333. doi:10.1073/pnas.1800352115

Habara, O., Logan, C. Y., Kanai-Azuma, M., Nusse, R., and Takase, H. M. (2021). WNT signaling in pre-granulosa cells is required for ovarian folliculogenesis and female fertility. *Development* 148 (9), dev198846. doi:10.1242/dev.198846

Hanrahan, J. P., Gregan, S. M., Mulsant, P., Mullen, M., Davis, G. H., Powell, R., et al. (2004). Mutations in the genes for oocyte-derived growth factors GDF9 and BMP15 are associated with both increased ovulation rate and sterility in cambridge and belclare sheep (*Ovis aries*). *Biol. Reproduction* 70, 900–909. doi:10.1095/biolreprod.103.023093

He, Y., Peng, X., Wu, T., Yang, W., Liu, W., Zhang, J., et al. (2017). Restricting the induction of NGF in ovarian stroma engenders selective follicular activation through the mTOR signaling pathway. *Cell Death Dis.* 8, e2817. doi:10.1038/cddis.2017.168

Heinrich, A., Bhandary, B., Potter, S. J., Ratner, N., and DeFalco, T. (2021). Cdc42 activity in Sertoli cells is essential for maintenance of spermatogenesis. *Cell Rep.* 37, 109885. doi:10.1016/j.celrep.2021.109885

Hirshfield, A. N. (1991). Development of follicles in the mammalian ovary. *Int. Rev. Cytol.* 124, 43–101. doi:10.1016/s0074-7696(08)61524-7

Hobert, O., and Westphal, H. (2000). Functions of LIM-homeobox genes. *Trends Genet. TIG* 16 (2), 75–83. doi:10.1016/s0168-9525(99)01883-1

Howard, J. A., Hart, K. N., and Thompson, T. B. (2022). Molecular mechanisms of AMH signaling. *Front. Endocrinol.* 13, 927824. doi:10.3389/fendo.2022.927824

Hoyos, L. R., Visser, J. A., McLuskey, A., Chazenbalk, G. D., Grogan, T. R., and Dumesic, D. A. (2020). Loss of anti-Müllerian hormone (AMH) immunoactivity due to a homozygous AMH gene variant rs10417628 in a woman with classical polycystic ovary syndrome (PCOS). *Hum. Reprod.* 35, 2294–2302. doi:10.1093/humrep/deaa199

Hsueh, A. J., Kawamura, K., Cheng, Y., and Fauser, B. C. (2015). Intraovarian control of early folliculogenesis. *Endocr. Rev.* 36 (1), 1–24. doi:10.1210/er.2014-1020

Hsueh, A. J. W., and Kawamura, K. (2020). Hippo signaling disruption and ovarian follicle activation in infertile patients. *Fertil. Steril.* 114, 458–464. doi:10.1016/j.fertnstert.2020.07.031

Huang, J., Wu, S., Barrera, J., Matthews, K., and Pan, D. (2005). The Hippo signaling pathway coordinately regulates cell proliferation and apoptosis by inactivating Yorkie, the Drosophila Homolog of YAP. *Cell* 122 (3), 421–434. doi:10.1016/j.cell.2005.06.007

Hutt, K. J., McLaughlin, E. A., and Holland, M. K. (2006). KIT/KIT ligand in mammalian oogenesis and folliculogenesis: Roles in rabbit and murine ovarian follicle activation and oocyte growth. *Biol. reproduction* 75 (3), 421–433. doi:10.1095/biolreprod.106.051516

Jaffe, L. A., and Egbert, J. R. (2017). Regulation of mammalian oocyte meiosis by intercellular communication within the ovarian follicle. *Annu. Rev. physiology* 79, 237–260. doi:10.1146/annurev-physiol-022516-034102

Jang, H., Na, Y., Hong, K., Lee, S., Moon, S., Cho, M., et al. (2017). Synergistic effect of melatonin and ghrelin in preventing cisplatin-induced ovarian damage via regulation of FOXO3a phosphorylation and binding to the p27Kip1 promoter in primordial follicles. *J. Pineal Res.* 63, e12432. doi:10.1111/jpi.12432

Kallen, A., Polotsky, A. J., and Johnson, J. (2018). Untapped reserves: Controlling primordial follicle growth activation. *Trends Mol. Med.* 24, 319–331. doi:10.1016/j.molmed.2018.01.008

Kawabata, M., Inoue, H., Hanyu, A., Imamura, T., and Miyazono, K. (1998). Smad proteins exist as monomers *in vivo* and undergo homo- and hetero-oligomerization upon activation by serine/threonine kinase receptors. *EMBO J.* 17 (14), 4056–4065. doi:10.1093/emboj/17.14.4056

Kawamura, K., Cheng, Y., Suzuki, N., Deguchi, M., Sato, Y., Takae, S., et al. (2013). Hippo signaling disruption and Akt stimulation of ovarian follicles for infertility treatment. *Proc. Natl. Acad. Sci.* 110, 17474–17479. doi:10.1073/pnas.1312830110

Kerr, B., Garcia-Rudaz, C., Dorfman, M., Paredes, A., and Ojeda, S. R. (2009). NTRK1 and NTRK2 receptors facilitate follicle assembly and early follicular development in the mouse ovary. *Reproduction* 138, 131–140. doi:10.1530/REP-08-0474

Kissel, H., Timokhina, I., Hardy, M. P., Rothschild, G., Tajima, Y., Soares, V., et al. (2000). Point mutation in kit receptor tyrosine kinase reveals essential roles for kit signaling in spermatogenesis and oogenesis without affecting other kit responses. *EMBO J.* 19 (6), 1312–1326. doi:10.1093/emboj/19.6.1312

Kocer, A., Pinheiro, I., Pannetier, M., Renault, L., Parma, P., Radi, O., et al. (2008). R-spondin1 and FOXL2 act into two distinct cellular types during goat ovarian differentiation. *BMC Dev. Biol.* 8, 36. doi:10.1186/1471-213X-8-36

Lee, H. N., and Chang, E. M. (2019). Primordial follicle activation as new treatment for primary ovarian insufficiency. *Clin. Exp. Reprod. Med.* 46, 43–49. doi:10.5653/cerm.2019.46.2.43

Lee, S.-H., Lee, J.-H., Lee, H.-Y., and Min, K.-J. (2019). Sirtuin signaling in cellular senescence and aging. *BMB Rep.* 52, 24–34. doi:10.5483/BMBRep.2019.52.1.290

Lee, W.-S., Otsuka, F., Moore, R. K., and Shimasaki, S. (2001). Effect of bone morphogenetic protein-7 on folliculogenesis and ovulation in the Rat. *Biol. Reproduction* 65, 994–999. doi:10.1095/biolreprod65.4.994

Li, J., Kawamura, K., Cheng, Y., Liu, S., Klein, C., Liu, S., et al. (2010). Activation of dormant ovarian follicles to generate mature eggs. *Proc. Natl. Acad. Sci. U. S. A.* 107 (22), 10280–10284. doi:10.1073/pnas.1001198107

Li, J., Zhang, Y., Zheng, N., Li, B., Yang, J., Zhang, C., et al. (2020). CREB activity is required for mTORC1 signaling-induced primordial follicle activation in mice. *Histochem. Cell Biol.* 154, 287–299. doi:10.1007/s00418-020-01888-4

Lintern-Moore, S., and Moore, G. P. (1979). The initiation of follicle and oocyte growth in the mouse ovary. *Biol. Reprod.* 20 (4), 773–778. doi:10.1095/biolreprod20.4.773

Liu, J., Wu, D.-C., Qu, L.-H., Liao, H.-Q., and Li, M.-X. (2018). The role of mTOR in ovarian Neoplasms, polycystic ovary syndrome, and ovarian aging. *Clin. Anat.* 31, 891–898. doi:10.1002/ca.23211

Liu, J., Xiao, Q., Xiao, J., Niu, C., Li, Y., Zhang, X., et al. (2022). Wnt/β-catenin signalling: Function, biological mechanisms, and therapeutic opportunities. *Signal Transduct. Target. Ther.* 7 (1), 3. doi:10.1038/s41392-021-00762-6

Liu, K., Rajareddy, S., Liu, L., Jagarlamudi, K., Boman, K., Selstam, G., et al. (2006). Control of mammalian oocyte growth and early follicular development by the oocyte PI3 kinase pathway: New roles for an old timer. *Dev. Biol.* 299 (1), 1–11. doi:10.1016/j.ydbio.2006.07.038

Liu, W., Xin, Q., Wang, X., Wang, S., Wang, H., Zhang, W., et al. (2017). Estrogen receptors in granulosa cells govern meiotic resumption of pre-ovulatory oocytes in mammals. *Cell Death Dis.* 8, e2662. doi:10.1038/cddis.2017.82

Long, G.-Y., Yang, J.-Y., Xu, J.-J., Ni, Y.-H., Zhou, X.-L., Ma, J.-Y., et al. (2019). SIRT1 knock-in mice preserve ovarian reserve resembling caloric restriction. *Gene* 686, 194–202. doi:10.1016/j.gene.2018.10.040

Ma, S., Meng, Z., Chen, R., and Guan, K. L. (2019). The Hippo pathway: Biology and pathophysiology. *Annu. Rev. Biochem.* 88, 577–604. doi:10.1146/annurev-biochem-013118-111829

Maidarti, M., Anderson, R. A., and Telfer, E. E. (2020). Crosstalk between PTEN/PI3K/Akt signalling and DNA damage in the oocyte: Implications for primordial follicle activation, oocyte quality and ageing. *Cells* 9, 200. doi:10.3390/cells9010200

McGee, E. A., and Hsueh, A. J. (2000). Initial and cyclic recruitment of ovarian follicles. *Endocr. Rev.* 21 (2), 200–214. doi:10.1210/edrv.21.2.0394

Monget, P., McNatty, K., and Monniaux, D. (2021). The crazy ovary. *Genes* 12 (6), 928. doi:10.3390/genes12060928

Moolhuijsen, L. M. E., and Visser, J. A. (2020). Anti-müllerian hormone and ovarian reserve: Update on assessing ovarian function. *J. Clin. Endocrinol. metabolism* 105 (11), 3361–3373. doi:10.1210/clinem/dgaa513

Mork, L., Maatouk, D. M., McMahon, J. A., Guo, J. J., Zhang, P., McMahon, A. P., et al. (2012). Temporal differences in granulosa cell specification in the ovary reflect distinct follicle fates in mice. *Biol. reproduction* 86 (2), 37. doi:10.1095/biolreprod.111.095208

Moya, I. M., and Halder, G. (2019). Hippo-YAP/TAZ signalling in organ regeneration and regenerative medicine. *Nat. Rev. Mol. cell Biol.* 20 (4), 211–226. doi:10.1038/s41580-018-0086-y

Nallathambi, J., Moumné, L., De Baere, E., Beysen, D., Usha, K., Sundaresan, P., et al. (2007). A novel polyalanine expansion in FOXL2: The first evidence for a recessive form of the blepharophimosis syndrome (BPES) associated with ovarian dysfunction. *Hum. Genet.* 121, 107–112. doi:10.1007/s00439-006-0276-0

Nelson, L. M. (2009). Clinical practice. Primary ovarian insufficiency. *N. Engl. J. Med.* 360 (6), 606–614. doi:10.1056/NEJMcp0808697

Nilsson, E. E., and Skinner, M. K. (2004). Kit ligand and basic fibroblast growth factor interactions in the induction of ovarian primordial to primary follicle transition. *Mol. Cell. Endocrinol.* 214 (1-2), 19–25. doi:10.1016/j.mce.2003.12.001

Nusse, R., and Clevers, H. (2017). Wnt/β-Catenin signaling, disease, and emerging therapeutic modalities. *Cell* 169, 985–999. doi:10.1016/j.cell.2017.05.016

Olzmann, J. A., Li, L., Chudaev, M. V., Chen, J., Perez, F. A., Palmiter, R. D., et al. (2007). Parkin-mediated K63-linked polyubiquitination targets misfolded DJ-1 to aggresomes via binding to HDAC6. *J. Cell Biol.* 178, 1025–1038. doi:10.1083/jcb.200611128

Osseni, A., Ravel-Chapuis, A., Thomas, J.-L., Gache, V., Schaeffer, L., and Jasmin, B. J. (2020). HDAC6 regulates microtubule stability and clustering of AChRs at neuromuscular junctions. *J. Cell Biol.* 219 (8), e201901099. doi:10.1083/jcb.201901099

Ou, M., Xu, P., Lin, H., Ma, K., and Liu, M. (2021). AMH is a good predictor of metabolic risk in women with PCOS: A cross-sectional study. *Int. J. Endocrinol.* 2021, 9511772. doi:10.1155/2021/9511772

Pedersen, T. (1970). Determination of follicle growth rate in the ovary of the immature mouse. *J. reproduction Fertil.* 21 (1), 81–93. doi:10.1530/jrf.0.0210081

Pepinsky, R. B., Sinclair, L. K., Chow, E. P., Mattaliano, R. J., Manganaro, T. F., Donahoe, P. K., et al. (1988). Proteolytic processing of mullerian inhibiting substance produces a transforming growth factor-beta-like fragment. *J. Biol. Chem.* 263 (35), 18961–18964. doi:10.1016/s0021-9258(18)37375-7

Pierini, S., Tanyi, J. L., Simpkins, F., George, E., Uribe-Herranz, M., Drapkin, R., et al. (2020). Ovarian granulosa cell tumor characterization identifies FOXL2 as an immunotherapeutic target. *JCI insight* 5 (16), e136773. doi:10.1172/jci.insight.136773

Polyak, K., Kato, J. Y., Solomon, M. J., Sherr, C. J., Massague, J., Roberts, J. M., et al. (1994). p27Kip1, a cyclin-Cdk inhibitor, links transforming growth factor-beta and contact inhibition to cell cycle arrest. *Genes and Dev.* 8 (1), 9–22. doi:10.1101/gad.8.1.9

Rajareddy, S., Reddy, P., Du, C., Liu, L., Jagarlamudi, K., Tang, W., et al. (2007). p27kip1 (Cyclin-Dependent Kinase Inhibitor 1B) Controls ovarian development by suppressing follicle endowment and activation and promoting follicle atresia in mice. *Mol. Endocrinol.* 21, 2189–2202. doi:10.1210/me.2007-0172

Razavipour, S. F., Harikumar, K. B., and Slingerland, J. M. (2020). p27 as a transcriptional regulator: New roles in development and cancer. *Cancer Res.* 80 (17), 3451–3458. doi:10.1158/0008-5472.CAN-19-3663

Reddy, P., Adhikari, D., Zheng, W., Liang, S., Hämäläinen, T., Tohonen, V., et al. (2009). PDK1 signaling in oocytes controls reproductive aging and lifespan by manipulating the survival of primordial follicles. *Hum. Mol. Genet.* 18, 2813–2824. doi:10.1093/hmg/ddp217

Reddy, P., Liu, L., Adhikari, D., Jagarlamudi, K., Rajareddy, S., Shen, Y., et al. (2008). Oocyte-specific deletion of Pten causes premature activation of the primordial follicle pool. *Science* 319, 611–613. doi:10.1126/science.1152257

Reddy, P., Shen, L., Ren, C., Boman, K., Lundin, E., Ottander, U., et al. (2005). Activation of Akt (PKB) and suppression of FKHRL1 in mouse and rat oocytes by stem cell factor during follicular activation and development. *Dev. Biol.* 281 (2), 160–170. doi:10.1016/j.ydbio.2005.02.013

Reddy, P., Zheng, W., and Liu, K. (2010). Mechanisms maintaining the dormancy and survival of mammalian primordial follicles. *Trends Endocrinol. metabolism TEM* 21 (2), 96–103. doi:10.1016/j.tem.2009.10.001

Ren, Y., Suzuki, H., Jagarlamudi, K., Golnoski, K., McGuire, M., Lopes, R., et al. (2015). Lhx8 regulates primordial follicle activation and postnatal folliculogenesis. *BMC Biol.* 13, 39. doi:10.1186/s12915-015-0151-3

Rim, E. Y., Clevers, H., and Nusse, R. (2022). The Wnt pathway: From signaling mechanisms to synthetic modulators. *Annu. Rev. Biochem.* 91, 571–598. doi:10.1146/annurev-biochem-040320-103615

Rudnicka, E., Kunicki, M., Calik-Ksepka, A., Suchta, K., Duszewska, A., Smolarczyk, K., et al. (2021). Anti-müllerian hormone in pathogenesis, diagnostic and treatment of PCOS. *Int. J. Mol. Sci.* 22, 12507. doi:10.3390/ijms222212507

Saatcioglu, H. D., Cuevas, I., and Castrillon, D. H. (2016). Control of oocyte reawakening by kit. *PLoS Genet.* 12 (8), e1006215. doi:10.1371/journal.pgen.1006215

Salussolia, C. L., Klonowska, K., Kwiatkowski, D. J., and Sahin, M. (2019). Genetic etiologies, diagnosis, and treatment of tuberous sclerosis complex. *Annu. Rev. Genomics Hum. Genet.* 20, 217–240. doi:10.1146/annurev-genom-083118-015354

Schmidt, D., Ovitt, C. E., Anlag, K., Fehsenfeld, S., Gredsted, L., Treier, A.-C., et al. (2004). The murine winged-helix transcription factor Foxl2 is required for granulosa cell differentiation and ovary maintenance. *Development* 131, 933–942. doi:10.1242/dev.00969

Schneider, M. R., and Wolf, E. (2009). The epidermal growth factor receptor ligands at a glance. *J. Cell. physiology* 218 (3), 460–466. doi:10.1002/jcp.21635

Seo, J., and Kim, J. (2018). Regulation of Hippo signaling by actin remodeling. *BMB Repeports* 51, 151–156. doi:10.5483/bmbrep.2018.51.3.012

Shoham, Z., and Schachter, M. (1996). Estrogen biosynthesis-regulation, action, remote effects, and value of monitoring in ovarian stimulation cycles. *Fertil. Steril.* 65 (4), 687–701. doi:10.1016/s0015-0282(16)58197-7

Shrikhande, L., Shrikhande, B., and Shrikhande, A. (2020). AMH and its clinical implications. *J. Obstetrics Gynecol. India* 70, 337–341. doi:10.1007/s13224-020-01362-0

Song, Y., Chen, W., Zhu, B., and Ge, W. (2022). Disruption of epidermal growth factor receptor but not EGF blocks follicle activation in zebrafish ovary. *Front. Cell Dev. Biol.* 9, 750888, doi:10.3389/fcell.2021.750888

Sonigo, C., Beau, I., Grynberg, M., and Binart, N. (2019). AMH prevents primordial ovarian follicle loss and fertility alteration in cyclophosphamide-treated mice. *FASEB J.* 33, 1278–1287. doi:10.1096/fj.201801089R

Sun, X., Su, Y., He, Y., Zhang, J., Liu, W., Zhang, H., et al. (2015). New strategy for *in vitro* activation of primordial follicles with mTOR and PI3K stimulators. *Cell Cycle* 14, 721–731. doi:10.1080/15384101.2014.995496

Tanaka, Y., Hsueh, A. J., and Kawamura, K. (2020). Surgical approaches of drug-free *in vitro* activation and laparoscopic ovarian incision to treat patients with ovarian infertility. *Fertil. Steril.* 114, 1355–1357. doi:10.1016/j.fertnstert.2020.07.029

Tang, Z. R., Zhang, R., Lian, Z. X., Deng, S. L., and Yu, K. (2019). Estrogen-receptor expression and function in female reproductive disease. *Cells* 8 (10), 1123. doi:10.3390/cells8101123

Teede, H., Misso, M., Tassone, E. C., Dewailly, D., Ng, E. H., Azziz, R., et al. (2019). Anti-müllerian hormone in PCOS: A review informing international guidelines. *Trends Endocrinol. Metabolism* 30, 467–478. doi:10.1016/j.tem.2019.04.006

Telfer, E. E., and Andersen, C. Y. (2021). *In vitro* growth and maturation of primordial follicles and immature oocytes. *Fertil. Steril.* 115 (5), 1116–1125. doi:10.1016/j.fertnstert.2021.03.004

Tomic, D., Brodie, S. G., Deng, C., Hickey, R. J., Babus, J. K., Malkas, L. H., et al. (2002). Smad 3 may regulate follicular growth in the mouse ovary. *Biol. Reproduction* 66, 917–923. doi:10.1095/biolreprod66.4.917

Vander Ark, A., Cao, J., and Li, X. (2018). TGF-β receptors: In and beyond TGF-β signaling. *Cell. Signal.* 52, 112–120. doi:10.1016/j.cellsig.2018.09.002

Vatansever, D., İncir, S., Bildik, G., Taskiran, C., and Oktem, O. (2020). *In-vitro* AMH production of ovarian tissue samples in culture correlates with their primordial follicle pool. *Eur. J. Obstetrics Gynecol. Reproductive Biol.* 254, 138–140. doi:10.1016/j.ejogrb.2020.09.002

Wang, M., Zhou, C., Yu, L., Kong, D., Ma, W., Lv, B., et al. (2022). Upregulation of MDH1 acetylation by HDAC6 inhibition protects against oxidative stress-derived neuronal apoptosis following intracerebral hemorrhage. *Cell. Mol. Life Sci.* 79, 356. doi:10.1007/s00018-022-04341-y

Wang, R., Tan, J., Chen, T., Han, H., Tian, R., Tan, Y., et al. (2018). ATP13A2 facilitates HDAC6 recruitment to lysosome to promote autophagosome-lysosome fusion. *J. Cell Biol.* 218, 267–284. doi:10.1083/jcb.201804165

Wang, W., Chen, J., and Guo, X. (2014). The role of nerve growth factor and its receptors in tumorigenesis and cancer pain. *Biosci. trends* 8 (2), 68–74. doi:10.5582/bst.8.68

Wang, Y., Wang, K., and Fu, J. (2020a). HDAC6 mediates poly (I:C)-Induced TBK1 and Akt phosphorylation in macrophages. *Front. Immunol.* 11, 1776. doi:10.3389/fimmu.2020.01776

Wang, Z.-P., Mu, X.-Y., Guo, M., Wang, Y.-J., Teng, Z., Mao, G.-P., et al. (2014). Transforming growth factor-β signaling participates in the maintenance of the primordial follicle pool in the mouse ovary. *J. Biol. Chem.* 289, 8299–8311. doi:10.1074/jbc.M113.532952

Wang, Z., Liu, C.-Y., Zhao, Y., and Dean, J. (2020b). FIGLA, LHX8 and SOHLH1 transcription factor networks regulate mouse oocyte growth and differentiation. *Nucleic Acids Res.* 48, 3525–3541. doi:10.1093/nar/gkaa101

Wirth, A., Labus, J., Abdel Galil, D., Schill, Y., Schmidt, S., Bunke, T., et al. (2022). Palmitoylation of the small GTPase Cdc42 by DHHC5 modulates spine formation and gene transcription. *J. Biol. Chem.* 298, 102048. doi:10.1016/j.jbc.2022.102048

Worby, C. A., and Dixon, J. E. (2014). Pten. *Annu. Rev. Biochem.* 83, 641–669. doi:10.1146/annurev-biochem-082411-113907

Wu, Z., and Guan, K.-L. (2021). Hippo signaling in embryogenesis and development. *Trends Biochem. Sci.* 46, 51–63. doi:10.1016/j.tibs.2020.08.008

Yan, H., Wen, J., Zhang, T., Zheng, W., He, M., Huang, K., et al. (2019). Oocyte-derived E-cadherin acts as a multiple functional factor maintaining the primordial follicle pool in mice. *Cell Death Dis.* 10, 160. doi:10.1038/s41419-018-1208-3

Yan, H., Zhang, J., Wen, J., Wang, Y., Niu, W., Teng, Z., et al. (2018). CDC42 controls the activation of primordial follicles by regulating PI3K signaling in mouse oocytes. *BMC Biol.* 16, 73. doi:10.1186/s12915-018-0541-4

Yao, H., and Rahman, I. (2012). Perspectives on translational and therapeutic aspects of SIRT1 in inflammaging and senescence. *Biochem. Pharmacol.* 84, 1332–1339. doi:10.1016/j.bcp.2012.06.031

Yehia, L., Keel, E., and Eng, C. (2020). The clinical spectrum of PTEN mutations. *Annu. Rev. Med.* 71, 103–116. doi:10.1146/annurev-med-052218-125823

Yin, O., Cayton, K., and Segars, J. H. (2016). *In vitro* activation: A dip into the primordial follicle pool? *J. Clin. Endocrinol. metabolism* 101 (10), 3568–3570. doi:10.1210/jc.2016-2837

Yu, F. X., Zhao, B., and Guan, K. L. (2015). Hippo pathway in organ size control, tissue homeostasis, and cancer. *Cell* 163 (4), 811–828. doi:10.1016/j.cell.2015.10.044

Zaidel-Bar, R. (2013). Cadherin adhesome at a glance. *J. Cell Sci.* 126, 373–378. doi:10.1242/jcs.111559

Zhai, J., Yao, G., Dong, F., Bu, Z., Cheng, Y., Sato, Y., et al. (2016). *In vitro* activation of follicles and fresh tissue auto-transplantation in primary ovarian insufficiency patients. *J. Clin. Endocrinol. Metabolism* 101, 4405–4412. doi:10.1210/jc.2016-1589

Zhang, H., and Liu, K. (2015). Cellular and molecular regulation of the activation of mammalian primordial follicles: Somatic cells initiate follicle activation in adulthood. *Hum. Reprod. update* 21 (6), 779–786. doi:10.1093/humupd/dmv037

Zhang, H., Panula, S., Petropoulos, S., Edsgärd, D., Busayavalasa, K., Liu, L., et al. (2015). Adult human and mouse ovaries lack DDX4-expressing functional oogonial stem cells. *Nat. Med.* 21, 1116–1118. doi:10.1038/nm.3775

Zhang, H., Risal, S., Gorre, N., Busayavalasa, K., Li, X., Shen, Y., et al. (2014). Somatic cells initiate primordial follicle activation and govern the development of dormant oocytes in mice. *Curr. Biol.* 24, 2501–2508. doi:10.1016/j.cub.2014.09.023

Zhang, J., Yan, L., Wang, Y., Zhang, S., Xu, X., Dai, Y., et al. (2020). *In vivo* and *in vitro* activation of dormant primordial follicles by EGF treatment in mouse and human. *Clin. Transl. Med.* 10, e182. doi:10.1002/ctm2.182

Zhang, L., Zhang, J., Zhai, J., Liu, X., Deng, W., Wang, H., et al. (2021a). Autotransplantation of the ovarian cortex after *in-vitro* activation for infertility treatment: A shortened procedure. *Hum. Reprod.* 36, 2134–2147. doi:10.1093/humrep/deab143

Zhang, T., Du, X., Zhao, L., He, M., Lin, L., Guo, C., et al. (2019). SIRT1 facilitates primordial follicle recruitment independent of deacetylase activity through directly modulating Akt1 and mTOR transcription. *FASEB J.* 33, 14703–14716. doi:10.1096/fj.201900782R

Zhang, T., He, M., Zhao, L., Qin, S., Zhu, Z., Du, X., et al. (2021b). HDAC6 regulates primordial follicle activation through mTOR signaling pathway. *Cell Death Dis.* 12, 559. doi:10.1038/s41419-021-03842-1

Zhang, X., Yang, J., Wang, H., Guo, R., Yin, Y., Zhang, D., et al. (2017). Overexpression of Hdac6 extends reproductive lifespan in mice. *Protein and Cell* 8, 360–364. doi:10.1007/s13238-017-0375-9

Zhang, X., Zhang, W., Wang, Z., Zheng, N., Yuan, F., Li, B., et al. (2022). Enhanced glycolysis in granulosa cells promotes the activation of primordial follicles through mTOR signaling. *Cell Death Dis.* 13, 87. doi:10.1038/s41419-022-04541-1

Zhao, L., Du, X., Huang, K., Zhang, T., Teng, Z., Niu, W., et al. (2016). Rac1 modulates the formation of primordial follicles by facilitating STAT3-directed Jagged1, GDF9 and BMP15 transcription in mice. *Sci. Rep.* 6, 23972. doi:10.1038/srep23972

Zhao, L., Li, Q., Kuang, Y., Xu, P., Sun, X., Meng, Q., et al. (2022). Heterozygous loss-of-function variants in LHX8 cause female infertility characterized by oocyte maturation arrest. *Genet. Med. official J. Am. Coll. Med. Genet.* 24 (11), 2274–2284. doi:10.1016/j.gim.2022.07.027

Zhao, Y., Feng, H., Zhang, Y., Zhang, J. V., Wang, X., Liu, D., et al. (2021). Current understandings of core pathways for the activation of mammalian primordial follicles. *Cells* 10, 1491. doi:10.3390/cells10061491

Zhao, Y., Zhang, Y., Li, J., Zheng, N., Xu, X., Yang, J., et al. (2018). MAPK3/1 participates in the activation of primordial follicles through mTORC1-KITL signaling. *J. Cell. Physiology* 233, 226–237. doi:10.1002/jcp.25868

Zheng, W., Zhang, H., Gorre, N., Risal, S., Shen, Y., and Liu, K. (2014). Two classes of ovarian primordial follicles exhibit distinct developmental dynamics and physiological functions. *Hum. Mol. Genet.* 23, 920–928. doi:10.1093/hmg/ddt486

Zhou, L., Charkraborty, T., Yu, X., Wu, L., Liu, G., Mohapatra, S., et al. (2012). R-spondins are involved in the ovarian differentiation in a teleost, medaka (*Oryzias latipes*). *BMC Dev. Biol.* 12, 36. doi:10.1186/1471-213X-12-36

frontiers | Frontiers in Endocrinology

TYPE Original Research
PUBLISHED 24 April 2023
DOI 10.3389/fendo.2023.1153289

OPEN ACCESS

EDITED BY
Bin Liu,
Jinan University, China

REVIEWED BY
Vikas Kumar Roy,
Mizoram University, India
Adesola Oniyide,
Afe Babalola University, Nigeria

*CORRESPONDENCE
Mohd Zahoor ul haq Shah
scholarendocrinology@gmail.com
Showkeen Muzamil Bashir
showkeen@skuastkashmir.ac.in
Ebtesam A. Al-Suhaimi
ealsuhaimi@iau.edu.sa

SPECIALTY SECTION
This article was submitted to Reproduction, a section of the journal Frontiers in Endocrinology

RECEIVED 30 January 2023
ACCEPTED 07 April 2023
PUBLISHED 24 April 2023

CITATION
Shah MZuh, Shrivastva Vk, Mir MA, Sheikh WM, Ganie MA, Rather GA, Shafi M, Bashir SM, Ansari MA, Al-Jafary MA, Al-Qahtani MH, Homeida AM and Al-Suhaimi EA (2023) Effect of quercetin on steroidogenesis and folliculogenesis in ovary of mice with experimentally-induced polycystic ovarian syndrome. *Front. Endocrinol.* 14:1153289. doi: 10.3389/fendo.2023.1153289

Effect of quercetin on steroidogenesis and folliculogenesis in ovary of mice with experimentally-induced polycystic ovarian syndrome

Mohd Zahoor ul haq Shah[1*], Vinoy kumar Shrivastva[1], Manzoor Ahmad Mir[2], Wajid Mohammad Sheikh[3], Mohd Ashraf Ganie[4], Gulzar Ahmed Rather[5], Majid Shafi[6], Showkeen Muzamil Bashir[3*], Mohammad Azam Ansari[7], Meneerah A. Al-Jafary[8], Mohammad H. Al-Qahtani[9], Abdalelgadir Musa Homeida[10] and Ebtesam A. Al-Suhaimi[8*]

[1]Laboratory of Endocrinology, Department of Bioscience, Barkatullah University, Bhopal, Madhya Pradesh, India, [2]Department of Bioresources, University of Kashmir, Srinagar, India, [3]Biochemistry & Molecular Biology Lab, Division of Veterinary Biochemistry, Faculty of Veterinary Sciences and Animal Husbandry, Sher-e-Kashmir University of Agricultural Sciences and Technology, Srinagar, India, [4]Department of Endocrinology and Metabolism, Sher-i-Kashmir Institute of Medical Sciences, Srinagar, India, [5]Department of Biomedical Engineering, Sathyabama Institute of Science & Technology, Chennai, Tamil Nadu, India, [6]Division of Veterinary Pathology, Faculty of Veterinary Sciences and Animal Husbandry, Sher-e-Kashmir University of Agricultural Sciences and Technology, Srinagar, India, [7]Department of Epidemic Disease Research, Institute for Research & Medical Consultations (IRMC), Imam Abdulrahman Bin Faisal University, Dammam, Saudi Arabia, [8]Biology Department, College of Science and Institute for Research and Medical Consultations (IRMC), Imam Abdulrahman Bin Faisal University, Dammam, Saudi Arabia, [9]Department of Paediatrics, College of Medicine, Imam Abdulrahman Bin Faisal University, Dammam, Saudi Arabia, [10]Department of Environmental Health Research, Institute for Research & Medical Consultations (IRMC), Imam Abdulrahman Bin Faisal University, Dammam, Saudi Arabia

Introduction: Polycystic Ovary syndrome (PCOS) affects the health of many women around the world. Apart from fundamental metabolic problems connected to PCOS, focus of our study is on the role of quercetin on genes relevant to steroidogenesis and folliculogenesis.

Methods: Eighteen mature parkes strain mice (4-5 weeks old) weighing 18–21 g were randomly divided into three groups of six each as follows: Group I serves as the control and was given water and a regular chow diet *ad lib* for 66 days; group II was given oral gavage administration of letrozole (LETZ) (6 mg/kg bw) for 21 days to induce PCOS and was left untreated for 45 days; For three weeks, Group III received oral gavage dose of LETZ (6 mg/kg), after which it received Quercetin (QUER) (125 mg/kg bw orally daily) for 45 days.

Results: In our study we observed that mice with PCOS had irregular estrous cycle with increased LH/FSH ratio, decreased estrogen level and decline in expression of *Kitl*, *Bmp1*, *Cyp11a1*, *Cyp19a1*, *Ar*, *Ihr*, *Fshr* and *Esr1* in ovary. Moreover, we observed increase in the expression of *CYP17a1*, as well as increase in cholesterol, triglycerides, testosterone, vascular endothelial growth factor VEGF and insulin levels. All these changes were reversed after the administration of quercetin in PCOS mice.

Discussion: Quercetin treatment reversed the molecular, functional and morphological abnormalities brought on due to letrozole in pathological and physiological setting, particularly the issues of reproduction connected to PCOS. Quercetin doesn't act locally only but it acts systematically as it works on Pituitary (LH/FSH)- Ovary (gonad hormones) axis. the Side effects of Quercetin have to be targeted in future researches. Quercetin may act as a promising candidate for medical management of human PCOS.

KEYWORDS

PCOS (polycystic ovarian syndrome), steroidogenesis, folliculogenesis, quercetin, VEGF

1 Introduction

Polycystic Ovary syndrome (PCOS) affects the health of many women around the world. Patients with PCOS are typically females in their reproductive years that have one or more of the following conditions: (A) obesity; (B) an irregular estrus cycle (C) sub/infertility or (D) hirsutism. Ovarian dysfunction, cysts in ovaries, and hyperandrogenism are some of its diagnostic markers. Despite the lack of a clear aetiology, it appears an imbalance of hormones, particularly elevated testosterone level, as well as insulin resistance (IR), can be taken into account (1–3). Patients with PCOS who have infertility are frequently upset about their inability to get pregnant. The hypothalamic-pituitary-ovarian axis is hypothesized to be impacted by the environment and genetics in around three and a half of PCOS patients who have elevated androgen levels (4). One of the intraovarian steroidogenesis abnormalities that are hypothesized to lead to ovarian failure in PCOS is a decrease in activity of aromatase enzyme, causing an imbalance of hormones, hyperandrogenism, and excess androgens within the ovaries leading to polycystic ovaries could be anticipated from decreased activity of the enzyme aromatase, which determines production rate of production of estrogen from androgen (5, 6).

As was already mentioned, a significant factor in PCOS is hyperandrogenism (7). In ovarian follicle granulosa cells, aromatase (*Cyp19a1*) changes testosterone (Testo) into oestrogen. As a way to create a model of PCOS having similar features of women with PCOS, we administered letrozole (LETZ) to female mice. LETZ is a non-steroidal inhibitor of aromatase which results in accumulation of androgen by decreasing the activity of aromatase, thereby lowers production of estrogen (8, 9).

Today, a variety of techniques are employed to combat PCOS and promote ovulation. However, a number of serious side effects, such as arthritis and joint or muscular pain have been observed (10). Consequently, natural medicines having no or few side effect are becoming more and more popular. A flavonoid molecule called quercetin (QUER) has biological properties that include, controlling blood lipid levels, controlling blood sugar and scavenging oxygen free radicals. Its molecular formula is C15H10O7, and its chemical name is 4h-1-benzopyran-4-one, 2-(3,4-dihydroxy phenyl), 3,5,7-trihydroxy-flavone. According to recent research, quercetin can boost healthy ovarian follicle development, restore healthy anatomy of ovary, as well as enhance histology of uterus. It's effects are comparable to those of metformin (11). According to reports, QUER lowers level of LH, and testo in PCOS patients (12). According to the most recent studies, quercetin can impact ovarian development and possesses estrogen-like effects (13) Researchers also discovered that quercetin can reduce insulin resistance, treat hyperinsulinemia, lower blood sugar levels, and block the expression of androgens (14). It has been observed that Oral QUER supplementation was effective in improving the adiponectin-mediated insulin resistance and hormonal profile of women with PCOS. It has been noted that taking oral QUER supplements helped women with PCOS with their adiponectin-mediated insulin resistance and hormonal profile (15). It has been demonstrated that quercetin lowers ovarian Bax and raises Bcl-2 protein abundance in PCOS rodents. Our findings suggest that QUER may increase oestrogen concentration, ovarian aromatase protein content, folliculogenesis, and decrease atresia by attenuating hyperandrogenism in PCOS rats. Q is as effective as metformin in reducing hyperandrogenism by lowering free Testosterone level and improving hypothalamic-pituitary-ovarian axis function. (16)

However, despite the fact that some researches have looked at the connection between QUER and PCOS, however they solely looked into impact of QUER on common signs of PCOS. Apart from fundamental metabolic problems connected to PCOS, focus of our study is on the role of quercetin on genes relevant to steroidogenesis and folliculogenesis.

2 Methods and materials

2.1 Chemicals

Sun Pharma Company and Sigma Aldrich were used to obtain the drugs letrozole and quercetin, respectively. The ELISA kits (ELK Biotechnology Wuhan, China) were bought from Clementia Biotech, New Delhi, India for the hormonal analysis. Analytical-grade chemicals were used in addition during the investigation.

2.2 Animals

Eighteen mature parkes strain mice (Age: 4-5 weeks) weighing 18-21 g were procured from Jeeva life sciences Hyderabad, mice having unrestricted access to water as well as food, and we gave them two weeks to acclimatize the environment. Following the acclimation period of two weeks, the animals were randomly into three groups of six each as follows: Group I serves as the control and was given water and a regular chow diet *ad lib* for 66 days; group II was given oral gavage administration of letrozole (LETZ) (6 mg/kg bw) (3) for 21 days to induce PCOS and was left untreated for 45 days; For three weeks, Group III received oral gavage dose of LETZ (6 mg/kg), after which it received Quercetin (QUER) (125 mg/kg bw orally daily) for 45 days. We kept mice under normal ambient temperature (22-25˚C), relative humidity of (55-60) and twelve hours of dark and light cycles respectively. A 50 mg/kg intraperitoneal dose of sodium pentobarbital was used to anaesthetize the mice and by puncturing the retro-orbital venous sinus, blood samples from all the mice were obtained at 66th day of the experiment, and serum was obtained which was then used to analyse hormones and biochemistry. A cervical dislocation was then used to kill the mice. The body had its ovaries removed and adipose tissues were cleansed for further biochemical and gene expression studies. The ethical committee of institution (Barkatullah University Bhopal) gave their consent under 1885/GO/Re/S/CPCSEA/IAEC/BU/21 to all experimental protocols.

2.3 Cholesterol and triglyceride (TG) analysis

Using easily accessible kits, triglycerides (TG) and total cholesterol (TC) were colorimetrically measured (Meril Diagnostics, Gujrat, India). Indirect measurements of low-density lipoprotein and very low-density lipoprotein were made while using Friedewald's equation.

Friedwald Equation: LDL = TC – HDL – (TG/5). VLDL= VLDL = TG/5 (17).

2.4 Analysis of hormones

The 67th day of the trial saw the collection of blood *via* retro-orbital venous sinus puncture. A centrifugation process was used to separate the serum, which was then put in storage until it was needed. The Enzyme-linked- Immunosorbent Assay ELISA kits that were used were obtained from ELK biotechnology, Wuhan, China, (CAT. numbers: ELK 368, ELK4808, ELK8407) and were built on the competitive inhibition enzyme immunoassay methodology. The kits' microtiter plate already has a specific protein pre-coated on it. An anti-testosterone, anti-LH, anti-FSH, and anti-oestrogen antibody biotin-conjugated was added to the appropriate microplate wells once the addition was made of standards or samples. The TMB substrate solution was then added to each microplate well, followed by the addition of an avidin-horseradish peroxidase (HRP) conjugate, which was then incubated for 45 minutes. The enzyme substrate reaction was stopped using the kits' stop solution, and the colour shift was detected using an ELISA reader that operates at a wavelength of 450 ± 10 nm.

2.5 Test procedure for vascular endothelial growth factor (VEGF) in ovarian tissue

The sandwich-ELISA method was used in the ELISA kit purchased from Elabscience Biotechnology Inc., (Wuhan, Hubei, P.R.C., China; CAT. No: E-EL-H0111; intra and inter –CV are <10%) This kit came with a micro ELISA plate (MEP) that was already coated with a vascular endothelial growth factor-specific antibody (VEGF). The wells of MEP comprised the particular antibody additionally to norms or examples. Then serial injections of an Avidin-Horseradish Peroxidase (HRP) solution and biotin - conjugated antibodies unique to VEGF were produced into each microplate well. The free bits were removed during washing. Each well received a dose of the substrate solution. Colour blue was only visible in the wells containing VEGF, biotinylated detecting antibody, and Avidin-HRP conjugate. Stop solution is added to stop the enzyme-substrate reaction was halted and the colour changed to yellow. At 450 nm, the optical density (OD) was measured using an ELISA reader. The OD value and VEGF levels are linearly correlated. Based on the OD of the data in respect to the conventional curves, the amount of VEGF present for each sample may be determined.

2.6 Reverse transcription and real-time PCR

Total RNA was extracted using Invitrogen's TRI Reagent, and 1μg of total RNA was used to create cDNA, both in accordance with the manufacturer's instructions (Invitrogen). The RT-PCR was performed using SYBR green and real-time PCR. To calculate the mRNA values, a standard curve for every gene's related expression level was developed. The SDS software was used to determine the threshold cycle (CT) of each sample and average CT was calculated for triplicate. Moreover Δ CT for each target gene was calculated by subtracting Δ CT for β-actin from average CT of the target gene of the sample. Table 1 lists the primers and internal controls that were employed, with additional data.

2.7 Histological assessment of ovaries

Ovarian tissue was fixated in 10% formol-saline for 24 hrs, dried, covered with paraffin, and sections were cut at a thickness of 5 microns for hematoxylin and eosin (H & E) stains. Motic microscope was used to examine and evaluate the sections (18).

10.3389/fendo.2023.1153289

TABLE 1 Description for RT-PCR primers.

Gene	Forward primer	Reverse primer
Kitl	GGTAGCCAGGAGTTTGTTCT	TTGTGTGGCATAAGGGCT
CYP11a1	TCCTCAAAGCCAGCATCA	ATCTCGACCCATGGCAAA
CYP19a1		ATGTTCTTGGAAATGCTGAACCC
		AGGACCTGGTATGAAGACGAG
Bmp1	GATATTGAGTCTCAGCCCGA	AACATGCGGTTGCCTGTA
fshr	CTCATCAAGCGACACCAAGA	GGAAAGGATTGGCACAAGAA
lhr	ACACTGCCCTCCAAAGAAAA	CCTCAAAGATGGCGGAATAA
Ar	CTGGGAAGGGTCTACCCAC	GGTGCTATGTTAGCGGCCTC
Esr1	GAA GGC TGC AAG GCT TTC TT	TCT TTT CGT ATC CCG CCT TT
CYP17a1	GCC CAA GTC AAA GAC ACC TAA T	GTA CCC AGG CGA AGA GAA TAG A
β Actin	TACGTCGCCCTGGATTTT	ATGAAAGAGGGCTGGAAGAG

2.8 Statistical analysis

A one-way analysis of variance as well as a *post hoc* evaluation utilizing Tukey's multiple comparison tests was utilized to decide the parameters' importance by using Graph Pad Prism version 9.3. Significance levels of 0.05, 0.01 and 0.001 accordingly have been used to indicate the statistically important, highly remarkable, and extremely significant level.

3 Results

3.1 Effects of quercetin (QUER) treatment on levels of insulin in mice with letrozole-induced polycystic ovary

Letrozole (LTZ) delivery in this trial caused a substantial rise in blood insulin levels (p 0.001) against healthy controls, and we also discovered a significant fall in insulin in the PCOS group receiving QUER in comparison to the PCOS group not receiving treatment (Figure 1).

3.2 Effect of quercetin (QUER) treatment on estrous cycle in mice with letrozole-induced polycystic ovary

The estrouscyclicity of the LETZ-induced PCOS mice was abnormal, and we saw a persistent diestrus condition that led to longer diestrous cycles than in the normal control mice. However, the estrous cycle was regularized after taking QUER, which returned the cycle duration to normal (Table 2).

3.3 Effect of oral quercetin (QUER) treatment on serum cholesterol and TG levels in mice with letrozole-induced polycystic ovary

When compared to the normal control mice, we saw that LETZ-induced PCOS mice had significantly higher levels of TG and cholesterol (P<0.001). In contrast, we saw that the PCOS group

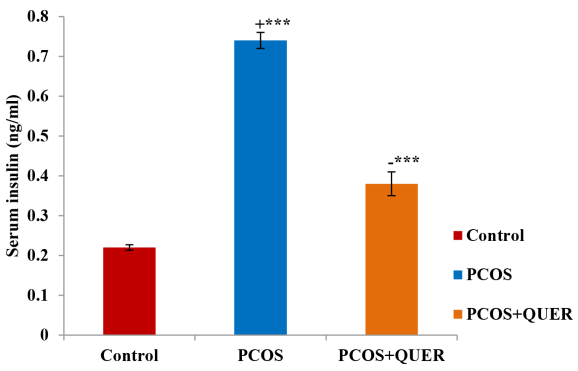

FIGURE 1
Effect of QUER on Serum insulin in mice with PCOS: With n=6 per group, all values are expressed as means with standard errors: Control: saline solution at 0.9%: PCOS (6 mg/kg of LETZ); PCOS+ QUER (6 mg/kg of LETZ and 125 mg/kg of QUER); += Control versus PCOS; -= PCOS versus PCOS+QUER; ***p 0.001.

TABLE 2 Effect of QUER therapy on estrous cycle, cholesterol and triglycerides PCOS mice.

Group	Cholesterol	Triglycerides	Average number of cycles in 30 days
Control	114.93 ± 1.01	119.76 ± 0.71	5.00 ± 0.31
PCOS	144.86 ± 1.95^{+***}	141.91 ± 2.49^{+***}	1.66 ± 0.21^{+***}
PCOS+QUER	124.71 ± 1.68^{-***}	131.55 ± 2.35^{-**}	4.00 ± 0.36^{-***}

With n=6 per group, all values are expressed as means with standard errors: Control: saline solution at 0.9%: PCOS (6 mg/kg of LETZ); PCOS+ QUER (6 mg/kg of LETZ and 125 mg/kg of QUER); += Control versus PCOS; -= PCOS versus PCOS+QUER; ***p 0.001, **p 0.01.

that received QUER had significantly lower levels of TG and cholesterol (P<0.001).

3.4 Effect of quercetin (QUER) on serum hormones in mice with letrozole-Induced polycystic ovary

We found that, in contrast normal control group, LETZ induced PCOS mice had significantly elevated levels of blood testosterone and LH : FSH ratio and significantly lower serum estrogen and FSH levels. However, QUER treatment significantly reduced (p<0.001) the testosterone as well as LH : FSH levels in PCOS mice, while increasing (p<0.01) the levels of estrogen and FSH compared with the PCOS group that isn't receiving treatment (Figure 2).

3.5 Effects of oral quercetin (QUER) treatment on plasma vascular endothelial growth factor in mice with LTZ induced polycystic ovary

This study's findings demonstrated that when letrozole was administered, VEGF levels significantly increased (p<0.001) when compared to the normal mice. However, in contrast to the LETZ-induced PCOS group, we noticed a significant (P<0.001) drop in VEGF levels in the group that received LETZ + QUER (Figure 3).

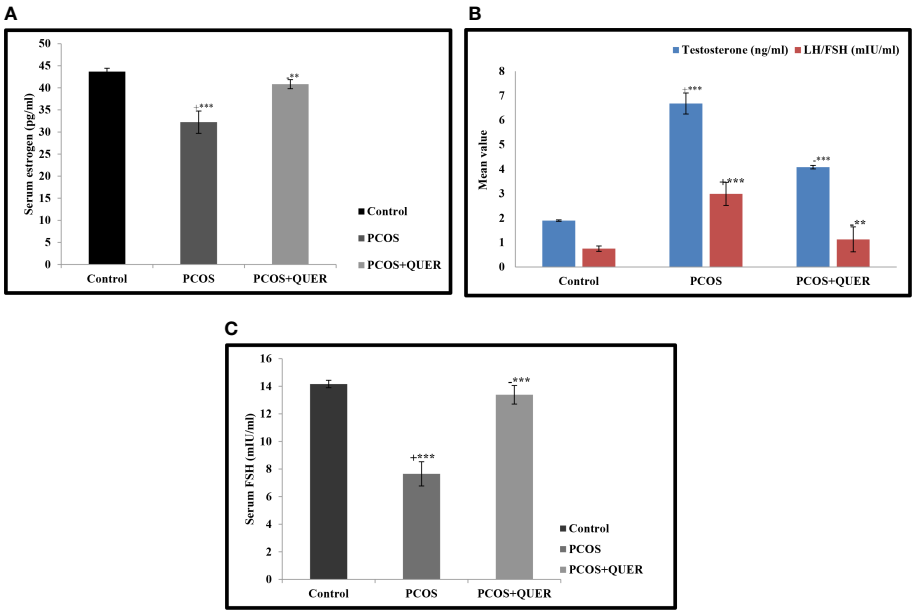

FIGURE 2
(A) Effect of QUER on Serum estrogen in mice with PCOS With n=6 per group, all values are expressed as means with standard errors: Control: saline solution at 0.9%: PCOS (6 mg/kg of LETZ); PCOS+ QUER (6 mg/kg of LETZ and 125 mg/kg of QUER); += Control versus PCOS; -= PCOS versus PCOS+QUER; ***p 0.001, **p 0.01 **(B)** Effect of QUER on LH/FSH and testosterone in PCOS mice. With n=6 per group, all values are expressed as means with standard errors: Control: saline solution at 0.9%: PCOS (6 mg/kg of LETZ); PCOS+ QUER (6 mg/kg of LETZ and 125 mg/kg of QUER); += Control versus PCOS; -= PCOS versus PCOS+QUER; ***p 0.001, **p 0.01. **(C)** Effect of QUER on serum FSH in PCOS mice. With n=6 per group, all values are expressed as means with standard errors: Control: saline solution at 0.9%: PCOS (6 mg/kg of LETZ); PCOS+ QUER (6 mg/kg of LETZ and 125 mg/kg of QUER); += Control versus PCOS; -= PCOS versus PCOS+QUER; ***p 0.001.

10.3389/fendo.2023.1153289

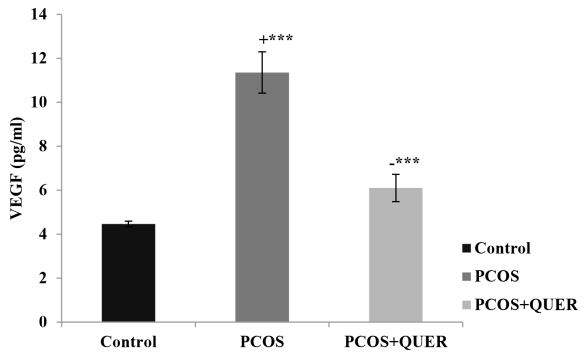

FIGURE 3
Effect of QUER on plasma VEGF in PCOS mice. With n=6 per group, all values are expressed as means with standard errors: Control: saline solution at 0.9%: PCOS (6 mg/kg of LETZ); PCOS+ QUER (6 mg/kg of LETZ and 125 mg/kg of QUER); += Control versus PCOS; -= PCOS versus PCOS+QUER; ***p 0.001.

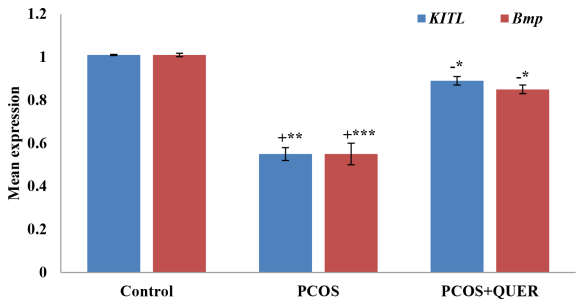

FIGURE 4
Effect of QUER on *KITL* and *Bmp1* in mice with polycystic ovary syndrome: With n=6 per group, all values are expressed as means with standard errors: Control: saline solution at 0.9%: PCOS (6 mg/kg of LETZ); PCOS+ QUER (6 mg/kg of LETZ and 125 mg/kg of QUER); += Control versus PCOS; -= PCOS versus PCOS+QUER; ***p 0.001, **p 0.01, *P<0.05.

3.6 Effects of oral administration of QUER expression of genes related to folliculogenesis in LETZ induced PCOS mice

Our findings demonstrated that, in comparison to the usual control, the expressions of *KITL* and *Bmp1* significantly decreased after LETZ treatment ($p<0.001$). The group that received LETZ + QUER, however, had levels that were importantly higher ($p<0.05$) in contrast to the mice with PCOS induced by letrozole (Figure 4).

3.7 Effect of oral QUER treatment on expression of genes related to generation of steroids in mice with LETZ induced PCOS

The findings demonstrated that mice with PCOS induced by LETZ had considerably increased levels of *CYP17a1* expression and low levels of *CYP19a1* and *CYP11a1* than control mice. *CYP17a1* expression in LETZ + QUER group, however, were significantly lower with the increase in *CYP19a1* and *CYP11a1* ($p<0.01$) than mice with LTZ induced PCOS (Figure 5).

3.8 Effect of oral treatment of QUER on expression of receptors of hormones in mice with LTZ induced PCOS

The findings demonstrated that *Ar*, *lhr*, *esr1*, and *fshr* expressions significantly decreased mice with PCOS induced by LETZ ($p<0.001$). However, we saw a substantial reduction ($p<0.01$) in the levels of *Ar*, *lhr*, *esr1*, and *fshr* in the LETZ + QUER group in contrast to the PCOS group subjected to LETZ (Figure 6).

3.9 Effects of oral QUER treatment on ovarian histology in mice with LETZ induced PCOS

Contrary to the normal control, we saw that letrozole treatment caused the corpus luteum to degenerate, producing more cystic follicles and no ovum. We saw a drop in cystic follicles and a regeneration of the corpus luteum and ovum in the group that underwent oral gavage treatment with LETZ+QUER in contrast to the mice with LETZ induced PCOS (Figure 7).

4 Discussion

We show here that quercetin (QUER) therapy is linked to anti-androgenic and anti- angiogenesis effects in the mouse ovary using a mice model of PCOS. We further show that the prolonged advantage of QUER improves ovarian function by increasing the control of genes involved to steroidogenesis and folliculogenesis. We demonstrate how QUER alters the functional, molecular, and morphological abnormalities caused by letrozole in pathological and physiological settings, particularly the problems with reproduction associated with PCOS, by regulating steroidogenesis and folliculogenesis in addition to regulating hormone receptors. The estrous cycle is known to cause changes in the hormones that control the activity of the ovaries, including follicle maturation (19). Prolonged estrus cycle with a continuous dioestrus phase was seen in our PCOS mice model, but the deficiencies were alleviated by giving the mice QUER. The PCOS rats also showed an extended diestrus phase and an irregular estrus cycle (20).

Other than type 2 diabetes, which has been previously established, women with polycystic ovarian syndrome also exhibit IR, impaired glucose tolerance, and obesity (14, 21). Result from this supported earlier research in that LETZ-induced PCOS in mice led toward increased levels of insulin, a sign of insulin resistance, a critical feature of metabolic disorders (MD'S) (14, 22). Additionally,

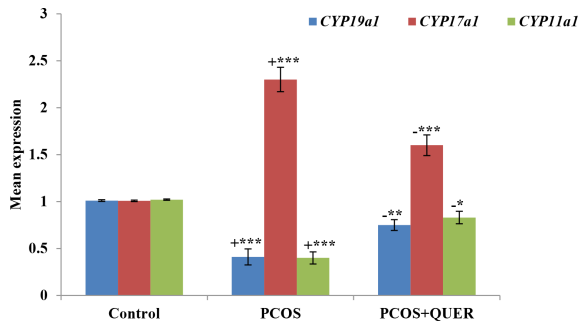

FIGURE 5
Effects of QUER on *CYP19A1*, *CYP17A1* & *CYP11a1* in mice with PCOS. With n=6 per group, all values are expressed as means with standard errors: Control: saline solution at 0.9%: PCOS (6 mg/kg of LETZ); PCOS+ QUER (6 mg/kg of LETZ and 125 mg/kg of QUER); += Control versus PCOS; -= PCOS versus PCOS+QUER; *p<0.05, **p<0.01, ***p<0.001.

previous studies have also shown that adiposity is exacerbated by IR which is a major contributing risk factor for obesity in metabolic and associated disorders (23, 24). Additionally, we discovered in this study that QUER treatment resulted in a considerable drop in blood insulin levels in PCOS mice, suggesting a potential function for QUER in the treatment of insulin resistance. Patients with PCOS experience hyperandrogenism as well as hyperinsulinemia, which causes adipocytes to increase catecholamine-induced lipolysis, which then results in increased serum free fatty acid levels and dyslipidemia (25). Due to the increased production of free fatty acids by the liver, TG levels in the blood are increased (3). In this work, we discovered that letrozole-treated mice had higher TC and TG levels than the control group. However, the levels significantly dropped after QUER treatment.

Pathological, physiological, and developmental angiogenesis all depend on the angiogenic factor VEGF. Oxidative stress initiates an inflammatory state that, within a feedback cycle, results in both insulin resistance and hyperandrogenism (26). According to reports, PCOS women release more VEGF (27). The mechanism is explained by the fact that the VEGF promoter region contains sites where the androgen receptor (AR) binds. When androgens bind to these locations, the VEGF gene is triggered (28).

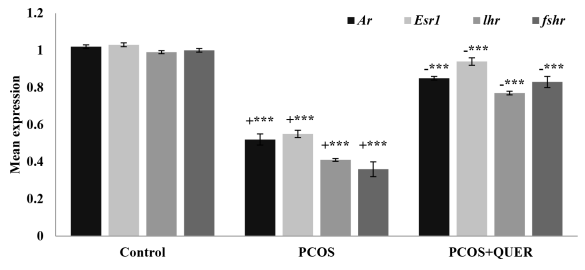

FIGURE 6
Effects of QUER treatment on *Ar, Esr1, Ihr* and *fshr* in mice with PCOS. With n=6 per group, all values are expressed as means with standard errors: Control: saline solution at 0.9%: PCOS (6 mg/kg of LETZ); PCOS+ QUER (6 mg/kg of LETZ and 125 mg/kg of QUER); += Control versus PCOS; -= PCOS versus PCOS+QUER; ***p 0.001.

Additionally, blood of women with PCOS has lower levels of soluble VEGF receptors, which increases the bioavailability of VEGF, as shown by (29). These outcomes are in agreement with the higher VEGF levels seen in this study in the letrozole group, Furthermore VEGF levels were decreased when mice treated with quercetin.

We observed serum hormone levels to confirm the impact of quercetin on hormonal alterations. The most consistent hormonal characteristic of PCOS-affected rats is increased serum levels of androgen and LH/FSH (6), and reduced oestrogen were also noted in PCOS-afflicted mice (18). In this investigation, in contrast to levels in PCOS-afflicted mice, quercetin decreased serum LH/FSH concentration. LH levels above normal and elevated LH and FSH ratio may be used as indicators of PCO among females (30). In addition, quercetin treatment in mice with PCOS significantly reduced serum testosterone levels. PCOS illnesses may benefit from the decreasing of these elevated testosterone levels, since it has already been shown that a high androgen level contributes to aetiology of PCOS (5, 31). Contrary to testosterone, LETZ-treated mice had lower serum oestrogen levels, and the decline was associated with mid or early-follicular growth as well as creation of morphology of follicles in ovary (32). The most successful treatments for atypical symptoms linked to female reproductive illnesses are hormones and chemicals; however, these treatments come with a number of side effects, including uterine haemorrhage, and hyperplasia (33, 34). Such findings imply, quercetin might be an effective medication in treating hormonal imbalances brought on by PCOS. Lower steroid hormone levels in the ovary are correlated with higher numbers of developing follicle's and different their shapes (35).

Kitl and *Bmp1* were used in our work to investigate the ovarian follicle components, and histological investigation was also carried out. In PCOS mice ovaries, the mRNA expression of *Kitl* and *Bmp1*, are declined; and the decline reversed after QUER injection. Histological examination revealed that the PCOS-afflicted mice similarly had many cysts, small follicles, and thin granulosa cell layers. In the past, letrozole-induced follicular dysfunction was also seen, including atretic and large cysts with few granulosa cells (35). Quercetin appears to be involved in the regulation of different parameters linked to follicular development in the ovary because treatment with the drug returned ovarian follicles and its other components in the present investigation, toward normal range.

Quercetin treatment in the current study raised expression of *CYP19a1* in ovary of PCOS-affected mice. Past research has shown that PCOS women have defective aromatase activity, and *CYP19a1* is essential for the normal advancement of the estrous or menstrual phases in PCOS rats (5). Contrarily, reduced aromatase activity in PCOS causes disturbances in oestrogen as well as androgeen generation (36). Here it is demonstrated that mice with PCOS had decreased aromatase activity, which is congruent with the *CYP19a1* and *CYP11a1* mRNA levels. On the other hand, the PCOS plus QUER mice had their aromatase activity restored because *CYP19a1* and *CYP11a1* was highly expressed. Our results on *CYP17A1* expression disagreed with Shah and Patel (37) who reported that quercetin owns useful impact in PCOS *via* suppressing PI3K that as a result of a reduction in *CYP17A1* gene expression which critically plays function in steroidogenesis process

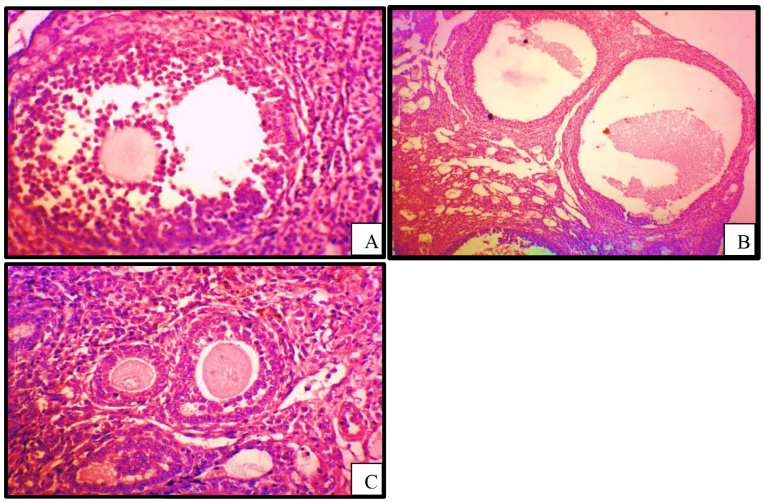

FIGURE 7
Photomicrographs of histological sections of ovary (H&E, magnificent x50): **(A)** PCOS; showing cystic follicles with degeneration of ovum **(B)** control; showing healthy follicle and ovum **(C)** PCOS treated with QUER; showing regenerated ovum with absence of cystic follicles.

in ovary. Additionally, the mRNA levels of *Ar* and *Esr1* were lowered; however, in our work, quercetin therapy corrected this downregulation in mice with PCOS. *Ar* and *Esr1* transcripts are shown to serve a function of proliferation in folllicular growth (38, 39) and elevated *Ar* levels could facilitate granulosa cell proliferation and differentiation (40). Additionally, quercetin treatment brought back to normal the transcriptional levels of *Fshr* and *Lhr* that had been changed in the ovaries of PCOS mice. *Fshr* moderately controls follicle growth during the baseline follicle growth phase by working in synergy with other stimulating substances like androgens (41). *Lhr* is also present on theca and granulosa cell surfaces, and *Lhr* levels have an impact on ovulation, the development of the corpus lutum, also on synthesis of additional steroids' such as oestrogen, androgen and progesterone (42). Such findings led us to discover cystic degeneration of the corpus luteum and follicles in PCOS-affected animals. It's interesting to note that the quercetin helped to slow down the degradation of ovarian follicle development by regenerating the corpus luteum and eliminating cystic follicles. It could be said that quercetinmarkedly reversing ovary physiological functions and regularity of estrous cycle. All these functions have been done *via* acting of quercetinon pituitary- ovary axis because of reversing normal ration of LH/FSH the main gonadotropic hormones.

Our results agree markedly with PourteymourFardTabrizi et al., (12) and Chen et al., (43) who reviewed Quercetin effects and concluded that it can recover disturbance of ovulation, decrease testosterone and Insulin resistance, adjust metabolism of lipid, ameliorate function of vascular endotheliaum and control intestinal microbiota, that all helps significantly in PCOS' treatment. Quercetin a bio-flavonoid compound, presents in the glycosylies in vegetables and fruits. Although Quercetin analogs have antioxidant effect attributed to the amount of free "OH" groups in its composition, but Quercetin shows essential hydrophobicity (13). This may cause the recovering effect of Quercetin on PCOS mice in our study. Quercetin medical advantages are attributed to flavanols which serve as ant-inflammatory, antivirus and antioxidative stress, which are considered as three main elements that threaten the health and cause diseases, (12, 17).

It is observed that quercetin impacted positively by recovering in the PCOS in different levels: 1) systematically indicated by insulin and lipid profile. 2) Organ level as shown by reserving the ovary histology. 3) Molecular level: it regulated related genes expression and hormones in ovary cells as shown in Figure 8.

5 Conclusion

This study was designed to illustrate recovering effect of quercetin PCOS induced in mice model. It has proven that quercetin administration reversed experimentally abnormalities in PCOS induced by letrozole. It can speculated that PCOS has modulating-effects on regulatory genes of steroidogenesis and folliculogenesis that leading to the pathophysiological changes include (disturbance in gonadotropin as a result of related gene dysregulation, which followed by regression of ovarian follicles. Interestingly, the study has found that quercetin prevented the degradation of ovarian follicle by regenerating the corpus luteum and eliminating cystic follicles which reset the estrous cycle. The curing action of quercetin on ovary has been seen by recovering gonadotropic and gonads steroids with their physiological functions and regularity of cycle. This indicated markedly that Pituitary- ovary axis was the target of quercetin effect as it reversed normal levels and rations of LH/FSH the main gonadotropic hormones. It worth to mention that quercetin has positively treated PCOS syndrome through different biological aspects: 1) metabolic path: systematically indicated by insulin and lipid profile. 2) histological level as shown by reserving the ovary tissue structure and components. 3) Molecular level: it regulated genes expression listed above. 4) through endocrine mechanism as seen in pituitary and ovary hormones. It could be concluded that

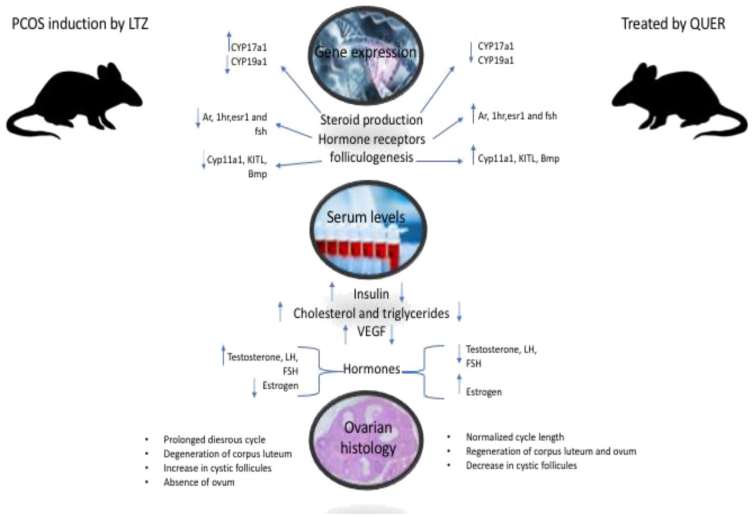

FIGURE 8
Shows the effect of quercetin on the tested animals in term of Genes expression that control ovary functions. It is observed that quercetin impacted positively by recovering in the PCOS in the ovary by regulating genes expression listed here and restoring hormones and lipid profile.

quercetin has systematic, histological and molecular improving effects on PCOC. Further research is needed to investigate safety of quercetin on body functions and organs

Data availability statement

The original contributions presented in the study are included in the article/supplementary material. Further inquiries can be directed to the corresponding authors.

Ethics statement

The animal study was reviewed and approved by Institutional ethical committee Barkatullah University Bhopal, India.

Author contributions

MZS: Conceptualization, Data curation, Software, Validation, Visualization, Writing-Review and editing, writing original draft, investigation, resources, analysis, Methodology; VS: Methodology, Project adminstration, Supervision, review and editing. MAM: Conceptualization, Methodology, Software, Review and editing; WMS, MAG, GAR, MS, SMB, MAA, MHA, AMH and EAA: Review and editing; MAA, MHA, AMH and EAA: Resources, Funding acquisition. EAA contributed in Scientific editing and revising the manuscript.

Conflict of interest

The authors declare that the research was conducted in the absence of any commercial or financial relationships that could be construed as a potential conflict of interest.

Publisher's note

References

1. Ul Haq Shah MZ, Soni M, Shrivastava VK, Mir MA, Muzamil S. Gallic Acid reverses ovarian disturbances in mice with letrozole-induced PCOS *via* modulating adipo R1 expression. *Toxicol Rep* (2022) 9:1938–49. doi: 10.1016/j.toxrep.2022.10.009

2. Bremer AA. Polycystic ovary syndrome in the pediatric population. *Metab Syndr Relat Disord* (2010) 8:375–94. doi: 10.1089/met.2010.0039

3. Ul haq Shah MZ, Shrivastava V, Mir MA. Metformin treatment ameliorates endocrine-metabolic disturbances in letrozole-induced PCOS mice model by modulating adiponectin status. *Obes Med Res* (2022) 31:100392. doi: 10.1016/j.obmed.2022.100392

4. Codner E, Escobar-Morreale HF. Clinical review: hyperandrogenism and polycystic ovary syndrome in women with type 1 diabetes mellitus. *J Clin Endocrinol Metab* (2007) 92:1209–16. doi: 10.1210/jc.2006-2641

5. Kafali H, Iriadam M, Ozardali I, Demir N. Letrozole-induced polycystic ovaries in the rat: a new model for cystic ovarian disease. *Arch Med Res* (2004) 35:103–8. doi: 10.1016/j.arcmed.2003.10.005

6. Wang MX, Yin Q, Xu X. A rat model of polycystic ovary syndrome with insulin resistance induced by letrozole combined with high fat diet. *Med Sci Monitor Int Med J Exp Clin Res* (2020) 26:e922136. doi: 10.12659/MSM.922136

7. Abbott DH, Barnett DK, Bruns CM, Dumesic DA. Androgen excess fetal programming of female reproduction: a developmental aetiology for polycystic ovary syndrome hum. *Reprod Update* (2005) 11:357–74. doi: 10.1093/humupd/dmi013

8. Daneasa A, Cucolas C, Lenghel LM, Olteanu D, Orasan R, Filip GA. Letrozole vsestradiolvalerate induced PCOS in rats: glycemic, oxidative and inflammatory status assessment. *Reproduction* (2016) 151:401–9. doi: 10.1530/REP-15-0352

9. Chen T, Jia F, Yu Y, Zhang W, Wang C, Zhu S, et al. Potential role of quercetin in polycystic ovary syndrome and its complications: a review. *Molecules* (2022) 27 (14):4476. doi: 10.3390/molecules27144476

10. Badawy A, Elnashar A. Treatment options for polycystic ovary syndrome. *Int J Womens Health* (2011) 3:25–35. doi: 10.2147/IJWH.S11304

11. Neisy A, Zal F, Seghatoleslam A, Alaee S. Amelioration by quercetin of insulin resistance and uterine GLUT4 and ERα gene expression in rats with polycystic ovary syndrome (PCOS). *Reprod Fertil Dev* (2019) 31(2):315–23. doi: 10.1071/RD18222

12. PourteymourFardTabrizi F, Hajizadeh-Sharafabad F, Vaezi M, Jafari-Vayghan H, Alizadeh M, Maleki V. Quercetin and polycystic ovary syndrome, current evidence and future directions: a systematic review. *J Ovarian Res* (2020) 13(1):11. doi: 10.1186/s13048-020-0616-z

13. Shu X, Hu XJ, Zhou SY, Xu CL, Qiu QQ, Nie SP, et al. Yao xuexuebao. *ActapharmaceuticaSinica* (2011) 46(9):1051–7.

14. Zheng S, Chen Y, Ma M, Li M. Mechanism of quercetin on the improvement of ovulation disorder and regulation of ovarian CNP/NPR2 in PCOS model rats. *J Formosan Med Assoc Taiwan Yizhi* (2022) 121(6):1081–92. doi: 10.1016/j.jfma.2021.08.015

15. Rezvan N, Moini A, Janani L, Mohammad K, Saedisomeolia A, Nourbakhsh M, et al. Effects of quercetin on adiponectin-mediated insulin sensitivity in polycystic ovary syndrome: a randomized placebo-controlled double-blind clinical trial. *Horm Metab Res* (2017) 49(2):115–21. doi: 10.1055/s-0042-118705

16. Mahmoud AA, Elfiky AM, Abo-Zeid FS. The anti-androgenic effect of quercetin on hyperandrogenism and ovarian dysfunction induced in a dehydroepiandrosterone rat model of polycystic ovary syndrome. *Steroids* (2022) 177:108936. doi: 10.1016/j.steroids.2021.108936

17. Soni M, Shah M, Shrivastava VK. The hypoglycemic and anti-hyperlipidemic activity of vitamin c in di(2-ethylhexyl) phthalate-induced toxicity in female mice, mus musculus. *Comp Clin Pathol* (2023). doi: 10.1007/s00580-023-03466-1

18. Shah M, Shrivastava VK. Turmeric extract alleviates endocrine-metabolic disturbances in letrozole-induced PCOS by increasing adiponectin circulation: a comparison with metformin. *Metab Open* (2021) 13:100160. doi: 10.1016/j.metop.2021.100160

19. Sun J, Jin C, Wu H, Zhao J, Cui Y, Liu H, et al. Effects of electroacupuncture on ovarian P450arom, P450c17alpha and mRNA expression induced by letrozole in PCOS rats. *PloS One* (2013) 8:e79382. doi: 10.1371/journal.pone.0079382

20. Soumya V, Muzib YI, Venkatesh P. A novel method of extraction of bamboo seed oil (BambusabambosDruce) and its promising effect on metabolic symptoms of experimentally induced polycystic ovarian disease. *Indian J Pharmacol* (2016) 48 (2):162–7. doi: 10.4103/0253-7613.178833

21. Joham AE, Teede HJ, Ranasinha S, Zoungas S, Boyle J. Prevalence of infertility and use of fertility treatment in women with polycystic ovary syndrome: data from a large community-based cohort study. *J Womens Health (Larchmt)* (2015) 24(4):299–307. doi: 10.1089/jwh.2014.5000

22. Cussons AJ, Watts GF, Burke V, Shaw JE, Zimmet PZ, Stuckey BG. Cardiometabolic risk in polycystic ovary syndrome: a comparison of different approaches to defining the metabolic syndrome. *Hum Reprod* (2008) 23(10):2352–8. doi: 10.1093/humrep/den263

23. Stanhope KL, Schwarz JM, Keim NL, Griffen SC, Bremer AA, Graham JL, et al. Consuming fructose-sweetened, not glucose-sweetened, beverages increases visceral adiposity and lipids and decreases insulin sensitivity in overweight/obese humans. *J Clin Invest* (2009) 119(5):1322–34. doi: 10.1172/JCI37385

24. Shah MZ, Shrivastava VK. Ameliorative effects of quercetin on endocrine and metabolic abnormalities associated with experimentally induced polycystic ovary syndrome in mice. *Comp Clin Pathol* (2023), 32–1. doi: 10.1007/s00580-023-03446-5

25. Diamanti-Kandarakis E, Papavassiliou AG, Kandarakis SA, Chrousos GP. Pathophysiology and types of dyslipidemia in PCOS. *Trends Endocrinol Metabol: TEM* (2007) 18(7):280–5. doi: 10.1016/j.tem.2007.07.004

26. El-bahya AAZ, Radwanb RA, Gadc MZ, Abdel SM. A closer insight into the role of vitamin d in polycystic ovary syndrome (Pcos). *Glob J Pharmaceu Sci* (2018) 6(4). doi: 10.19080/GJPPS.2018.06.555692

27. Artini PG, Ruggiero M, ParisenToldin MR, Monteleone P, Monti M, Cela V, et al. Vascular endothelial growth factor and its soluble receptor in patients with polycystic ovary syndrome undergoing IVF, hum. *Fertil* (2009) 12(1):40–4. doi: 10.1080/14647270802621358

28. Eisermann K, Broderick CJ, Bazarov A, Moazam MM, Fraizer GC. Androgen up-regulates vascular endothelial growth factor expression in prostate cancer cells *via* an Sp1 binding site, mol. *Cancer* (2013) 12:(1). doi: 10.1186/1476-4598-12-7

29. Almawi WY, Gammoh E, Malalla ZH, Al-Madhi SA. Analysis of VEGFA variants and changes in VEGF levels underscores the contribution of VEGF to polycystic ovary syndrome. *PloS One* (2016) 11(11):e0165636. doi: 10.1371/journal.pone.0165636

30. Saadia Z. Follicle stimulating hormone (LH: FSH) ratio in polycystic ovary syndrome (PCOS) - obese vs. non- obese women. *Med Arch (Sarajevo Bosnia Herzegovina)* (2020) 74(4):289–93. doi: 10.5455/medarh.2020.74.289-293

31. Abbott DH, Dumesic DA, Franks S. Developmental origin of polycystic ovary syndrome - a hypothesis. *J Endocrinol* (2002) 174:1–5. doi: 10.1677/joe.0.1740001

32. Dewailly D, Robin G, Peigne M, Decanter C, Pigny P, CatteauJonard S. Interactions between androgens, FSH, anti-mullerian hormone and estradiol during folliculogenesis in the human normal and polycystic ovary. *Hum Reprod Update* (2016) 22:709–24. doi: 10.1093/humupd/dmw027

33. Hidaka T, Yonezawa R, Saito S. Kami-shoyo-san, kampo (Japanese traditional medicine), is effective for climacteric syndrome, especially in hormone-replacement-therapy-resistant patients who strongly complain of psychological symptoms. *J Obstet Gynaecol Res* (2013) 39:223–8. doi: 10.1111/j.1447-0756.2012.01936.x

34. Yang H, Kim HJ, Pyun BJ, Lee HW. Licorice ethanol extract improves symptoms of polycytic ovary syndrome in letrozole-induced female rats. *Integr Med Res* (2018) 7:264–70. doi: 10.1016/j.imr.2018.05.003

35. Baravalle C, Salvetti NR, Mira GA, Pezzone N, Ortega HH. Microscopic characterization of follicular structures in letrozoleinduced polycystic ovarian syndrome in the rat. *Arch Med Res* (2006) 37:830–9. doi: 10.1016/j.arcmed.2006.04.006\

36. Chen J, Shen S, Tan Y, Xia D, Xia Y, Cao Y, et al. The correlation of aromatase activity and obesity in women with or without polycystic ovary syndrome. *J Ovarian Res* (2015) 8:11. doi: 10.1186/s13048-015-0139-1

37. Shah KN, Patel SS. Phosphatidylinositide 3-kinase inhibition: a new potential target for the treatment of polycystic ovarian syndrome. *Pharm Biol* (2016) 54(6):975–83. doi: 10.3109/13880209.2015.1091482

38. Hammes SR. Androgens regulate ovarian follicular development by increasing follicle stimulating hormone receptor and microRNA-125b expression. *Proc Natl Acad Sci United States America* (2014) 111(8):3008–13. doi: 10.1073/pnas.1318978111

39. Chauvin S, Cohen-Tannoudji J, Guigon ,CJ. EstradiolSignaling at the heart of folliculogenesis: its potential deregulation in human ovarian pathologies. *Int J Mol Sci* (2022) 23(1):512. doi: 10.3390/ijms23010512

40. Hasegawa T, Kamada Y, Hosoya T, Fujita S, Nishiyama Y, Iwata N, et al. A regulatory role of androgen in ovarian steroidogenesis by rat granulosa cells. *J Steroid Biochem Mol Biol* (2017) 172:160–5. doi: 10.1016/j.jsbmb.2017.07.002

41. George JW, Dille EA, Heckert LL. Current concepts of follicle-stimulating hormone receptor gene regulation. *Biol Reprod* (2011) 84(1):7–17. doi: 10.1095/biolreprod.110.085043

42. Edson MA, Nagaraja AK, Matzuk MM. The mammalian ovary from genesis to revelation.Endocr. *Rev* (2009) 30:624–712. doi: 10.1210/er.2009-0012

43. Rathod S, Arya S, Kanike S, Shah SA, Bahadur P, Tiwari S. Advances on nanoformulation approaches for delivering plant-derived antioxidants: a case of quercetin. *Int J Pharm* (2022) 625:122093. doi: 10.1016/j.ijpharm.2022.122093

frontiers | Frontiers in Physiology

TYPE Review
PUBLISHED 12 May 2023
DOI 10.3389/fphys.2023.1177443

OPEN ACCESS

EDITED BY
Fengxiang Wei,
Shenzhen Longgang District Maternal and Child Healthcare Hospital, China

REVIEWED BY
Jiaqiang Xiong,
Wuhan University, China
Fabiana Fernandes Bressan,
University of São Paulo, Brazil

*CORRESPONDENCE
Shujie Liao,
sjliao@tjh.tjmu.edu.cn
Chaoyang Sun,
suncydoctor@gmail.com

RECEIVED 01 March 2023
ACCEPTED 04 May 2023
PUBLISHED 12 May 2023

CITATION
Hu B, Wang R, Wu D, Long R, Ruan J, Jin L, Ma D, Sun C and Liao S (2023), Prospects for fertility preservation: the ovarian organ function reconstruction techniques for oogenesis, growth and maturation *in vitro*.
Front. Physiol. 14:1177443.
doi: 10.3389/fphys.2023.1177443

Prospects for fertility preservation: the ovarian organ function reconstruction techniques for oogenesis, growth and maturation *in vitro*

Bai Hu[1,2], Renjie Wang[1,2], Di Wu[1,2], Rui Long[1,2], Jinghan Ruan[1,2], Lei Jin[1], Ding Ma[1,2], Chaoyang Sun[1,2]* and Shujie Liao[1,2]*

[1]Department of Gynecological Oncology, Tongji Hospital, Tongji Medical College, Huazhong University of Science and Technology, Wuhan, China, [2]National Clinical Research Center for Obstetrics and Gynecology, Cancer Biology Research Center (Key Laboratory of the Ministry of Education), Tongji Hospital, Tongji Medical College, Huazhong University of Science and Technology, Wuhan, China

Today, fertility preservation is receiving more attention than ever. Cryopreservation, which preserves ovarian tissue to preserve fertility in young women and reduce the risk of infertility, is currently the most widely practiced. Transplantation, however, is less feasible for women with blood-borne leukemia or cancers with a high risk of ovarian metastasis because of the risk of cancer recurrence. In addition to cryopreservation and re-implantation of embryos, *in vitro* ovarian organ reconstruction techniques have been considered as an alternative strategy for fertility preservation. *In vitro* culture of oocytes in vitro Culture, female germ cells induction from pluripotent stem cells (PSC) *in vitro*, artificial ovary construction, and ovaria-related organoids construction have provided new solutions for fertility preservation, which will therefore maximize the potential for all patients undergoing fertility preservation. In this review, we discussed and thought about the latest ovarian organ function reconstruction techniques *in vitro* to provide new ideas for future ovarian disease research and fertility preservation of patients with cancer and premature ovarian failure.

KEYWORDS

ovarian organ function reconstruction techniques, fertility preservation, tissue engineering, *in vitro* culture of oocytes, artificial ovary, organoids, artificial oocytes, reproduction

1 Introduction

Nowadays, with the development of malignant tumors at a younger age (Gershenson, 2019), chemotherapy and radiotherapy have immediate and long-term side effects on ovarian function. The first effect of chemotherapy on the ovarian is immediate. It is cytotoxicity to dividing cells, which may directly kill growing follicles and induce premature ovarian failure (POF). Chemotherapy may also induce inflammation and destruction of vascular and stroma, which is harmful to the growth of the follicle. Moreover, the acute decrease in growing follicles, which leads to the reduction of sex steroid hormones and inhibin, may activate primordial follicles, enhance the rate of recruitment, accelerate the depletion of the reserve, and finally lead to POF (Sciorio and Anderson, 2020). The frequency of POF after radiotherapy is

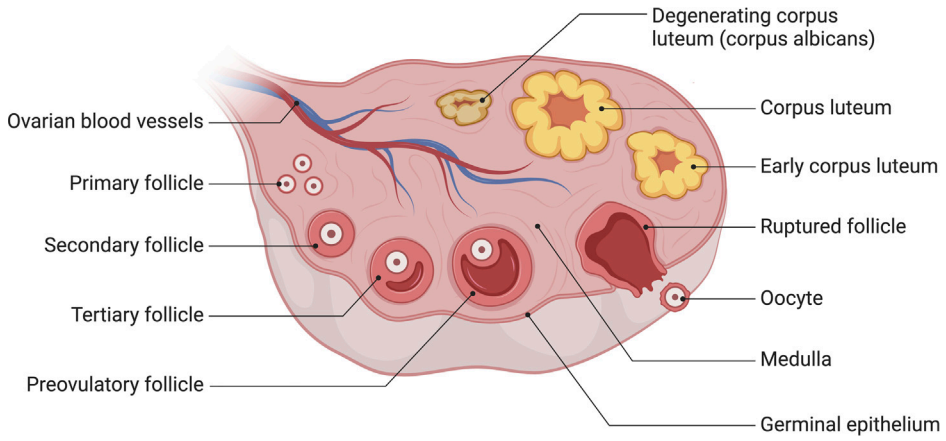

FIGURE 1
The anatomy of human ovary. The cortex is the principal part of the ovary, containing various levels of developing follicles, corpus luteum, interstitial tissue, *etc.*, whereas the medulla is mainly composed of blood vessels, nerves, lymphatics, and loose connective tissue. Created with BioRender.com.

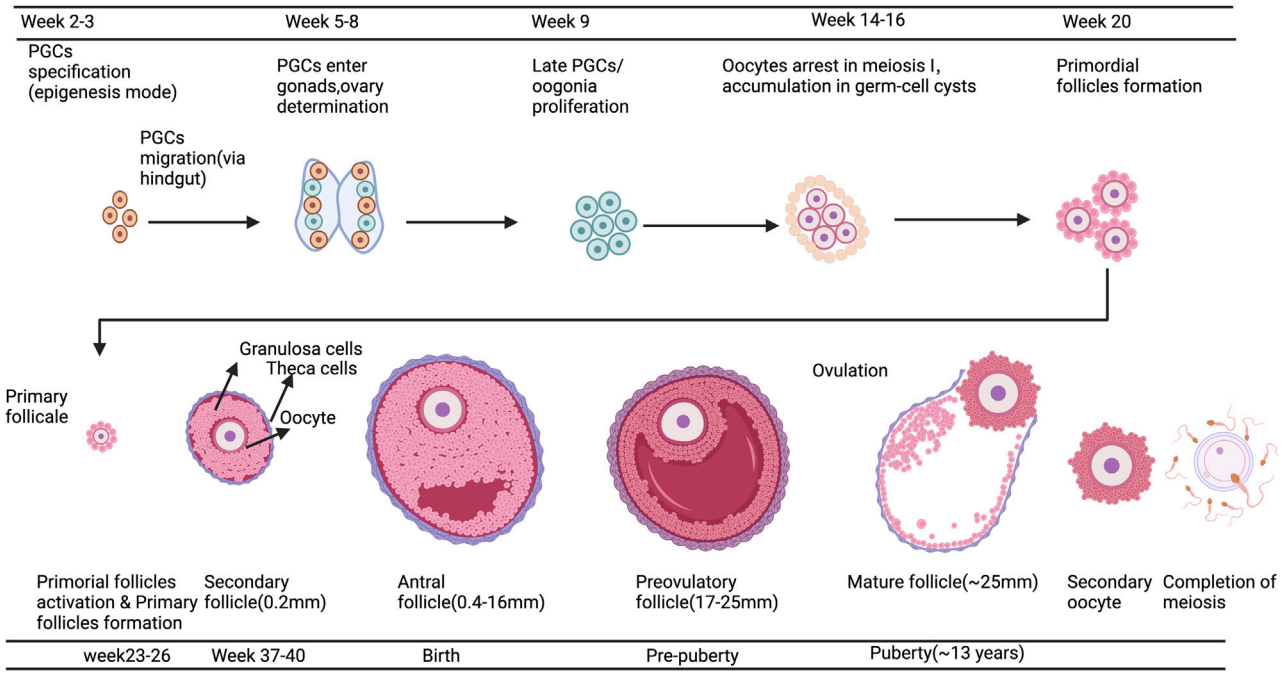

FIGURE 2
A Schematic comparison of developing germ cells, oocytes, and ovarian follicles in humans. The primordial germ cells (PGCs) are specified by the epigenesis mode in humans. After specification, PGCs migrate to the gonads; this occurs via the hindgut in humans. Further physiological events in the differentiated ovary, including oogonia proliferation and entry into meiosis, oocyte arrest in meiotic prophase I, the accumulation of oocytes in germ-cell cysts, and the formation of early follicles, are all essentially the same in humans. Created with BioRender.com.

related to the used dose of radiation. Whole irradiation doses at 3–5 Gy, 60% of the follicles are destroyed; with irradiation at doses of 5 Gy, 100% of the follicles are destroyed (Dinas, 2020). To meet reproductive and endocrine needs, cryopreservation of ovarian tissue for transplantation before starting anti-cancer treatment is the main means of fertility preservation. However, this method has the risk of reintroducing malignant tumor cells. For patients with ovarian diseases such as POF, the search for safe and efficient fertility preservation methods is also of great importance. In order to solve this problem, the ovarian organ function reconstruction techniques for oogenesis, growth and maturation *in vitro* are gradually becoming the core of research.

Histologically, human ovarian germinal epithelium (OSE) is divided into the outer cortex and the inner medulla. The cortex is the principal part of the ovary, containing various levels of developing follicles, corpus luteum, interstitial tissue, *etc.*, whereas the medulla is mainly composed of blood vessels, nerves, lymphatics, and loose connective tissue (Frances-Herrero et al., 2022) (Figure 1).

Follicles are the primary functional units of mammalian ovaries. In most mammals, follicle development starts before birth and continues throughout the reproductive years. Generally, the development of the follicle includes three processes:1) primordial follicle is activated and grows to the preantral follicle stage; 2) preantral follicle goes through antral follicular stage to preovulatory follicle as follicular fluid increases to form a follicular cavity; 3) due to the effect of luteinizing hormone/follicle-stimulating hormone releasing hormone (LH/FSH) peak, preovulatory follicle releases oocyte corona cumulus complex (OCCC) and oocyte (Telfer and Zelinski, 2013).

The process of human oocyte growth and development is continuous and complex: during early embryonic development, primordial germ cells (PGCS) actively migrate to the gonads, undergo pluripotency recapture, epigenetic reprogramming (including histone modifications, X-stained weight activation, genome-wide DNA demethylation, and blot erases) and sexual differentiation to form oogonia. Finally, Meiosis II(MII) oocytes are generated through Meiosis, and the second Meiosis is completed when spermatozoa meet (Garcia-Alonso et al., 2022) (Figure 2). Oocyte development and growth depend on the follicular environment; as a result, the ovarian organ function reconstruction system should promote follicle activation, growth, and maturity or provide a follicle-like microenvironment for oocyte development. It will allow complex dynamic bidirectional communication between the oocyte and surrounding granulosa cells and follicle theca cells, completing the critical process of oocyte meiosis. By establishing a safe and effective ovarian organ rebuilding system, it will be feasible for oogenesis, growth and maturation *in vitro* to make the most of the ovarian follicular reserve and even restore fertility in the absence of ovarian follicle reserves.

Recently, the ovarian organ function reconstruction techniques for oogenesis, growth and maturation *in vitro* mainly include *in vitro* follicle culture (IVC), induction using pluripotent stem cells (PSCs) *in vitro*, artificial ovary construction technology and ovarian organoids. In addition, tissue engineering techniques, which combine biology, medicine, and materials engineering (Langer and Vacanti, 2016), are also being extensively studied to reconstruct or repair ovarian structures. In order to provide fresh perspectives on the preservation of patients' fertility who have cancer, POF, *etc.*, as well as on future research on ovarian diseases, this article reviews the most recent techniques for ovarian organ function reconstruction techniques for oogenesis, growth and maturation *in vitro*.

2 Follicle *in vitro* culture (IVC)

IVC refers to the isolation of immature follicles from ovarian tissue, *in vitro* culture to maturity, and subsequent *in vitro* fertilization (IVF), which can avoid the risk of tumor reimplantation and utilize a large number of immature follicles in the ovary. The follicular multistage IVC system has been applied into practice in many species: in mice, it can be cultured from primordial follicles to live birth (Mochida et al., 2013); In primates, it can be cultured from secondary follicles to morula stage (Xu et al., 2013); and in humans, there have been reports of MII stage oocytes cultured from primary or secondary follicles (Xu et al., 2021). However, compared with humans, the prolonged growth period of complete follicular formation in mice, larger follicles in humans, and different effects of growth factors and hormones between species are factors that hinder the cross-species translation of these technologies (Herta et al., 2018; Telfer, 2019a; Telfer, 2019b; Telfer et al., 2019). The follicular multistage IVC system is mainly carried out in three steps: 1) Culturing the small ovarian cortex to support primordial follicle activation (*in vitro* activation, IVA) and early growth and supporting its early growth; 2) Isolating and culturing growing presinus follicles to achieve oocyte growth and development to the sinus stage (*In vitro* growth, IVG); 3) *In vitro* maturation (IVM) of oocytes (Yang et al., 2020a). Figure 3 shows the whole multistep culture system to support *in vitro* growth of oocytes

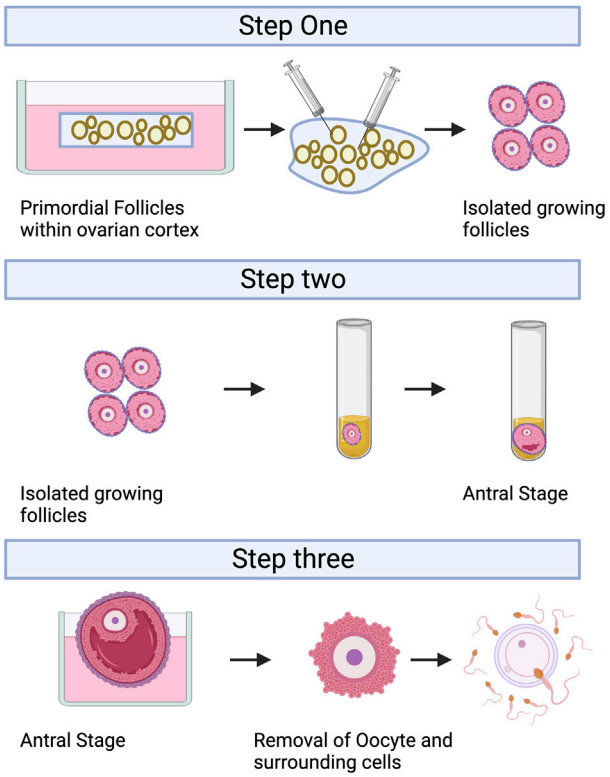

FIGURE 3
A multistep culture system to support *in vitro* growth (IVG) of oocytes from human primordial follicles through to maturation. Step one: Flattened strips of ovarian tissue are cultured free-floating in medium containing human serum albumin, ascorbic acid, and basal levels of follicle-stimulating hormone. Once follicles have reached multilaminar stages, they can be isolated mechanically using needles. Step two: Isolated follicles are cultured individually from the preantral to the antral stages. Step three: The final stages of oocyte growth and development are achieved by removing the oocyte-cumulus complex from the antral follicle and culturing the oocyte and its surrounding somatic cells. Oocyte-cumulus complexes are placed within medium for *in vitro* maturation (IVM). Oocytes are then analyzed for the presence of a metaphase II spindle and a polar body. Created with BioRender.com.

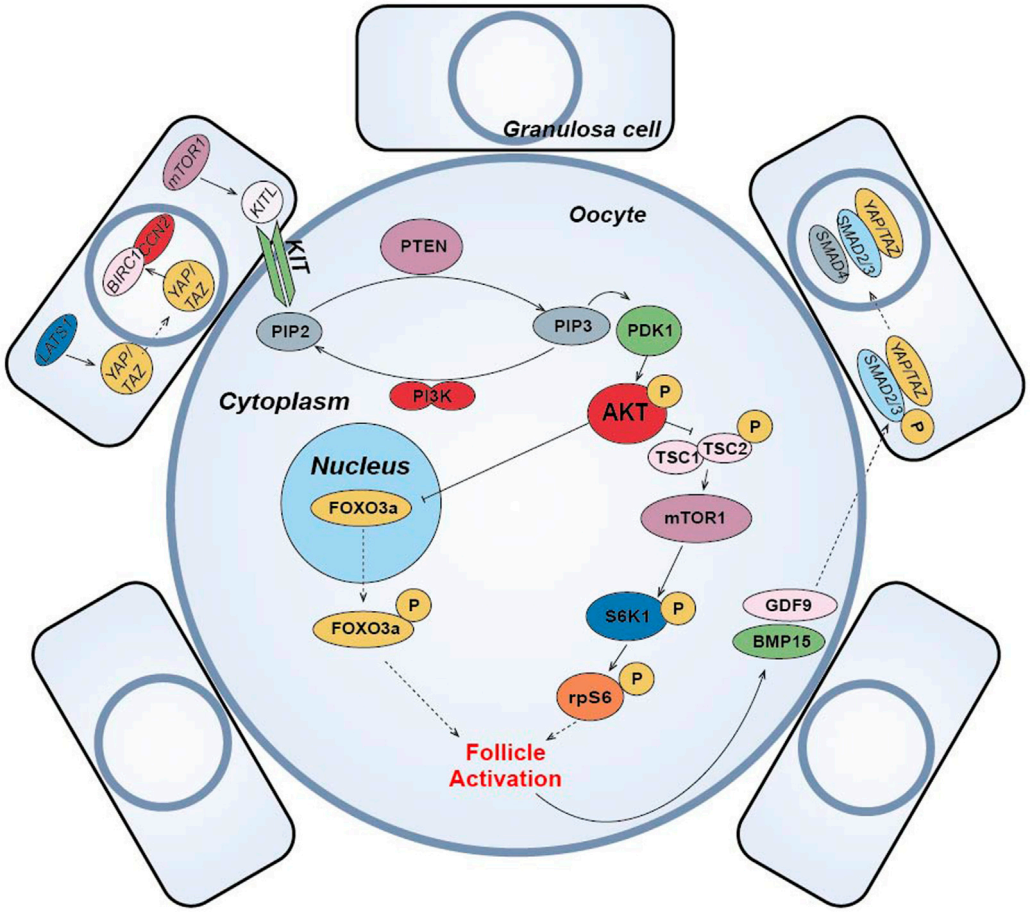

FIGURE 4
Schematic diagram of primordial follicle activation signaling pathway. The "p" represents phosphorylation, the solid arrow represents activation, the solid T-shaped arrow represents inhibition, and the dotted arrow represents entering or exiting the nucleus or cell membrane.

from human primordial follicles through to maturation. The ovarian environment is dynamic, controlled by cyclical changes in the receptor cycle of hormones and local signals from the ovary itself. The significant principle of using tissue engineering to construct IVC system is to accurately present the changes of various signals (including growth factors, hormones, extracellular matrix (ECM), mechanics, *etc.*), so as to allow the coordinated growth of multiple cell compartments (oocytes and surrounding granulosa cells, follicular theca cells) in the follicle. When simulating the ovarian environment *in vitro,* the follicles must be provided with signals such as growth factors and hormones at appropriate times and concentrations. Therefore, it can promote cell growth and development and promote cell-cell communication, maintain the complex interaction between oocyte and ovarian somatic cells (granulosa cells and follicular theca cells), and meet the changing needs of oocyte and ovarian somatic cells.

2.1 Follicle *in vitro* activation (IVA)

Activation of primordial follicles is a key initial step in oocyte development. In females, dormant primordial follicles consist of a single layer of primordial follicle granulosa cells (pfGCs) wrapped around primary oocytes, and the dormant state is influenced by forkheadbox O3 (FOXO3), the phosphatase and tensin homolog deleted on chromosome 10(PTEN), TSC complex subunit 1 (TSC1), TSC complex subunit 2 (TSC2), forkheadbox L2(FOXL2), p27KIP1 gene (p27), ribosomal protein S6 (rpS6), 3-phosphatidylinositol-dependent protein kinase 1 (PDK1), and anti-mullerian hormone (AMH) (Reddy et al., 2010; Chen et al., 2020), *etc.* When the regulation of certain factors is altered, the dormant state of the primordial follicle is broken and thus activated to continue development, or degeneration or atresia occurs. IVA can be used to activate growth before transplantation to cause a burst of sinus follicle development 4–6 months later, from which oocytes can be harvested, which would benefit women with no ovarian reserve or who produce only a small number of follicles even after intense ovarian stimulation (Kawamura et al., 2013; Suzuki et al., 2015; Zhai et al., 2016). Notably, when human primordial follicles are isolated from human ovarian cortical tissue, the survival rate of culturing isolated primordial follicles is extremely low (Hovatta et al., 1997; Oktay et al., 1997); therefore, primordial follicle-based cultures need to incorporate both human ovarian cortex and not isolated primordial follicles. Because mechanical signals modulate the

activation pathway, ovarian cortical tissue containing primordial follicles was activated more quickly in flat "sheets" culture than in cube culture (Yding Andersen et al., 2019).

Currently, the commonly used IVA basal media mainly include α-MEM, D-MEM, Waymouth and McCoys 5a (Yang et al., 2020a), and researchers alter culture environment by modulating key pathways and adding small molecule compounds to improve IVC follicle number and quality.

(1) The PI3K-PTEN-AKT-FOXO3 signaling pathway is the main non-gonadotropin growth factor signaling pathway that has been agreed upon to regulate ovarian follicle growth and differentiation (Reddy et al., 2008; Li et al., 2010; Grosbois and Demeestere, 2018; Maidarti et al., 2019) (Figure 4). PI3K, consisting of a regulatory subunit (p85) and a catalytic subunit (p110), is a key factor in the reception of granulosa cell signaling in the primary oocyte membrane (Hsueh et al., 2015). PI3K-mediated signaling converges at PDK1 (Telfer and Zelinski, 2013), where PI3K in the primary oocyte membrane is stimulated by the upstream receptor complex kinase to phosphorylate phosphatidylinositol 4,5-bisphosphate (PIP2) to phosphatidylinositol 3,4,5-trisphosphate (PIP3), while PDK1 transduces the signal to free intracellular Akt, which is stimulated to phosphorylate and transmit the signal from the cell membrane to the nucleus. The follicular dormancy factor Foxo3a in the nucleus is inhibited by receiving signals from Akt and moves out of the nucleus (Hsueh et al., 2015). Upon release from the dormant inhibition of Foxo3a, primary oocytes are activated and continue to develop, thus inducing the activation of the initiating follicle development. Among them, PTEN plays a negative regulatory role in this signaling pathway and is involved in the activation and dormancy regulation of the initiating follicle by dephosphorylating PIP3 to PIP2, and inhibition of PTEN expression has a facilitative effect on the activation of the initiating follicle (Hsueh et al., 2015; Novella-Maestre et al., 2015). In 2013, scientist Kazuhiro Kawamura reported for the first time that *in vitro* addition of PI3K activator 740Y-P and PTEN inhibitor bpV (HOpic) to human ovarian tissue successfully activated the follicles of POI patients to achieve live births, opening a new paradigm of IVA for infertility treatment (Kawamura et al., 2013). Notably, more than 50% of the POI patients in this study did not contain residual follicles and did not respond to IVA drugs, limiting the use of IVA procedures in infertility treatment. In addition, PTEN inhibition affects ovarian DNA repair (Martin et al., 2019), and a process to study IVC in bovine ovarian cortex showed that PTEN inhibition activated non-growing follicles in cattle, but simultaneously increased follicular DNA damage and decreased DNA repair responses (Maidarti et al., 2019). Recently, a drug-free IVA approach has led to successful pregnancies in POI patients (Ferreri et al., 2020), which eliminates the negative effects of activators on follicles, but may also reduce follicle production sufficiently for subsequent culture.

(2) In pfGCs, mTORC1 is a key factor in the reception of follicle activation signals (Zhang et al., 2014) (Figure 4). PfGCs induce primary oocyte activation through signaling via the mTORC1-KIT ligand (KITL) signaling pathway to dormant primary oocytes (Zhang and Liu, 2015). When pfGCs are affected by changes in nutrition, oxygen concentration and growth factors, mTORC1 activity on pfGCs is enhanced and further stimulates KITL, resulting in upregulation of KITL secretion. KIT receptors on primary oocytes bind to secreted KITL and continue to stimulate PI3K in primary oocytes (Zhang and Liu, 2015), thereby activating the PI3K/PTEN/Akt signaling pathway. In primary oocytes, mTORC1 is also a regulator of dormancy and activation and is negatively regulated by a heterodimeric complex composed of the tumor suppressors Tsc1 and Tsc2 (Reddy et al., 2010). When Akt inhibits the TSC1/2 complex and subsequently inhibits downstream mTORC1 expression, resulting in reduced mTORC1 activity, the inhibited mTORC1 promotes phosphorylation of the downstream ribosomal protein S6 Kinase 1 (S6K1), which continues to stimulate downstream rpS6 and subsequently promotes primary oocyte protein translation and ribosome genesis (Adhikari et al., 2010), initiating primary oocyte development. Moreover, it has been suggested that mTORC2 is also involved in regulating Akt and thus mediating the downstream activation mechanism (Sarbassov et al., 2005).

(3) Hippo signaling pathway can be activated by cutting ovarian tissue under *in vitro* culture conditions to induce follicle activation and early development (Figure 4). In 2018, the results of J. Grosbois et al. confirmed that in chopped cultured ovarian tissue, more follicles were activated at the margins of the tissue than at the middle of the tissue and that the activation mechanism was due to the disruption of the Hippo signaling pathway by inhibition (Grosbois and Demeestere, 2018). In dormant primordial follicles, Hippo signaling pathway-mediated activation mechanisms take place mainly in pfGCs. When ovarian tissue is fragmented, contact inhibition between pfGCs at the tissue margin is released and expression of large tumor suppressor gene 1 (LATS1) in the Hippo signaling pathway increases. Highly expressed LATS1 inhibits phosphorylated YES-associated protein (YAP)/PDZ-binding domain transcriptional co-activator (TAZ) specifically expressed by pfGCs, allowing its translocation into the nucleus. Accumulation of YAP/TAZ in the nucleus enhances transcription of connective tissue growth factor (CTGF/CCN2) and baculovirus repetition 1 protein (BIRC1), both of which promote the development of pfGCs (Pan, 2007; Herta et al., 2018). The developed pfGCs then transmit signals to primary oocytes through the mTORC1-KITL signaling pathway and induce activation. After activation, GDF9 and BMP15 secreted by primary oocytes can coordinate with YAP in pfGCs to promote the phosphorylation of receptor-regulated SMAD2/3 protein. Then, it binds with co-modulating SMAD4 protein to form AP-Smad2/3/4 complex into the nucleus, which can also promote the development of pfGCs (Grosbois and Demeestere, 2018). In conclusion, Hippo signaling can cooperate with PI3K/PTEN/Akt signaling to promote the activation and development of dormant primordial follicles (Grosbois and Demeestere, 2018). Disruption of Hippo signaling pathway-mediated follicle activation has the advantage of using only physical cutting methods without the

addition of other chemicals to achieve *in vitro* activation of dormant primordial follicles, effectively reducing the *in vitro* culture time of ovarian tissue and improving the safety of the IVA technique. Usually, the regulation of PI3K/PTEN/Akt signaling pathway is accompanied by the activation of Hippo signaling pathway when implementing IVA technology, which synergistically promotes the effect of IVA.

(4) In addition to the important role of the above pathways in IVA, some studies have found that the Wnt/β-catenin signaling pathway is not only closely related to embryonic development, organogenesis and disease occurrence (Clevers and Nusse, 2012), but also related to the development and regulation of follicular granulosa cells in mammalian ovarian tissue (Li et al., 2014) (Figure 4). Wnt/β-catenin plays a role in the dormancy and activation of mammalian primordial follicles by mediating Foxo3a expression (Li et al., 2014). Like Foxo3a, p27 gene also plays a dormancy inhibitory role in primordial follicle regulation, but p27 gene and Foxo3a are regulated independently. Only when p27 gene is absent, primordial follicle is activated through PI3K/PTEN/Akt/p27 pathway (Zhang and Liu, 2015). Other studies have suggested that glycogen synthetase kinase 3 (GSK-3) also regulates primordial-follicular activation and development through the PI3K/PTEN/Akt/GSK-3 pathway (Liu et al., 2007). By stimulating mitogen activated protein kinase 3/1 (MAPK3/1), the development of primordia follicles was also activated through the mTORC1-KITL pathway (Zhao et al., 2018). E.H. Ernst et al. also analyzed the development process of human primordia follicles to primary follicles by transcriptome, and found that FOXL2 gene and FOG2 gene expression changed significantly. This indicates that FOXL2 and FOG2 genes also play important roles in the regulation of human primordial follicle activation (Ernst et al., 2018) (Figure 4).

(5) Other small molecule compounds similarly act to stimulate primordial follicle development:In α-MEM basal medium, the addition of human albumin and ITS (insulin, transferrin, selenium) is beneficial to the activation and growth of human follicles and leaves fewer atretic follicles. Meanwhile, the addition of FSH can greatly reduce the number of atretic follicles while increasing the diameter of follicles (Wright et al., 1999). Anti-mullerian hormone (AMH) may affect initiation follicle activation and follicle growth in a dose-dependent manner. Studies have found that the addition of 300 ng/mL AMH in the culture medium can promote the recruitment and activation of human follicles (Schmidt et al., 2005), while the addition of 100 ng/mL AMH inhibits follicle activation (Carlsson et al., 2006). Members of the TGF-β superfamily, such as growth differentiation factor-9 (GDF-9) and bone morphogenetic protein-15(BMP-15) (Sanfins et al., 2018) (**Figure 4**) were found to affect the cell communication between oocytes and somatic cells and promote the activation of human primordial follicle (Kedem et al., 2011). In addition, basic fibroblast growth factor (bFGF), keratinocyte growth factor (keratinocyte growth factor), KGF, leukemia inhibitory factor (LIF), stem cell factor (SCF), vascular endothelial growth factor (VEGF), VEGF and cyclic adenosine monophosphate (cAMP) have both been proved that can improve the activation and survival of cultured follicles *in vitro* (Asadi et al., 2017; Bertoldo et al., 2018). Shown in Table 1.

2.2 Follicle *in vitro* growth (IVG)

Once the follicle reaches the secondary follicle stage with multiple layers of granulosa cells, it needs to be separated from the cortex, as this would otherwise inhibit its further development (Telfer et al., 2008; Anderson et al., 2014; McLaughlin et al., 2018). Mechanical separation by fine syringe needles is now commonly used (Spears et al., 1994; Cortvrindt et al., 1996; McLaughlin et al., 2018), and this method is commonly used to obtain secondary follicles from mouse ovarian tissue, preserving the complete follicular morphology including an intact theca cell layer and a normal basement membra. However, this method is time-consuming and the production of mature follicles obtained by this method is relatively low. In order to improve the efficiency of follicle separation and for higher density of ovarian tissues such as human and bovine, the efficiency of follicle acquisition can now also be improved by enzymatic methods or a combination of enzymatic and mechanical methods (Telfer et al., 2000). Enzymes such as collagenase and DNase are commonly used to isolate growing follicles from the ovarian cortex, but these enzymes may damage follicular theca cells and may be detrimental to follicle morphology and survival (Telfer et al., 2000; Telfer et al., 2008; Kim et al., 2018; Yang et al., 2020b). However, methods such as improving the purity of enzymes can reduce the damage observed after treatment with collagenase (Dolmans et al., 2006; Rice et al., 2008). A recent study comparing the isolation efficiency of four isolation methods (two mechanical and two enzymatic methods) applied to secondary follicles in mice concluded that the mechanical method had better follicle growth, survival and MII rates, while the method using a cell isolation kit (Sigma Aldrich) was more efficient than traditional mechanical isolation (Kim et al., 2018). In general, each method is unique and requires a carefully designed isolation method based on differences in ovarian tissue of different species.

After isolation of secondary follicles, it is challenging to grow them while maintaining their normal structural state. In the previous multi-step IVC system for human follicles, the isolated secondary follicles were placed directly in 96-well V-bottomed plates without any extracellular matrix or scaffold, and the serum-free medium contained low doses of follicle stimulating hormone (FSH), activin-A, and ascorbic acid (Telfer et al., 2008; Anderson et al., 2014; McLaughlin et al., 2018). 62% of follicles completed the process of growth, differentiation and follicular antrum formation, but only 8% of follicles eventually reached the MII stage (McLaughlin et al., 2018). Growing human antral follicles to preovulatory size *in vivo* is technically challenging, and maintaining the growth of multilayered follicles *in vitro* depends on the maintenance of oocyte-somite interactions, which can be well supported by tissue engineering applications. Using biological matrix such as alginate to encase human antral follicles can support their structure and promote their growth *in vitro* (Xu et al., 2009; Shea et al., 2014; Yin et al., 2016; Jones and Shikanov, 2019). Alginate and other biological materials provide an extracellular matrix-like substance for follicles. At the same time,

TABLE 1 Additives and Operation in human follicle in IVA stage.

Additives/ Operation	Dose	Pathway/Mechanism	Effect	Author
740Y-P	150 μg/mL	PI3K/AKT activator	More follicles activated, no survival difference; Higher serum AMH	Grosbois et al. (Grosbois and Demeestere, 2018); Suzuki N et al. (Suzuki et al., 2015)
				Kawamura K (Kawamura et al., 2013) et al
bpV(HOpic)	30 μM	PTEN inhibitor	More follicles activated	Grosbois et al. (Grosbois and Demeestere, 2018); Suzuki N et al. (Suzuki et al., 2015)
				Kawamura K (Kawamura et al., 2013) et al
Cutting ovarian tissue	—	Hippo signaling pathway	Reduce the *in vitro* culture time of ovarian tissue and improve the safety of the IVA technique	Grosbois et al. (Grosbois and Demeestere, 2018)
rhAMH[a]	300 ng/mL	May rescue some follicles from entering atresia	Enhance follicles recruitment, survival and growth	Schmidt KL et al. (Schmidt et al., 2005)
rrAMH[b]	100 ng/mL	Act as a negative paracrine feedback signal	Suppress the initiation of the growth of primordial follicles, without detrimental effect on viability or follicle density	Carlsson IB et al. (Carlsson et al., 2006)
FSH	300mIU/mL	Prevent apoptotic atresia; Mitogenic function	Reduce the proportion of atretic follicles; Increase follicle size and healthy follicles	Wright CS et al. (Wright et al., 1999)
HAS + ITS	2.5% HSA; 1% ITS[c]	Promote cell proliferation; Act as free-radical scavengers	Reduce the proportion of atretic follicles; Increase follicle size and healthy follicles	Wright CS et al. (Wright et al., 1999)
GDF9	10 ng/mL	BMP15 activates the intracellular signal-mediated pathways Smad1, Smad5, and Smad8	More follicles activated; More follicles activated; increase PCNA expression	Kedem A et al. (Kedem et al., 2011)
	100 ng/mL			
BMP15	10 ng/mL	GDF9 activates Smad2 and Smad3	More follicles activated; increase PCNA expression	Kedem A et al. (Kedem et al., 2011)
	100 ng/mL			

[a]rhAMH:recombinant human anti-Mullerian hormone.
[b]rrAMH: recombinant rat anti-Mullerian hormone.
[c]HSA, human serum albumin; 1% ITS:10 mg/mL insulin, 5.5 mg/mL transferrin, and 6.7 ng/mL sodium selenite.

they have good toughness and rigidity, which can satisfy the growth and expansion of follicles while maintaining the integrity of follicle units. At the same time, the follicle and the outer medium can exchange molecules (Skory et al., 2015). Based on the physiological process that displaces follicles from the cortex to the proximal medulla during development, it has also been proposed that biomechanical features and the physical environment within the ovary affect follicle development, with follicles located in the ovarian cortex is less likely to grow due to high collagen density, while follicles located in the medulla are exposed to easier growth due to a biomechanical environment that promotes hormonal responses (Woodruff and Shea, 2011). A team showed that alginate-encapsulated follicles could reach 110 μm in diameter in culture after 30 days, but the oocytes in these follicles could not reach MII stage (Xu et al., 2009), after which the team released some of antral follicles from the alginate hydrogel and then continued to culture them in low attachment plates for 40 days. The results showed that follicles cultured with alginate only produced oocytes that either remained at the germinal vesicle (GV) stage or degenerated, whereas 20% (5/20) of the follicles cultured using the two-step strategy reached the MII stage (Xiao et al., 2015). Studies using microfluidic techniques to wrap follicles have also demonstrated the role of mechanical heterogeneity in follicle development and ovulation (Choi et al., 2014). The finding that follicle function was influenced by the physical environment of three-dimensional (3D) follicle culture when hormonal stimulation was maintained (Xu et al., 2006; West et al., 2007; West-Farrell et al., 2009) further emphasized the importance of 3D culture for the isolated follicle culture environment. A range of 3D scaffolds has been developed to support follicle growth *in vitro*, including decellularized ovarian tissue (Laronda et al., 2015; Pors et al., 2019) and 3D microporous scaffolds (Laronda et al., 2017; Liverani et al., 2019). 3D scaffolds have great potential to provide a versatile option for engineering artificial ovarian creation due to their producibility (Dolmans and Amorim, 2019; Liverani et al., 2019; Dolmans et al., 2021). The most successful current culture systems that could support the full development of mouse oocytes from the primordial oocyte stage focused exclusively on the integrity of the oocyte-granulosa cell complexes (OGCs) and promote oocyte development (O'Brien et al., 2003) without attempting to grow intact antral follicles to the preovulatory stage *in vitro*. Isolated follicles cultured alone formed antral cavities within 6–8 days, followed by the release of the OGCs therein by slight squeezing of the follicle. Complexes with complete cumulus and adherent mural granulosa cells were then selected for further growth on membranes. After this step, oocytes of at least 100 mm with meiosis potential could be obtained

TABLE 2 Additives in human follicle in IVG stage.

Additives	Dose	Mechanism	Follicles growth rate	MII rate	Author
FSH	1.5U/mL	Increase E2 production	62%	8%	McLaughlin M et al. (McLaughlin et al., 2018)
	1 ng/mL		42.7%	11%	R.A. Anderson et al. (Anderson et al., 2014)
	100 ng/mL		69.7%	—	McLaughlin et al. (McLaughlin et al., 2010)
	50 ng/mL		71.1%		
Actin-a	100 ng/mL	Regulate granulosa cell growth and differentiation	62%	8%	McLaughlin M et al. (McLaughlin et al., 2018)
			58%	30%	Evelyn E et al. (Telfer et al., 2008)
			69.7%; 71.1%	—	McLaughlin et al. (McLaughlin et al., 2010)
Ascorbic acid	50 μg/mL	Antioxidant that inhibits oocyte mitochondrial damage	62%	8%	McLaughlin M et al. (McLaughlin et al., 2018)
			42.7%	11%	R.A. Anderson et al. (Anderson et al., 2014)
			58%	30%	Evelyn E et al. (Telfer et al., 2008)
bFGF	200 ng/mL	Promote GC proliferation, suppress apoptosis in preantral follicles, and enhance early follicle cell differentiation	60%	30%	Tian-ren Wang (Wang et al., 2014)

(McLaughlin et al., 2018). The study removed oocyte complexes from surrounding cells and, further, may include transplants in women with leukemia, where IVG fertilization has previously been associated with continued transmission of cancerous cells.

Oocyte-somite interactions can also be enhanced by additive interventions (Li and Albertini, 2013). At the IVG stage, the addition of activin and low-dose FSH to IVA medium helps maintain intercellular connections, improves oocyte quality, and promotes follicle health and the formation of antrum, as demonstrated in experiments in dogs, cattle, and humans (Abir et al., 1997; Telfer et al., 2008; McLaughlin et al., 2010; McLaughlin et al., 2018). The addition of 200 ng/mL bFGF to IVG medium also promotes early follicle development in the human ovary (Wang et al., 2014). Supporting substrates or scaffolds may be beneficial, but they are not absolutely necessary to promote isolated follicle development, and the complex hormonal regulation of combined follicle growth suggests that the *in vitro* growth and development of human follicles need to address multiple challenges. More studies are needed in the future to compare different culture environments to find out which environment is most conducive to *in vitro* follicle development. Shown in Table 2.

2.3 Follicle *in vitro* maturation (IVM)

The IVM method for immature human oocytes has been in development for over 50 years (Edwards et al., 1969), but the first live birth after IVM was not reported until 1991 (Cha et al., 1991). IVM success is closely related to the oocyte source, with immature oocytes having a lower rate of successful maturation than oocytes harvested from stimulated ovaries (Nogueira et al., 2012; Chian et al., 2013). Oocytes generated during IVG must transfer to IVM medium for final meiosis and maturation. Most studies focus only on the maturation stage of oocytes, so the oocytes used in experiments are mainly from the COH cycle, while the maturation of IVG-derived oocytes has been less reported, but a review of these literature results is still helpful to optimize IVM after IVG. It was previously thought that oocyte diameter was critical for maintaining nuclear maturation and the ability to perform MII. In 2015, a study comparing alginate encapsulated culture with a two-step culture of separating follicles showed no significant difference in the diameter of oocytes that reached the MII stage and those that remained in the GV stage. This suggests that meiosis can be achieved in oocytes, although the size of the final follicle cannot reach the size of the preovulatory follicle *in vivo* (Xiao et al., 2015). In a later modified multi-step IVC system, follicular cavity formation was observed within 6–8 days after isolation of follicle culture and without waiting for follicle diameter to increase to pre-ovulation follicle level when COCs were removed for follow-up culture. Oocytes with diameters greater than 100 μm were obtained after IVM, and few oocytes developed to MII stage (McLaughlin et al., 2018). Alain Goughon (Gougeon, 1996) previously observed a 15%–24% atresia rate in human follicles with diameters between 0.9 and 2mm, and a 55%–77% atresia rate in follicles with diameters between 2 and 8 mm. The expression of FSH receptors on follicles in small sinuses was significantly higher than that in late follicular development (Jeppesen et al., 2013; Kristensen et al., 2018). The response to FSH stimulation may be enhanced and they may be

more susceptible to stimulation and less prone to atresia. These results suggest that the IVC process can be implemented more directly and efficiently based on oocyte development, rather than follicle diameter.

At the end of the IVG process, IVM is performed on the harvested oocyte-cumulus complex to support meiosis recovery to the MII site. More recently, promising progress has been made in refining and optimizing IVM regimens through the use of a biphasic system (oocytes pretreated with C-type natriuretic peptide followed by routine IVM), with recent results showing significant improvements in maturation and oocyte quality (Sanchez et al., 2019). cAMP plays a crucial role in regulating oocyte maturation. The granulosa cells in the outer layer of the follicle contain C-type natriuretic peptide (CNP), while the surface natriuretic peptide receptor (NPR2) in cumulus cells around the oocyte. And the oocyte secretes paracrine factors that can promote the activation of NPR2 in cumulus cells. CNP of granulosa cells combines with activated NPR2 to produce cyclic guanosine monophosphate (cGMP) in oocytes and inhibit the activity of phosphodiesterase (PDE3A) in oocytes. Thus, high levels of cAMP in oocytes are maintained, leading to meiotic arrest of oocytes. When the LH level rises in the blood circulation, LH activates PDE3A and then downregulates the cAMP level in oocytes, which can restore the meiosis process of immature oocytes. Subsequently, oocytes reach the MII stage and fully mature (Grzesk and Nowaczyk, 2021). Therefore, the combination therapy of silotamide (PDE3-specific inhibitor) and capillarin (adenylate cyclase activator) can control the cAMP level in the cumulus complex, synchronize the maturation process of oocyte core and cytoplasm, and improve oocyte development and subsequent embryo development (Nogueira et al., 2006; Roy et al., 2021). The application of CNP in the culture medium can improve the success rate of meiosis of oocyte IVM (Sanchez et al., 2017). In addition to cAMP level, some other factors have also been proved that can promote oocyte maturation or benefit the subsequent embryonic development process: The addition of GDF9 can significantly increase the survival rate of fertilization and blastocysts, but does not affect the maturation rate of oocytes (Chatroudi et al., 2019). Growth hormone (GH) can increase the IVM maturation rate of human oocytes (Li et al., 2019). Melatonin has no apparent effect on the maturation rate of oocytes, but it can increase the blastocyst formation rate from 24.5% to 49.3% after fertilization by protecting mitochondria (Zou et al., 2020).

Based on the current exploration of the follicular multistage IVC system, it seems promising to obtain progeny by culturing human immature follicles *in vitro*. However, the current IVC system of human follicles is still limited by low MII rate, stability of fertilization ability and low safety. Thus, future research can be optimized for the three parts of the IVC system: (1)IVA: Clarifying the safe concentration and safe exposure time of existing activators to further explore the effective way of non-toxic activation of primordial follicles; (2)IVG: Exploring the best method and timing for separating follicle cells from the cortex, and developing a 3D follicle culture system to simulate the follicle development environment *in vivo* by combining microfluidics and other tissue engineering technologies; (3)IVM: Establishing a whole-process culture system to improve the maturation rate, fertilization ability and subsequent embryo development potential of IVG-derived oocytes. In conclusion, It is necessary to conduct a large number of studies to optimize the various stages of follicle development *in vitro* and establish a relatively unified, standardized, efficient and safe culture system before applying multistage IVC technology to the clinical practice. Shown in Table 3.

3 Oogenesis, growth, and maturation induced by pluripotent stem cells (PSCs)

Utilizing pluripotent stem cells (PSCs) to induce oocytes has emerged as a new method of fertility preservation with the introduction of induced pluripotent stem cell (iPSC) technology in 2006. Since the oocytes of mice and human originate differently, mouse PSCs (mPSCs) and human PSCs (hPSCs) have slightly different induction techniques.

3.1 *In vitro* induction of mouse female oocytes by mouse PSCs

The researchers discovered that mPSCs demonstrate more potent germ cell capacity in 2iLIF medium including inhibitors of LIF and MAPK/GSK3 pathway. The subsequent induction of mPSCs in 2iLIF media including ActA, bFGF, and GMEM/KSR for 2 days resulted in the formation of ectoderm epiblast-like cells (EpiLCs). EpiLCs are appropriate precursors for producing mouse primordial germ cell like-cells (PGCLC), as they have gaenteral ectoderm cellular features (Sarma et al., 2019). About 30% of EpiLCs were transformed to PGCLCs after subsequent induction for 4–6 days under BMP4, LIF, SCF, and EGF conditions (Hayashi et al., 2011). These mouse PGCLCs displayed comparable transcriptome and epigenetic profiles to mouse PGCS, and the process of their production underwent dynamic epigenetic regulation similar to that of PGC differentiation. However, it is more challenging to promote mouse PGCLCs undergoing further differentiation. Previously, “reconstituted ovaries” were created by aggregating mouse PGCLCs with mouse female gonadal somatic cells, undergo X-reactivation, imprint erasure, and cyst formation, and exhibit meiotic potential and then transplanted under mouse ovarian bursa (Hayashi et al., 2012). Upon transplantation, mouse PGCLCs in the reconstituted ovaries mature into germinal vesicle-stage oocytes (Hayashi et al., 2012). These oocytes can develop into MII oocytes following IVM and obtain healthy fertile offspring after IVF fertilization (Hayashi et al., 2012). However, oogenesis in this method is not completely done *in vitro*. In subsequent studies, esearchers have attempted to rebuild mammalian oogenesis entirely from mouse PGC *in vitro* using an estrogen-receptor antagonist that promotes normal follicle formation, which in turn is crucial for supporting oocyte growth (Morohaku et al., 2016). The fundamental events in oogenesis (i.e., meiosis, oocyte growth, and genomic imprinting) were then reproduced in the culture system. The IVA, IVG, and IVM processes are continued after *in vitro* differentiation (IVD), and the ultimately generated MII oocytes can result in healthy and fertile offspring through IVF (Morohaku et al., 2016). Taking the above breakthroughs into account, it is not difficult to connect the entire process of *in vitro* induction of mouse

TABLE 3 Additives in human follicle in IVM stage.

Additives	Mechanism/Pathway	Effect	Author
Silotamide and capillarin	Silotamide (PDE3-specific inhibitor) and capillarin (adenylate cyclase activator)	Control the cAMP level in the cumulus complex, synchronize the maturation process of oocyte core and cytoplasm, and improve oocyte development and subsequent embryo development	Nogueira, D. et al. (Nogueira et al., 2006)
			Roy, P. K. et al. (Roy et al., 2021)
GDF-9	Induce the mitotic division of granulosa cells to suppress the FSH receptor expression those cells; Induce the expression of kit ligand mRNA in granulosa cells	Increase the survival rate of fertilization and blastocysts, but has no effect on the maturation rate of oocytes	Chatroudi, M. H. et al. (Chatroudi et al., 2019)
Growth hormone	Accelerate meiotic progression	Increase the IVM maturation rate of human oocytes	Li, Y. et al. (Li et al., 2019)
Melatonin	A potent antioxidant	has no apparent effect on the maturation rate of oocytes, but it can increase the blastocyst formation rate from 24.5% to 49.3% after fertilization by protecting mitochondria	Zou, H. et al. (Zou et al., 2020)

PSC into mouse oocytes by combining the induction of mouse PGCLC and *in vitro* oogenesis of PGC. Namely, mouse PSCs were initially differentiated into mouse EpiLCs, and then mouse PGCLCs were produced under the influence of BMP4, LIF, SCF, and EGF. Via IVD, IVA, IVG, and IVM procedures, the MII oocytes were gradually produced, undergo fertilization to produce healthy, viable offspring which show normal levels of body weight, survival rate, fertility, and gene expression (Hikabe et al., 2016).

According to the landmark study above, "reconstituted ovaries" containing female gonadal somatic cells played a vital role in promoting further oocyte differentiation (Hayashi et al., 2012; Hikabe et al., 2016). However, to clarify the unclear mechanism of oocyte differentiation, it is crucial to investigate how to induce oocytes without ovarian somatic cells. Overexpression of the pluripotency gene NANOG individually could promote the formation of PGC. NANOG is upstream of PRDM14 and BLIMP1, and NANOG binds to their enhancers (Murakami et al., 2016). Germline induction can be facilitated by the overexpression of PRDM14 alone or by the combined expression of the three germline genes BLIMP1, PRDM14, and TFAP2C (Nakaki et al., 2013). Transient overexpression of DAZL, which is required for the differentiation and growth of germ cells, can inhibit the expression of NANOG and promote the formation and meiosis progression of oocyte-like cells (Yu et al., 2009). Additionally, a cluster of transcription factors, including Nobox, Figla, Tbpl2, Sohlh1, Stat3, Dynll1, Sub1, and Lhx8 (Hamazaki et al., 2020), can encourage the development of primordial follicles into primary follicles. The primary follicles are placed in the reconstituted ovarian environment after being cultivated. Even though there was no distinct epigenetic reprogramming or meiosis process at the end, the fact that the procured oocyte-like cells could mature, fertilize, divide, and progress to the 8-cell stage also demonstrated the independence of mouse oocyte maturation, epigenetic reprogramming, and meiosis. PGCLCs can be amplified by the enhanced cAMP expression (Ohta et al., 2017). BMP and RA can commence initiation differentiation without the involvement of ovarian somatic cells since BMP2 and RA cooperate to further induce PGCLCs to differentiate into primitive oocyst-like cells that express VASA and SCP3 (Ohta et al., 2017). The discovery of the cytokines and transcription factors mentioned above provides a basis for encouraging oocyte differentiation and starting meiosis.

In conclusion, researchers have been able to induce MII oocytes from mouse PSC and obtain healthy and fertile offspring after 2 decades of effort. Both the technique of overexpressing the relevant genes by regulating the genetic level and the strategy of constructing an ovarian-like microenvironment using ovarian somatic cells were successful in generating mouse female GCs from mouse PSC. Therefore, the most effective method for inducing female GCs in mice has been recognized as the production of PGCLCs from PSCs by EpiLCs and subsequent binding of PGCLCs to mouse female gonadal somatic cells (Irie et al., 2018; Hayashi, 2019). The mechanism of female GCs can be revealed through further induction scheme optimization, which can increase the culture system's induction efficiency.

3.2 *In vitro* induction of human female oocytes by human PSCs

Treated with 4i medium (an inhibitor of MAPK, GSK3, p38, and JNK), hPSCs can be brought back to the naive stage (Gafni et al., 2013), at which hPSCs at the naive state can be exposed to TGFβ, βFGF, and LIF for 2 days in a similar method to the induction of mouse PGCLC. Then, after 8 days of induction by BMP2/4, LIF, SCF, and EGF (Irie et al., 2015), it is possible to differentiate into human PGCLCs (hPGCLCs). In a different study, hiPSCs were grown with FGF and a free-feeding layer, then stimulated for 2 days with ActA and the WNT signaling agonist (CHIR99021). The acquired cells displayed increased pluripotency and expressed mesodermal genes that corresponded to incipient mesoderm-like cells (iMeLCs) Then, for a further 4 days, it was cultured in GMEM/KSR, BMP4, LIF, SCF, and EGF to produce hPGCLCs that corresponded to the seventh week of embryonic development (Sasaki et al., 2015) In addition, Another team has accomplished the differentiation of hPSCs into hPGCLCs in a concentration-dependent manner. ActA, FGF, and low concentration (5 ng/mL) BMP4 were first utilized to convert hPSCs into mesodermal cells, and subsequently high concentration (100 ng/mL) BMP4 was used to stimulate the differentiation of mesodermal cells into hPGCLCs (Sugawa et al., 2015). The mechanism of female GCs differentiation was increasingly clarified by successful *in vitro* reconstruction of hPGCLCs, which promoted the induction of hPGCLCs differentiation in more efficient ways.

As for mice, the coculture of mouse PGCLCs with mouse female gonadal somatic cells can be applied to the next step of induction. But obtaining human female gonadal somatic cells is challenging. Therefore, it is necessary to explore an induction strategy without the coculture of human female gonadal somatic cells. According to Jung et al., overexpressing DAZL and BOULE can lead hESC to leave the pluripotent state and enter meiosis. GDF9 and BMP15 can then be added to speed up the induction of FLCs, which can subsequently express ZP2 and NOBOX and generate estradiol after implantation in the renal sac of the mouse. Currently, ovarian somatic cells are necessary for initiating oocyte differentiation due to the interaction between oocytes and somatic cells. In a recent study, researchers swapped over human embryonic ovarian cells with mouse ovarian cells and then incubated the resulting "xenorecombinant ovary" for 121 days (Yamashiro et al., 2018). The early PGC genes BLIMP1, TFAP2C, SOX17, and NANOS3 were discovered to undergo downregulation upon induction. The critical meiosis genes DMC1, H2AX, or SCP1 were not adequately upregulated during induction, while DAZL, VASA, and RA response genes (STR8 and SCP3) were. The cells inducing in "xenogeneic recombination ovary" correspond to oocytes and have DNA demethylation and imprint erasability similar to those of embryos at 10 weeks of development *in vivo*. It indicates that the cells are in the process of entering meiosis but have not yet done so, which might be a consequence of inadequate meiotic signaling in xenogeneic mouse ovarian cells. Theoretically, human ovarian somatic cells induced by hPSCs may be applied in the induction of hPGCLCs. By transplanting hipScS-induced granulosa cells into POF mice ovaries, previous research has demonstrated that these cells can secrete hormones that improve POF and promote follicle formation (Liu et al., 2016; Lipskind et al., 2018). Additionally, one of the future study objectives might be to determine whether hipScS-derived granulosa cells can be employed as substitutes for human ovarian somatic cells and combine with PGCLCs to generate recombinant ovaries to further accelerate oocyte differentiation and production.

Up to now, human oogonium-like cells have been successfully induced by constructing hiPSCs and mouse female gonadal somatic cells in "xenogenic recombinant ovary" (Yamashiro et al., 2018). These efforts and advancements offer opportunities for additional research into the genes specific to female GCs, PGCs migratory pathways, sexual differentiation, and initiation of meiosis, even if there is still a long way to go before oocytes can be utilized clinically to create fertile babies. Besides developing effective and securing protocols for the differentiation of PGCLC into genetically and epigenetically normal, patient-specific oocytes, it is now more important to identify the critical molecules that facilitate the maturation of hPGCLCs and to understand the mechanisms of the ovarian microenvironment.

Recently, genome-wide DNA methylation maps during human preimplantation development were revealed by global scale landscape sequencing of single-cell chromatin in human preimplantation embryos (Li et al., 2018), offering us some information on how humans PGC differentiation before the second week of embryonic development. Furthermore, female GCs differentiation was split into three stages, including the RA response stage, premeiotic stage, and primordial follicle stage, using single-cell transcriptome and epigenome sequencing technology (Wen and Tang, 2019). Each stage corresponded to a distinctive level of gene expression and epigenetic regulation. Single-cell methods for genome-wide DNA methylation and chromatin analysis can be employed to investigate the epigenetic regulation network of female GC at various developmental stages (Wang et al., 2019). Likewise, methods to improve the cultural environment are being researched. Recently, a redesigned approach that combines a low adhesion cell culture plate with a 3D induction system based on methylcellulose has made it feasible to induce PGCLC on a massive scale to boost production efficiency (Wang et al., 2019). The 3D artificial ovary mentioned above, except for the 3D induction system, can facilitate oocyte development. Future research will examine whether a 3D artificial ovary can provide a condition for PSC induction that is more comparable to the ovarian microenvironment *in vivo*. Ultimately, ethical issues in reproductive medicine have been receiving attention from both the scientific community and the public. Especially concerning the ethical issues expressed by the induction of GCs in human females, questions regarding stem cell origin, technical safety, clinical application of generated cells, and epigenetic regulation of offspring remain common.

Although hPSCs have not yet been properly converted into human MII oocytes, it is theoretically feasible to combine the already used approaches to produce MII oocytes *in vitro* through hPGCLCs induction, iPSC to granulosa cell induction, IVD, IVA, IVG and IVM. If the idea was successful, this will result in a breakthrough in our comprehension of the complicated biological processes involved in oocyte development, an innovative cell model for testing sterility-related drugs, and fresh perspectives on ovarian disease research and the preservation of future fertility in OC and POF patients.

4 Artificial ovary construction technology

The artificial ovaries focus on constructing biological material used to construct a stromal environment in which follicles can proliferate and ensure sex hormone secretion. This biological material should be 1) biosafety and tolerable by the human body, 2) high-temperature resistant due to the human body temperature (Chen et al., 2022), 3) liable for cell adhesion, proliferation, and differentiation, and 4) allow the dissemination of nutrients, growth factors, and oxygen. The final goal of artificial ovaries is to be retransplanted into the human body, so the tolerability and biosafety of its components are very important. Since human follicles vary greatly in diameter during growth (from 19 to 30 μm to 100–110 μm), the material should be degradable and conducive to follicle growth and migration. Furthermore, given the close signaling exchange between the follicle and the endofollicular and intrafollicular environment, this material should be highly permeable to allow diffusion of nutrients and signaling in and out of it. A number of tissue engineering materials suitable for artificial ovaries have been developed, ranging from natural materials (collagen, plasma clots, alginate, fibrin, decellularized tissue, *etc.*) to synthetic polymers (polyethylene glycol, 3D printed ovaries, *etc.*) as shown in Table 4, with encouraging results in animal research models. Laronda et al. isolated follicles from cryopreserved human ovarian tissues to form an artificial ovary and transplanted them into ovariectomized adult mice,6 out of

TABLE 4 Meterials applied in the artificial ovary construction technology.

Materials	Advantages	Disadvantages	Author	Specie	Year	Outcomes
Collagen	Plasma clots allow follicles to progress to the sinus stage	The plasma clot's poor composition and quick degradation lead to greater follicle loss	Telfe et al. (Telfer et al., 1990)	Mice	1990	The follicles could develop and mature 5 days after transplantation, and mature follicles from this grafted gel could eventually form embryos by IVF.
Plasma clots			Gosden et al. (Gosden, 1990)	Mice	1990	11 of 15 mice became pregnant and 2 produced offspring
Plasma clots			Dolmans et al. (Dolmans et al., 2007; Dolmans et al., 2008)	Human	2007	Five months after transplantation, stage II and antral follicles could be found in the clot, but the plasma clot degraded rapidly, resulting in the loss of a large number of follicles
Alginate	The rigidity prevents structural degradation	Human follicles lack alginate lyase, which would limit angiogenesis and further follicle	Rios et al. (Rios et al., 2018)	Mice	2018	Many follicles could develop into antral follicles, and mature follicles could be successfully fertilized by ICSI.
			Wang, T. R. et al. (Wang et al., 2014)	Human	2014	Human primordial follicles encapsulated in alginate gel and cultured *in vitro* for 8 days can develop, and some of them can reach the preantral stage
Fibrin	High bioadhesive properties and low inflammation after transplantation into humans	high rate of degradation and after degradation follicles lose structural support	Paulini et al. (Paulini et al., 2016)	Human	2016	Many follicles could grow to secondary follicles after 7 days
			Smith, R. M. *et al* (Smith et al., 2014)	Mice	2014	Isolated primary mouse follicles could also develop to the antral stage and hormone production can be detected
Fibrin-alginate	It has good degradability and rigidity, maintains the connection communication between the internal cells and follicle structure	—	Shikanov, A. et al. (Shikanov et al., 2009)	Mice	2009	Short-term culture of mice secondly follicle encapsulated with an interpenetrating network composed of fibrin-alginate resulted in higher oocyte MII rates than culture with alginate or fibrin alone
			Brito, I. R. et al. (Brito et al., 2016)	Goat	2016	The maturation rate of isolated caprine follicles cultured in a fibrin-alginate matrix for a longer period of time (30 days) was higher than that cultured with alginate alone
The decellularized ovarian extracellular matrix	Highly mimic the natural ovary *in vivo*, allowing for cell adhesion and growth	Xenogeneic scaffolds may induce a high risk of immune response and may also induce certain diseases, such as viruses or cells residues from the donor	Laronda et al. (Laronda et al., 2015)	Mouse follicles and decellularized bovine ovarian scaffolds	2015	After 2 weeks of transplantation, an antral follicle could be found in the transplanted scaffold
			Hassanpour et al. (Hassanpour et al., 2018)	Rat follicles and decellularized human ovary	2018	Four weeks after surgery, hormones and primordial or primary follicle-like structures were detected in this suitable cytocompatibility scaffold
			Pors et al. (Pors et al., 2019)	Human follicles and decellularized human scaffold	2019	They successfully implanted isolated human follicles in a decellularized human scaffold and reimplanted them in rats for 3 weeks

(Continued on following page)

TABLE 4 (*Continued*) Meterials applied in the artificial ovary construction technology.

Materials	Advantages	Disadvantages	Author	Specie	Year	Outcomes
Polyethylene glycol (PEG)	Synthetic polymers can be tailored to the different stiffness of natural ovaries to meet different clinical requirements	Degradation of synthetic polymers is toxic and the degradation products tend to cause immune reactions	Kim et al. (Kim et al., 2016)	Mouse	2016	All stages of follicles and corpora lutea could be found in the scaffold 30 days after transplantation
Bio-3D printing	Bio-3D printing allows precise adjustment of the pore diameter and thickness of the scaffold, and also controls properties such as rigidity of the scaffold to meet clinical needs	—	laronda et al. (Laronda et al., 2017)	Mice	2020	Mature follicles were found 3 weeks after implantation, and after 10 weeks, these transplanted mice could be mated to produce normal offspring
			Raffel, N. et al. (Raffel et al., 2019)	Pig	2019	After 10 days of *in vitro* culture, the follicles adhered well to the scaffold, developed well, and had a high survival rate
			Yoon, H. J. et al. (Yoon et al., 2021)	Rat	2021	The release of hormones that significantly aid the restoration of endocrine function can completely regenerate the endometrium

7 ovariectomized mice with artificial ovary implanted had recovered hormone cycle in 4 weeks (Laronda et al., 2015). Kniazeva et al. extracted follicles from young female mice and encapsulated them with artificial ovaries, mice for subsequent transplantation, 33% of female mice deliver offspring (Kniazeva et al., 2015). Natural polymers are usually less rigid but have advantages in cell adhesion, migration and signal communication. Synthetic polymers have better mechanical properties to support human transplantation but are not conducive to nutrient exchange and signal crosstalk (Reddy et al., 2021), and current research is directed at combining the two to better prepare artificial ovarian materials.

Collagen and plasma clots were the first natural 3D scaffolding materials used for isolated primordial follicle encapsulation. In 1990, Telfe et al. cultured isolated primary mouse follicles in collagen for 5 days and then transplanted them into ovariectomized mice; the follicles could develop and mature 5 days after transplantation, and mature follicles from this grafted gel could eventually form embryos by IVF, while sufficient hormones were produced within the grafted gel to support the vaginal opening and keratinization of the vaginal epithelium, and angiogenesis appeared in the gel as well (Telfer et al., 1990). Gosden et al. isolated primordial follicles from mice, cultured them in plasma clots, and then transplanted them back into ovariectomized mice. 11 of 15 mice became pregnant and 2 produced offspring (Gosden, 1990). Dolmans et al. isolated human primordial follicles, encapsulated them in plasma clots, and xenotransplanted them into immunodeficient mice. Five months after transplantation, stage II and antral follicles could be found in the clot, but the plasma clot degraded rapidly, resulting in the loss of a large number of follicles (Dolmans et al., 2007; Dolmans et al., 2008). Overall, plasma clots allow follicles to progress to the sinus stage, however the plasma clot's poor composition and quick degradation lead to greater follicle loss (Dolmans et al., 2007; Dolmans et al., 2008).

To address the problem of degradation, researchers developed alginate, a polysaccharide-based natural polymer derived from algae whose rigidity prevents structural degradation. Rios et al. encapsulated mouse isolated follicles into an alginate matrix and transplanted them back into ovariectomized mice. Many follicles could develop into antral follicles, and mature follicles could be successfully fertilized by intracytoplasmic sperm injection (ICSI) (Rios et al., 2018). It has been reported that isolated human primordial follicles encapsulated in alginate gel and cultured *in vitro* for 8 days can develop, and some of them can reach the preantral stage (Wang et al., 2014). However, when the culture *in vitro* last for a longer period of time (about 30 days), follicles grew to the antral stage, but many follicles degenerated and stopped growing after further incubation (Yin et al., 2016). The reason for this may be that human follicles are 2-fold larger than mice, and the lack of alginate lyase, which prevents degradation of alginate, would limit angiogenesis and further follicle (Chiti et al., 2016).

Fibrin is an alternative natural polymer to plasma colt with high bioadhesive properties and low inflammation after transplantation into humans, and has been widely used in tissue engineering. Paulini et al. encapsulated isolated human primordial follicles in fibrin gel and transplanted them into mice, and many follicles could grow to secondary follicles after 7 days (Paulini et al., 2016). Isolated primary mouse follicles cultured in fibronectin gels for long periods (21 days) could also develop to the antral stage and hormone production can be detected in mice (Smith et al., 2014). However, fibrin has the same high rate of degradation as plasma clots and collagen in humans, and after degradation follicles lose structural support due to inherent inhibitors such as fibrinolytic enzymes in humans. Follicles migrate and grow in different ovarian structures due to the different cortices and medullae of the natural ovary (Laronda, 2020). Short-term culture of mice secondly follicle encapsulated with an interpenetrating network composed of fibrin-alginate resulted in higher oocyte MII rates than culture with alginate or fibrin alone (Shikanov et al., 2009). The maturation rate of isolated caprine follicles cultured in a fibrin-alginate matrix for a longer period (30 days) was higher than that cultured with alginate alone

(Brito et al., 2016). Thus, the fibrin-alginate matrix combination has better degradability and rigidity, which facilitates follicle survival and proliferation. Moreover, to build a synthetic ovarian scaffold, slowly degrading alginate and fibrin can combine their benefits while maintaining the connection communication between the internal cells and follicle structure (Zhou et al., 2015).

The decellularized ovarian extracellular matrix is another natural matrix obtained by removing the cellular components of the natural ovary and can highly mimic the natural ovary *in vivo*, allowing for cell adhesion and growth. Decellularized tissues have been applied in the liver (Fares et al., 2021), lung (Dabaghi et al., 2021), and heart (Ercan et al., 2021). Laronda et al. implanted isolated mouse follicles into decellularized bovine ovarian scaffolds and transplanted them into immunocompetent normal ovariectomized mice. After 2 weeks of transplantation, an antral follicle could be found in the transplanted scaffold (Laronda et al., 2015). Hassanpour et al. decellularized human ovary and encapsulated it with isolated rat follicles, then reimplanted it in rats. Four weeks after surgery, hormones and primordial or primary follicle-like structures were detected in this suitable cytocompatibility scaffold (Hassanpour et al., 2018). Pors et al. also successfully implanted isolated human follicles in a decellularized human scaffold and reimplanted them in rats for 3 weeks (Pors et al., 2019). However, xenogeneic scaffolds may induce a high risk of immune response and may also induce certain diseases, such as viruses or cells residues from the donor (Massaro et al., 2021).

In contrast to natural polymers, synthetic polymers can be tailored to the different stiffness of natural ovaries to meet different clinical requirements (Dolmans and Amorim, 2019). Polyethylene glycol (PEG) is widely used in engineering, and oxygen and carbon are the main components of PEG. Kim et al. used PEG hydrogels to encapsulate isolated mouse follicles and transplant them into ovariectomized mice, and all stages of follicles and corpora lutea could be found in the scaffold 30 days after transplantation. After 60 days of transplantation, hormone levels were significantly increased and functional vessels could also be detected in the scaffold (Kim et al., 2016). In other studies, PEG-superoxide dismutase, which promotes follicle growth, has been combined with polytetrafluoroethylene membrane, which successfully prevents graft immune recognition and restores endocrine function in mice with ovariectomies (David et al., 2017). However, degradation of synthetic polymers is toxic and the degradation products tend to cause immune reactions (Shiraishi and Yokoyama, 2019).

Bio-3D printing allows precise adjustment of the pore diameter and thickness of the scaffold, and also controls properties such as rigidity of the scaffold to meet clinical needs. It can fabricate scaffolds layer by layer to produce tissue-mimicking structures (Zubizarreta and Xiao, 2020). Laronda et al. used gelatin as3D ink to print 3D scaffold crosslink with a support diameter of 250 μm and a pore diameter of 350 μm. After implanting isolated mouse follicles into 3D printed scaffolds, the scaffolds were transplanted into ovariectomized mice for 7 days after implantation without the addition of exogenous angiogenic factors. Mature follicles were found 3 weeks after implantation, and after 10 weeks, these transplanted mice could be mated to produce normal offspring (Laronda et al., 2017). It has also been reported that isolated porcine follicles were implanted in gelatin and poly (epsilon-caprolactone) (PCL)-printed scaffolds to construct scaffold structures with a pore size of 300 μm and a scaffold diameter of 1 μm. After 10 days of *in vitro* culture, the follicles adhered well to the scaffold, developed well, and had a high survival rate (Raffel et al., 2019). In terms of the crucial limitations of how vascularization can be achieved in the artificial ovary, a recent research team used 3D printing technology to create numerous microvascular channels in hydrogels. They then coated rat oocytes layer by layer with autologous granulosa cells, follicular theca cells, basal basal-like ECM, gelatin, and hydrogels with microchannels, and implanted them into the ischemic hind limbs of ovaries removed rats. The release of hormones that significantly aid the restoration of endocrine function can completely regenerate the endometrium (Yoon et al., 2021).

Growth factors play an equally important role. Growth factors such as vascular endothelial growth factor (VEGF) and basic fibroblast growth factor (bFGF) promote artificial ovarian angiogenesis and reduce apoptosis *in vivo*. Shikanov et al. encapsulated ovarian tissue with VEGF in a fibrin gel and transplanted it back into bilateral oophorectomy mice. After 2 weeks of transplantation, the VEGF-containing gel survived two times (Shikanov et al., 2011) as many follicles and blood vessels as the control group (102). In another study, ovarian tissue was also wrapped in a fibrin gel along with bFGF and then transplanted under the skin of mice. Seven days after transplantation, the bFGF group had higher follicle survival and proliferation rates, lower rates of follicular and ovarian apoptosis, and higher rates of angiogenesis compared to the non-bFGF group (Gao et al., 2013). The apoptosis suppressor sphingosine-1-phosphate (S1P) is an apoptosis suppressor capable of inducing cell survival and proliferation. It is a signaling sphingolipid that can act as an intracellular second messenger and extracellular ligand for G protein-coupled receptors. It also regulates angiogenesis and vascular stability (Soleimani et al., 2011). Soleimani et al. reported that human ovaries were transplanted with S1P into severe combined immunodeficient (SCID) mice. Ten days after transplantation, the grafts showed significantly increased vascular density, angiogenesis, and ovarian cell proliferation, and lower follicular apoptosis compared to controls (Soleimani et al., 2011). Another study implanted follicles with S1P and VEGF in a fibrin scaffold and produced twice as many primordial follicles, vessels, and progeny as controls (Ladanyi et al., 2017). Besides, the addition of platelet-derived growth factor (PDGF), BMP4 (Felder et al., 2019), and other substances can help to further increase the vascularization of the graft and the restoration of follicular activity.

Although artificial ovary technology has made tremendous progress in mice, it is still in the preliminary stages of study in large animals and humans since their grafts are much larger than those of mice in terms of size, quantity, and size of follicles. Therefore, when graft scaffold gets larger, it is an urgent problem to be solved how to design vascular channels in the scaffold or advance the vascularization (Yoon et al., 2021) of the implant with the graft scaffold growing larger while maintaining follicle vitality. The ovary's cortex and medulla have different functions, and the arrangement of the follicle and its constituent parts in space (Quan et al., 2020) will also have an impact on how well it performs. In order to maximize cell-cell interaction, enhance ovarian function,

and lengthen the implant's longevity, structure of ovary should be considered when building the ovarian organ.

5 Construction technology of ovarian organoids

Organoid technology is one of the most important breakthroughs in the area of tissue engineering research in the past decade and was rated as one of the top ten discoveries by ⟪Science⟫. It refers to the application of 3D culture technology to produce matrix glue as a growth scaffold, regulate a range of cell internal and external signals, and encourage the cells with stem cell potential to generate tissue structures resembling those derived from corresponding organs. Organoids, particularly tumor organoids, have the generally stable phenotypes and genetic properties and exhibit a high degree of histological similarity to real organs. The morphology and size of organoids among individuals remain largely uniform, in contrast to tumor cell lines and xenotransplantation models, maintaining the heterogeneity of the source tumor and the heterogeneity between patients. It offers a quick and excellent technical platform for the study of tumor pathogenesis, drug screening, personalized precision medicine, regenerative medicine, and other fields. At present, organogenesis has been reported in ovaries, fallopian tubes, endometrium, cervix and trophoblasts.

In terms of ovaries, Jung et al. (Jung et al., 2017) first established FLCs structures similar to follicular organoids by using HESCs in 2017. Four years later, Ji Wu et al. first used female germline stem cells (FGSCs) and a three-dimensional culture system to induce the generation of ovarian organoids. FGSCs were sorted by magnetic activated cell sorting (MACS) and cultured with α-MEM supplement with 10% fetal bovine serum, 10 ng/mL mouse leukemia inhibitory factor, 10 ng/mL mouse bFGF, 10 ng/mL EGF, 40 ng/mL mouse glial cell line-derived neurotrophic factor, 1 mM non-essential amino acids, 2 mM L-glutamine, 10 mg/mL penicillin, 30 mg/mL pyruvate and β-mercaptoethanol (Li et al., 2021). The ovarian organoids contained six kinds of ovarian cells, including germ cells, granulosa cells and theca cells. Oocytes could be produced and had endocrine functions. Using this model, normal mouse offspring could be produced. In addition, drug toxicity could be tested and it was found that ascorbic acid treatment had a beneficial effect on the maintenance of germ cell numbers, whereas salinomycin affects the formation of ovarian organoids and the maintenance of germ cell populations by inducing apoptosis (Li et al., 2021). Ovarian organoid model can play an important role in the study of oocyte development and screening of drugs promoting oocyte development *in vitro*. Using ovarian organoids, it was found that topologically dependent domains were stable during germ stem cell differentiation, but chromatin interactions changed in surprising ways, altering 35 percent of inactive and active chromosomal compartments throughout the genome (Luo et al., 2021). Recently, George Church et al. published a study on the directed differentiation of human iPSC cells into functional, fully human ovarian organoids, which can support oocyte maturation, follicle development and sex hormone secretion (Pierson Smela et al., 2023). The results showed that simultaneous overexpression of transcription factors NR5A1 and RUNX1/RUNX2 could induce the redifferentiation of iPSCs into granulosa cells. These granuloid cells had a transcriptome similar to that of human fetal ovarian cells. More importantly, these granuloid cells induced from human iPSCs could be co-cultured with hPGCLC also induced from human iPSCs to form ovarian organoids to aid oocyte development.

Currently, a two-step approach to bioengineering ovaries using ovarian organoids combined with artificial ovarian technology has been summarized: the first step aims to create 3D biological scaffolds, obtained mainly through whole-organ acellular technology, which can simulate the natural ovarian environment *in vitro*, allowing the maintenance of the original tissue microstructure and biological signals. The second step involves the isolation of purified FGSCs using MACS, which are capable of further differentiation when organoid techniques are used and can be used for the refilling of the ovarian acellular biological scaffold (Pennarossa et al., 2021). The combination of these two techniques provides a powerful tool for *in vitro* reconstruction of bioengineered ovaries, which may be a promising solution for restoring hormonal and reproductive function. However, the current problem is that the ability of organoids to generate oocytes *in vitro* is generally low, especially the low IVM rate (Luo et al., 2021), and it is necessary to establish a culture system that can not only effectively expand FGSCs but also maintain the uniformity of FGSCs differentiation into oocytes. Changing the culture substrate, such as water-soluble, Fzd subtype-specific "next-generation surrogate" (NGS) Wnts that hetero-dimerize Fzd and Lrp6 solves the problem of Wnt lipidation and Wnt-Frizzled (Fzd) cross-reactivity, supports the long-term expansion of many different types of organoids such as ovaries. This culture condition is considered to be superior to Wnt3a conditioned medium in organoid dilatation and single cell organoid growth (Miao et al., 2020). Recently, 3D microenvironments have been shown to trigger mitochondrial dysfunction during follicular growth *in vitro* (Takashima et al., 2021). Adding 100 nM MitoQ to the medium promotes follicular growth and maturation *in vitro* during organoid growth, while removing ROS, reducing oxidative damage, and restoring mitochondrial membrane potential in oocytes (Wang et al., 2023a). Inhibition of EED activity could promote the survival of FGSCs and significantly inhibit their apoptosis during *in vitro* differentiation. EED226 treatment and processing of FGSCs can enhance the expression of Oct4 and inhibit the expression of P53 and P63 by reducing the enrichment of H3K27me3 in Oct4 promoter and exon. Specifically improve the survival rate of FGSC (Wang et al., 2023b).

In addition to ovarian organoids, organoids of various pathological types of ovarian cancer have been reported, including epithelial ovarian cancers such as serous carcinoma, endometrioid carcinoma, clear cell carcinoma and mucous carcinoma (Kopper et al., 2019), as well as ovarian sarcoma (Phan et al., 2019) and even borderline ovarian tumor (Maru et al., 2019). The construction of ovarian organoids is shown in Table 5. Patient-derived ovarian cancer organoids can be successfully modeled in a short period and compare drug high-throughput *experimentations* in different patients, contributing to the accurate screening of anti-ovarian cancer drugs. Generally, the present cultured organoids own a simple construction, while their lack of immune cells, blood vessels, innervation, matrix, and vasculature distinguish them from real organs. Future studies will

TABLE 5 Organoids derived from healthy and pathological ovary tissues.

Tissue source	Organoid medium	Specie	Application	References
Female germline stem cells (FGSCs) from 6- or 16-week-old mice	Three-dimensional culture medium was based on Glasgow MEM supplemented with 15% Knockout serum replacement, 1.5 μM retinoic acid, 2 mM L-glutamine, 1 mM non-essential amino acids, 2 mM L-glutamine, 30 mg/mL pyruvate, 100 mM β-mercaptoethanol, 20 ng/mL mEGF, 10 ng/mL bFGF, 10 ng/mL mouse glial cell line-derived neurotrophic factor, and 10 ng/mL mouse leukemia inhibitory factor, 30 mg/mL penicillin, and 75 mg/mL streptomycin. The α-MEM-based medium was α-MEM supplemented with 2% FBS, 2 mM L-glutamine, 100–300 μM ascorbic acid, 20 ng/mL mEGF, 50 mM β-mercaptoethanol, 30 mg/mL penicillin and 75 mg/mL streptomycin. StemPro-34-based medium was StemPro-34 SFM supplemented with 10% FBS, 2 mM L-glutamine, 100–300 μM ascorbic acid, 20 ng/mL mEGF, 50 mM β-mercaptoethanol, 30 mg/mL penicillin, and 75 mg/mL streptomycin, and 800 nM ICI182780 was used depending on the experimental context	Mice	Production of oocytes and offspring; Secretion of hormones; drug toxicological detection	Li et al. (2021)
Spermatogonial stem cells (SSCs) were isolated from Testes of 6-day-old pou5f1-GFP transgenic mice or pou5f1/GFP transgenic mice × C57BL/6 F1 hybrid mice FGSCs were isolated and purified from ovaries collected from 5-day-old pou5f1/GFP transgenic mice × C57BL/6 F1 hybrid mice	GMEM supplemented with 15% Knockout serum replacement, 1.5 μM retinoic acid, 2 mM L-glutamine, 1 mM non-essential amino acids, 2 mM L-glutamine, 30 mg/mL pyruvate, 100 mM β-mercaptoethanol, 30 mg/L penicillin, and 75 mg/L streptomycin.The α-MEM supplemented with 2% FBS, 2 mM L-glutamine, 200 μM ascorbic acid, 50 mM β-mercaptoethanol, 30 mg/lpenicillin, and 75 mg/L streptomycin. The StemPro-34 SFM supplemented with 10% FBS, 2 mM L-glutamine, 200 μM ascorbic acid, 50 mM β-mercaptoethanol, 30 mg/L penicillin, and 75 mg/L streptomycin. From 7 to 10 days of culture, 800 nM ICI182780 was added to the StemPro-34-based medium. At 11 days of culture, the culture medium was changed to StemPro-34-based medium without ICI182780	Mice	Production successful offspring; These findings have important implications in various areas including mammalian gametogenesis, genetic and epigenetic reprogramming, biotechnology, and medicine	Luo et al. (2021)
BXS0115 hiPSC line	STO-conditioned medium (Glasgow Minimum Essential Medium [GMEM] with 13% KSR and 1× non-essential amino acids, sodium pyruvate, and GlutaMax), supplemented with 100 ng/mL stem cell factor (SCF), 50 μg/mL ascorbic acid, and 25 μM 2-mercaptoethanol GK15 medium (GMEM, 15% KSR, with 1× GlutaMax, sodium pyruvate, and non-essential amino acids) supplemented with 10 mM Y-27632, 0.1 mM 2-mercaptoethanol, 1 μg/mL doxycycline, 100 ng/mL SCF, and 50 μg/mL primocin Alpha Minimum Essential Medium, 10% KSR, 55 μM 2-mercaptoethanol, 500 ng/mL doxycycline, and 50 μg/mL primocin	Human	Provide unique opportunities for studying human ovarian biology and may enable the development of therapies for female reproductive health	Pierson Smela et al. (2023)
Human ovarian samples	AdDE+++[a] supplement with 50% v/v Wnt3aCM, Noggin, Rspo1, B27 (50x), 500 mM N-Acetylcysteine, Primocin, 1M Nicotinamide, 5 mM A83-01, 100 μg/mL Fgf10, 75 μg/mL Heregulinβ-1, 100 mM Y27632, 500 μg/mL EGF, 10 mM Forskolin, 250 μg/mL Hydrocortisone, 100 μM β-Estradiol	Human	NGS Wnts offer a unified organoid expansion protocol and a laboratory "tool kit" for dissecting the functions of Fzd subtypes in stem cell biology	Miao et al. (2020)

(Continued on following page)

TABLE 5 (*Continued*) Organoids derived from healthy and pathological ovary tissues.

Tissue source	Organoid medium	Specie	Application	References
Human ovarian cancer, fallopian tube and ovarian surface epithelium	AdDE+++[a] supplement with WNT (CM), Noggin, Rspo1, B27 (50x), 500 mM N-Acetylcysteine, Primocin, 1M Nicotinamide, 5 mM A83-01, 100 μg/mL Fgf10, 75 μg/mL Heregulinβ-1, 100 mM Y27632, 500 μg/mL EGF, 10 mM Forskolin, 250 μg/mL Hydrocortisone, 100 μM β-Estradiol	Human	Drug-screening assays; *in vivo* drug-sensitivity assays	Kopper et al. (2019)
FGSCs isolate from ovaries of 1–3 dpp female mice	GK15+ RA medium (Glasgow MEM supplemented with 15% Knockout serum replacement, 1.5 μM retinoic acid, 2 mM Glutamax, 1 mM MEM non-essential amino acids, 1 mM Sodium Pyruvate, 100 mM β-mercaptoethanol, 20 ng/mL EGF, 10 ng/mL bFGF, 10 ng/mL GDNF, 10 ng/mL LIF, and 100 IU/mL Penicillin-streptomycin). α-MEM-based medium (α-MEM supplemented with 2% FBS, 2 mM Glutamax, 100 μM ascorbic acid, 20 ng/mL EGF, 50 mM β-mercaptoethanol and 100 IU/mL penicillin-streptomycin) and StemPro-34-based medium (StemPro34 SFM supplemented with 10% FBS, 2 mM Glutamax, 100 μM ascorbic acid, 20 ng/mL EGF, 50 mM β-mercaptoethanol, 800 nM ICI182780, 100 IU/mL penicillin-streptomycin)	Mice	Basic research; pre-clinical drug screening	Wang et al. (2023a)
FGSCs isolate from ovaries of 1–3 dpp female mice	GK15+ RA medium (Glasgow MEM supplemented with 15% Knockout serum replacement, 1.5 μM retinoic acid, 2 mM Glutamax, 1 mM MEM non-essential amino acids, 1 mM Sodium Pyruvate, 100 mM β-mercaptoethanol, 20 ng/mL EGF, 10 ng/mL bFGF, 10 ng/mL GDNF, 10 ng/mL LIF, and 100 IU/mL Penicillin-streptomycin)	Mice	Establish a culture system that effectively expands FGSCs *in vitro*	Wang et al. (2023b)
Ovarian, peritoneal high-grade serous carcinomas, carcinosarcoma	AdDE+++[a] supplement with WNT (CM), Noggin, Rspo1, B27 (50x), 500 mM N-Acetylcysteine, Primocin, 1M Nicotinamide, 5 mM A83-01, 100 μg/mL Fgf10, 75 μg/mL Heregulinβ-1, 100 mM Y27632, 500 μg/mL EGF, 10 mM Forskolin, 250 μg/mL Hydrocortisone, 100 μM β-Estradiol	Human	Drug development; personalized medicine applications	Phan et al. (2019)

[a]AdDE+++:Advanced DMEM/F12 containing 1x Glutamax, 10 mM HEPES, and Pen Strep.

concentrate on how to create a tumor microenvironment in an *in vitro* culture system. The recently reported gas-liquid interface culture (Ye et al., 2020) and microfluidic technology (Li et al., 2017) will make it possible to co-culture organoids with immune cells and mesenchymal cells, advancing the study of organoids in immunotherapy. Besides, organoid development will be greatly accelerated by other innovations, such as refining the composition of culture medium, reducing the variety of culture conditions, using CRISPR/Cas9 gene editing technology, RNA-seq technology, bioprinting, and organoids-on-chips technology.

6 Summary and outlook

In conclusion, the ovarian organ function reconstruction techniques *in vitro* rebuilding technique can offer a fresh perspective on the study of ovaria-related disorders and fertility preservation in patients with cancers and POF. Future development direction in fertility preservation would focus on IVC, female GCs induction from PSC *in vitro*, artificial ovary construction, and ovaria-related organoids construction, all of which have promising futures. However, there are still problems to be resolved, including how to increase the primordial follicle maturation rate, establish a productive culture system with 3D technology, maintain the viability of follicles, build artificial human ovaries, and induce hPGCLCs to undergo meiosis. The construction of ovarian organoids is still a new method for ovarian reconstruction. However, it is extremely difficult to obtain human ovarian stem cells, so it is necessary to establish a single culture system that can efficiently expand FGSCs and maintain the differentiation of FGSCs into oocytes, and effectively improve the IVM rate of oocytes by combining with IVC technology. Organoid construction of ovarian cancer provides ideas for the study of the

pathogenesis, drug screening and individualized therapy, gene function and immunotherapy of ovarian cancer. Meanwhile, the construction of tumor microenvironment of patient-derived tumor organoids should be further increased to reflect the specific situation more truly. Despite the numerous challenges, it is reasonable to assume that with the continued development of tissue engineering, new replacement options will eventually appear to offer new solutions to solve human reproductive problems like fertility preservation and ovarian diseases.

Author contributions

Conceptualization, SL and CS, literature search, BH, RW, DW, and JR, literature collation and analysis, BH, manuscript writing, BH, manuscript modification, SL, DM, and CS, resources, SL, DM, LJ, and CS. All authors listed have made a substantial, direct, and intellectual contribution to the work and approved it for publication. All authors contributed to the article and approved the submitted version.

Funding

The National Natural Science Foundation of China (81672085); The Hubei Provincial Natural Science Foundation of China (2019CFA062); Reproductive Health Fund of Huiling Stem Cell Innovation Institute (FIRMSCOV05); Gynecological tumor special research Fund of Beijing Kanghua Traditional Chinese and Western Medicine Development Foundation (KH-2021-LLZX-074); National Medical Professional Postgraduate Education Steering Committee research topic (B2-YX20190502-01); Open Fund of State Key Laboratory of Reproductive Medicine (SKLRM-K201802).

Conflict of interest

The authors declare that the research was conducted in the absence of any commercial or financial relationships that could be construed as a potential conflict of interest.

Publisher's note

All claims expressed in this article are solely those of the authors and do not necessarily represent those of their affiliated organizations, or those of the publisher, the editors and the reviewers. Any product that may be evaluated in this article, or claim that may be made by its manufacturer, is not guaranteed or endorsed by the publisher.

References

Abir, R., Franks, S., Mobberley, M. A., Moore, P. A., Margara, R. A., and Winston, R. M. (1997). Mechanical isolation and *in vitro* growth of preantral and small antral human follicles. *Fertil. Steril.* 68, 682–688. doi:10.1016/s0015-0282(97)00264-1

Adhikari, D., Zheng, W., Shen, Y., Gorre, N., Hämäläinen, T., Cooney, A. J., et al. (2010). Tsc/mTORC1 signaling in oocytes governs the quiescence and activation of primordial follicles. *Hum. Mol. Genet.* 19, 397–410. doi:10.1093/hmg/ddp483

Anderson, R. A., McLaughlin, M., Wallace, W. H., Albertini, D. F., and Telfer, E. E. (2014). The immature human ovary shows loss of abnormal follicles and increasing follicle developmental competence through childhood and adolescence. *Hum. Reprod.* 29, 97–106. doi:10.1093/humrep/det388

Asadi, E., Najafi, A., Moeini, A., Pirjani, R., Hassanzadeh, G., Mikaeili, S., et al. (2017). Ovarian tissue culture in the presence of VEGF and fetuin stimulates follicle growth and steroidogenesis. *J. Endocrinol.* 232, 205–219. doi:10.1530/JOE-16-0368

Bertoldo, M. J., Walters, K. A., Ledger, W. L., Gilchrist, R. B., Mermillod, P., and Locatelli, Y. (2018). *In-vitro* regulation of primordial follicle activation: Challenges for fertility preservation strategies. *Reprod. Biomed. Online* 36, 491–499. doi:10.1016/j.rbmo.2018.01.014

Brito, I. R., Silva, G. M., Sales, A. D., Lobo, C. H., Rodrigues, G. Q., Sousa, R. F., et al. (2016). Fibrin-alginate hydrogel supports steroidogenesis, *in vitro* maturation of oocytes and parthenotes production from caprine preantral follicles cultured in group. *Reprod. Domest. Anim.* 51, 997–1009. doi:10.1111/rda.12779

Carlsson, I. B., Scott, J. E., Visser, J. A., Ritvos, O., Themmen, A. P. N., and Hovatta, O. (2006). Anti-Mullerian hormone inhibits initiation of growth of human primordial ovarian follicles *in vitro*. *Hum. Reprod.* 21, 2223–2227. doi:10.1093/humrep/del165

Cha, K. Y., Koo, J. J., Ko, J. J., Choi, D. H., Han, S. Y., and Yoon, T. K. (1991). Pregnancy after *in vitro* fertilization of human follicular oocytes collected from nonstimulated cycles, their culture *in vitro* and their transfer in a donor oocyte program. *Fertil. Steril.* 55, 109–113. doi:10.1016/s0015-0282(16)54068-0

Chatroudi, M. H., Khalili, M. A., Ashourzadeh, S., Anbari, F., Shahedi, A., and Safari, S. (2019). Growth differentiation factor 9 and cumulus cell supplementation in *in vitro* maturation culture media enhances the viability of human blastocysts. *Clin. Exp. Reprod. Med.* 46, 166–172. doi:10.5653/cerm.2019.00402

Chen, J., Todorov, P., Isachenko, E., Rahimi, G., Mallmann, P., and Isachenko, V. (2022). Construction and cryopreservation of an artificial ovary in cancer patients as an element of cancer therapy and a promising approach to fertility restoration. *Hum. Fertil. (Camb)* 25, 651–661. doi:10.1080/14647273.2021.1885756

Chen, Y., Yang, W., Shi, X., Zhang, C., Song, G., and Huang, D. (2020). The factors and pathways regulating the activation of mammalian primordial follicles *in vivo*. *Front. Cell Dev. Biol.* 8, 575706. doi:10.3389/fcell.2020.575706

Chian, R. C., Uzelac, P. S., and Nargund, G. (2013). *In vitro* maturation of human immature oocytes for fertility preservation. *Fertil. Steril.* 99, 1173–1181. doi:10.1016/j.fertnstert.2013.01.141

Chiti, M. C., Dolmans, M. M., Orellana, O., Soares, M., Paulini, F., Donnez, J., et al. (2016). Influence of follicle stage on artificial ovary outcome using fibrin as a matrix. *Hum. Reprod.* 31, 2898. doi:10.1093/humrep/dew254

Choi, J. K., Agarwal, P., Huang, H., Zhao, S., and He, X. (2014). The crucial role of mechanical heterogeneity in regulating follicle development and ovulation with engineered ovarian microtissue. *Biomaterials* 35, 5122–5128. doi:10.1016/j.biomaterials.2014.03.028

Clevers, H., and Nusse, R. (2012). Wnt/β-catenin signaling and disease. *Cell* 149, 1192–1205. doi:10.1016/j.cell.2012.05.012

Cortvrindt, R., Smitz, J., and Van Steirteghem, A. C. (1996). *In-vitro* maturation, fertilization and embryo development of immature oocytes from early preantral follicles from prepuberal mice in a simplified culture system. *Hum. Reprod.* 11, 2656–2666. doi:10.1093/oxfordjournals.humrep.a019188

Dabaghi, M., Saraei, N., Carpio, M. B, Nanduri, V., Ungureanu, J., Babi, M., et al. (2021). A robust protocol for decellularized human lung bioink generation amenable to 2D and 3D lung cell culture. *Cells* 10 (6), 1538. doi:10.3390/cells10061538

David, A., Day, J. R., Cichon, A. L., Lefferts, A., Cascalho, M., and Shikanov, A. (2017). Restoring ovarian endocrine function with encapsulated ovarian allograft in immune competent mice. *Ann. Biomed. Eng.* 45, 1685–1696. doi:10.1007/s10439-016-1780-6

Dinas, K. D. (2020). Impact of breast cancer treatment on fertility. *Adv. Exp. Med. Biol.* 1252, 175–179. doi:10.1007/978-3-030-41596-9_24

Dolmans, M. M., and Amorim, C. A. (2019). Fertility preservation: Construction and use of artificial ovaries. *Reproduction* 158, F15–F25. doi:10.1530/REP-18-0536

Dolmans, M. M., Donnez, J., and Cacciottola, L. (2021). Fertility preservation: The challenge of freezing and transplanting ovarian tissue. *Trends Mol. Med.* 27, 777–791. doi:10.1016/j.molmed.2020.11.003

Dolmans, M. M., Martinez-Madrid, B., Gadisseux, E., Guiot, Y., Yuan, W. Y., Torre, A., et al. (2007). Short-term transplantation of isolated human ovarian follicles and cortical tissue into nude mice. *Reproduction* 134, 253–262. doi:10.1530/REP-07-0131

Dolmans, M. M., Michaux, N., Camboni, A., Martinez-Madrid, B., Van Langendonckt, A., Nottola, S. A., et al. (2006). Evaluation of Liberase, a purified

enzyme blend, for the isolation of human primordial and primary ovarian follicles. *Hum. Reprod.* 21, 413–420. doi:10.1093/humrep/dei320

Dolmans, M. M., Yuan, W. Y., Camboni, A., Torre, A., Van Langendonckt, A., Martinez-Madrid, B., et al. (2008). Development of antral follicles after xenografting of isolated small human preantral follicles. *Reprod. Biomed. Online* 16, 705–711. doi:10.1016/s1472-6483(10)60485-3

Edwards, R. G., Bavister, B. D., and Steptoe, P. C. (1969). Early stages of fertilization *in vitro* of human oocytes matured *in vitro*. *Nature* 221, 632–635. doi:10.1038/221632a0

Ercan, H., Elcin, A. E., and Elcin, Y. M. (2021). Preliminary assessment of an injectable extracellular matrix from decellularized bovine myocardial tissue. *Z Naturforsch C J. Biosci.* 76, 491–501. doi:10.1515/znc-2021-0039

Ernst, E. H., Franks, S., Hardy, K., Villesen, P., and Lykke-Hartmann, K. (2018). Granulosa cells from human primordial and primary follicles show differential global gene expression profiles. *Hum. Reprod.* 33, 666–679. doi:10.1093/humrep/dey011

Fares, A. E., Gabr, H., ShamsEldeen, A. M., Farghali, H. A. M., Rizk, M. M. S. M., Mahmoud, B. E., et al. (2021). Implanted subcutaneous versus intraperitoneal bioscaffold seeded with hepatocyte-like cells: Functional evaluation. *Stem Cell Res. Ther.* 12, 441. doi:10.1186/s13287-021-02531-2

Felder, S., Masasa, H., Orenbuch, A., Levaot, N., Shachar Goldenberg, M., and Cohen, S. (2019). Reconstruction of the ovary microenvironment utilizing macroporous scaffold with affinity-bound growth factors. *Biomaterials* 205, 11–22. doi:10.1016/j.biomaterials.2019.03.013

Ferreri, J., Fàbregues, F., Calafell, J. M., Solernou, R., Borrás, A., Saco, A., et al. (2020). Drug-free *in-vitro* activation of follicles and fresh tissue autotransplantation as a therapeutic option in patients with primary ovarian insufficiency. *Reprod. Biomed. Online* 40, 254–260. doi:10.1016/j.rbmo.2019.11.009

Frances-Herrero, E., Lopez, R., Hellström, M., de Miguel-Gómez, L., Herraiz, S., Brännström, M., et al. (2022). Bioengineering trends in female reproduction: A systematic review. *Hum. Reprod. Update* 28, 798–837. doi:10.1093/humupd/dmac025

Gafni, O., Weinberger, L., Mansour, A. A., Manor, Y. S., Chomsky, E., Ben-Yosef, D., et al. (2013). Derivation of novel human ground state naive pluripotent stem cells. *Nature* 504, 282–286. doi:10.1038/nature12745

Gao, J. M., Yan, J., Li, R., Li, M., Yan, L. Y., Wang, T. R., et al. (2013). Improvement in the quality of heterotopic allotransplanted mouse ovarian tissues with basic fibroblast growth factor and fibrin hydrogel. *Hum. Reprod.* 28 (10), 2784–2793. doi:10.1093/humrep/det296

Garcia-Alonso, L., Lorenzi, V., Mazzeo, C. I., Alves-Lopes, J. P., Roberts, K., Sancho-Serra, C., et al. (2022). Single-cell roadmap of human gonadal development. *Nature* 607, 540–547. doi:10.1038/s41586-022-04918-4

Gershenson, D. M. (2019). Management of rare epithelial ovarian cancers. *Clin. Adv. Hematol. Oncol.* 17, 444–446.

Gosden, R. G. (1990). Restitution of fertility in sterilized mice by transferring primordial ovarian follicles. *Hum. Reprod.* 5, 499–504. doi:10.1093/oxfordjournals.humrep.a137132

Gougeon, A. (1996). Regulation of ovarian follicular development in primates: Facts and hypotheses. *Endocr. Rev.* 17, 121–155. doi:10.1210/edrv-17-2-121

Grosbois, J., and Demeestere, I. (2018). Dynamics of PI3K and Hippo signaling pathways during *in vitro* human follicle activation. *Hum. Reprod.* 33, 1705–1714. doi:10.1093/humrep/dey250

Grzesk, G., and Nowaczyk, A. (2021). Current modulation of guanylate cyclase pathway activity-mechanism and clinical implications. *Molecules* 26, 3418. doi:10.3390/molecules26113418

Hamazaki, N., Kyogoku, H., Araki, H., Miura, F., Horikawa, C., Hamada, N., et al. (2020). Reconstitution of the oocyte transcriptional network with transcription factors. *Nature* 589, 264–269. doi:10.1038/s41586-020-3027-9

Hassanpour, A., Talaei-Khozani, T., Kargar-Abarghouei, E., Razban, V., and Vojdani, Z. (2018). Decellularized human ovarian scaffold based on a sodium lauryl ester sulfate (SLES)-treated protocol, as a natural three-dimensional scaffold for construction of bioengineered ovaries. *Stem Cell Res. Ther.* 9, 252. doi:10.1186/s13287-018-0971-5

Hayashi, K. (2019). *In vitro* reconstitution of germ cell development†. *Biol. Reprod.* 101, 567–578. doi:10.1093/biolre/ioz111

Hayashi, K., Ogushi, S., Kurimoto, K., Shimamoto, S., Ohta, H., and Saitou, M. (2012). Offspring from oocytes derived from *in vitro* primordial germ cell-like cells in mice. *Science* 338, 971–975. doi:10.1126/science.1226889

Hayashi, K., Ohta, H., Kurimoto, K., Aramaki, S., and Saitou, M. (2011). Reconstitution of the mouse germ cell specification pathway in culture by pluripotent stem cells. *Cell* 146, 519–532. doi:10.1016/j.cell.2011.06.052

Herta, A. C., Lolicato, F., and Smitz, J. E. J. (2018). *In vitro* follicle culture in the context of IVF. *Reproduction* 156, F59–F73. doi:10.1530/REP-18-0173

Hikabe, O., Hamazaki, N., Nagamatsu, G., Obata, Y., Hirao, Y., Hamada, N., et al. (2016). Reconstitution *in vitro* of the entire cycle of the mouse female germ line. *Nature* 539, 299–303. doi:10.1038/nature20104

Hovatta, O., Silye, R., Abir, R., Krausz, T., and Winston, R. M. (1997). Extracellular matrix improves survival of both stored and fresh human primordial and primary ovarian follicles in long-term culture. *Hum. Reprod.* 12, 1032–1036. doi:10.1093/humrep/12.5.1032

Hsueh, A. J., Kawamura, K., Cheng, Y., and Fauser, B. C. (2015). Intraovarian control of early folliculogenesis. *Endocr. Rev.* 36, 1–24. doi:10.1210/er.2014-1020

Irie, N., Sybirna, A., and Surani, M. A. (2018). What can stem cell models tell us about human germ cell biology? *Curr. Top. Dev. Biol.* 129, 25–65. doi:10.1016/bs.ctdb.2018.02.010

Irie, N., Weinberger, L., Tang, W. W. C., Kobayashi, T., Viukov, S., Manor, Y. S., et al. (2015). SOX17 is a critical specifier of human primordial germ cell fate. *Cell* 160, 253–268. doi:10.1016/j.cell.2014.12.013

Jeppesen, J. V., Anderson, R. A., Kelsey, T. W., Christiansen, S. L., Kristensen, S. G., Jayaprakasan, K., et al. (2013). Which follicles make the most anti-mullerian hormone in humans? Evidence for an abrupt decline in AMH production at the time of follicle selection. *Mol. Hum. Reprod.* 19, 519–527. doi:10.1093/molehr/gat024

Jones, A. S. K., and Shikanov, A. (2019). Follicle development as an orchestrated signaling network in a 3D organoid. *J. Biol. Eng.* 13, 2. doi:10.1186/s13036-018-0134-3

Jung, D., Xiong, J., Ye, M., Qin, X., Li, L., Cheng, S., et al. (2017). *In vitro* differentiation of human embryonic stem cells into ovarian follicle-like cells. *Nat. Commun.* 8, 15680. doi:10.1038/ncomms15680

Kawamura, K., Cheng, Y., Suzuki, N., Deguchi, M., Sato, Y., Takae, S., et al. (2013). Hippo signaling disruption and Akt stimulation of ovarian follicles for infertility treatment. *Proc. Natl. Acad. Sci. U. S. A.* 110, 17474–17479. doi:10.1073/pnas.1312830110

Kedem, A., Fisch, B., Garor, R., Ben-Zaken, A., Gizunterman, T., Felz, C., et al. (2011). Growth differentiating factor 9 (GDF9) and bone morphogenetic protein 15 both activate development of human primordial follicles *in vitro*, with seemingly more beneficial effects of GDF9. *J. Clin. Endocrinol. Metab.* 96, E1246–E1254. doi:10.1210/jc.2011-0410

Kim, E. J., Lee, J., Youm, H. W., Kim, S. K., Lee, J. R., Suh, C. S., et al. (2018). Comparison of follicle isolation methods for mouse ovarian follicle culture *in vitro*. *Reprod. Sci.* 25, 1270–1278. doi:10.1177/1933719117737851

Kim, J., Perez, A. S., Claflin, J., David, A., Zhou, H., and Shikanov, A. (2016). Synthetic hydrogel supports the function and regeneration of artificial ovarian tissue in mice. *NPJ Regen. Med.* 1, 16010. doi:10.1038/npjregenmed.2016.10

Kniazeva, E., Hardy, A. N., Boukaidi, S. A., Woodruff, T. K., Jeruss, J. S., and Shea, L. D. (2015). Primordial follicle transplantation within designer biomaterial grafts produce live births in a mouse infertility model. *Sci. Rep.* 5, 17709. doi:10.1038/srep17709

Kopper, O., de Witte, C. J., Lõhmussaar, K., Valle-Inclan, J. E., Hami, N., Kester, L., et al. (2019). An organoid platform for ovarian cancer captures intra- and interpatient heterogeneity. *Nat. Med.* 25, 838–849. doi:10.1038/s41591-019-0422-6

Kristensen, S. G., Liu, Q., Mamsen, L. S., Greve, T., Pors, S. E., Bjørn, A. B., et al. (2018). A simple method to quantify follicle survival in cryopreserved human ovarian tissue. *Hum. Reprod.* 33, 2276–2284. doi:10.1093/humrep/dey318

Ladanyi, C., Mor, A., Christianson, M. S., Dhillon, N., and Segars, J. H. (2017). Recent advances in the field of ovarian tissue cryopreservation and opportunities for research. *J. Assist. Reprod. Genet.* 34, 709–722. doi:10.1007/s10815-017-0899-1

Langer, R., and Vacanti, J. (2016). Advances in tissue engineering. *J. Pediatr. Surg.* 51, 8–12. doi:10.1016/j.jpedsurg.2015.10.022

Laronda, M. M. (2020). Engineering a bioprosthetic ovary for fertility and hormone restoration. *Theriogenology* 150, 8–14. doi:10.1016/j.theriogenology.2020.01.021

Laronda, M. M., Jakus, A. E., Whelan, K. A., Wertheim, J. A., Shah, R. N., and Woodruff, T. K. (2015). Initiation of puberty in mice following decellularized ovary transplant. *Biomaterials* 50, 20–29. doi:10.1016/j.biomaterials.2015.01.051

Laronda, M. M., Rutz, A. L., Xiao, S., Whelan, K. A., Duncan, F. E., Roth, E. W., et al. (2017). A bioprosthetic ovary created using 3D printed microporous scaffolds restores ovarian function in sterilized mice. *Nat. Commun.* 8, 15261. doi:10.1038/ncomms15261

Li, J., Kawamura, K., Cheng, Y., Liu, S., Klein, C., Liu, S., et al. (2010). Activation of dormant ovarian follicles to generate mature eggs. *Proc. Natl. Acad. Sci. U. S. A.* 107, 10280–10284. doi:10.1073/pnas.1001198107

Li, L., Guo, F., Gao, Y., Ren, Y., Yuan, P., Yan, L., et al. (2018). Single-cell multi-omics sequencing of human early embryos. *Nat. Cell Biol.* 20, 847–858. doi:10.1038/s41556-018-0123-2

Li, L., Ji, S. Y., Yang, J. L., Li, X. X., Zhang, J., Zhang, Y., et al. (2014). Wnt/β-catenin signaling regulates follicular development by modulating the expression of Foxo3a signaling components. *Mol. Cell Endocrinol.* 382, 915–925. doi:10.1016/j.mce.2013.11.007

Li, R., and Albertini, D. F. (2013). The road to maturation: Somatic cell interaction and self-organization of the mammalian oocyte. *Nat. Rev. Mol. Cell Biol.* 14, 141–152. doi:10.1038/nrm3531

Li, S. S., Ip, C. K., Tang, M. Y., Sy, S. K., Yung, S., Chan, T. M., et al. (2017). Modeling ovarian cancer multicellular spheroid behavior in a dynamic 3D peritoneal microdevice. *J. Vis. Exp.* (120), 55337. doi:10.3791/55337

Li, X., Zheng, M., Xu, B., Li, D., Shen, Y., Nie, Y., et al. (2021). Generation of offspring-producing 3D ovarian organoids derived from female germline stem cells and their

application in toxicological detection. *Biomaterials* 279, 121213. doi:10.1016/j.biomaterials.2021.121213

Li, Y., Liu, H., Yu, Q., Liu, H., Huang, T., Zhao, S., et al. (2019). Growth hormone promotes *in vitro* maturation of human oocytes. *Front. Endocrinol. (Lausanne)* 10, 485. doi:10.3389/fendo.2019.00485

Lipskind, S., Lindsey, J. S., Gerami-Naini, B., Eaton, J. L., O'Connell, D., Kiezun, A., et al. (2018). An embryonic and induced pluripotent stem cell model for ovarian granulosa cell development and steroidogenesis. *Reprod. Sci.* 25, 712–726. doi:10.1177/1933719117725814

Liu, L., Rajareddy, S., Reddy, P., Jagarlamudi, K., Du, C., Shen, Y., et al. (2007). Phosphorylation and inactivation of glycogen synthase kinase-3 by soluble kit ligand in mouse oocytes during early follicular development. *J. Mol. Endocrinol.* 38, 137–146. doi:10.1677/jme.1.02027

Liu, T., Li, Q., Wang, S., Chen, C., and Zheng, J. (2016). Transplantation of ovarian granulosa-like cells derived from human induced pluripotent stem cells for the treatment of murine premature ovarian failure. *Mol. Med. Rep.* 13, 5053–5058. doi:10.3892/mmr.2016.5191

Liverani, L., Raffel, N., Fattahi, A., Preis, A., Hoffmann, I., Boccaccini, A. R., et al. (2019). Electrospun patterned porous scaffolds for the support of ovarian follicles growth: A feasibility study. *Sci. Rep.* 9, 1150. doi:10.1038/s41598-018-37640-1

Luo, H., Li, X., Tian, G. G., Li, D., Hou, C., Ding, X., et al. (2021). Offspring production of ovarian organoids derived from spermatogonial stem cells by defined factors with chromatin reorganization. *J. Adv. Res.* 33, 81–98. doi:10.1016/j.jare.2021.03.006

Maidarti, M., Clarkson, Y. L., McLaughlin, M., Anderson, R. A., and Telfer, E. E. (2019). Inhibition of PTEN activates bovine non-growing follicles *in vitro* but increases DNA damage and reduces DNA repair response. *Hum. Reprod.* 34, 297–307. doi:10.1093/humrep/dey354

Martin, J. H., Aitken, R. J., Bromfield, E. G., and Nixon, B. (2019). DNA damage and repair in the female germline: Contributions to ART. *Hum. Reprod. Update* 25, 180–201. doi:10.1093/humupd/dmy040

Maru, Y., Tanaka, N., Itami, M., and Hippo, Y. (2019). Efficient use of patient-derived organoids as a preclinical model for gynecologic tumors. *Gynecol. Oncol.* 154, 189–198. doi:10.1016/j.ygyno.2019.05.005

Massaro, M. S., Pálek, R., Rosendorf, J., Červenková, L., Liška, V., and Moulisová, V. (2021). Decellularized xenogeneic scaffolds in transplantation and tissue engineering: Immunogenicity versus positive cell stimulation. *Mater Sci. Eng. C Mater Biol. Appl.* 127, 112203. doi:10.1016/j.msec.2021.112203

McLaughlin, M., Albertini, D. F., Wallace, W. H. B., Anderson, R. A., and Telfer, E. E. (2018). Metaphase II oocytes from human unilaminar follicles grown in a multi-step culture system. *Mol. Hum. Reprod.* 24, 135–142. doi:10.1093/molehr/gay002

McLaughlin, M., Bromfield, J. J., Albertini, D. F., and Telfer, E. E. (2010). Activin promotes follicular integrity and oogenesis in cultured pre-antral bovine follicles. *Mol. Hum. Reprod.* 16, 644–653. doi:10.1093/molehr/gaq021

Miao, Y., Ha, A., de Lau, W., Yuki, K., Santos, A. J. M., You, C., et al. (2020). Next-generation surrogate Wnts support organoid growth and deconvolute frizzled pleiotropy *in vivo*. *Cell Stem Cell* 27, 840–851. doi:10.1016/j.stem.2020.07.020

Mochida, N., Akatani-Hasegawa, A., Saka, K., Ogino, M., Hosoda, Y., Wada, R., et al. (2013). Live births from isolated primary/early secondary follicles following a multistep culture without organ culture in mice. *Reproduction* 146, 37–47. doi:10.1530/REP-13-0020

Morohaku, K., Tanimoto, R., Sasaki, K., Kawahara-Miki, R., Kono, T., Hayashi, K., et al. (2016). Complete *in vitro* generation of fertile oocytes from mouse primordial germ cells. *Proc. Natl. Acad. Sci. U. S. A.* 113, 9021–9026. doi:10.1073/pnas.1603817113

Murakami, K., Günesdogan, U., Zylicz, J. J., Tang, W. W. C., Sengupta, R., Kobayashi, T., et al. (2016). NANOG alone induces germ cells in primed epiblast *in vitro* by activation of enhancers. *Nature* 529, 403–407. doi:10.1038/nature16480

Nakaki, F., Hayashi, K., Ohta, H., Kurimoto, K., Yabuta, Y., and Saitou, M. (2013). Induction of mouse germ-cell fate by transcription factors *in vitro*. *Nature* 501, 222–226. doi:10.1038/nature12417

Nogueira, D., Ron-El, R., Friedler, S., Schachter, M., Raziel, A., Cortvrindt, R., et al. (2006). Meiotic arrest *in vitro* by phosphodiesterase 3-inhibitor enhances maturation capacity of human oocytes and allows subsequent embryonic development. *Biol. Reprod.* 74, 177–184. doi:10.1095/biolreprod.105.040485

Nogueira, D., Sadeu, J. C., and Montagut, J. (2012). *In vitro* oocyte maturation: Current status. *Semin. Reprod. Med.* 30, 199–213. doi:10.1055/s-0032-1311522

Novella-Maestre, E., Herraiz, S., Rodriguez-Iglesias, B., Diaz-Garcia, C., and Pellicer, A. (2015). Short-term PTEN inhibition improves *in vitro* activation of primordial follicles, preserves follicular viability, and restores AMH levels in cryopreserved ovarian tissue from cancer patients. *PLoS One* 10, e0127786. doi:10.1371/journal.pone.0127786

O'Brien, M. J., Pendola, J. K., and Eppig, J. J. (2003). A revised protocol for *in vitro* development of mouse oocytes from primordial follicles dramatically improves their developmental competence. *Biol. Reprod.* 68, 1682–1686. doi:10.1095/biolreprod.102.013029

Ohta, H., Kurimoto, K., Okamoto, I., Nakamura, T., Yabuta, Y., Miyauchi, H., et al. (2017). *In vitro* expansion of mouse primordial germ cell-like cells recapitulates an epigenetic blank slate. *EMBO J.* 36, 1888–1907. doi:10.15252/embj.201695862

Oktay, K., Nugent, D., Newton, H., Salha, O., Chatterjee, P., and Gosden, R. G. (1997). Isolation and characterization of primordial follicles from fresh and cryopreserved human ovarian tissue. *Fertil. Steril.* 67, 481–486. doi:10.1016/s0015-0282(97)80073-8

Pan, D. (2007). Hippo signaling in organ size control. *Genes Dev.* 21, 886–897. doi:10.1101/gad.1536007

Paulini, F., Vilela, J. M. V., Chiti, M. C., Donnez, J., Jadoul, P., Dolmans, M. M., et al. (2016). Survival and growth of human preantral follicles after cryopreservation of ovarian tissue, follicle isolation and short-term xenografting. *Reprod. Biomed. Online* 33, 425–432. doi:10.1016/j.rbmo.2016.05.003

Pennarossa, G., Ghiringhelli, M., Gandolfi, F., and Brevini, T. A. L. (2021). Creation of a bioengineered ovary: Isolation of female germline stem cells for the repopulation of a decellularized ovarian bioscaffold. *Methods Mol. Biol.* 2273, 139–149. doi:10.1007/978-1-0716-1246-0_9

Phan, N., Hong, J. J., Tofig, B., Mapua, M., Elashoff, D., Moatamed, N. A., et al. (2019). A simple high-throughput approach identifies actionable drug sensitivities in patient-derived tumor organoids. *Commun. Biol.* 2, 78. doi:10.1038/s42003-019-0305-x

Pierson Smela, M. D., Kramme, C. C., Fortuna, P. R. J., Adams, J. L., Su, R., Dong, E., et al. (2023). Directed differentiation of human iPSCs to functional ovarian granulosa-like cells via transcription factor overexpression. *Elife* 12, e83291. doi:10.7554/eLife.83291

Pors, S. E., Ramløse, M., Nikiforov, D., Lundsgaard, K., Cheng, J., Andersen, C. Y., et al. (2019). Initial steps in reconstruction of the human ovary: Survival of pre-antral stage follicles in a decellularized human ovarian scaffold. *Hum. Reprod.* 34, 1523–1535. doi:10.1093/humrep/dez077

Quan, N., Mara, J. N., Grover, A. R., Pavone, M. E., and Duncan, F. E. (2020). Spatial analysis of growing follicles in the human ovary to inform tissue engineering strategies. *Tissue Eng. Part A* 26, 733–746. doi:10.1089/ten.tea.2020.0051

Raffel, N., Dittrich, R., Bäuerle, T., Seyler, L., Fattahi, A., Hoffmann, I., et al. (2019). Novel approach for the assessment of ovarian follicles infiltration in polymeric electrospun patterned scaffolds. *PLoS One* 14, e0215985. doi:10.1371/journal.pone.0215985

Reddy, M. S. B., Ponnamma, D., Choudhary, R., and Sadasivuni, K. K. (2021). A comparative review of natural and synthetic biopolymer composite scaffolds. *Polym. (Basel)* 13, 1105. doi:10.3390/polym13071105

Reddy, P., Liu, L., Adhikari, D., Jagarlamudi, K., Rajareddy, S., Shen, Y., et al. (2008). Oocyte-specific deletion of Pten causes premature activation of the primordial follicle pool. *Science* 319, 611–613. doi:10.1126/science.1152257

Reddy, P., Zheng, W., and Liu, K. (2010). Mechanisms maintaining the dormancy and survival of mammalian primordial follicles. *Trends Endocrinol. Metab.* 21, 96–103. doi:10.1016/j.tem.2009.10.001

Rice, S., Ojha, K., and Mason, H. (2008). Human ovarian biopsies as a viable source of pre-antral follicles. *Hum. Reprod.* 23, 600–605. doi:10.1093/humrep/dem390

Rios, P. D., Kniazeva, E., Lee, H. C., Xiao, S., Oakes, R. S., Saito, E., et al. (2018). Retrievable hydrogels for ovarian follicle transplantation and oocyte collection. *Biotechnol. Bioeng.* 115, 2075–2086. doi:10.1002/bit.26721

Roy, P. K., Qamar, A. Y., Tanga, B. M., Fang, X., Kim, G., Bang, S., et al. (2021). Enhancing oocyte competence with milrinone as a phosphodiesterase 3A inhibitor to improve the development of porcine cloned embryos. *Front. Cell Dev. Biol.* 9, 647616. doi:10.3389/fcell.2021.647616

Sanchez, F., Le, A. H., Ho, V. N. A., Romero, S., Van Ranst, H., De Vos, M., et al. (2019). Biphasic *in vitro* maturation (CAPA-IVM) specifically improves the developmental capacity of oocytes from small antral follicles. *J. Assist. Reprod. Genet.* 36, 2135–2144. doi:10.1007/s10815-019-01551-5

Sanchez, F., Lolicato, F., Romero, S., De Vos, M., Van Ranst, H., Verheyen, G., et al. (2017). An improved IVM method for cumulus-oocyte complexes from small follicles in polycystic ovary syndrome patients enhances oocyte competence and embryo yield. *Hum. Reprod.* 32, 2056–2068. doi:10.1093/humrep/dex262

Sanfins, A., Rodrigues, P., and Albertini, D. F. (2018). GDF-9 and BMP-15 direct the follicle symphony. *J. Assist. Reprod. Genet.* 35, 1741–1750. doi:10.1007/s10815-018-1268-4

Sarbassov, D. D., Guertin, D. A., Ali, S. M., and Sabatini, D. M. (2005). Phosphorylation and regulation of Akt/PKB by the rictor-mTOR complex. *Science* 307, 1098–1101. doi:10.1126/science.1106148

Sarma, U. C., Findlay, J. K., and Hutt, K. J. (2019). Oocytes from stem cells. *Best. Pract. Res. Clin. Obstet. Gynaecol.* 55, 14–22. doi:10.1016/j.bpobgyn.2018.07.006

Sasaki, K., Yokobayashi, S., Nakamura, T., Okamoto, I., Yabuta, Y., Kurimoto, K., et al. (2015). Robust *in vitro* induction of human germ cell fate from pluripotent stem cells. *Cell Stem Cell* 17, 178–194. doi:10.1016/j.stem.2015.06.014

Schmidt, K. L., Kryger-Baggesen, N., Byskov, A. G., and Andersen, C. Y. (2005). Anti-Mullerian hormone initiates growth of human primordial follicles *in vitro*. *Mol. Cell Endocrinol.* 234, 87–93. doi:10.1016/j.mce.2004.12.010

Sciorio, R., and Anderson, R. A. (2020). Fertility preservation and preimplantation genetic assessment for women with breast cancer. *Cryobiology* 92, 1–8. doi:10.1016/j.cryobiol.2019.12.001

Shea, L. D., Woodruff, T. K., and Shikanov, A. (2014). Bioengineering the ovarian follicle microenvironment. *Annu. Rev. Biomed. Eng.* 16, 29–52. doi:10.1146/annurev-bioeng-071813-105131

Shikanov, A., Xu, M., Woodruff, T. K., and Shea, L. D. (2009). Interpenetrating fibrin-alginate matrices for *in vitro* ovarian follicle development. *Biomaterials* 30, 5476–5485. doi:10.1016/j.biomaterials.2009.06.054

Shikanov, A., Zhang, Z., Xu, M., Smith, R. M., Rajan, A., Woodruff, T. K., et al. (2011). Fibrin encapsulation and vascular endothelial growth factor delivery promotes ovarian graft survival in mice. *Tissue Eng. Part A* 17, 3095–3104. doi:10.1089/ten.TEA.2011.0204

Shiraishi, K., and Yokoyama, M. (2019). Toxicity and immunogenicity concerns related to PEGylated-micelle carrier systems: A review. *Sci. Technol. Adv. Mater* 20, 324–336. doi:10.1080/14686996.2019.1590126

Skory, R. M., Xu, Y., Shea, L. D., and Woodruff, T. K. (2015). Engineering the ovarian cycle using *in vitro* follicle culture. *Hum. Reprod.* 30, 1386–1395. doi:10.1093/humrep/dev052

Smith, R. M., Shikanov, A., Kniazeva, E., Ramadurai, D., Woodruff, T. K., and Shea, L. D. (2014). Fibrin-mediated delivery of an ovarian follicle pool in a mouse model of infertility. *Tissue Eng. Part A* 20, 3021–3030. doi:10.1089/ten.TEA.2013.0675

Soleimani, R., Heytens, E., and Oktay, K. (2011). Enhancement of neoangiogenesis and follicle survival by sphingosine-1-phosphate in human ovarian tissue xenotransplants. *PLoS One* 6, e19475. doi:10.1371/journal.pone.0019475

Spears, N., Boland, N. I., Murray, A. A., and Gosden, R. G. (1994). Mouse oocytes derived from *in vitro* grown primary ovarian follicles are fertile. *Hum. Reprod.* 9, 527–532. doi:10.1093/oxfordjournals.humrep.a138539

Sugawa, F., Araúzo-Bravo, M. J., Yoon, J., Kim, K. P., Aramaki, S., Wu, G., et al. (2015). Human primordial germ cell commitment *in vitro* associates with a unique PRDM14 expression profile. *EMBO J.* 34, 1009–1024. doi:10.15252/embj.201488049

Suzuki, N., Yoshioka, N., Takae, S., Sugishita, Y., Tamura, M., Hashimoto, S., et al. (2015). Successful fertility preservation following ovarian tissue vitrification in patients with primary ovarian insufficiency. *Hum. Reprod.* 30, 608–615. doi:10.1093/humrep/deu353

Takashima, T., Fujimaru, T., and Obata, Y. (2021). Effect of *in vitro* growth on mouse oocyte competency, mitochondria and transcriptome. *Reproduction* 162, 307–318. doi:10.1530/REP-21-0209

Telfer, E. E., Binnie, J. P., McCaffery, F. H., and Campbell, B. K. (2000). *In vitro* development of oocytes from porcine and bovine primary follicles. *Mol. Cell Endocrinol.* 163, 117–123. doi:10.1016/s0303-7207(00)00216-1

Telfer, E. E. (2019). Fertility preservation: Progress and prospects for developing human immature oocytes *in vitro*. *Reproduction* 158, F45–F54. doi:10.1530/REP-19-0077

Telfer, E. E. (2019). Future developments: *In vitro* growth (IVG) of human ovarian follicles. *Acta Obstet. Gynecol. Scand.* 98, 653–658. doi:10.1111/aogs.13592

Telfer, E. E., McLaughlin, M., Ding, C., and Thong, K. J. (2008). A two-step serum-free culture system supports development of human oocytes from primordial follicles in the presence of activin. *Hum. Reprod.* 23, 1151–1158. doi:10.1093/humrep/den070

Telfer, E. E., Sakaguchi, K., Clarkson, Y. L., and McLaughlin, M. (2019). *In vitro* growth of immature bovine follicles and oocytes. *Reprod. Fertil. Dev.* 32, 1–6. doi:10.1071/RD19270

Telfer, E. E., and Zelinski, M. B. (2013). Ovarian follicle culture: Advances and challenges for human and nonhuman primates. *Fertil. Steril.* 99, 1523–1533. doi:10.1016/j.fertnstert.2013.03.043

Telfer, E., Torrance, C., and Gosden, R. G. (1990). Morphological study of cultured preantral ovarian follicles of mice after transplantation under the kidney capsule. *J. Reprod. Fertil.* 89, 565–571. doi:10.1530/jrf.0.0890565

Wang, J., Du, H., Ma, L., Feng, M., Li, L., Zhao, X., et al. (2023). MitoQ protects ovarian organoids against oxidative stress during oogenesis and folliculogenesis *in vitro*. *Int. J. Mol. Sci.* 24 (2), 924. doi:10.3390/ijms24020924

Wang, J., Fang, J., Feng, M., Li, L., Ma, L., Zhao, X., et al. (2023). Inhibition of EED activity enhances cell survival of female germline stem cell and improves the oocytes production during oogenesis *in vitro*. *Open Biol.* 13 (1), 220211. doi:10.1098/rsob.220211

Wang, T. R., Yan, L. y., Yan, J., Lu, C. l., Xia, X., Yin, T. l., et al. (2014). Basic fibroblast growth factor promotes the development of human ovarian early follicles during growth *in vitro*. *Hum. Reprod.* 29, 568–576. doi:10.1093/humrep/det465

Wang, X., Liao, T., Wan, C., Yang, X., Zhao, J., Fu, R., et al. (2019). Efficient generation of human primordial germ cell-like cells from pluripotent stem cells in a methylcellulose-based 3D system at large scale. *PeerJ* 6, e6143. doi:10.7717/peerj.6143

Wen, L., and Tang, F. (2019). Human germline cell development: From the perspective of single-cell sequencing. *Mol. Cell* 76, 320–328. doi:10.1016/j.molcel.2019.08.025

West, E. R., Xu, M., Woodruff, T. K., and Shea, L. D. (2007). Physical properties of alginate hydrogels and their effects on *in vitro* follicle development. *Biomaterials* 28, 4439–4448. doi:10.1016/j.biomaterials.2007.07.001

West-Farrell, E. R., Xu, M., Gomberg, M. A., Chow, Y. H., Woodruff, T. K., and Shea, L. D. (2009). The mouse follicle microenvironment regulates antrum formation and steroid production: Alterations in gene expression profiles. *Biol. Reprod.* 80, 432–439. doi:10.1095/biolreprod.108.071142

Woodruff, T. K., and Shea, L. D. (2011). A new hypothesis regarding ovarian follicle development: Ovarian rigidity as a regulator of selection and health. *J. Assist. Reprod. Genet.* 28, 3–6. doi:10.1007/s10815-010-9478-4

Wright, C. S., Hovatta, O., Margara, R., Trew, G., Winston, R. M., Franks, S., et al. (1999). Effects of follicle-stimulating hormone and serum substitution on the *in-vitro* growth of human ovarian follicles. *Hum. Reprod.* 14, 1555–1562. doi:10.1093/humrep/14.6.1555

Xiao, S., Zhang, J., Romero, M. M., Smith, K. N., Shea, L. D., and Woodruff, T. K. (2015). *In vitro* follicle growth supports human oocyte meiotic maturation. *Sci. Rep.* 5, 17323. doi:10.1038/srep17323

Xu, F., Lawson, M. S., Bean, Y., Ting, A. Y., Pejovic, T., De Geest, K., et al. (2021). Matrix-free 3D culture supports human follicular development from the unilaminar to the antral stage *in vitro* yielding morphologically normal metaphase II oocytes. *Hum. Reprod.* 36, 1326–1338. doi:10.1093/humrep/deab003

Xu, J., Lawson, M. S., Yeoman, R. R., Molskness, T. A., Ting, A. Y., Stouffer, R. L., et al. (2013). Fibrin promotes development and function of macaque primary follicles during encapsulated three-dimensional culture. *Hum. Reprod.* 28, 2187–2200. doi:10.1093/humrep/det093

Xu, M., Barrett, S. L., West-Farrell, E., Kondapalli, L. A., Kiesewetter, S. E., Shea, L. D., et al. (2009). *In vitro* grown human ovarian follicles from cancer patients support oocyte growth. *Hum. Reprod.* 24, 2531–2540. doi:10.1093/humrep/dep228

Xu, M., West, E., Shea, L. D., and Woodruff, T. K. (2006). Identification of a stage-specific permissive *in vitro* culture environment for follicle growth and oocyte development. *Biol. Reprod.* 75, 916–923. doi:10.1095/biolreprod.106.054833

Yamashiro, C., Sasaki, K., Yabuta, Y., Kojima, Y., Nakamura, T., Okamoto, I., et al. (2018). Generation of human oogonia from induced pluripotent stem cells *in vitro*. *Science* 362, 356–360. doi:10.1126/science.aat1674

Yang, Q., Zhu, L., and Jin, L. (2020). Human follicle *in vitro* culture including activation, growth, and maturation: A review of research progress. *Front. Endocrinol. (Lausanne)* 11, 548. doi:10.3389/fendo.2020.00548

Yang, Y., Kanno, C., Sakaguchi, K., Katagiri, S., Yanagawa, Y., and Nagano, M. (2020). Theca cells can support bovine oocyte growth *in vitro* without the addition of steroid hormones. *Theriogenology* 142, 41–47. doi:10.1016/j.theriogenology.2019.09.037

Yding Andersen, C., Mamsen, L. S., and Kristensen, S. G. (2019). Fertility preservation: Freezing of ovarian tissue and clinical opportunities. *Reproduction* 158, F27–F34. doi:10.1530/REP-18-0635

Ye, W., Luo, C., Li, C., Huang, J., and Liu, F. (2020). Organoids to study immune functions, immunological diseases and immunotherapy. *Cancer Lett.* 477, 31–40. doi:10.1016/j.canlet.2020.02.027

Yin, H., Kristensen, S. G., Jiang, H., Rasmussen, A., and Andersen, C. Y. (2016). Survival and growth of isolated pre-antral follicles from human ovarian medulla tissue during long-term 3D culture. *Hum. Reprod.* 31, 1531–1539. doi:10.1093/humrep/dew049

Yoon, H. J., Lee, Y. J., Baek, S., Chung, Y. S., Kim, D. H., Lee, J. H., et al. (2021). Hormone autocrination by vascularized hydrogel delivery of ovary spheroids to rescue ovarian dysfunctions. *Sci. Adv.* 7, eabe8873. doi:10.1126/sciadv.abe8873

Yu, Z., Ji, P., Cao, J., Zhu, S., Li, Y., Zheng, L., et al. (2009). Dazl promotes germ cell differentiation from embryonic stem cells. *J. Mol. Cell Biol.* 1, 93–103. doi:10.1093/jmcb/mjp026

Zhai, J., Yao, G., Dong, F., Bu, Z., Cheng, Y., Sato, Y., et al. (2016). *In vitro* activation of follicles and fresh tissue auto-transplantation in primary ovarian insufficiency patients. *J. Clin. Endocrinol. Metab.* 101, 4405–4412. doi:10.1210/jc.2016-1589

Zhang, H., and Liu, K. (2015). Cellular and molecular regulation of the activation of mammalian primordial follicles: Somatic cells initiate follicle activation in adulthood. *Hum. Reprod. Update* 21, 779–786. doi:10.1093/humupd/dmv037

Zhang, H., Risal, S., Gorre, N., Busayavalasa, K., Li, X., Shen, Y., et al. (2014). Somatic cells initiate primordial follicle activation and govern the development of dormant oocytes in mice. *Curr. Biol.* 24, 2501–2508. doi:10.1016/j.cub.2014.09.023

Zhao, Y., Zhang, Y., Li, J., Zheng, N., Xu, X., Yang, J., et al. (2018). MAPK3/1 participates in the activation of primordial follicles through mTORC1-KITL signaling. *J. Cell Physiol.* 233, 226–237. doi:10.1002/jcp.25868

Zhou, H., Malik, M. A., Arab, A., Hill, M. T., and Shikanov, A. (2015). Hydrogel based 3-dimensional (3D) system for toxicity and high-throughput (HTP) analysis for cultured murine ovarian follicles. *PLoS One* 10, e0140205. doi:10.1371/journal.pone.0140205

Zou, H., Chen, B., Ding, D., Gao, M., Chen, D., Liu, Y., et al. (2020). Melatonin promotes the development of immature oocytes from the COH cycle into healthy offspring by protecting mitochondrial function. *J. Pineal Res.* 68, e12621. doi:10.1111/jpi.12621

Zubizarreta, M. E., and Xiao, S. (2020). Bioengineering models of female reproduction. *Biodes Manuf.* 3, 237–251. doi:10.1007/s42242-020-00082-8

frontiers | Frontiers in Physiology

TYPE Original Research
PUBLISHED 18 May 2023
DOI 10.3389/fphys.2023.1166827

OPEN ACCESS

EDITED BY
Gendie Lash,
Guangzhou Medical University, China

REVIEWED BY
Céline Aguer,
McGill University, Canada
Perrie O'Tierney-Ginn,
Tufts Medical Center, United States

*CORRESPONDENCE
Shiao-Yng Chan,
obgchan@nus.edu.sg

†These authors have contributed equally to this work

RECEIVED 21 February 2023
ACCEPTED 04 May 2023
PUBLISHED 18 May 2023

CITATION
Yong HEJ, Watkins OC, Mah TKL, Cracknell-Hazra VKB, Pillai RA, Selvam P, Islam MO, Sharma N, Cazenave-Gassiot A, Bendt AK, Wenk MR, Godfrey KM, Lewis RM and Chan S-Y (2023), Increasing maternal age associates with lower placental *CPT1B* mRNA expression and acylcarnitines, particularly in overweight women. *Front. Physiol.* 14:1166827. doi: 10.3389/fphys.2023.1166827

Increasing maternal age associates with lower placental *CPT1B* mRNA expression and acylcarnitines, particularly in overweight women

Hannah E. J. Yong[1†], Oliver C. Watkins[2†], Tania K. L. Mah[1], Victoria K. B. Cracknell-Hazra[1,3], Reshma Appukuttan Pillai[2], Preben Selvam[2], Mohammad O. Islam[2], Neha Sharma[2], Amaury Cazenave-Gassiot[4,5], Anne K. Bendt[5], Markus R. Wenk[4,5], Keith M. Godfrey[3,6], Rohan M. Lewis[3,7] and Shiao-Yng Chan[1,2]*

[1]Singapore Institute for Clinical Sciences (SICS), Agency for Science, Technology and Research (A*STAR), Singapore, Singapore, [2]Department of Obstetrics and Gynaecology, Yong Loo Lin School of Medicine, National University of Singapore, Singapore, Singapore, [3]NIHR Southampton Biomedical Research Centre, University of Southampton and University Hospital Southampton NHS Foundation Trust, Southampton, United Kingdom, [4]Department of Biochemistry and Precision Medicine Translational Research Programme, Yong Loo Lin School of Medicine, National University of Singapore, Singapore, Singapore, [5]Singapore Lipidomics Incubator, Life Sciences Institute, National University of Singapore, Singapore, Singapore, [6]MRC Lifecourse Epidemiology Centre, University of Southampton, Southampton, United Kingdom, [7]Institute of Developmental Sciences, Faculty of Medicine, University of Southampton, Southampton, United Kingdom

Older pregnant women have increased risks of complications including gestational diabetes and stillbirth. Carnitine palmitoyl transferase (CPT) expression declines with age in several tissues and is linked with poorer metabolic health. Mitochondrial CPTs catalyze acylcarnitine synthesis, which facilitates fatty acid oxidization as fuel. We hypothesized that the placenta, containing maternally-inherited mitochondria, shows an age-related CPT decline that lowers placental acylcarnitine synthesis, increasing vulnerability to pregnancy complications. We assessed *CPT1A*, *CPT1B*, *CPT1C* and *CPT2* mRNA expression by qPCR in 77 placentas and quantified 10 medium and long-chain acylcarnitines by LC-MS/MS in a subset of 50 placentas. Older maternal age associated with lower expression of placental *CPT1B*, but not *CPT1A*, *CPT1C* or *CPT2*. *CPT1B* expression positively associated with eight acylcarnitines and *CPT1C* with three acylcarnitines, *CPT1A* negatively associated with nine acylcarnitines, while *CPT2* did not associate with any acylcarnitine. Older maternal age associated with reductions in five acylcarnitines, only in those with BMI≥ 25 kg/m^2, and not after adjusting for *CPT1B* expression. Our findings suggest that *CPT1B* is the main transferase for placental long-chain acylcarnitine synthesis, and age-related *CPT1B* decline may underlie decreased placental metabolic flexibility, potentially contributing to pregnancy complications in older women, particularly if they are overweight.

KEYWORDS

placenta, maternal age, lipid metabolism, carnitine palmitoyltransferases, obesity, overweight, CPT1B

1 Introduction

More women are entering pregnancy at an older age worldwide, particularly in developed countries. These women are at increased risk of pregnancy complications including gestational diabetes, pre-eclampsia and stillbirth (Flenady et al., 2011; Lean et al., 2017; Saccone et al., 2022). Nonetheless, the mechanistic pathways by which older age contributes to adverse pregnancy outcomes are still unclear (Huang et al., 2008; Plows et al., 2018). It is thus important to examine potential mechanisms by which advanced maternal age might affect pregnancy outcomes to aid development of strategies to reduce risk.

Outside of pregnancy, several studies have reported that expression and activity of carnitine palmitoyltransferases (CPTs) decline with age in multiple tissues and that these changes associate with poorer metabolic health. Aging is associated with decreased CPT1 activity in rodent hearts (McMillin et al., 1993; Odiet et al., 1995), where the predominant CPT1 isoform is CPT1B. In mice, genetically-induced deficiency or age-associated reduction of skeletal muscle CPT1B expression leads to the development of insulin resistance provoked by a high fat diet challenge (Kim et al., 2014; Vieira-Lara et al., 2021). Such relationships are consistent with a study in elderly humans showing that higher skeletal *CPT1B* mRNA expression associated with insulin sensitivity and better metabolic health (Bétry et al., 2019). A negative association of CPT1 expression with age is also observed in peripheral blood mononuclear cells (Karlic et al., 2003).

CPTs catalyze the synthesis of acylcarnitines from fatty-acyl CoAs, a process essential to facilitate the transport of fatty acids into mitochondria for fatty acid oxidation (also known as beta oxidation), and for the production of acylcarnitines for cellular use, secretion and signaling (Ceccarelli et al., 2011; Houten et al., 2020). CPTs are expressed in most tissues with the ratios of isoforms dependent on the tissue type and species (Ceccarelli et al., 2011; Houten et al., 2020). CPT1 and CPT2 are present on the outer and inner mitochondrial membrane respectively and together enable fatty acids to be transported across the mitochondrial membrane as acylcarnitines for utilization (Ceccarelli et al., 2011; Houten et al., 2020). CPT1 is the main regulator of fatty acid oxidation and occurs as three isoforms—CPT1A, CPT1B and CPT1C; their individual characteristics remain under investigation (Ceccarelli et al., 2011; Virmani et al., 2015; Houten et al., 2020). CPTs are also active in peroxisomes and the endoplasmic reticulum, but their role in these organelles is not well understood (Sierra et al., 2008; Ceccarelli et al., 2011; Houten et al., 2020).

In the placenta, CPTs are important for generating acylcarnitines, for use locally as well as for release into both fetal and maternal circulations to serve as both a fuel source and a precursor of activated fatty acids for lipid remodeling and protein palmitoylation (Novak et al., 1981; Schmidt-Sommerfeld et al., 1985; Arduini et al., 1992; Arduini et al., 1994; Lahjouji et al., 2004; Jones et al., 2010). These exported acylcarnitines act as signaling molecules, anti-oxidants and as an alternative fetal fuel source to glucose (Jones et al., 2010; Yli and Kjellmer, 2016; Kolb et al., 2021). Hence, acylcarnitine supply is vital to the fetus when glucose and oxygen supply is limited and when anaerobic metabolism and oxidative stress is high such as during parturition (Jones et al., 2010; Yli and Kjellmer, 2016; Kolb et al., 2021). Indeed, increased umbilical cord blood acylcarnitines are associated with both extremes of birthweight (Giannacopoulou et al., 1998; Sánchez-Pintos et al., 2016; El-Wahed et al., 2017; Sánchez-Pintos et al., 2017), where there is often either a lack or oversupply of nutrients relative to fetal needs.

Therefore, given that developmentally, mitochondria in conceptuses and, hence, placental mitochondrial CPTs are maternally-inherited, we hypothesized that a maternal age-related decline in placental CPT expression and activity may contribute to the development of pregnancy adversity. As an initial step, our study aimed to determine the relationship between maternal age and the placental expression of four CPT isoforms, and associated alterations in placental acylcarnitine abundance.

2 Materials and methods

2.1 Subject recruitment and placental collection

Placentas were collected at term elective cesarean sections of singleton pregnancies at the National University Hospital, Singapore with written informed consent. Only elective cesarean section cases were included to reduce the possible effects of labor on placental expression of CPTs and acylcarnitine content. Indications for elective cesarean section were previous cesarean section, breech presentation, suspected macrosomia or maternal request/social reasons. Participants were of Asian ethnicity (classified as Chinese and non-Chinese: Malay or Indian), self-reported non-smokers, conceived spontaneously and delivered neonates that were not small-for-gestational age (birthweight >10th centile). All participants underwent a routine 75 g oral glucose tolerance test (OGTT) after an overnight fast during pregnancy. Gestational diabetes mellitus (GDM) was diagnosed according to World Health Organization 2013 criteria of a fasting glucose 5.1—6.9 mmol/L, and/or 1 h glucose ≥10.0 mmol/L, and/or 2 h glucose 8.5—11.0 mmol/L (World Health Organization Guideline, 2014). With the exception of GDM in 39 subjects, all participants were otherwise healthy and had uncomplicated pregnancies (Table 1). Ethics approval was granted by the National Healthcare Group Domain Specific Research Board (References 2000/00524 and 2016/00183).

2.2 Sample processing

Five villous tissue biopsies were obtained from random sampling across each placenta. Following removal of the maternal decidua, biopsies were snap frozen in liquid nitrogen within 10 min of delivery and stored at −80°C until use. Considering variation across each placenta, biopsies for each placenta were subsequently pulverized in liquid nitrogen and mixed together for RNA and lipid extractions.

2.3 RNA extraction, cDNA synthesis and real-time quantitative polymerase chain reaction (RT-qPCR)

Placental mRNA expression of carnitine palmitoyltransferases was determined as described previously (Watkins et al., 2022).

TABLE 1 Participant characteristics by molecular analysis method.

Characteristics[a]	RT-qPCR analysis (n = 77)	Lipidomic analysis (n = 50)
Maternal age (years)	33.1 ± 3.5	32.8 ± 3.8
Maternal ethnicity (n)	45 Chinese, 32 non-Chinese	27 Chinese, 23 non-Chinese
Maternal BMI in early pregnancy (kg/m^2)	25.5 ± 5.1	25.7 ± 5.1
Gestational diabetes mellitus status (n, %)	39 (50.6%)	24 (48.0%)
Antenatal fasting glycemia (mmol/L)[b]	4.5 ± 0.3	4.5 ± 0.4
Antenatal 2h glycemia (mmol/L)[b]	7.4 ± 1.8	7.3 ± 2.0
Gestational age at delivery (weeks)	38.6 ± 0.6	38.5 ± 0.5
Infant sex (n males, n females)	44 Males, 33 Females	30 Males, 20 Females
Infant birthweight (g)	3276.9 ± 313.3	3310.8 ± 297.3
Customized infant birthweight percentiles (%)[c]	56.8 ± 25.5	60.2 ± 23.4

[a]Data presented as mean ± standard deviation unless stated otherwise.
[b]Subjects underwent a 75 g oral glucose tolerance test conducted during pregnancy.
[c]Customized for maternal BMI, ethnicity, parity, gestational age at delivery and infant sex.

Briefly, following phenol-chloroform extraction, placental RNA was purified with the RNeasy Mini Kit (Qiagen) and reverse transcribed to cDNA with Superscript III reverse transcriptase (Thermo Fisher Scientific) according to manufacturer's instructions. RT-qPCR was performed with TaqMan Fast Advanced Master Mix (Thermo Fisher Scientific) on an Applied Biosystems 7500 Fast Real-Time PCR System (Thermo Fisher Scientific). Samples were run in duplicate 10 µL reactions containing 5 ng cDNA at the following settings: 95°C for 20 s, followed by 45 cycles of 95°C for 3 s and 60°C for 30 s. Inventoried FAM-labeled TaqMan probes were used for three housekeeping genes—*CYC1* (cytochrome C1, Hs00357718_m1), *SDHA* (succinate dehydrogenase complex, subunit A, Hs00188166_m1) and *TBP* (TATA-box binding protein, Hs00427620_m1); and four CPT family genes—*CPT1A* (Hs00912671_m1), *CPT1B* (Hs00993896_g1), *CPT1C* (Hs00380581_m1) and *CPT2* (Hs00988962_m1). The average threshold cycle (C_T) value of non-GDM subjects served as the calibrator (assigned value of 1) for relative quantification. Relative expression of each CPT isoform was calculated using formula $2^{(-\Delta CT)}$ and normalized to the geometric mean expression of the three housekeeping genes.

2.4 Lipid extraction and quantification by liquid chromatography tandem mass spectrometry (LC-MS/MS)

Lipid extraction and quantification by LC-MS/MS was performed on a subset of 50 placentas using methods similar to previous work on the placental lipidome (Wong et al., 2021; Watkins et al., 2022). In brief, approximately 250 mg of each placental sample was freeze-dried, weighed and homogenized in 1 ml phosphate buffered saline. Following an addition of 800 µL butanol/methanol (1:1) to 40 µL of placental homogenate and 10 µL of internal standard mix containing 151.1 pmol acylcarnitine 16:0 d3 (Larodan Chemicals, Solna, Sweden), samples were vortexed briefly, sonicated for 30 min in an ice bath and shaken for 30 min at 4°C. After centrifugation at 13,000 rpm for 10 min, the supernatant was collected into a La-Pha-Pack HPLC tube (Langerwehe, Germany) and stored at -80°C until LC-MS/MS analysis. Quality control (QC) samples were similarly prepared from placental homogenates pooled from several subjects. Lipid extracts (5 µL) were then injected into an Agilent 6490 triple quadrupole LC-MS/MS instrument with chromatography performed as described in Supplementary Methods. Metabolite peak areas were integrated using Mass Hunter QQQ Quantitative Analysis Version 10. Lipids were considered quantifiable if their %RSD in QC samples was less than 25% and the peak area at least 10 times that of a blank sample extracted under the same conditions. Placental lipid content was expressed as µmol lipid/mg tissue dry weight. Ten medium and long chain acylcarnitines (12:0, 14:0, 14:1, 14:2, 15:0, 16:0, 16:1, 18:0, 18:1 and 18:2) were measured.

2.5 Statistical analysis

To ensure a normal distribution and to standardize comparisons between genes and lipids that had different degrees of interindividual variability, gene expression and lipid data were log2-transformed and then converted to Z-scores for analysis. Linear regression models were run in R version "Kick Things" with 'tidyverse' Version: 1.3.1 (Wickham et al., 2019). To account for multiple testing and minimize false discovery, Benjamini–Hochberg correction was applied with statistical significance set at $p < 0.05$. For each CPT, linear regression was first performed between gene expression (outcome) and maternal age. This model was then rerun with covariate adjustment for maternal fasting glycemia, ethnicity, maternal BMI, gestational age and infant sex. To determine how CPT expression might influence the production of placental acylcarnitines, linear

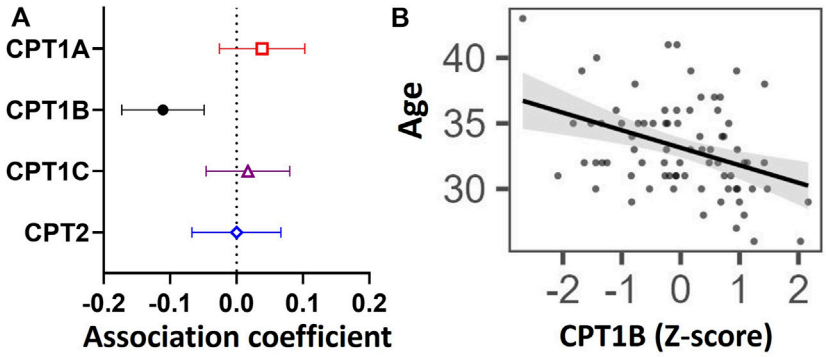

FIGURE 1
Associations between placental mRNA expression of CPT isoforms and maternal age in n = 77 placentas. Forest plot **(A)** shows coefficient estimates and 95% confidence intervals of associations between each CPT isoform (outcome) and age (years), after adjusting for maternal fasting glycemia, ethnicity, maternal BMI, gestational age and fetal sex. Scatter plot **(B)** shows the unadjusted relationship between maternal age and Z-score for *CPT1B* mRNA expression. A black line denotes a significant association. The shaded grey area represents the 95% confidence interval of the regression. Placental mRNA expression data of CPTs were log_2-transformed then converted to Z-scores prior to linear regression.

regression was performed between placental acylcarnitine abundance (outcome) and gene expression (for each CPT). Lastly, to explore if maternal factors such as high maternal glycemia and BMI affected the relationship between placental CPT expression with maternal age and acylcarnitine abundance, these associations were examined in the study population as a whole, as well as following stratification by GDM or BMI status, as decided *a priori*.

3 Results

3.1 Clinical characteristics of study participants

Study participants (n = 77) for the RT-qPCR analysis were predominantly of Chinese ethnicity, with a mean age of 33 years, a mean BMI in early pregnancy of 25.5 kg/m^2 and delivered at an average of 38.6 weeks of gestation (Table 1). Approximately 50% of these women had GDM, with an average antenatal OGTT fasting and 2 h glucose of 4.5 and 7.4 mmol/L respectively. The maternal characteristics of the subset (n = 50) used for the lipidomic analysis were similar to those used for the RT-qPCR analysis. The proportion of male to female infants, birthweight mean and average birthweight centiles were also comparable between both groups.

3.2 Participant characteristics associated with placental expression of CPT isoforms

Older maternal age was associated with lower placental *CPT1B* expression [coefficient estimate: -0.107 (-0.167, -0.047) Z-score of expression per year, $p = 0.001$], but not with that of *CPT1A* [0.043 (-0.021, 0.108), $p > 0.05$], *CPT1C* [0.018 (-0.047, 0.083), $p > 0.05$] or *CPT2* [0.003 (-0.062, 0.068), $p > 0.05$] (Figure 1). Associations remained similar [*CPT1B* coefficient estimate: -0.111 (-0.173, -0.049), $p = 0.006$] after covariate adjustment for maternal fasting glycemia, ethnicity, maternal BMI, gestational age and infant sex. No associations were observed between maternal fasting glycemia, ethnicity, maternal BMI, gestational age or fetal sex and the expression of any CPT isoform.

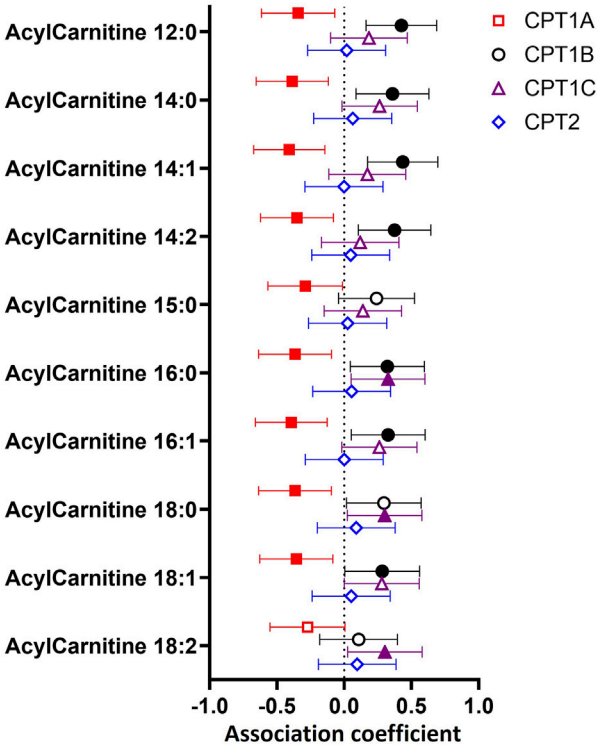

FIGURE 2
Associations between mRNA expression of CPT isoforms and placental acylcarnitines by linear regression. The forest plot shows coefficient estimates and 95% confidence intervals of associations between CPT isoforms and placental acylcarnitines (outcome, n = 50 placentas). Filled symbols show acylcarnitines that are significantly associated after adjustment by Benjamini–Hochberg's correction. Data for placental acylcarnitine abundance and mRNA expression data of CPT isoforms were log2-transformed then converted to Z-scores prior to linear regression.

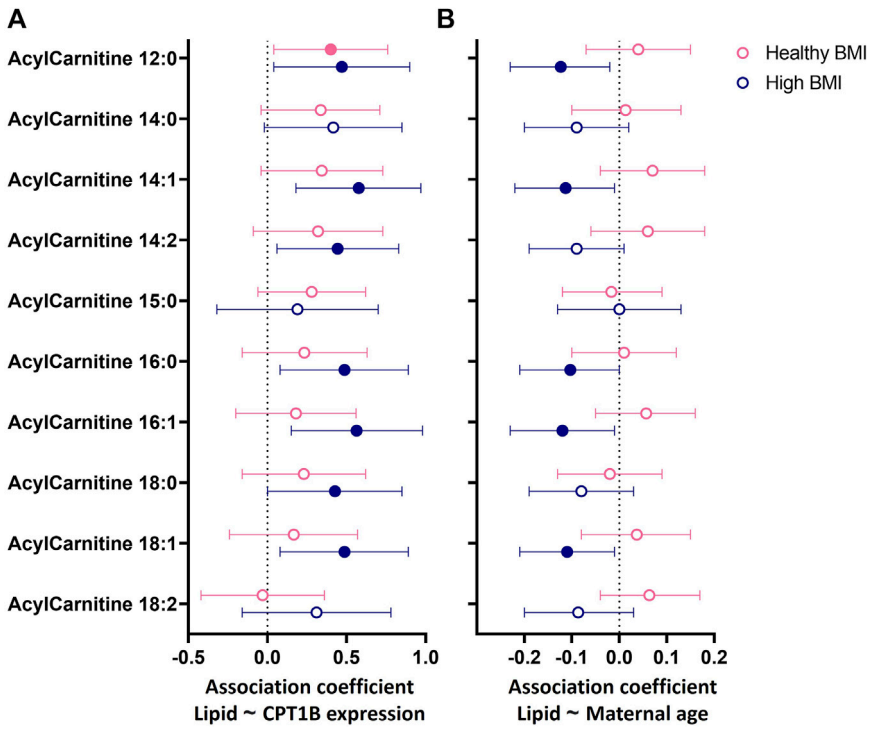

FIGURE 3
Associations between **(A)** placental *CPT1B* mRNA expression or **(B)** maternal age with the abundance of placental acylcarnitines by linear regression stratified by maternal BMI status. The forest plots show coefficient estimates and 95% confidence intervals of associations between placental *CPT1B* mRNA expression **(A)** or maternal age (years, **(B)** with placental acylcarnitines (outcome) in subjects with healthy (<25 kg/m^2, n = 25) and high (≥25 kg/m^2, n = 25) BMI. Filled symbols show acylcarnitines that are significantly associated after adjustment by Benjamini–Hochberg's correction. Data for placental acylcarnitine abundance and mRNA expression data of *CPT1B* were $\log_2$-transformed then converted to Z-scores prior to linear regression.

3.3 Association of expression of CPT isoforms with acylcarnitines in the placenta

To determine whether variations in CPT isoform expression related to differences in transferase activity represented by placental acylcarnitine content, we examined the relationship between expression of each CPT isoform with 10 medium and long-chain acylcarnitines in the placenta (Figure 2). Placental *CPT1A* expression negatively associated with nine acylcarnitines (12:0, 14:0, 14:1, 14:2, 15:0, 16.0, 16:1, 18:0, 18:1), while *CPT1B* positively associated with eight acylcarnitines (12:0, 14:0, 14:1, 14:2, 16.0, 16:1, 18:0, 18:1) and *CPT1C* positively associated with three long chain acylcarnitines (16:0, 18:0 and 18:2). The exception was *CPT2,* which showed no associations with any acylcarnitine.

3.4 Associations between *CPT1B* expression and maternal age with placental acylcarnitines following stratification by maternal BMI or GDM status

Both a high maternal BMI (≥25 kg/m^2) and GDM are known to increase the supply and availability of fatty acids to the placenta (Duttaroy and Basak, 2021), which could place greater stress on the placenta's capacity for fatty acid processing. Thus, to determine whether such factors altered the relationships of *CPT1B* expression and maternal age with placental acylcarnitines, we examined these associations following stratification by BMI (Figure 3) and GDM status (Supplementary Figure S1).

In BMI-stratified analyses (Figure 3), among participants with a healthy BMI (<25 kg/m^2; n = 25), *CPT1B* expression positively associated with only one acylcarnitine (12:0). In contrast, in those with a high BMI (≥25 kg/m^2; n = 25), *CPT1B* expression remained strongly positively associated with seven acylcarnitines (12:0, 14:1, 14:2, 16.0, 16:1, 18:0, 18:1). Only acylcarnitine 12:0 was significantly associated with *CPT1B* expression with similar coefficient estimates in both BMI groups. Differences by GDM status were less apparent, with the normoglycemic group showing significant positive associations for two acylcarnitines (12:0, 14:1) and the GDM group for three acylcarnitines (14:1, 16:0, 16:1), with an overlap observed for acylcarnitine 14:1 (Supplementary Figure S1A).

Since placental *CPT1B* expression declined with older maternal age, it was expected that placental acylcarnitines would be negatively associated with age. However, no direct relationships between maternal age and placental acylcarnitines were observed (Supplementary Table S3). Instead, we only observed such a relationship of older maternal age with lower acylcarnitines (12:0, 14:1, 16:0, 16:1, 18:1) in those with a high BMI and not in those with a healthy BMI (Figure 3B). No relationships were seen when

stratified by GDM status (Supplementary Figure S1B). The associations seen for the high BMI group remained similar after adjusting for maternal ethnicity, fasting glycemia, gestational age at delivery and infant sex. Following adjustment for placental *CPT1B* expression, all associations between maternal age and placental acylcarnitines were attenuated and no longer significant.

4 Discussion

4.1 Main findings

Our study demonstrates that older maternal age is associated with lower placental expression of *CPT1B*, but not that of *CPT1A*, *CPT1C* or *CPT2*. Furthermore, placental *CPT1B* expression positively associated with eight out of 10 acylcarnitines quantified in the placenta, suggesting it may play a prominent role in placental long-chain acylcarnitine synthesis. Placental acylcarnitines were only reduced with older maternal age in overweight/obese participants. These associations between maternal age and placental acylcarnitines were attenuated after accounting for *CPT1B* expression.

4.2 Implications of reduced CPT1B expression in the placenta

The inverse relationship between maternal age and placental *CPT1B* mRNA expression is consistent with past studies in elderly humans and aged rodents demonstrating decreased expression and activity of CPT in tissues such as the heart and skeletal muscles, where the CPT1B is the predominant isoform (McMillin et al., 1993; Odiet et al., 1995; Bétry et al., 2019; Vieira-Lara et al., 2021). Curiously, despite the relatively "young" age of placental tissue (originating from the recent conception), the conceptus and placenta inherits maternal mitochondria—a major site where CPT1B is active. Thus, in certain respects, the placenta may share maternal age-related physiological characteristics.

In a human study, participants with lower skeletal muscle *CPT1B* mRNA expression were less able to oxidize lipids in a fasted state and were more insulin-resistant (Bétry et al., 2019). In mice, the age-associated decrease in skeletal muscle CPT1B protein exacerbated insulin resistance induced by a high fat diet, indicating that older mice had reduced metabolic flexibility in response to an obesogenic dietary challenge compared with their younger counterparts (Vieira-Lara et al., 2021). Meanwhile, loss of CPT1B activity in the heart increases myocardial lipids in obese mice and causes cardiac lipotoxicity in a heart failure mouse model (He et al., 2012; Zhang et al., 2016). These studies particularly highlight the importance of CPT1B in buffering metabolic stress and its contribution to overall metabolic health. As such, the age-related decline in placental CPT1B may similarly impair the placenta's ability to appropriately regulate fatty acid oxidation in response to metabolic challenges such as maternal obesity; this could lead to dysregulated placental lipid metabolism and altered lipid-derived signaling, and ultimately placental dysfunction. Nonetheless, while our sample population encompassed a range of maternal BMI and glycemia, our study was restricted to those with relatively uncomplicated pregnancies with a livebirth following an elective cesarean section and thus not representative of the general obstetric population. Therefore, we were unable to test for associations of placental *CPT1B* expression with adverse pregnancy outcomes such as pre-eclampsia and stillbirth that are linked with placental dysfunction and advanced maternal age. Future studies in large cohorts that are adequately powered could be used to further investigate the link between placental *CPT1B* expression with these relatively infrequent adverse pregnancy outcomes.

4.3 Significance of the role of maternal BMI in influencing placental fatty oxidation

In addition to advanced maternal age, high BMI is another risk factor for stillbirth and antenatal complications such as GDM (Flenady et al., 2011; Plows et al., 2018). Studies of placentas from women with obesity generally report lower expression of CPTs, reduced acylcarnitines and impaired fatty acid oxidation, although the changes in expression of specific CPT isoforms differed between studies. For instance, Calabuig-Navarro et al. found that obesity increased placental *CPT2* mRNA expression, but decreased that of *CPT1B* and acylcarnitine content (Calabuig-Navarro et al., 2017), while Bucher et al. showed that CPT1A and CPT2 protein expression and acylcarnitines (16:0, 18:2, and 20:4) were reduced only in the placentas of female offspring (female placenta) among women with obesity (Bucher et al., 2021). In contrast, Powell et al. did not observe any changes with placental protein expression of CPTs, though they also demonstrated less fatty acid oxidation in female placentas of women with obesity (Powell et al., 2021). Similarly, we did not identify any associations of maternal BMI or infant sex with placental expression of CPTs. The discrepancies between studies may arise from different BMI cutoffs (i.e. overweight *versus* obese) and baseline population differences (e.g. Asian and non-Asian). Nonetheless, our finding of a maternal age-associated decline in placental acylcarnitines only among overweight women, provides additional supporting evidence that high BMI may contribute to reduced ability to process excess fatty acids.

Therefore, while maternal age is associated with decreased placental *CPT1B* expression, this only appears to impact acylcarnitine production when BMI is high, when the placenta is presumably already experiencing an increased fatty acid load. Hence, CPT1B may become the limiting factor in acylcarnitine production in an environment of excess fatty acids. Indeed, placental *CPT1B* mRNA expression positively associated with more acylcarnitines among overweight participants (BMI $\geq$25 kg/m^2) as compared to just one significant association seen among the non-overweight participants (BMI <25 kg/m^2), further highlighting the close relationship between maternal BMI, *CPT1B* expression and acylcarnitines in the placenta. Moreover, while placental fatty acid oxidation is reportedly reduced with GDM (Visiedo et al., 2013), GDM status had minor implications on the associations of placental *CPT1B* expression and of maternal age with placental acylcarnitines in our cohort, which suggests that differences in BMI are more important than differences in maternal glycemia.

4.4 Role of other placental CPTs

In addition to being the only CPT associated with age, *CPT1B* mRNA expression was positively associated with the largest number of placental acylcarnitines, suggesting it may be the main transferase for converting medium and long-chain fatty acids into acylcarnitines in the human placenta. This is similar to a previous finding showing that placental *CPT1B* mRNA expression positively correlated with total placental acylcarnitine content (Calabuig-Navarro et al., 2017). The positive relationships of placental *CPT1C* mRNA expression with only the longer chain acylcarnitines (16:0, 18:0 and 18:2) suggests its particular importance in generating the very long chain acylcarnitines. This is corroborated by the localization of CPT1C mainly in the endoplasmic reticulum, hinting at its role in biosynthesis as opposed to catabolism (in mitochondria) and that the loss of CPT1C results in decreased long chain signaling endocannabinoid production (Sierra et al., 2008; Lee and Wolfgang, 2012). Unexpectedly, placental *CPT1A* expression was negatively associated with acylcarnitines. The underlying reasons remain unclear, but one possibility is that placental increases in CPT1A enhances fatty acid oxidation overall, such that longer chain acylcarnitines become depleted. This is similar to the negative relationship seen in patients with chronic kidney disease, where decreased kidney *CPT1A* mRNA expression was linked with increased accumulation of short and middle chain acylcarnitines (Miguel et al., 2021). In contrast, CPT2 was not associated with any placental acylcarnitine in our cohort, which suggests it is not the limiting factor in the placenta for synthesis of the medium and long-chain acylcarnitines examined. Nonetheless, as there are no inhibitors currently available to selectively block the activity of each CPT in isolation, we are limited in our ability to determine the specific role of each CPT in *vitro* studies of the human placenta.

4.5 Possible mechanisms for CPT1B decline with age and potential reversal with carnitine supplementation

The mechanisms by which maternal age affects placental *CPT1B* expression are unknown. However, insights may be gained from non-placental studies. For example, decreased CPT1 expression with increasing age in tissues such as the heart and skeletal muscle is speculated to result from cumulative mitochondrial oxidative damage over time (Odiet et al., 1995; Vieira-Lara et al., 2021). As such, oxidative damage accumulated in the maternal mitochondria of the aging oocyte that are subsequently inherited by the fetus may be one contributing factor. *In vitro* studies conducted on placental explants show that acute oxidative stress of up to 4 h does not affect placental CPT1B expression at the mRNA or protein level (Thomas et al., 2019), but the effects of chronic oxidative stress remain to be investigated. Direct signaling from the maternal tissues to the placenta may also influence placental CPT expression, given that advanced maternal age can impair decidualisation and thus alter the biochemical and hormonal environment that the developing placenta is exposed to (Woods et al., 2017; Mendes et al., 2020). Alternatively, a decline in CPT may be due to deficiency of micronutrients needed for optimal fatty acid oxidation. For instance, in conjunction with the age-associated drop in CPT (Bétry et al., 2019; Vieira-Lara et al., 2021), skeletal muscle carnitine content also decreases with age in humans and mice (Costell et al., 1989). Interestingly, carnitine supplementation was able to enhance CPT1 transcription in the liver of aged rats (Karlic et al., 2002). In humans, pregnancy also results in a decline in circulating carnitine (Keller et al., 2009), and dietary carnitine supplementation can increase hepatic CPT1B activity in pregnant pigs (Xi et al., 2008). Furthermore, carnitine supplementation was previously shown to decrease the stillbirth rate in sows (Eder, 2009). Exercise can also increase skeletal muscle and adipose tissue *CPT1B* mRNA expression in young and middle adults across the BMI spectrum (Lohninger et al., 2005; Otero-Díaz et al., 2018) but whether exercise in pregnancy can increase placental CPT1B remains to be investigated. The notion that maternal physical activity can influence fetal-placental tissues at a molecular level was suggested in a study by Chaves et al. (Chaves et al., 2022), which demonstrated that maternal exercise altered metabolism in isolated umbilical cord mesenchymal stromal cells. It is thus tantalizing to speculate that the CPT-promoting effects of carnitine supplementation and exercise individually or in combination may be able to counter the age-associated placental CPT decline in pregnancy and possibly reduce advanced maternal age-linked stillbirths and other pregnancy adversity, which could be explored in future studies. Therefore, further studies are warranted to improve understanding of CPT regulation at the maternal-fetal interface.

5 Conclusion

In summary, older maternal age is specifically associated with lower placental *CPT1B* expression and *CPT1B* appears to be the main CPT that catalyzes acylcarnitine production in the placenta. However, placental acylcarnitines are only lower with older maternal age in overweight/obese women. These findings may underlie decreased placental metabolic flexibility and ability to adapt to adverse intrauterine environments, which may contribute to greater risk of pregnancy complications in older women, particularly if they are overweight/obese.

Data availability statement

The raw data supporting the conclusion of this article will be made available by the authors upon reasonable request.

Ethics statement

The studies involving human participants were reviewed and approved by the National Healthcare Group Domain Specific Research Board. The patients/participants provided their written informed consent to participate in this study.

Author contributions

Conception and/or study design HY, OW, and S-YC. Data acquisition: HY, OW, TM, VC-H, RP, PS, MI, and NS. Data analysis and interpretation: HY, OW, TM, VC-H, and S-YC. Drafting the manuscript HY and OW. Critical revision of the manuscript for intellectual content: HY, OW, TM, VC-H, RP, PS, MI, NS, AC-G, AB, MW, KG, RL, and S-YC. Funding acquisition: AC-G, AB, MW, KG, RL, and S-YC. All authors have approved the submitted version of the manuscript.

Funding

This research is supported by a Clinician Scientist Award awarded to SYC from the Singapore National Medical Research Council (NMRC/CSA-INV/0010/2016, MOH-CSAINV19nov-0002), by the National University of Singapore, National University Health System Singapore and the Singapore Institute for Clinical Sciences A*STAR. The Singapore Lipidomics Incubator receives funding from the Life Sciences Institute, the National University of Singapore Yong Loo Lin School of Medicine, the National Research Foundation (NRFI 2015–05) and A*STAR (IAF-ICP I1901E0040). KMG is supported by the United Kingdom Medical Research Council (MC_UU_12011/4), the National Institute for Health Research (NIHR Senior Investigator (NF-SI-0515–10042) and NIHR Southampton Biomedical Research Centre (NIHR203319)), the European Union (Erasmus + Programme ImpENSA 598488-EPP-1–2018-1-DE-EPPKA2-CBHE-JP), and the US National Institute On Aging of the National Institutes of Health (Award No. U24AG047867). For the purpose of Open Access, the authors have applied a Creative Commons Attribution (CC BY) licence to any Author Accepted Manuscript version arising from this submission. Funders played no role in study design; in the collection, analysis, and interpretation of data; in the writing of the report; and in the decision to submit the paper for publication.

Acknowledgments

The authors would like to thank Samantha Grace Loon Magadia, Celes Maria Catherine Dado and Zhenzhi Chen in coordinating the recruitment of the women involved in this study, the staff of the National University Hospital who kindly assisted with placental collection, and the women who generously donated their placentas for research.

Conflict of interest

S-YC and KG are part of an academic consortium that has received research funding from Société Des Produits Nestlé S.A. and BenevolentAI Bio Ltd for work unrelated to this manuscript. S-YC and KMG are co-inventors on patent filings by Nestlé S.A. which covers the use of inositol in human health applications, but which do not draw on the work in this manuscript.

The remaining authors declare that the research was conducted in the absence of any commercial or financial relationships that could be construed as a potential conflict of interest.

Publisher's note

Supplementary material

The Supplementary Material for this article can be found online at: https://www.frontiersin.org/articles/10.3389/fphys.2023.1166827/full#supplementary-material

References

Arduini, A., Denisova, N., Virmani, A., Avrova, N., Federici, G., and Arrigoni-Martelli, E. (1994). Evidence for the involvement of carnitine-dependent long-chain acyltransferases in neuronal triglyceride and phospholipid fatty acid turnover. *J. Neurochem.* 62 (4), 1530–1538. doi:10.1046/j.1471-4159.1994.62041530.x

Arduini, A., Mancinelli, G., Radatti, G. L., Dottori, S., Molajoni, F., and Ramsay, R. R. (1992). Role of carnitine and carnitine palmitoyltransferase as integral components of the pathway for membrane phospholipid fatty acid turnover in intact human erythrocytes. *J. Biol. Chem.* 267 (18), 12673–12681. doi:10.1016/s0021-9258(18)42330-7

Bétry, C., Meugnier, E., Pflieger, M., Grenet, G., Hercberg, S., Galan, P., et al. (2019). High expression of CPT1b in skeletal muscle in metabolically healthy older subjects. *Diabetes & Metabolism* 45 (2), 152–159. doi:10.1016/j.diabet.2018.01.018

Bucher, M., Montaniel, K. R. C., Myatt, L., Weintraub, S., Tavori, H., and Maloyan, A. (2021). Dyslipidemia, insulin resistance, and impairment of placental metabolism in the offspring of obese mothers. *J. Dev. Orig. Health Dis.* 12 (5), 738–747. doi:10.1017/S2040174420001026

Calabuig-Navarro, V., Haghiac, M., Minium, J., Glazebrook, P., Ranasinghe, G. C., Hoppel, C., et al. (2017). Effect of maternal obesity on placental lipid metabolism. *Endocrinology* 158 (8), 2543–2555. doi:10.1210/en.2017-00152

Ceccarelli, S. M., Chomienne, O., Gubler, M., and Arduini, A. (2011). Carnitine palmitoyltransferase (CPT) modulators: A medicinal chemistry perspective on 35 years of research. *J. Med. Chem.* 54 (9), 3109–3152. doi:10.1021/jm100809g

Chaves, A., Weyrauch, L. A., Zheng, D., Biagioni, E. M., Krassovskaia, P. M., Davidson, B. L., et al. (2022). Influence of maternal exercise on glucose and lipid metabolism in offspring stem cells: ENHANCED by mom. *J. Clin. Endocrinol. Metab.* 107 (8), e3353–e3365. doi:10.1210/clinem/dgac270

Costell, M., O'Connor, J. E., and Grisolía, S. (1989). Age-dependent decrease of carnitine content in muscle of mice and humans. *Biochem. Biophysical Res. Commun.* 161 (3), 1135–1143. doi:10.1016/0006-291x(89)91360-0

Duttaroy, A. K., and Basak, S. (2021). Maternal fatty acid metabolism in pregnancy and its consequences in the feto-placental development. *Front. Physiol.* 12, 787848. doi:10.3389/fphys.2021.787848

Eder, K. (2009). Influence of l-carnitine on metabolism and performance of sows. *Br. J. Nutr.* 102 (5), 645–654. doi:10.1017/S0007114509990778

El-Wahed, M. A., El-Farghali, O., ElAbd, H., El-Desouky, E., and Hassan, S. (2017). Metabolic derangements in IUGR neonates detected at birth using UPLC-MS. *Egypt. J. Med. Hum. Genet.* 18 (3), 281–287. doi:10.1016/j.ejmhg.2016.12.002

Flenady, V., Koopmans, L., Middleton, P., Froen, J. F., Smith, G. C., Gibbons, K., et al. (2011). Major risk factors for stillbirth in high-income countries: A systematic review and meta-analysis. *Lancet* 377 (9774), 1331–1340. doi:10.1016/S0140-6736(10)62233-7

Giannacopoulou, C., Evangeliou, A., Matalliotakis, I., Relakis, K., Sbirakis, N., Hatzidaki, E., et al. (1998). Effects of gestation age and of birth weight in the concentration of carnitine in the umbilical plasma. *Clin. Exp. Obstetrics Gynaecol.* 25 (1), 42–45.

He, L., Kim, T., Long, Q., Liu, J., Wang, P., Zhou, Y., et al. (2012). Carnitine palmitoyltransferase-1b deficiency aggravates pressure overload-induced cardiac hypertrophy caused by lipotoxicity. *Circulation* 126 (14), 1705–1716. doi:10.1161/CIRCULATIONAHA.111.075978

Houten, S. M., Wanders, R. J. A., and Ranea-Robles, P. (2020). Metabolic interactions between peroxisomes and mitochondria with a special focus on acylcarnitine metabolism. *Biochimica Biophysica Acta (BBA) - Mol. Basis Dis.* 1866 (5), 165720. doi:10.1016/j.bbadis.2020.165720

Huang, L., Sauve, R., Birkett, N., Fergusson, D., and van Walraven, C. (2008). Maternal age and risk of stillbirth: A systematic review. *Can. Med. Assoc. J.* 178 (2), 165–172. doi:10.1503/cmaj.070150

Jones, L L., McDonald, D. A., and Borum, P. R. (2010). Acylcarnitines: Role in brain. *Prog. Lipid Res.* 49 (1), 61–75. doi:10.1016/j.plipres.2009.08.004

Karlic, H., Lohninger, A., Laschan, C., Lapin, A., Böhmer, F., Huemer, M., et al. (2003). Downregulation of carnitine acyltransferases and organic cation transporter OCTN2 in mononuclear cells in healthy elderly and patients with myelodysplastic syndromes. *J. Mol. Med.* 81 (7), 435–442. doi:10.1007/s00109-003-0447-6

Karlic, H., Lohninger, S., Koeck, T., and Lohninger, A. (2002). Dietary L-carnitine stimulates carnitine acyltransferases in the liver of aged rats. *J. Histochem. Cytochem.* 50 (2), 205–212. doi:10.1177/002215540205000208

Keller, U., van der Wal, C., Seliger, G., Scheler, C., Röpke, F., and Eder, K. (2009). Carnitine status of pregnant women: Effect of carnitine supplementation and correlation between iron status and plasma carnitine concentration. *Eur. J. Clin. Nutr.* 63 (9), 1098–1105. doi:10.1038/ejcn.2009.36

Kim, T., Moore, J. F., Sharer, J. D., Yang, K., Wood, P. A., and Yang, Q. (2014). Carnitine palmitoyltransferase 1b deficient mice develop severe insulin resistance after prolonged high fat diet feeding. *J. diabetes & metabolism* 5, 1000401. doi:10.4172/2155-6156.1000401

Kolb, H., Kempf, K., Röhling, M., Lenzen-Schulte, M., Schloot, N. C., and Martin, S. (2021). Ketone bodies: From enemy to friend and guardian angel. *BMC Med.* 19 (1), 313–315. doi:10.1186/s12916-021-02185-0

Lahjouji, K., Elimrani, I., Lafond, J., Leduc, L., Qureshi, I. A., and Mitchell, G. A. (2004). L-Carnitine transport in human placental brush-border membranes is mediated by the sodium-dependent organic cation transporter OCTN2. *Am. J. Physiology-Cell Physiology* 287 (2), C263–C269. doi:10.1152/ajpcell.00333.2003

Lean, S. C., Derricott, H., Jones, R. L., and Heazell, A. E. P. (2017). Advanced maternal age and adverse pregnancy outcomes: A systematic review and meta-analysis. *PLoS One* 12 (10), e0186287. doi:10.1371/journal.pone.0186287

Lee, J., and Wolfgang, M. J. (2012). Metabolomic profiling reveals a role for CPT1c in neuronal oxidative metabolism. *BMC Biochem.* 13 (1), 23. doi:10.1186/1471-2091-13-23

Lohninger, A., Sendic, A., Litzlbauer, E., Hofbauer, R., Staniek, H., Blesky, D., et al. (2005). Endurance exercise training and L-carnitine supplementation stimulates gene expression in the blood and muscle cells in young athletes and middle aged subjects. *Monatsh. für Chem./Chem. Mon.* 136 (8), 1425–1442. doi:10.1007/s00706-005-0335-6

McMillin, J. B., Taffet, G. E., Taegtmeyer, H., Hudson, E. K., and Tate, C. A. (1993). Mitochondrial metabolism and substrate competition in the aging Fischer rat heart. *Cardiovasc. Res.* 27 (12), 2222–2228. doi:10.1093/cvr/27.12.2222

Mendes, S., Timoteo-Ferreira, F., Soares, A. I., Rodrigues, A. R., Silva, A. M. N., Silveira, S., et al. (2020). Age-related oxidative modifications to uterine albumin impair extravillous trophoblast cells function. *Free Radic. Biol. Med.* 152, 313–322. doi:10.1016/j.freeradbiomed.2020.03.020

Miguel, V., Tituaña, J., Herrero, J. I., Herrero, L., Serra, D., Cuevas, P., et al. (2021). Renal tubule Cpt1a overexpression protects from kidney fibrosis by restoring mitochondrial homeostasis. *J. Clin. Investigation* 131 (5), e140695. doi:10.1172/JCI140695

Novak, M., Monkus, E. F., Chung, D., and Buch, M. (1981). Carnitine in the perinatal metabolism of lipids I. Relationship between maternal and fetal plasma levels of carnitine and acylcarnitines. *Pediatrics* 67 (1), 95–100. doi:10.1542/peds.67.1.95

Odiet, J A., Boerrigter, M. E. T. I., and Wei, J. Y. (1995). Carnitine palmitoyl transferase-I activity in the aging mouse heart. *Mech. Ageing Dev.* 79 (2), 127–136. doi:10.1016/0047-6374(94)01552-w

Otero-Díaz, B., Rodríguez-Flores, M., Sánchez-Muñoz, V., Monraz-Preciado, F., Ordoñez-Ortega, S., Becerril-Elias, V., et al. (2018). Exercise induces white adipose tissue browning across the weight spectrum in humans. *Front. Physiology* 9, 1781. doi:10.3389/fphys.2018.01781

Plows, J. F., Stanley, J. L., Baker, P. N., Reynolds, C. M., and Vickers, M. H. (2018). The pathophysiology of gestational diabetes mellitus. *Int. J. Mol. Sci.* 19 (11), 3342. doi:10.3390/ijms19113342

Powell, T. L., Barner, K., Madi, L., Armstrong, M., Manke, J., Uhlson, C., et al. (2021). Sex-specific responses in placental fatty acid oxidation, esterification and transfer capacity to maternal obesity. *Biochim. Biophys. Acta Mol. Cell. Biol. Lipids* 1866 (3), 158861. doi:10.1016/j.bbalip.2020.158861

Saccone, G., Gragnano, E., Ilardi, B., Marrone, V., Strina, I., Venturella, R., et al. (2022). Maternal and perinatal complications according to maternal age: A systematic review and meta-analysis. *Int. J. Gynecol. Obstetrics* 159, 43–55. doi:10.1002/ijgo.14100

Sánchez-Pintos, P., de Castro, M. J., Roca, I., Rite, S., López, M., and Couce, M. L. (2017). Similarities between acylcarnitine profiles in large for gestational age newborns and obesity. *Sci. Rep.* 7 (1), 16267–16269. doi:10.1038/s41598-017-15809-4

Sánchez-Pintos, P., Perez-Munuzuri, A., Ja, C., Fernández-Lorenzo, J. R., Fraga, J. M., and Couce, M. L. (2016). Evaluation of carnitine deficit in very low birth weight preterm newborns small for their gestational age. *J. Maternal-Fetal Neonatal Med.* 29 (6), 933–937. doi:10.3109/14767058.2015.1024647

Schmidt-Sommerfeld, E., Penn, D., Sodha, R. J., Prögler, M., Novak, M., and Schneider, H. (1985). Transfer and metabolism of carnitine and carnitine esters in the *in vitro* perfused human placenta. *Pediatr. Res.* 19 (7), 700–706. doi:10.1203/00006450-198507000-00013

Sierra, A. Y., Gratacós, E., Carrasco, P., Clotet, J., Ureña, J., Serra, D., et al. (2008). CPT1c is localized in endoplasmic reticulum of neurons and has carnitine palmitoyltransferase activity. *J. Biol. Chem.* 283 (11), 6878–6885. doi:10.1074/jbc.M707965200

Thomas, M. M., Haghiac, M., Grozav, C., Minium, J., Calabuig-Navarro, V., and O'Tierney-Ginn, P. (2019). Oxidative stress impairs fatty acid oxidation and mitochondrial function in the term placenta. *Reprod. Sci.* 26 (7), 972–978. doi:10.1177/1933719118802054

Vieira-Lara, M. A., Dommerholt, M. B., Zhang, W., Blankestijn, M., Wolters, J C., Abegaz, F., et al. (2021). Age-related susceptibility to insulin resistance arises from a combination of CPT1B decline and lipid overload. *BMC Biol.* 19 (1), 154. doi:10.1186/s12915-021-01082-5

Virmani, A., Pinto, L., Bauermann, O., Zerelli, S., Diedenhofen, A., Binienda, Z. K., et al. (2015). The carnitine palmitoyl transferase (CPT) System and possible relevance for neuropsychiatric and neurological conditions. *Mol. Neurobiol.* 52 (2), 826–836. doi:10.1007/s12035-015-9238-7

Visiedo, F., Bugatto, F., Sanchez, V., Cozar-Castellano, I., Bartha, J. L., and Perdomo, G. (2013). High glucose levels reduce fatty acid oxidation and increase triglyceride accumulation in human placenta. *Am. J. Physiol. Endocrinol. Metab.* 305 (2), E205–E212. doi:10.1152/ajpendo.00032.2013

Watkins, O. C., Yong, H. E. J., Mah, T. K. L., Cracknell-Hazra, V. K. B., Pillai, R. A., Selvam, P., et al. (2022). Sex-dependent regulation of placental oleic acid and palmitic acid metabolism by maternal glycemia and associations with birthweight. *Int. J. Mol. Sci.* 23 (15), 8685. doi:10.3390/ijms23158685

Wickham, H., Averick, M., Bryan, J., Chang, W., McGowan, L. D A., François, R., et al. (2019). Welcome to the tidyverse. *J. open source Softw.* 4 (43), 1686. doi:10.21105/joss.01686

Wong, G., Weir, J. M., Mishra, P., Huynh, K., Nijagal, B., Gupta, V., et al. (2021). The placental lipidome of maternal antenatal depression predicts socio-emotional problems in the offspring. *Transl. Psychiatry* 11 (1), 107. doi:10.1038/s41398-021-01208-x

Woods, L., Perez-Garcia, V., Kieckbusch, J., Wang, X., DeMayo, F., Colucci, F., et al. (2017). Decidualisation and placentation defects are a major cause of age-related reproductive decline. *Nat. Commun.* 8 (1), 352. doi:10.1038/s41467-017-00308-x

World Health Organization Guideline (2014). Diagnostic criteria and classification of hyperglycaemia first detected in pregnancy: A World health organization guideline. *Diabetes Res. Clin. Pract.* 103 (3), 341–363. doi:10.1016/j.diabres.2013.10.012

Xi, L., Brown, K., Woodworth, J., Shim, K., Johnson, B., and Odle, J. (2008). Maternal dietary L-carnitine supplementation influences fetal carnitine status and stimulates carnitine palmitoyltransferase and pyruvate dehydrogenase complex activities in swine. *J. Nutr.* 138 (12), 2356–2362. doi:10.3945/jn.108.095638

Yli, B. M., and Kjellmer, I. (2016). Pathophysiology of foetal oxygenation and cell damage during labour. *Best Pract. Res. Clin. Obstetrics Gynaecol.* 30, 9–21. doi:10.1016/j.bpobgyn.2015.05.004

Zhang, Y., Fang, X., Dai, M., Cao, Q., Tan, T., He, W., et al. (2016). Cardiac-specific down-regulation of carnitine palmitoyltransferase-1b (CPT-1b) prevents cardiac remodeling in obese mice. *Obes. (Silver Spring)* 24 (12), 2533–2543. doi:10.1002/oby.21665

frontiers | Frontiers in Physiology

TYPE Original Research
PUBLISHED 22 June 2023
DOI 10.3389/fphys.2023.1197658

OPEN ACCESS

EDITED BY
Gendie Lash,
Guangzhou Medical University, China

REVIEWED BY
Christophe Millie,
Partners In Health, United States
Bin Liu,
Baoan Women's and Children's Hospital, China

*CORRESPONDENCE
Shixuan Wang,
shixuanwang@tjh.tjmu.edu.cn

RECEIVED 18 April 2023
ACCEPTED 12 June 2023
PUBLISHED 22 June 2023

CITATION
Liu X, Wang B, Zhang Q, Zhang J and Wang S (2023), The long-term trend of uterine fibroid burden in China from 1990 to 2019: A Joinpoint and Age–Period–Cohort study. *Front. Physiol.* 14:1197658. doi: 10.3389/fphys.2023.1197658

The long-term trend of uterine fibroid burden in China from 1990 to 2019: A Joinpoint and Age–Period–Cohort study

Xingyu Liu[1,2,3], Bo Wang[1,2,3], Qianyu Zhang[1,2,3], Jinjin Zhang[1,2,3] and Shixuan Wang[1,2,3]*

[1]Department of Obstetrics and Gynecology, Tongji Hospital, Tongji Medical College, Huazhong University of Science and Technology, Wuhan, China, [2]National Clinical Research Center for Obstetrical and Gynecological Diseases, Huazhong University of Science and Technology, Wuhan, China, [3]Key Laboratory of Cancer Invasion and Metastasis, Ministry of Education, Huazhong University of Science and Technology, Wuhan, China

Purpose: Uterine fibroids occur in 40%–60% of women and are symptomatic in 30% of the patients by causing abnormal uterine bleeding, pelvic pressure, pain, and infertility. The study aims to evaluate the long-term trend of uterine fibroids mortality and disability-adjusted life years (DALYs) in China and the relative risks of age, period, and birth cohort effects.

Methods: The mortality and DALYs of uterine fibroids from 1990 to 2019 were derived from the Global Burden of Disease 2019. The annual percentage change and average annual percent change (AAPC) were assessed using the Joinpoint regression. The effects of age, period, and birth cohort on death and DALYs were analyzed by the Age–Period–Cohort framework.

Results: The age-standardized rates were all on the ascending trend, with the greatest increase in the age-standardized mortality rate (AAPC, 1.53; 95% CI, 1.04–2.02). The net drift was found to be 3.51% (95% CI, 2.25%–4.78%) per year for mortality and 0.34% (95% CI, 0.14%–0.53%) per year for DALYs. Significant age, period, and birth cohort effects were found for mortality and DALYs ($p < 0.001$ for all). The mortality risk increased overall with age, but the DALYs risk increased first and then decreased with age. The period and birth cohort risks for mortality and DALYs showed different trends.

Conclusion: These secular time trends and changes of mortality and DALYs reveal the socioeconomic alterations, reform of diagnosis and therapy, and changes in social lifestyles and behaviors. Uterine fibroids are still the most common benign gynecological tumors in women, and more epidemiological investigations and social health prevention and control should be applied.

KEYWORDS

uterine fibroids, mortality, disability-adjusted life years, Joinpoint regression analysis, Age–Period–Cohort analysis

Introduction

Uterine fibroids are the most common benign gynecological tumors in women (Bulun, 2013; Drayer and Catherino, 2015), which are derived from uterine smooth muscle cells and consist of massive extracellular matrices (Kim and Sefton, 2012). Due to their hormonally responsive nature, fibroids increase with age during a women's reproductive years, are rare

before puberty, and regress after menopause (Wise and Laughlin-Tommaso, 2016). The incidence of uterine fibroids was 60% and 40% by the age of 35 years in African–American women and white women, respectively, growing to >80% and 70% by the age of 50 years (Baird et al., 2003). In 2014, the estimated incidence of uterine fibroids among women was 101.4/10,000 person-years, with the highest incidence rate in the age group of 45–49 years (240.3/10,000 person-year) in the United States (Yu et al., 2018). Besides, the prevalence of fibroids varies from 4.5% to 68.8% depending on different countries and studies (Stewart et al., 2017). Although the data varies widely, uterine fibroids are recognized to affect a large number of women.

Although benign, the lesions of fibroids may lead to the dysfunction of the uterus and cause increased menstrual flow, prolonged periods, anemia, pelvic discomfort, obstruction of fertilized eggs, miscarriage, abnormal fetal positioning, placental abruption, postpartum hemorrhage, preterm labor, and malignancy (Bulun, 2013). Up to 25% of all women and 30%–40% of perimenopausal women may be influenced by symptomatic uterine fibroids (Cramer and Patel, 1990); surgery is the main option for women with severe symptoms. Given the high incidence of uterine fibroids, they are a heavy healthcare burden for women. Nearly 29% of gynecological hospitalizations are attributable to fibroids (Whiteman et al., 2010). In the United States, approximately 200,000 hysterectomies, 30,000 myomectomies, and thousands of uterine artery embolizations and high-intensity focused ultrasound procedures are performed each year for the removal or destruction of fibroids (Bulun, 2013), which occupy 40%–60% of all performed hysterectomies and account for 30% of hysterectomies among women aged 18–44 years (Merrill, 2008).

The high prevalence, hospitalization rates, and surgery rates of uterine fibroids have a profoundly negative impact on healthcare and economic costs worldwide, which include direct costs and indirect costs. The direct annual costs of uterine fibroids, such as the cost of surgeries, hospital admissions, outpatient visits, and medications, are 4.1–9.4 billion dollars (Cardozo et al., 2012). Nevertheless, the indirect annual costs include $1.55–$17.2 billion of the estimated lost work costs and $238 million–$7.76 billion of obstetric outcomes attributed to uterine fibroids (Cardozo et al., 2012). Totally, the costs of uterine fibroids are estimated to be $5.9–$34.4 billion annually in the United States. The mean total cost of hysterectomy for uterine fibroids ranges from 7,370 yuan to 10,064 yuan in China (Gu et al., 2015). Obviously, uterine fibroids remain a problematic issue for women's healthcare and health economies, especially in a developing country like China with a large number of women. However, relevant studies have scarcely evaluated the long-term trend of uterine fibroids in China. Moreover, the potential cause of the long-term trend is underdetermined, and the relative risks of age, period, and birth cohort effects remain to be elucidated.

To gain insight into this area, we aim to interrogate the long-term trend in death and disability-adjusted life years (DALYs) and investigate the specific effects of age, period, and birth cohort in China from 1990 to 2019 using the Joinpoint regression and Age–Period–Cohort analyses, based on detailed and comparable information of the Global Burden of Disease 2019 (GBD 2019) (Mattiuzzi and Lippi, 2020). Our findings may provide evidence for uterine fibroids intervention by integration and allocation of health resources.

Materials and methods

Data resource

The mortality and DALYs of uterine fibroids from 1990 to 2019 were derived from the GBD 2019, which provides a comprehensive and internally consistent estimation of the health losses from hundreds of diseases, injuries, and risk factors to improve health systems and eliminate disparities (Lancet, 2018a; Lancet, 2018b). The GBD 2019 comprised assessments of age–sex-specific all-cause and cause-specific mortality and DALYs from 369 diseases and 87 risk factors in 204 countries and territories (Lancet, 2020a; Lancet, 2020b). The methods of GBD 2019 were fully understood as reported previously (GBD, 2019 Demographics Collaborators, 2020; Lancet, 2020a). Uterine fibroids were diagnosed based on the International Statistical Classification of Diseases and the International Classification of Diseases and Injuries (ICD-10). The mortality and DALY rates of uterine fibroids in Chinese women were age-standardized based on the GBD global age-standardized population (Zhou et al., 2016). The study enrolled a national population–based Chinese cohort from the GBD, and no interaction with human subjects or personal private information was involved.

Statistical analysis

Joinpoint regression analysis

Trends of the mortality or DALY rate over a specific time interval could be depicted by a Joinpoint regression model under the assumption that the change of rates is constant over each time partition defined by the transition points, but varies among different time partitions (Clegg et al., 2009). The basic theory of the Joinpoint regression model is to separate the whole specific-time-interval regression trend into several segmented regression trends by transition points, of which the maximum number is five. This analysis postulates that dependent variables follow a Poisson distribution, exploiting the year as the predictor (Iannuzzi et al., 2022). The significance level of each segmented regression trend was evaluated by using Monte Carlo methods and the significance level of the whole specific-time-interval regression trend was obtained by a Bonferroni correction (Clegg et al., 2009). The segmented regression trends were presented as the annual percentage change (APC) and 95% confidence intervals (CI), while the whole specific-time-interval regression trend was presented as the average annual percent change (AAPC) and 95% CI. The Joinpoint Regression Program 4.9.1.0 (National Cancer Institute, Washington, DC) was used to calculate the APC and AAPC. A two-tailed p-value < 0.05 was considered statistically significant.

Age–Period–Cohort analysis

The Age–Period–Cohort (APC) model was designed to evaluate the effects of age, period, and birth cohort on outcomes, especially in the sociology and epidemiology fields. It is based on a log-linear

model for the outcome variable with additional effects from the age, period, and birth cohort, as shown in the following formula:

$$Y_{ijk} = u + \alpha_i + \beta_j + \gamma_k + \varepsilon_{ijk}.$$

where Y_{ijk} is the outcome variable, such as the mortality rate; μ is the intercept; α_i represents the i-th age effect; β_j represents the j-th period effect; γ_k represents the k-th birth cohort effect; and ε_{ijk} is the error term (Fosse and Winship, 2019). In this model, the age effect represents the effect of outcome risk changes related to different age groups; the period effect represents the effect of outcome risk changes of all age groups at different time intervals; the birth cohort effect represents the effect of outcome risk changes associated with different birth cohorts (Yang and Land, 2013). Net drift, the overall logarithmic linear trend by period and birth cohort, indicates the overall annual percentage change; local drifts, the logarithmic linear trend by period and birth cohort for each age group, indicate annual percentage changes for each age group; longitudinal age curve indicates the fitted longitudinal age-specific rates in the reference birth cohort adjusted for period deviations; the period relative risk (RR) indicates the RR adjusted for age and non-linear birth cohort effects in a certain period versus the reference period, which represents the period effect; the birth cohort RR indicates the relative risk adjusted for age and non-linear period effects in a certain birth cohort versus the reference birth cohort, which represents the birth cohort effect (Rosenberg et al., 2014; Wang et al., 2017; Wang et al., 2021).

For the APC analysis, the mortality and population data for uterine fibroids were divided into continuous 5-year periods from 1990 to 2019 and consecutive 5-year age intervals from 10–14 to 90–94 years. Uterine fibroids were rare in age groups under 10 years, and the data for age groups over 94 years in China were not provided in GBD 2019. The age-specific rates were appropriately recoded into successive 5-year age groups (10–14, 15–19, . . ., and 90–94 years), consecutive 5-year periods from 1990 to 2019 (1990–1994, 1995–1999, . . ., and 2015–2019), and correspondingly consecutive 5-year birth cohorts (1898–1902, 1903–1907, . . ., 1998–2002, and 2003–2007) to estimate net age, period, and birth cohort effects of uterine fibroids mortality and DALYs. The central period (2000–2004) and birth cohort (1948–1952) were defined as the references, respectively. The estimable parameters were obtained by using the APC web tool (Biostatistics Branch, National Cancer Institute, Bethesda, MD, http://analysistools.nci.nih.gov/apc/) (Rosenberg et al., 2014). The central age group, period, and birth cohort were defined as the respective references in the APC analysis. The significance of the estimable functions was tested by the Wald chi-squared test. Other analyses were performed by the R Project for Statistical Computing (version 4.0.5, http://www.r-project.org/). All statistical tests were two-tailed, and a p-value < 0.05 was considered statistically significant.

Results

Trends of uterine fibroids incidence, death, and DALY rates in China

By and large, there were 747,648 incidences, 138 deaths, and 90,389 DALYs in China in 1990 and 1,046,738 incidences, 473 deaths, and 159,558 DALYs in China in 2019, with a 40.0% increase in incidence, 242.8% increase in death, and 75.6% increase in DALYs. Trends of uterine fibroids incidence, death, and DALY rates in China from 1990 to 2019 are shown in Figure 1. In general, the crude incidence rate and age-standardized incidence rate (ASIR) exhibited a binormal distribution with peaks in 2004 and 2005. The crude mortality rate and age-standardized mortality rate (ASMR) were elevated fast from 2000 and began to fall since 2013. The crude DALY rate and age-standardized mortality rate showed an obvious upward trend since 1990 and stabilized after 2000.

Table 1 displays the AAPCs and APCs in uterine fibroids incidence, death, and DALYs in China from 1990 to 2019. The age-standardized rates were all on the ascending trend, with the greatest increase in ASMR (AAPC, 1.53; 95% CI, 1.04–2.02). As shown in Supplementary Table S1, for age-specific incidence rates, significant increases were observed in the 30–34, 35–39, and 40–44 years age groups, in which age-specific DALY rates also showed significant increases. A stable trend was observed in the 25–29 years age group, while the other age groups were on the decline. The age-specific mortality rates were on the ascending trend in most age groups. The age-specific DALY rates were on the decline in the younger age groups (10–14, 15–19, 20–24, and 25–29 years) and on the increase in the older age groups (75–79,80–84, 85–89, and 90–94 years).

Effect of age, period, and birth cohort on uterine fibroid mortality and DALY

The net drift indicating the overall annual percentage change was 3.51% (95% CI, 2.25%–4.78%) per year for mortality and 0.34% (95% CI, 0.14%–0.53%) per year for DALY. The local drifts, which represent annual percentage changes for each age group, are shown in Figure 2. The local shift values of mortality were above 0 in all age groups (Figure 2A). The local shift value of DALY exhibited an overall upward trend, where the values were below 0 for younger age groups (10–14, 15–19, 20–24, 25–29, and 30–34 years) and above 0 for age groups over 34 years (Figure 2B).

Figure 3 displays the longitudinal age curves of uterine fibroids mortality and DALY. Chinese women in the same birth cohort witnessed a stable growth in the mortality risk for uterine fibroids with age (Figure 3A). Contrary to the steady growth of mortality, DALYs showed a binormal distribution with a peak in the 40–44 years age group (Figure 3B).

The estimation of the period RR of mortality and DALYs is shown in Figure 4. The mortality of uterine fibroids shows an increasing trend between the period 1995 and 2015 and a declining trend for the periods 1990–1994 and 2015–2019 (Figure 4A). The mortality RR increased by approximately 74.6% in the period 2015–2019 when compared to that in the period 1990–1994. The DALY RRs of uterine fibroids were on an increase for most periods except for the period 2005–2014 (Figure 4B). When compared to the reference period 2000–2004, the period RRs of DALYs in other periods did not differ much. Detailed information on the period RR is shown in Supplementary Table S2.

The estimated birth cohort RR of mortality and DALYs is displayed in Figure 5. The overall trend of mortality RR is on the increase (Figure 5A). Compared with the birth cohort 1898–1902, the RR of mortality in the birth cohort 2003–2007 is increased by

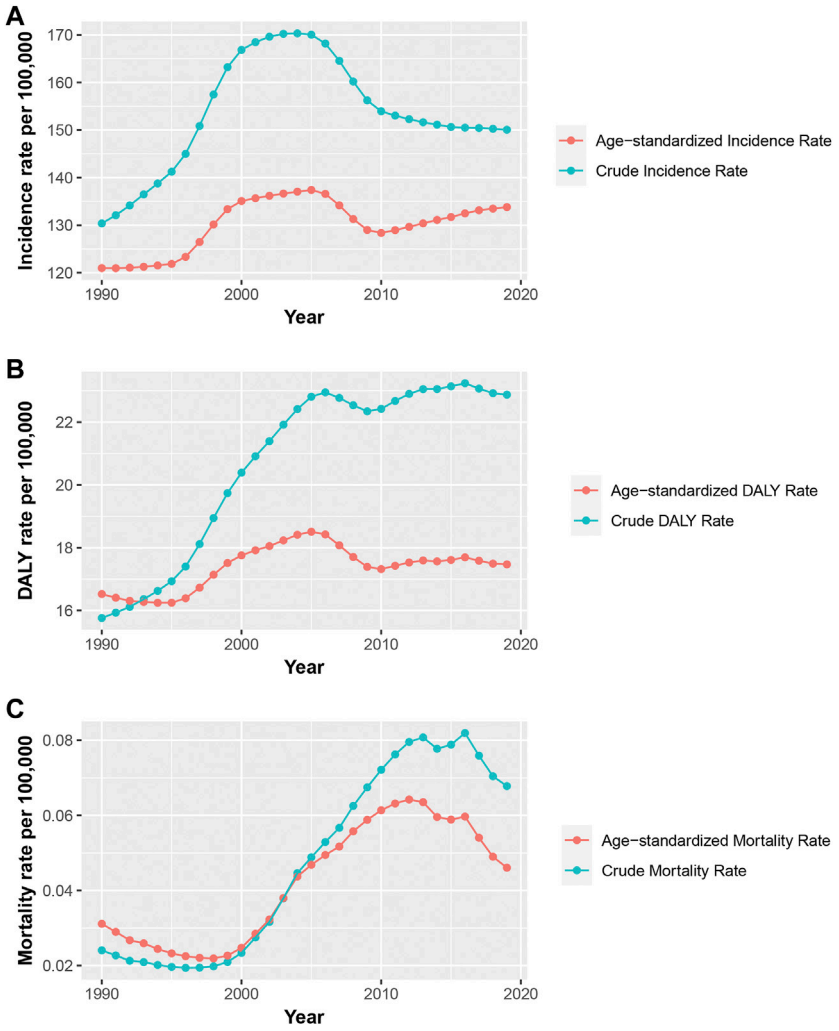

FIGURE 1
Trends of the crude rates and the age-standardized rates per 100,000 persons for incidence **(A)**, mortality **(B)**, and DALY **(C)** of uterine fibroids in China, 1990–2019 **(A)**, The crude rates and the age-standardized rates per 100,000 persons for incidence of uterine fibroids in China, 1990–2019; **(B)**, The crude rates and the age-standardized rates per 100,000 persons for mortality of uterine fibroids in China, 1990–2019; **(C)**, The crude rates and the age-standardized rates per 100,000 persons for DALY of uterine fibroids in China, 1990–2019; DALY, disability-adjusted life years.

427.2% for uterine fibroids. Different from the steady growth of mortality, the DALY risk shows a binormal distribution with a peak in the birth cohort 1973–1977 (Figure 5B). The RRs of DALYs in the birth cohort 1973–1977 is increased by 115.8% when compared to that in the birth cohort 1898–1902. Detailed information on the period RR is shown in Supplementary Table S2.

Finally, the net drifts of mortality and DALYs and the local shifts of DALYs are statistically significant according to the Wald test results (p-value < 0.001 for all), and the birth cohort and period RRs of mortality and DALYs were also statistically significant (p-value < 0.001 for all). However, the local shifts of death are not significant (p = 0.999).

Discussion

To our knowledge, this is the first study to investigate the long-term trend of mortality and DALYs of uterine fibroids in China from 1990 to 2019 and evaluate the specific effects of age, period, and birth cohort based on the APC framework analysis. The trends of incidence, mortality, and DALY rates in China were not consistent with the trends of the corresponding global rates (Cheng et al., 2022). When compared with an overall upward trend in ASIR and downward trends in ASMR and age-standardized DALY rate at the global level, the ASIR, ASMR, and age-standardized DALY rates of uterine fibroids in China fluctuated, increased, and decreased, respectively, over the past 30 years. Overall, the age-standardized rates were all on the ascending trend, with the greatest increase in ASMR (AAPC, 1.53; 95% CI, 1.04–2.02). The findings of our study provide valuable evidence for uterine fibroids control through policy and health system planning.

Uterine fibroids are the most common and frequently occurring benign gynecological tumors in women of productive age. Increasing age is one of the most important risk factors for uterine fibroids, especially in women aged over 40 years and

TABLE 1 Trends of ASIR, ASMR, and age-standardized DALY rates in uterine fibroids in China.

ASR	Period	APC (95% CI)	*p*-value
ASIR			
Trend1	1990–2004	1.17 (0.99, 1.35)	<0.001
Trend2	2004–2010	−1.30 (−2.11, −0.50)	0.003
Trend3	2010–2019	0.50 (0.19, 0.82)	0.003
AAPC	1990–2019	0.45 (0.24, 0.65)	<0.001
ASMR			
Trend1	1990–1999	−3.66 (−4.60, −2.71)	<0.001
Trend2	1999–2004	16.00 (13.85, 18.20)	<0.001
Trend3	2004–2011	5.63 (5.11, 6.16)	<0.001
Trend4	2011–2016	−2.02 (−3.00, −1.04)	0.001
Trend5	2016–2019	−7.92 (−9.44, −6.38)	<0.001
AAPC	1990–2019	1.53 (1.04, 2.02)	<0.001
Age-standardized DALY rate			
Trend1	1990–1995	−0.39 (−0.54, −0.24)	<0.001
Trend2	1995–2000	1.90 (1.68, 2.12)	<0.001
Trend3	2000–2005	0.94 (0.72, 1.16)	<0.001
Trend4	2005–2009	−1.69 (−2.01, −1.37)	<0.001
Trend5	2009–2016	0.23 (0.12, 0.34)	<0.001
Trend6	2016–2019	−0.41 (−0.74, −0.09)	0.016
AAPC	1990–2019	0.20 (0.12, 0.27)	<0.001

Abbreviations: ASR, age-standardized rate; ASIR, age-standardized incidence rate; ASMR, age-standardized mortality rate; APC, annual percentage change; AAPC, average annual percent change; CI, confidence interval; DALYs, disability-adjusted life years.

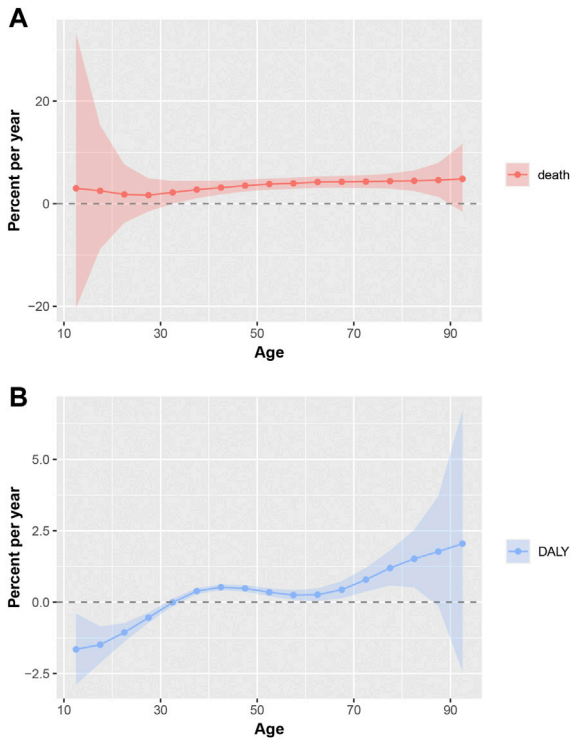

FIGURE 2
Local drifts of mortality and DALY for uterine fibroids in China. Age group-specific annual percent change (%) in mortality and DALY rate and the corresponding 95% CI. **(A)**, Local drifts of mortality for uterine fibroids in China; **(B)**, Local drifts of DALY for uterine fibroids in China; DALY, disability-adjusted life years.

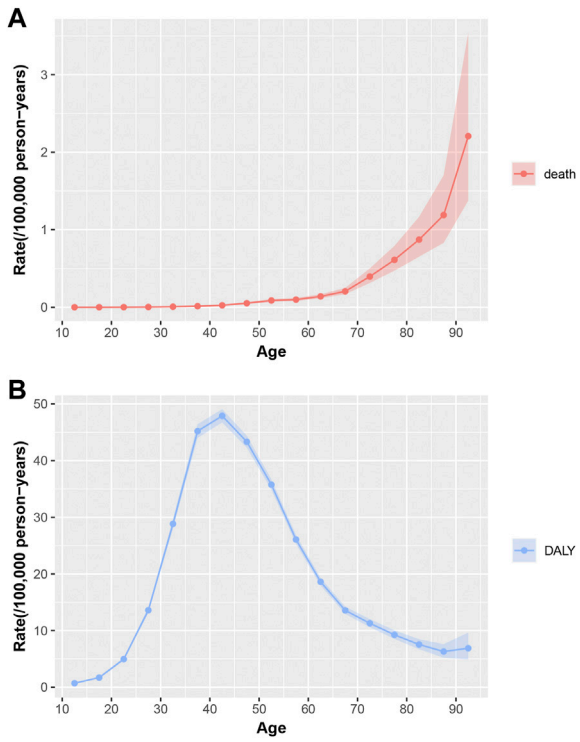

FIGURE 3
Longitudinal age curves of mortality and DALY for uterine fibroids in China. Fitted longitudinal age-specific rates of mortality and DALY (per 100,000 person-years) and the corresponding 95% CI. **(A)**, Longitudinal age curves of mortality for uterine fibroids in China; **(B)**, Longitudinal age curves of DALY for uterine fibroids in China; DALY, disability-adjusted life years; CI, confidence interval.

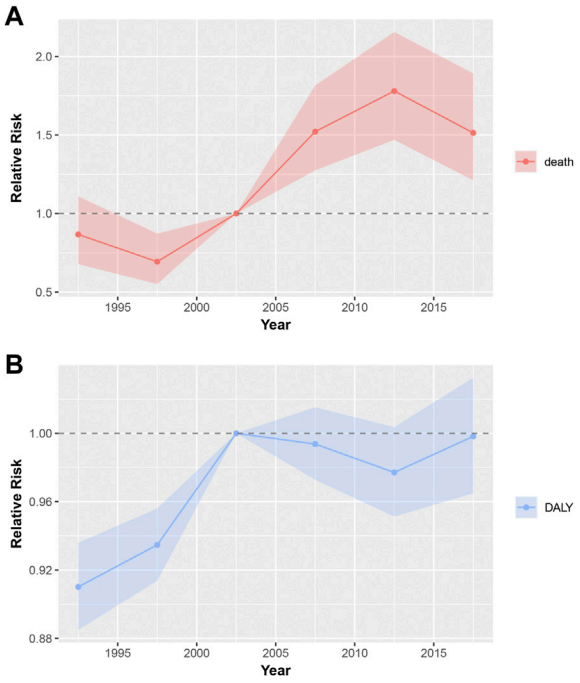

FIGURE 4
Period RRs of mortality and DALY for uterine fibroids in China. The RR of each period adjusted for age and non-linear cohort effects and the corresponding 95% CI. **(A)**, Period RRs of mortality for uterine fibroids in China; **(B)**, Period RRs of DALY for uterine fibroids in China; DALY, disability-adjusted life years; RR, relatively risk; CI, confidence interval.

women at the premenopausal stage (Faerstein et al., 2001; Wise et al., 2005). According to the longitudinal age curve results of mortality and DALYs, it is clear that the mortality risk increased overall with age, but the DALY risk increased first and then decreased with age. Since DALY is mainly influenced by incidence, the incidence of uterine fibroids reaches a peak at premenopausal age. The peak of the DALY risk was in the 40–44 years age group.

The period effects reflected the influence of different time periods on death and DALYs among all age groups, generally through social, economic, and medical measures, especially the changes in guidelines. So, when we wonder about the reasons for the mortality risk due to period effects, the impact of the International Classification of Diseases (ICD) coding issues should be taken into consideration (Wang et al., 2017). The improvement in cause-of-death reporting in China may be closely associated with the increase in the period RRs of mortality for uterine fibroids. Uterine fibroids–related deaths were possibly underestimated when the quality of reporting of the cause-of-death codes was suboptimal in the past. For instance, an old woman with uterine fibroids had likely died of severe anemia, massive uterine bleeding, or other complications; however, the physician responsible for reporting the cause-of-death may have ignored fibroids and instead filled in the underlying cause of death as severe anemia, massive uterine bleeding, or other fatal illness. A similar phenomenon was found in a study of reported causes of injury and poisoning deaths in China (Gao and Li, 2013).

The decline of DALY RRs after 2004 might be due to improvements of therapy; advancements in medical and uterine-preserving treatment options have been made in the past decade. A step-up approach, beginning with pharmacological and minimally invasive treatments before moving to surgery, is recommended by many international obstetrical and gynecology societies when treating uterine fibroids (ACOG practice bulletin, 2008). Available medical therapies include non-hormonal treatment and hormonal treatment, which work together to manage symptoms. Minimally invasive treatments such as uterine artery embolization and magnetic resonance–guided focused radiofrequency ablation are shorter procedures with faster recovery and quicker return to normal activities (ACOG practice bulletin, 2008). These improvements in medical and minimally invasive therapy have helped decrease the DALYs in recent years.

The birth cohort effects reflect different risk factors in early life, such as environmental, behavioral, and socioeconomic factors. The birth cohort RRs of mortality increased gradually in all birth cohorts, and the birth cohort RRs of DALY increased before the birth cohort 1973–1977 and then decreased somehow. The increase in mortality might be mainly due to unhealthy lifestyles. Obesity prevalence and the rate of increase have been high in women (Afshin et al., 2017). The rapid growth of obesity in women probably leads to an increase in the occurrence and growth of uterine fibroids through hormonal and inflammatory mechanisms (Wise and Laughlin-Tommaso, 2016; Ciavattini et al., 2017). Apart from obesity, the alteration of lifestyle might also increase the risk of uterine fibroids. Less physical activity, stress of work and family, unhealthy diet, smoking, alcohol,

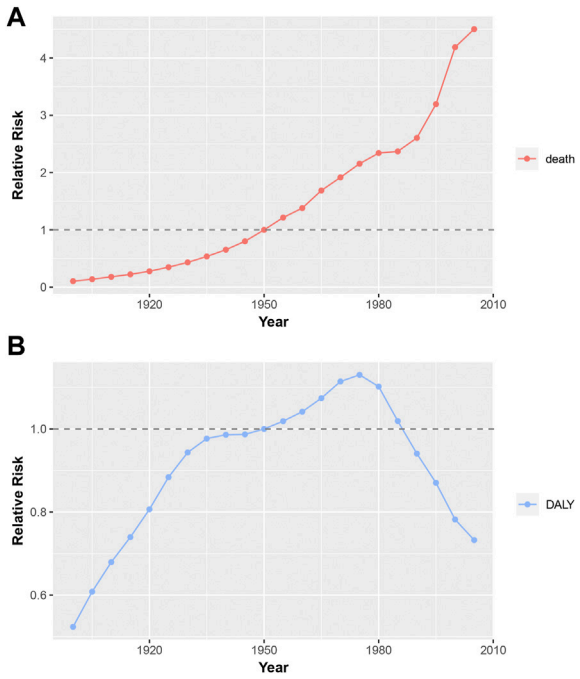

FIGURE 5
Birth cohort RRs of mortality and DALY for uterine fibroids in China. The RR of each birth cohort adjusted for age and non-linear period effects. **(A)**, Birth cohort RRs of mortality for uterine fibroids in China; **(B)**, Birth cohort RRs of DALY for uterine fibroids in China; DALY, disability-adjusted life years; RR, relatively risk.

and too much caffeine consumption all contribute to a higher risk of uterine fibroids (Pavone et al., 2018). Since fibroids are estrogen related, birth control methods (such as oral contraceptives and intrauterine devices) for the policy of one child per family might be partially responsible for the birth cohort risk increase in DALYs before the birth cohort 1973–1977 (Wang, 2012). The possible reason for the following decline in DALY period risks might be the widespread use of condoms.

Strengths of this study include a comprehensive and up-to-date analysis of uterine fibroid death and DALYs in China between 1990 and 2019 and the illustrated effects of age, period, and birth cohort through the Age–Period–Cohort analysis. Due to the inherent deficiencies of GBD 2019, some limitations are unavoidable in this study. First, the accuracy of the results of this study depends on the quality and quantity of GBD data, although there were many adjustment steps, such as the correction of incompleteness, underreporting, and misclassification, as well as redistribution of garbage codes, to improve data quality and comparability of data in GBD 2019. Second, due to the limitation of GBD 2019 data, we could not investigate the incidence and burden of uterine fibroids subtypes by location (intermural, subplasma, and submucosa). Third, since the GBD study took the country as its basic unit, we cannot investigate the differences in race. Finally, GBD 2019 only includes DALY, YLL, and YLD as the indicators of disease burden, therefore the recurrence rate, malignancy rate, and impact on fertility cannot be estimated.

The study investigates the secular time trends of mortality and the DALY trend of uterine fibroids from 1990 to 2019 in China. The age-standardized rates were all on the ascending trend, with the greatest increase in ASMR. The net drift was found to be 3.51% (95% CI, 2.25%–4.78%) per year for mortality and 0.34% (95% CI, 0.14%–0.53%) per year for DALYs. Significant age, period, and birth cohort effects were found for mortality and DALYs. These secular time trends and effects of mortality and DALYs reveal socioeconomic alterations, reforms of diagnosis and therapy, and changes in social lifestyles and behaviors. More epidemiological investigations and social health prevention and control should be applied to uterine fibroids. Our results suggest an exaggeration of the epidemic among older individuals. Timely intervention should be conducted, especially for earlier birth cohorts at high risk.

Data availability statement

The data sets presented in this study can be found in online repositories. The names of the repository/repositories and accession number(s) can be found at http://ghdx.healthdata.org/gbd-results-tool.

Author contributions

Conceptualization: SW and JZ; data curation: XL and BW; formal analysis: XL; funding acquisition: SW and JZ; methodology: XL and QZ; software: XL and BW; supervision: SW and JZ; visualization: XL and QZ; roles/writing of manuscript—original draft: XL; writing of manuscript—review and editing: all authors. All authors contributed to the article and approved the submitted version.

Funding

This study was supported by the National Key Research and Development Program of China (grant no. 2022YFC2704100) and the National Natural Science Foundation of China (grant no. 82001498).

Acknowledgments

The authors would like to thank the collaborators of the Global Burden of Disease (GBD) Study 2019 for their work and all the individuals who contributed to the GBD 2019 for their extensive support in finding, cataloging, and analyzing data and facilitating communications.

Conflict of interest

The authors declare that the research was conducted in the absence of any commercial or financial relationships that could be construed as a potential conflict of interest.

Publisher's note

Supplementary material

The Supplementary Material for this article can be found online at: https://www.frontiersin.org/articles/10.3389/fphys.2023.1197658/full#supplementary-material

References

American College of Obstetricians and Gynecologists (2008). ACOG practice bulletin. Alternatives to hysterectomy in the management of leiomyomas. *Obstetrics Gynecol.* 112 (2), 387–400. doi:10.1097/AOG.0b013e318183fbab

Afshin, A., Forouzanfar, M. H., Reitsma, M. B., Sur, P., Estep, K., Lee, A., et al. (2017). Health effects of overweight and obesity in 195 countries over 25 years. *N. Engl. J. Med.* 377 (1), 13–27. doi:10.1056/NEJMoa1614362

Baird, D. D., Dunson, D. B., Hill, M. C., Cousins, D., and Schectman, J. M. (2003). High cumulative incidence of uterine leiomyoma in black and white women: Ultrasound evidence. *Am. J. obstetrics Gynecol.* 188 (1), 100–107. doi:10.1067/mob.2003.99

Bulun, S. E. (2013). Uterine fibroids. *N. Engl. J. Med.* 369 (14), 1344–1355. doi:10.1056/NEJMra1209993

Cardozo, E. R., Clark, A. D., Banks, N. K., Henne, M. B., Stegmann, B. J., and Segars, J. H. (2012). The estimated annual cost of uterine leiomyomata in the United States. *Am. J. obstetrics Gynecol.* 206 (3), 211.e1–e9. doi:10.1016/j.ajog.2011.12.002

Cheng, L. C., Li, H. Y., Gong, Q. Q., Huang, C. Y., Zhang, C., and Yan, J. Z. (2022). Global, regional, and national burden of uterine fibroids in the last 30 years: Estimates from the 1990 to 2019 Global Burden of Disease Study. *Front. Med.* 9, 1003605. doi:10.3389/fmed.2022.1003605

Ciavattini, A., Delli Carpini, G., Moriconi, L., Clemente, N., Orici, F., Boschi, A. C., et al. (2017). The association between ultrasound-estimated visceral fat deposition and uterine fibroids: An observational study. *Gynecol. Endocrinol.* 33 (8), 634–637. doi:10.1080/09513590.2017.1302418

Clegg, L. X., Hankey, B. F., Tiwari, R., Feuer, E. J., and Edwards, B. K. (2009). Estimating average annual per cent change in trend analysis. *Statistics Med.* 28 (29), 3670–3682. doi:10.1002/sim.3733

Cramer, S. F., and Patel, A. (1990). The frequency of uterine leiomyomas. *Am. J. Clin. pathology* 94 (4), 435–438. doi:10.1093/ajcp/94.4.435

Drayer, S. M., and Catherino, W. H. (2015). Prevalence, morbidity, and current medical management of uterine leiomyomas. *Int. J. Gynaecol. obstetrics* 131 (2), 117–122. doi:10.1016/j.ijgo.2015.04.051

Faerstein, E., Szklo, M., and Rosenshein, N. (2001). Risk factors for uterine leiomyoma: A practice-based case-control study. I. African-American heritage, reproductive history, body size, and smoking. *Am. J. Epidemiol.* 153 (1), 1–10. doi:10.1093/aje/153.1.1

Fosse, E., and Winship, C. (2019). Bounding analyses of age-periodperiod-cohort effects. *Demography* 56 (5), 1975–2004. doi:10.1007/s13524-019-00801-6

Gao, L. R. Y., and Li, X. (2013). Analysis of the problems existing in the reporting of underlying cause of death. *J. Aerosp. Med.* 24 (723–4).

GBD 2019 Demographics Collaborators (2020). Global age-sex-specific fertility, mortality, healthy life expectancy (HALE), and population estimates in 204 countries and territories, 1950-2019: A comprehensive demographic analysis for the global burden of disease study 2019. *Lancet (London, Engl.* 396 (10258), 1160–1203. doi:10.1016/S0140-6736(20)30977-6

Gu, Y., Zhu, L., Liu, A., Ma, J., and Lang, J. (2015). Analysis of hysterectomies for patients with uterine leiomyomas in China in 2010. *Int. J. Gynaecol. obstetrics* 129 (1), 71–74. doi:10.1016/j.ijgo.2014.10.031

Iannuzzi, J. P., King, J. A., Leong, J. H., Quan, J., Windsor, J. W., Tanyingoh, D., et al. (2022). Global incidence of acute pancreatitis is increasing over time: A systematic review and meta-analysis. *Gastroenterology* 162 (1), 122–134. doi:10.1053/j.gastro.2021.09.043

Kim, J. J., and Sefton, E. C. (2012). The role of progesterone signaling in the pathogenesis of uterine leiomyoma. *Mol. Cell. Endocrinol.* 358 (2), 223–231. doi:10.1016/j.mce.2011.05.044

Lancet (2020a). Global burden of 369 diseases and injuries in 204 countries and territories, 1990-2019: A systematic analysis for the global burden of disease study 2019. *Lancet (London, Engl.* 396 (10258), 1204–1222. doi:10.1016/S0140-6736(20)30925-9

Lancet (2020b). Global burden of 87 risk factors in 204 countries and territories, 1990-2019: A systematic analysis for the global burden of disease study 2019. *Lancet (London, Engl.* 396 (10258), 1223–1249. doi:10.1016/S0140-6736(20)30752-2

Lancet (2018b). Global, regional, and national comparative risk assessment of 84 behavioural, environmental and occupational, and metabolic risks or clusters of risks for 195 countries and territories, 1990-2017: A systematic analysis for the global burden of disease study 2017. *Lancet (London, Engl.* 392 (10159), 1923–1994. doi:10.1016/S0140-6736(18)32225-6

Lancet (2018a). Global, regional, and national incidence, prevalence, and years lived with disability for 354 diseases and injuries for 195 countries and territories, 1990-2017: A systematic analysis for the global burden of disease study 2017. *Lancet (London, Engl.* 392 (10159), 1789–1858. doi:10.1016/S0140-6736(18)32279-7

Mattiuzzi, C., and Lippi, G. (2020). Cancer statistics: A comparison between world health organization (WHO) and global burden of disease (GBD). *Eur. J. public health* 30 (5), 1026–1027. doi:10.1093/eurpub/ckz216

Merrill, R. M. (2008). Hysterectomy surveillance in the United States, 1997 through 2005. *Med. Sci. Monit. Int. Med. J. Exp. Clin. Res.* 14 (1), Cr24–31.

Pavone, D., Clemenza, S., Sorbi, F., Fambrini, M., and Petraglia, F. (2018). Epidemiology and risk factors of uterine fibroids. *Best Pract. Res. Clin. obstetrics Gynaecol.* 46, 3–11. doi:10.1016/j.bpobgyn.2017.09.004

Rosenberg, P. S., Check, D. P., and Anderson, W. F. (2014). A web tool for age-period-cohort analysis of cancer incidence and mortality rates. *Cancer Epidemiol. biomarkers Prev.* 23 (11), 2296–2302. doi:10.1158/1055-9965.EPI-14-0300

Stewart, E. A., Cookson, C. L., Gandolfo, R. A., and Schulze-Rath, R. (2017). Epidemiology of uterine fibroids: A systematic review. *BJOG Int. J. obstetrics Gynaecol.* 124 (10), 1501–1512. doi:10.1111/1471-0528.14640

Wang, C. (2012). Trends in contraceptive use and determinants of choice in China: 1980-2010. *Contraception* 85 (6), 570–579. doi:10.1016/j.contraception.2011.10.014

Wang, Z., Guo, E., Yang, B., Xiao, R., Lu, F., You, L., et al. (2021). Trends and age-period-cohort effects on mortality of the three major gynecologic cancers in China from 1990 to 2019: Cervical, ovarian and uterine cancer. *Gynecol. Oncol.* 163 (2), 358–363. doi:10.1016/j.ygyno.2021.08.029

Wang, Z., Hu, S., Sang, S., Luo, L., and Yu, C. (2017). Age-Period-cohort analysis of stroke mortality in China: Data from the global burden of disease study 2013. *Stroke* 48 (2), 271–275. doi:10.1161/STROKEAHA.116.015031

Whiteman, M. K., Kuklina, E., Jamieson, D. J., Hillis, S. D., and Marchbanks, P. A. (2010). Inpatient hospitalization for gynecologic disorders in the United States. *Am. J. obstetrics Gynecol.* 202 (6), 541.e1–e6. doi:10.1016/j.ajog.2009.12.013

Wise, L. A., and Laughlin-Tommaso, S. K. (2016). Epidemiology of uterine fibroids: From menarche to menopause. *Clin. obstetrics Gynecol.* 59 (1), 2–24. doi:10.1097/GRF.0000000000000164

Wise, L. A., Palmer, J. R., Stewart, E. A., and Rosenberg, L. (2005). Age-specific incidence rates for self-reported uterine leiomyomata in the Black Women's Health Study. *Obstetrics Gynecol.* 105 (3), 563–568. doi:10.1097/01.AOG.0000154161.03418.e3

Yang, Y., and Land, K. C. (2013). *Age-period-cohort analysis: New models, methods, and empirical applications*. United Kingdom: Taylor & Francis.

Yu, O., Scholes, D., Schulze-Rath, R., Grafton, J., Hansen, K., and Reed, S. D. (2018). A US population-based study of uterine fibroid diagnosis incidence, trends, and prevalence: 2005 through 2014. *Am. J. obstetrics Gynecol.* 219 (6), 591. doi:10.1016/j.ajog.2018.09.039

Zhou, M., Wang, H., Zhu, J., Chen, W., Wang, L., Liu, S., et al. (2016). Cause-specific mortality for 240 causes in China during 1990-2013: A systematic subnational analysis for the global burden of disease study 2013. *Lancet (London, Engl.* 387 (10015), 251–272. doi:10.1016/S0140-6736(15)00551-6

frontiers | Frontiers in Endocrinology

TYPE Review
PUBLISHED 07 September 2023
DOI 10.3389/fendo.2023.1191721

OPEN ACCESS

EDITED BY
Fengxiang Wei,
Shenzhen Longgang District Maternal and Child Health Care Hospital, China

REVIEWED BY
Chao Zhang,
Capital Medical University, China
Shilin Li,
Fudan University, China

*CORRESPONDENCE
Shuli Yang
yangsl@jlu.edu.cn

RECEIVED 22 March 2023
ACCEPTED 21 August 2023
PUBLISHED 07 September 2023

CITATION
Wang M, Zheng L, Ma S, Lin R, Li J and Yang S (2023) Biogenesis and function of exosome lncRNAs and their role in female pathological pregnancy. *Front. Endocrinol.* 14:1191721. doi: 10.3389/fendo.2023.1191721

Biogenesis and function of exosome lncRNAs and their role in female pathological pregnancy

Min Wang[1], Lianwen Zheng[1], Shuai Ma[1], Ruixin Lin[2], Jiahui Li[1] and Shuli Yang[1]*

[1]Department of Obstetrics and Gynecology, The Second Hospital of Jilin University, Changchun, China, [2]Department of Hepato-Biliary-Pancreatic Surgery, The Second Hospital of Jilin University, Changchun, China

Preeclampsia, gestational diabetes mellitus, and recurrent spontaneous abortion are common maternal pregnancy complications that seriously endanger women's lives and health, and their occurrence is increasing year after year with a rejuvenation trend. In contrast to biomarkers found freely in tissues or body fluids, exosomes exist in a relatively independent environment and provide a higher level of stability. As backbone molecules, guidance molecules, and signaling molecules in the nucleus, lncRNAs can regulate gene expression. In the cytoplasm, lncRNAs can influence gene expression levels by modifying mRNA stability, acting as competitive endogenous RNAs to bind miRNAs, and so on. Exosomal lncRNAs can exist indefinitely and are important in intercellular communication and signal transduction. Changes in maternal serum exosome lncRNA expression can accurately and timely reflect the progression and regression of pregnancy-related diseases. The purpose of this paper is to provide a reference for clinical research on the pathogenesis, diagnosis, and treatment methods of pregnancy-related diseases by reviewing the role of exosome lncRNAs in female pathological pregnancy and related molecular mechanisms.

KEYWORDS

exosome lncRNA, pregnancy, pre-eclampsia, diabetes, gestational, abortion, biomarkers

1 Introduction

Exosomes are membrane vesicles that are released into the extracellular fluid by various cells (1). The exosome membrane is high in cholesterol, sphingolipids, and other components, and it contains a variety of proteins, mRNA, and lncRNA, including mother cell-specific proteins and exosome-associated proteins. Exosomes are the best markers for determining the levels of various substances expressed within the mother cell (2). Scholars have paid close attention to the non-coding RNAs found in the non-coding region in recent years (3). lncRNAs are expressed in low amounts in cells or tissues and

have a length of more than 200 nt. Their regulation primarily consists of epigenetic regulation, transcriptional regulation, and post-transcriptional regulation, all of which affect cell proliferation, apoptosis, and differentiation and play an essential role in the development of many diseases (4, 5). Research has found that lncRNA plays an important role in the homeostasis of cells or tissues during development. Although LncRNAs cannot directly regulate protein translation, they can exert regulatory power through miRNAs, which may be mediated as a mediator (6). Some lncRNAs are enriched in exosomes, while others are almost absent, implying that lncRNAs are selectively sorted into exosomes (7). Pathological pregnancy is becoming more common, and the resulting problem of reduced fertility cannot be ignored (8). Exosomal lncRNA, which is abundant and stable in plasma and has high ribonuclease activity, can serve as a reference for clinicians in the diagnosis of pregnancy-related disorders (9). As a result, it is clinically significant to investigate the exosome lncRNAs that affect women's pathological pregnancy behavior, as this can help to further investigate the disease's development mechanism and provide new ideas and strategies for disease treatment, thereby genuinely protecting women's reproductive health (10).

2 Overview of exosomes

2.1 Biogenesis of exosomes

Exosomes are made up of a double-layered lipid membrane structure that ranges in size from 30nm to 150nm and contains DNA, mRNA, and lncRNA (11, 12). Exosomes are present in almost all eukaryotic body fluids (13), including uterine fluid, urine, amniotic fluid, breast milk, peritoneal fluid, and cell culture fluid, according to recent research (14). When exposed to extracellular stimuli, microbial attack, or other stress conditions, the cell membrane invaginates, allowing material from outside the cell membrane to enter the cell along with the cell membrane surface proteins, resulting in the formation of the early-sorting endosome (ESE) (15). By "budding," the ESE membrane generates multivesicular bodies (MVBs) or late endosomes. Finally, MVBs are secreted extracellularly to form exosomes under the control of the endosomal sorting complex required for transport (ESCRT) and specific proteins (16). Exosomes and target cells interact in three ways: exosome surface membrane proteins directly bind to target cell receptors, activating intracellular signaling pathways; target cells take up exosomes via endocytosis; and exosomes can directly fuse with the plasma membrane of target cells, releasing the miRNAs and lncRNAs they carry into the target cells (17) (Figure 1).

2.2 Function of exosomes

Exosomes are critical intercellular messengers that regulate cellular physiological functions such as immune regulation, cell proliferation, antigen expression and presentation, and bioenergetic conversion (18, 19). Exosomes transport nucleic acids, which play an essential role in cellular communication (20). Exosomes contain at least ten different types of RNA, and actively secreted exosomes can package a large amount of intracellular information material for transmission from one cell to another, achieving cross-cellular regulation and participating in intercellular communication and microenvironment regulation (21). Because cell membrane transmembrane proteins are also expressed on the exosome membrane, it is critical for exosome identification (22). Glycoproteins and transmembrane proteins are enriched in intercellular communication and adhesion events, which can be utilized to determine their cellular or tissue origin, such as placental-derived exosomes that express placental-like alkaline phosphatase (PLAP) (23). Exosomes can control morphogenetic signaling, immune cell recruitment, and genetic material transport to carry out a range of cell biological tasks in the cellular microenvironment (24). The majority of methods for detecting exosomal nucleic acid information rely on the presence of mRNA and microRNA in exosomes (25). In recent years, the importance of targeting exosomal lncRNAs has gained more attention. LncRNAs protected by the exosomal tegument exhibit higher expression and better stability than lncRNAs isolated directly from peripheral bodily fluids, and their results are trustworthy.

3 Overview of lncRNAs

3.1 lncRNAs play a role in the regulation of pre-transcription

By controlling the regulation of target genes by the epimodification complex before transcription takes place through chromatin modification, genomic imprinting, and dosage compensation effects, lncRNAs in the nucleus play an epigenetic function in gene expression (26, 27). The chromatin state and the way proteins attach to chromatin are both altered by the different ways that lncRNAs can modify histones, including methylation, acetylation, and ubiquitination. In order to interact with the histone modification complex Polycomb Repressive Complex 2 (PRC2) and mediate histone methylation and demethylation, LncRNA HOX antisense intergenic RNA (HOTAIR) may serve as a molecular scaffold. The ATP-dependent chromatin remodeling complex plays a major role in controlling chromatin remodeling, an enzymatic co-process that enables nucleosomal DNA acquisition by altering the structure, composition, and placement of nucleosomes. BRG1, the central component of the chromatin remodeling complex SWI/SNF, can interact with lncRNA MANTIS, stabilizing it. An open chromatin conformation is induced by the interaction of BRG1 with BAFl55, another chromatin remodeling factor, and this increases the transcription of genes involved in angiogenesis. MANTIS is a lncRNA that is thought to have pro-endothelial angiogenic potential (Figure 2).

3.2 LncRNAs play a role in controlling gene transcription

By preventing the RNA Pol II complex from attaching to the promoter, LncRNA can interfere with transcription (28). According

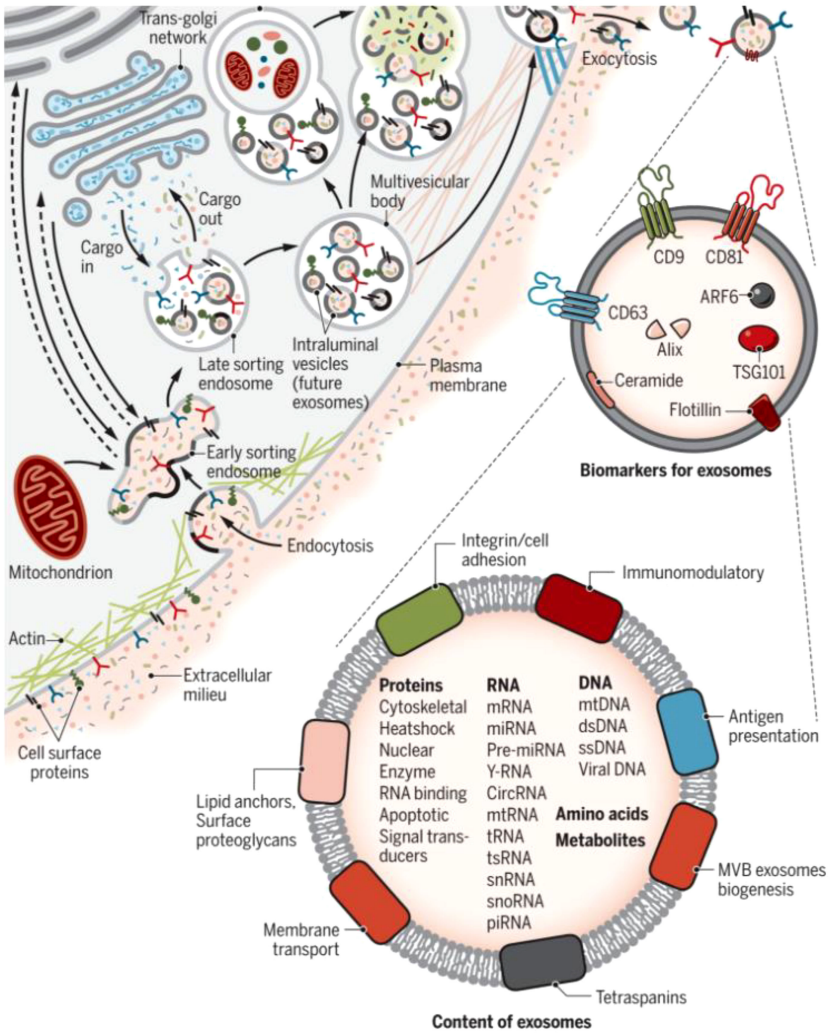

FIGURE 1
Biogenesis and identification of exosomes. Fluid and extracellular constituents such as proteins, lipids, metabolites, small molecules, and ions can enter cells, along with cell surface proteins, through endocytosis and plasma membrane invagination. The resulting plasma membrane bud formation in the luminal side of the cell presents with outside-in plasma membrane orientation. Several proteins are implicated in exosome biogenesis and include ESCRT proteins, as well as others that are also used as markers for exosomes (CD9, CD81, CD63, flotillin, ceramide, and Alix). Exosome surface proteins include tetraspanins, integrins, immunomodulatory proteins, and more. Exosomes can contain different types of cell surface proteins, intracellular proteins, RNA, DNA, amino acids, and metabolites (15).

to Latos et al., the lncRNA Aim transcript covers the lgf2r promoter region and prevents the recruitment of RNA Pol II, preventing the transcription of lgf2r. LncRNA can directly activate the downstream genes by bridging the gap between the enhancer and promoter regions (29). It is crucial for the transcriptional activation of Snail that activating lncRNAs interact with enhancers and transcription factors, be present inside the enhancer, and have enhancer activity. Studies demonstrate that the binding of activating lncRNAs to the Snail promoter region is mediated by the transcriptional co-activation complex Mediator, acting in concert with CDK8-catalyzed histone modifications to promote transcriptional activation of Snail, underscoring the significance of activating lncRNAs in human disease. lncRNA LNMAT2 is loaded into exosomes through direct interaction with heterogeneous ribonucleoprotein A2B1 (hnRNPA2B1) by direct interaction to exosomes and delivery to human lymphatic vessel endothelial cells (HLEC); subsequently, LncRNALNMAT2 forms a triple complex with the PROX1 promoter by inducing hnRNPA2B1-mediated H3K4me3 and enhances PROX1 transcription, thereby promoting lymphangiogenesis and lymph node metastasis.

3.3 LncRNAs participate in the selective shear regulation process

Genetic information from DNA is translated into mature mRNA by biological processes, including shearing and splicing; this process does not function directly (30). More than 95% of gene transcripts go through a process called selective splicing, which makes biological gene expression more complex and plays a

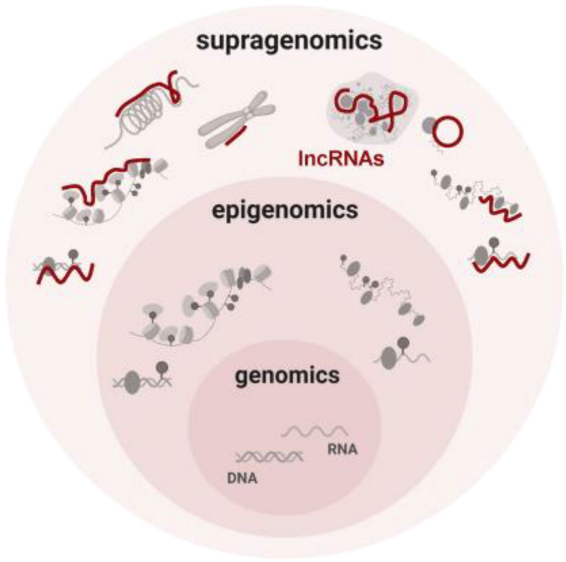

FIGURE 2
Conceptual summary of supragenomic regulation by lncRNAs Vast and heterogeneous lncRNAs interact broadly with gene regulatory machineries. By providing a supragenomic layer of control built upon genomic and epigenomic processes, lncRNAs modulate many levels of gene regulation, from transcription to protein modification (26).

regulatory function in the growth and development of living things (31). LncRNA participates in gene expression regulation by constructing different variable splicing forms through splicing factors, regulating miRNA precursor transcripts and upstream differentially methylated regions (DMR) (32). In order to control the phosphorylation level of the serine/arginine-rich (SR) protein family, which controls mRNA splicing, lncRNAs have been shown to function as regulatory factors (33). It has been demonstrated that the lncRNA metastasis-associated lung adenocarcinoma transcript 1 (MALAT1) associates with numerous proteins to form a nuclear speckle that takes part in varied pre-mRNA shearing (34). Vidisha et al. discovered that the lncRNA MALAT1 selectively binds to the nuclear protein TDP-43, resulting in the recruitment of the SR protein family to the nucleus. The nuclear speckle was recruited by splicing factors like TDP-43, which improved the SR protein family's capacity to splice and thus raised its level of phosphorylation.

4 Exosomal lncRNA offers excellent clinical use potential

Specificity, as exosomes include particular indicators of tissue or cellular origin, is one of the properties of exosome-derived lncRNAs as biomarkers. Notably, the RNase activity is high in the extracellular environment, but extracellular ncRNAs remain relatively stable in plasma, suggesting that circulating ncRNAs may be protected and circumvented from harsh conditions (35). Exosome stability: Exosomes remain in a stable state in bodily fluids, and RNA is not significantly exposed because of the protection of lipid bilayer membranes, where enzymes cannot easily digest the contents of exosomes (36). Although the lncRNA expression is low in some cells, it is highly expressed in their secreted exosomes and correlates with the development of disease. Exosomes are widely distributed in different body fluids. The primary techniques for isolating exosomes are gradient density centrifugation, differential ultracentrifugation, polymer immunoprecipitation, gel exclusion separation, and membrane affinity kits (37, 38). Exosomal lncRNAs combine the benefits of exosomes and lncRNAs in a way that enhances the effectiveness of treatment and the prognosis of patients (39). Exosomes can be employed as specialized targets for treating disease. As a result, the non-invasive detection of lncRNA produced from exosomes has the potential to be exploited as a biomarker for future diagnosis and therapy (40).

5 Correlation of exosomal lncRNA with pregnancy

5.1 Endometrial tolerance

Fertilization, implantation, endometrial metaphase, placental development, and birth are significant, complex, and irreversible aspects of pregnancy in humans and other mammals (41). Abnormalities or the failure of any one of these processes can have an impact on the pregnancy's outcome (9) (Figure 3). By directly influencing embryonic development and regulating the expression of important adhesion molecules, the endometrium can leak exosomes into the uterine fluid and govern implantation (42). h19 is a naturally occurring lncRNA that is widely produced, developmentally controlled, and affects Let-7 target genes (43). Reduced expression of the H19 gene and the ITG-3 protein was found in the recurrent implantation failure (RIF) group, proving that the expression of the lncRNAH19 is positively associated with that of the ITG-3 protein, reducing endometrial tolerance and ultimately causing implantation failure.lncRNATUNAR was initially expressed in the human endometrium and is thought to play a role in embryo implantation by controlling the attachment of blastocysts to the endometrial epithelium as well as the proliferation and ecdysis of embryonic stem cells. In healthy females, the expression of lncRNATUNAR was increased in LH+2 and downregulated in LH+7. Due to the cyclic expression of the endometrium and its abnormal expression in RIF patients, lncRNATUNAR may have a role in controlling the embryonic implantation process. lncRNATUNAR was found to be increased in LH+7 endometrium from RIF patients.

5.2 Promote the establishment of immune tolerance at the maternal-fetal interface

The maternal-fetal interface, which is made up of extra-embryonic tissues and the meconium, is a crucial component that helps the mother's immune system adapt to the fetus during pregnancy (44). By triggering the JNK and p38 signaling

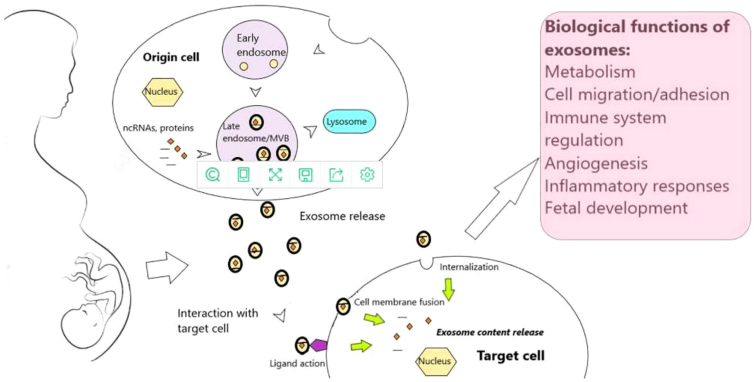

FIGURE 3
Exosomes and exosomal noncoding RNAs throughout human gestation (9).

pathways in meconium macrophages via the exosomal lncRNA Zinc finger E-box-binding homeobox 2 antisense RNA 1 (ZEB2-AS1), trophoblast cells can create and maintain the maternal-fetal immune tolerance microenvironment. This promotes the polarization of macrophages toward the inhibitory M2 phenotype. In order to support the orderly development of a typical pregnancy, the induced M2 can also operate on trophoblast cells and encourage their proliferation and differentiation at the same time. The decline in recurrent spontaneous abortion patients' metaphase macrophage M2 may be brought on by low expression of ZEB2-AS 1 in their trophoblast exosomes. The preservation of a stable pregnancy may be made possible by apoptosis, which may allow the human placenta and fetal allografts to avoid a detrimental maternal immune attack while pregnant and enjoy immunological privileges in the uterine cavity (45). The results point to functional FasL and TRAIL being secreted by human early and term placentas, which help deliver apoptosis and shield the fetal placenta from activated maternal immune cells. This suggests placental exosome-mediated fetal immunological privilege. Exosomes play a key role in preserving homeostasis at the maternal-fetal interface throughout pregnancy and are a cutting-edge instrument for intercellular communication (46).

5.3 Promote successful embryo implantation

Embryo implantation, a crucial stage in pregnancy, is the process by which the blastocyst interacts with the uterus in a receptive condition while in an activated state before making close contact with the endometrium (47). Mammalian reproduction depends on the embryo's successful implantation into the mother (48). Placenta-derived exosome (PEXO) can be ingested by epithelial and stromal cells in the meconium, changing the regional immunological milieu, according to *in vitro* research. In order to start and maintain pregnancy, cell-to-cell communication at the maternal-fetal interface is crucial. Exosomes, which the embryo secretes to help with implantation, enhance the embryo's natural adaptability and support successful implantation and the start of pregnancy, allowing the embryo to control its growth. Before embryo implantation, extracellular vesicles of decidual epithelial cells can activate the expression of Bcl2, Bax, Casp3, and Tp53 genes in endometrial epithelial cell apoptosis pathways. Exosomes primarily increase the expression of endometrial epithelial cell adhesion-related proteins following embryo implantation to aid subsequent adherence (49). Exosomes from human ectodermal stromal cells can upregulate the production of trophoblast calmodulin and so boost invasive activity in addition to that of epithelial cells. They can also promote the creation of endothelial cell tubes and may be crucial for angiogenesis. In mouse trials, embryos treated with embryonic-derived exosomes were able to increase implantation rates and improve implantation ability. They could also improve blastocyst formation rate, embryo quality, and future growth and development.

6 Exosomal lncRNA and pathological pregnancy

Exosomes contain various proteins and nucleic acids, serving as diagnostic markers for obstetric diseases with high specificity. The study of exosome lncRNA can explore the pathogenesis of various diseases in pathological pregnancy, screen biomarkers, and provide a new basic basis for the diagnosis and treatment of diseases. Many lncRNAs associated with tumor cell function may also play significant regulatory roles for trophoblasts because placental trophoblasts share characteristics with tumor cells during proliferation, migration, and invasion (50). This is especially true for pathways involved in angiogenesis, cell cycle regulation, cell migration, and invasion (51). Through interacting with miR-216a-5p and controlling recombinant hexokinase 2(HK2), LncRNA MALAT1 prevents placental trophoblast growth, migration, and invasion, as well as angiogenesis, cell cycle arrest, and apoptosis. In addition to the syncytial trophoblast-specific protein PLAP and the trophoblast-specific protein human leukocyte antigen G(HLAG), PEXO is abundant in the exosomal marker proteins CD9, CD63, and CD81 (52–54). These two proteins can be separated to form PEXO in maternal peripheral blood, and the quantity of PEXO can

be used to forecast fetal growth and ascertain the success of a pregnancy. Exosomes carry a variety of payloads in maternal peripheral blood, and histological study of these exosomes in various disorders has shown that changes in their type and amount may negatively impact the function of target cells (55).

6.1 Exosomal lncRNA and Preeclampsia

6.1.1 Exosomes participate in the occurrence of PE

A key contributor to increased maternal and neonatal mortality, Preeclampsia is a pregnancy problem that manifests beyond 20 weeks of gestation with proteinuria, hypertension, or other systemic damage (56–60). To lower maternal and neonatal mortality and enhance mother and baby health, early Preeclampsia diagnosis is crucial (61). The number of placental exosomes, changes in their composition, and their impact on the maternal immune system are thought to be the key ways that PEXO contributes to Preeclampsia pathogenesis (62).

Preeclampsia patients exhibit decreased expression of functional proteins such as matrix metalloproteinase (MMP) 2 and MMP9, as well as increased levels of phosphatidylserine (PS) and lower levels of phosphatidic acid and phosphatidylglycerol in exosomes when compared to the normal pregnancy group (63, 64). The remodeling of spiral arteries, fetal growth, superficial placentation, reduced blood flow, and ultimately the development of Preeclampsia can all be impacted by decreased expression of any one of these proteins. Human umbilical cord mesenchymal stem cells (HUCMSCs)- exosomes can increase IL-10, TNF-, IFN-, and the local recruitment of NK cells and macrophages *in utero*, modulating the immunological balance at the maternal-fetal plane and indirectly affecting pregnancy outcomes. Compared to women who had normal pregnancies, the placentas of Preeclampsia patients had a significant number of differently expressed lncRNAs, according to research using lncRNA microarray technology. They were implicated in the development of Preeclampsia by interfering with trophoblast cell activity, among other things (65).

6.1.2 Decreased expression of exosomal lncRNA in Preeclampsia

A lncRNA called MALAT1 is linked to placental implantation and penetration (66). When compared to healthy pregnant women, Preeclampsia sufferers' placental tissues express less of the lncRNA MALAT1 (67). When lncRNAMALAT1 levels are low, EMT is induced with less trophoblast invasion, migration, and angiogenesis, which can result in a higher uterine spiral artery remodeling injury (68). According to research, lncRNA MALAT1 levels in plasma exosomes from pregnant women with Preeclampsia were positively correlated with vascular endothelial growth factor (VEGF) expression levels. This suggests that downregulating lncRNA MALAT1 levels in plasma exosomes may speed up the progression of Preeclampsia by controlling VEGF expression, which in turn suppresses angiogenesis (69). Wu et al. discovered that lncRNAMALAT1 could bind to miR-206, prevent the latter from degrading IGF-1 mRNA, boost IGF-1 expression, and activate the PI3K/AKT signaling pathway, which in turn encouraged trophoblast migration and invasion (70).

Preeclampsia patients had a lower placental expression of the short nucleolar RNA host gene 22 (SNHG22) than healthy pregnant women did. By interacting with miR-128-3p to encourage PCDH11X expression and open up downstream pathways, lncRNASNHG22 can have a role in Preeclampsia. In comparison to normal pregnant placental tissues, the expression of lncRNA XIST was found to be considerably reduced in the placentas of Preeclampsia patients. lncRNA XIST is involved in the development of Preeclampsia by regulating the proliferation and invasive ability of trophoblast HTR-8/SVneo through miR-135b. The lncRNA TUG1 was downregulated in the placental tissue of Preeclampsia patients compared to healthy pregnant women, and this downregulation decreased cell proliferation, migration, and invasion while promoting trophoblast death. While TUG1 downregulation boosted the expression of the enhancer of zeste homolog 2 (EZH2) and decreased the levels of the Rho family GTPase 3 (RND3) in Preeclampsia, it prevented remodeling of the uterine spiral artery. Studies have shown that downregulating lnc-dendritic cell (DC), a lncRNA expressed in DC, prevents monocytes from differentiating into DC, diminishing the inhibitory effect of DC on Treg, encouraging the proliferation of Th1 cells in the meconium of Preeclampsia patients, and ultimately promoting Preeclampsia (71, 72).

6.1.3 Increased expression of exosomal lncRNA in Preeclampsia

Compared to normal pregnancies, the placenta of Preeclampsi patients has higher levels of lncRNAH19 expression (73). In the human choriocarcinoma cell line JEG-3 and the human choriocapillaris trophoblast cell line HTR-8/SVneo, lncRNAH19 regulates the PI3K/Akt/mTOR pathway and boosts autophagy and invasiveness (74). Moreover, the lncRNAH19 gene encodes miR-675, which can suppress cell growth by lowering the expression of the nodal modulator 1 (NOMO1) in JEG-3 cells (75). In the placental tissues of Preeclampsia patients, lncRNA GAS5 expression is elevated, and its level rises as the severity of the disease does as well (76). The development of atherosclerosis can be aided by the lncRNA GAS5, which can encourage the death of vascular endothelial cells as well as aberrant proliferation and migration of vascular smooth muscle cells. The degree to which lncRNA GAS5 was expressed in Preeclampsia patients was inversely correlated with spiral artery lumen area and positively correlated with spiral artery wall thickness, suggesting that lncRNA GAS5 may be connected to the process of placental spiral artery recasting. Many lncRNAs have an impact on trophoblast cells' physiological processes, which are intimately associated with the development of Preeclampsia and include migration, invasion, proliferation, and apoptosis (77). Determining the regulatory roles that Preeclampsia-related lncRNAs play in various pathways can therefore assist in clarifying the interactions that contribute to Preeclampsia pathophysiology, identify essential molecules for diagnosis and therapy, and provide potential targets for Preeclampsia prevention and treatment (78).

6.2 Exosomal lncRNA and gestational diabetes mellitus

6.2.1 Exosomal lncRNA's role in the emergence of gestational diabetes mellitus

The condition known as gestational diabetes mellitus is characterized by aberrant glucose metabolism in the body, which is brought on by insulin insufficiency and hormonal changes during pregnancy (79). In extreme cases, gestational diabetes mellitus can result in maternal and neonatal death. The incidence of gestational diabetes mellitus is increasing as people's lifestyles and diets change (80). Research has revealed that gestational diabetes mellitus is a risk factor for cardiovascular disease and type 2 diabetes (T2DM), which can raise the risk of immediate or long-term issues in expecting mothers and children and gravely jeopardize the physical and mental health of women and neonates (81, 82). Insulin resistance (IR), one of the primary causes of gestational diabetes mellitus, has a complex etiology and unknown pathophysiology (83, 84). Hence, a contemporary topic that requires attention is the quest for biomarkers with high sensitivity and specificity for the early diagnosis and treatment of gestational diabetes mellitus as well as the maternal postpartum state (85).

Exosome levels and biological activity were shown to vary with gestational stage in pregnant women with gestational diabetes mellitus and normal glucose tolerance (NGT) (86). When matched for gestational weeks, the concentration of placental exosomes in the plasma of gestational diabetes mellitus patients is significantly higher than that of healthy pregnant women and may positively correlate with baby weight. Between 22 and 28 weeks of gestation, the plasma exosomes mostly displayed altered expression of proteins related to insulin sensitivity, including CAMK2b and pregnancy-as-sociated plasma protein A (PAPPA). As a result, gestational diabetes mellitus patients' plasma exosomes play a significant role in controlling glucose homeostasis during pregnancy (87).

6.2.2 Decreased expression of exosomal lncRNA in gestational diabetes mellitus

An endogenous lncRNA called SNHG17 can bind and inhibit the transcription of miRNAs, which control the transcription and expression of target genes and contribute to the onset and progression of gestational diabetes mellitus (88). Research suggests that lncRNASNHG17, which is connected to vascular endothelial cell survival and angiogenesis, is abnormally underexpressed in the peripheral blood of T2DM patients (89). Serum lncRNASNHG17 levels are significantly lower in pregnant women with gestational diabetes mellitus than in healthy pregnant women, and they are correlated with fasting blood glucose (FBG), glycosylated hemoglobin, type A1c (HbA1c), and Homeostasis model assessment(HOMA)-IR negatively and HOMA-β positively. This suggests that lncRNASNHG17 may be involved in the pathological lesion process of gestational diabetes mellitus by influencing these variables (90). In gestational diabetes mellitus patients, the expression level of lncRNAMALAT1 was discovered to be correlated with the disease severity and to have a strong negative relationship with the maternal BMI and FBG at delivery (91). Compared to healthy pregnant women, gestational diabetes mellitus patients had significantly lower serum levels of the lncRNAMALAT1 gene (92). By increasing miR-155-5p expression, suppressing IGF2 expression, enhancing trophoblast cell survival, migration, and invasion, and reviving the biological activity of high glucose-induced trophoblast cells, *in vitro* cellular assays demonstrated that silencing lncRNAMALAT1 plays a role in the development of gestational diabetes mellitus (93).

6.2.3 Increased expression of exosomal lncRNA in gestational diabetes mellitus

Maternally expressed gene 3 (MEG3) has been linked to abnormal placental expression, trophoblast migration, and apoptosis. It also has an impact on the expression of the NF-B, caspase-3, and Bax proteins in the placenta. Human umbilical vein endothelial cells (HUVEC) from gestational diabetes mellitus have elevated MEG3 expression, which affects fetal endothelial function through the PI3K signaling pathway (94). MEG3 overexpression, meanwhile, was able to prevent human villous trophoblast HTR-8/SVneo from proliferating, migrating, and invading while inducing apoptosis, indicating that MEG3 may be implicated in the development of gestational diabetes mellitus and playing a significant role (95). The conserved family SNX member sortingnexin17 (SNX17) is crucial for the endocytic, intracellular transport of cell surface proteins. It is crucial for endocytosis and the intracellular activities that involve cell surface proteins. It was discovered that lncRNA-SNX17 was elevated and miR-517a was downregulated in the blood of gestational diabetes mellitus patients and that the two together were more useful for the diagnosis of gestational diabetes mellitus than the single index test (96). Both the lncRNA P21 and the lncRNA H19 were shown to be elevated in the serum and placental tissues of gestational diabetes mellitus patients. These two lncRNAs may cooperate to promote the development of gestational diabetes mellitus and correlate with newborns' birth weights. The incidence of gigantic newborns in gestational diabetes mellitus patients was connected with serum lncRNA HOXA transcript expression at the distal tip (HOTTIP), which was considerably increased in gestational diabetes mellitus patients. Both miR-21 and lncRNA HOTTIP were discovered to be abnormally expressed in gestational diabetes mellitus and connected with a poor pregnancy outcome, which could be used as a prediction for early identification of gestational diabetes mellitus (97). In order to identify other potential targets for the therapy of gestational diabetes mellitus, we will keep screening exosomal lncRNAs strongly associated with IR and glucose metabolism and investigate their potential participation in regulatory networks (98, 99).

6.3 Exosomal lncRNA and recurrent spontaneous abortion

6.3.1 The emergence of recurrent spontaneous abortion is intimately related to exosomal lncRNA

Two or more consecutive spontaneous abortions constitute the incidence of recurrent spontaneous abortion (100). Early superficial

placental implantation, poor trophoblast migration and invasion, and defective placental microvascular formation are three significant pathophysiological causes for the development of recurrent spontaneous abortion, all of which are becoming more common (101, 102). Exosomal lncRNAs participate in the regulation of trophoblast invasive capacity, the expression of cyclin-dependent kinases (CDKs), and various physiological processes like lipid metabolism and protein synthesis. These actions have an impact on early embryonic implantation. Exosomes produced by mesenchymal stem cells can operate on trophoblast cells to cause them to secrete MMP, which in turn makes trophoblasts more invasive. By being endocytosed by trophoblast cells, exosomes from metaphase macrophages can carry out the corresponding biological action (103). When we co-cultured exosomes from patients with unexplained recurrent spontaneous abortion (URSA) and patients with normal early pregnancy abortion with trophoblast HTR-8/SVneo cells, we discovered that the number of cells migrating in URSA patients was significantly lower than that in patients with normal early pregnancy abortion. Both the number of cells migrating and the viability of the cells were much lower in URSA patients. This shows that meconium macrophages can control trophoblast cells' biological behavior by secreting exosomes, leading to embryonic arrest and playing a role in the emergence of URSA (104).

The regulation of embryonic development, endometrial tolerance, trophoblast function, stimulation of inflammation, placental vascular development, and the regulation of embryonic stem cells are the key ways that lncRNAs contribute to miscarriage (105, 106). It was discovered that the p53-regulated lncRNA lncPRESS1 safeguards embryonic stem cells by inhibiting the function of the silent information regulator (SIRT) 6 (107). Meanwhile, lncKdm2b stimulates the production of transcription factor zinc finger and BTB structural domain protein 3, promoting early embryonic development and embryonic stem cell self-renewal (108). Small interfering RNA-silenced mouse embryonic stem cells may suffer harm or even miscarry if appropriate lncRNAs are administered (109). LncRNA screening before embryo implantation can lower the chance of a failed transfer and miscarriage since lncRNAs play a significant role in controlling embryonic stem cell development (110, 111).

6.3.2 Exosomal lncRNA offers fresh approaches to identifying and treating recurrent spontaneous abortion

Defective gene expression and aberrant cell proliferation are brought on by the increased expression of LncRNA H19 in recurrent spontaneous abortion patients' embryonic tissues (112). Through its binding to let-7, lncRNA H19 inhibits ITG3 expression. This has an impact on how cells adhere to the basement membrane and lowers endometrial tolerance. As a result, embryos are lost (113). Apoptosis and iron death are promoted by IncRNA H19 by downregulating the expression of Bax and upregulating the expression of Bcl2 and GPX4 in recurrent spontaneous abortion. Nuclear enriched transcript 1 (NEAT1) and MALAT levels in recurrent spontaneous abortion patients are much lower than in healthy women, and trophoblast cell proliferation, migration, invasiveness, and apoptosis were all reduced when the MALAT1 gene was knocked down (114). The human plasmacytoma variant translocation 1 (PVT1) promoter is directly impacted by lncRNA regulation, which also lowers the ability of trophoblast cells to invade (115).

Patients with recurrent spontaneous abortion had increased villous tissue LINC01088 expression. ARG1 can be bound by LINC01088, which is mostly found in the nucleus of trophoblast cells (116). This increases ARG1's protein stability and suppresses the expression of NOS. When LINC01088 is overexpressed, ARG1's protein stability is improved, which in turn lowers the expression

TABLE 1 The expression of exosomal lncRNAs in pathological pregnancy.

Type of disease	Exosomal lncRNAs	Expression increases/decreases	References
Preeclampsia	SNHG22	decreases	(77)
Preeclampsia	MALAT1	decreases	(67)
Preeclampsia	HIF1A-AS1	decreases	(77)
Preeclampsia	SNHG12	decreases	(77)
Preeclampsia	MVIH	decreases	(77)
Preeclampsia	GHET1	decreases	(77)
Preeclampsia	DANCR	decreases	(77)
Preeclampsia	SNHG5	decreases	(77)
Preeclampsia	TUG1	decreases	(77)
Preeclampsia	lnc-DC	decreases	(72)
Preeclampsia	H19	increases	(73)
Preeclampsia	GAS5	increases	(76)
Preeclampsia	HIF1A	increases	(77)

(Continued)

TABLE 1 Continued

Type of disease	Exosomal lncRNAs	Expression increases/decreases	References
Preeclampsia	SH3PXD2A-AS1	increases	(77)
Preeclampsia	LINC01410	increases	(77)
Preeclampsia	INHBA-AS1	increases	(77)
Preeclampsia	RPAIN	increases	(77)
Preeclampsia	TINCR	increases	(77)
Gestational diabetes mellitus	MALAT1	decreases	(92)
Gestational diabetes mellitus	PVT1	decreases	(98)
Gestational diabetes mellitus	SNHG17	decreases	(90)
Gestational diabetes mellitus	MEG3	increases	(94)
Gestational diabetes mellitus	SNX17	increases	(96)
Gestational diabetes mellitus	P21	increases	(98)
Gestational diabetes mellitus	H19	increases	(98)
Gestational diabetes mellitus	HOTTIP	increases	(97)
Gestational diabetes mellitus	p3134	increases	(98)
Gestational diabetes mellitus	ANRIL	increases	(98)
Gestational diabetes mellitus	AC092159.2	increases	(98)
Recurrent spontaneous abortion	NEAT1	decreases	(122)
Recurrent spontaneous abortion	MALAT	decreases	(114)
Recurrent spontaneous abortion	SNHG7	decreases	(120)
Recurrent spontaneous abortion	ANRIL	decreases	(122)
Recurrent spontaneous abortion	PVT1	decreases	(122)
Recurrent spontaneous abortion	HOTAIR	decreases	(121)
Recurrent spontaneous abortion	SNHG5	decreases	(119)
Recurrent spontaneous abortion	H19	increases	(113)
Recurrent spontaneous abortion	MEG8	increases	(122)
Recurrent spontaneous abortion	LINC01088	increases	(116)
Recurrent spontaneous abortion	SLC4A1-1	increases	(117)

of NOS and lowers NO expression. The JNK/P38 MAPK signaling pathway is further activated by the decreased NO, which impairs trophoblast cell proliferation, invasion, and migration and contributes to the development of recurrent spontaneous abortion. The lnc-SLC4A1-1 gene was discovered to be significantly expressed in the villi of URSA patients and to be able to trigger an immunological response via the NF-B/CXCL8 axis (117). In peripheral blood mononuclear cells from pregnant women with URSA, the expression levels of the lncRNAs SNHG5 and KLF4 were aberrant, and both of these were risk factors for the development of URSA (118, 119). We discovered that the lncRNA types HOTAIR and SNHG7 are related to recurrent spontaneous abortion pathogenesis and control trophoblast proliferation, apoptosis, invasion, and chorionic villus angiogenesis (120, 121). These investigations revealed prospective biomarkers and therapeutic targets, offering fresh perspectives on the early detection and management of recurrent spontaneous abortion (122) (Table 1).

Conclusion

Exosomal lncRNAs have a wide range of potential for investigation (123). Exosomal lncRNAs have the power to control a wide range of cellular biological processes, including the recasting of the helical arteries, the inflammatory response, immunological control, cellular metabolism, and autophagy (124–126). Exosomal lncRNAs are more

durable and less prone to degradation than serum-derived lncRNAs, allowing them to move unaltered from their "origin" to their "destination" and carry out their intended functions (127–130). Exosomal lncRNAs at the maternal-fetal interface have been shown in numerous studies to play an essential role in pregnancy-specific illnesses and to support embryo implantation and maintenance. Hence, it is necessary to address the issue of how to harvest exosomes that more accurately depict the cellular environment *in vivo* (126, 131, 132). Pregnancy-specific disorders have been linked to abnormal changes in placenta-derived exosomes seen in the peripheral blood of pregnant women, although larger sample sizes are still required to confirm their utility as biomarkers for clinical testing. Exosomes can also forecast embryonic developmental potential, and shortly, using exosomes as markers in clinical testing will be a promising and significant noninvasive test (133, 134).

Author contributions

MW, LZ, SM, RL, JL, and SY performed literature searches and selected the studies and reviews discussed in the manuscript. The first draft of the manuscript was prepared by MW. LZ, SM, RL, and JL made subsequent amendments. SY revised the manuscript. All authors read and approved the final manuscript and contributed to the conception of this review.

Funding

Funding for this work was provided by the Jilin Provincial Department of Finance Project and Jilin Provincial Development and Reform Commission Health Special Fund (No. 2020SCZT078 and No. 3D5204901429).

Conflict of interest

The authors declare that the research was conducted in the absence of any commercial or financial relationships that could be construed as a potential conflict of interest.

Publisher's note

References

1. Han J, Zhang Y, Ge P, Dakal TC, Wen H, Tang S, et al. Exosome-derived CIRP: An amplifier of inflammatory diseases. *Front Immunol* (2023) 14. doi: 10.3389/fimmu.2023.1066721

2. Zhu L, Sun H-T, Wang S, Huang S-L, Zheng Y, Wang C-Q, et al. Isolation and characterization of exosomes for cancer research. *J Hematol Oncol* (2020) 13(1):152. doi: 10.1186/s13045-020-00987-y

3. Bridges MC, Daulagala AC, Kourtidis A. LNCcation: lncRNA localization and function. *J Cell Biol* (2021) 220(2):e202009045. doi: 10.1083/jcb.202009045

4. Chen A, Yu R, Jiang S, Xia Y, Chen Y. Recent advances of microRNAs, long non-coding RNAs, and circular RNAs in preeclampsia. *Front Physiol* (2021) 12. doi: 10.3389/fphys.2021.659638

5. Nojima T, Proudfoot NJ. Mechanisms of lncRNA biogenesis as revealed by nascent transcriptomics (vol 23, pg 389, 2022). *Nat Rev Mol Cell Biol* (2022) 23 (12):853–. doi: 10.1038/s41580-022-00551-1

6. Yang J, Yang FJ, Wang YG, Su GF, Mao X. LncRNA MIR497HG inhibits proliferation and migration of retinal endothelial cells under high-level glucose treatment via miRNA-128-3p/SIRT1 axis. *Eur Rev Med Pharmacol Sci* (2020) 24 (11):5871–7. doi: 10.26355/eurrev_202006_21479

7. Wen SW, Lima LG, Lobb RJ, Norris EL, Hastie ML, Krumeich S, et al. Breast cancer-derived exosomes reflect the cell-of-origin phenotype. *Proteomics* (2019) 19(8): e1800180. doi: 10.1002/pmic.201800180

8. Vatish M, Powys VR, Cerdeira AS. Novel therapeutic and diagnostic approaches for preeclampsia. *Curr Opin Nephrol Hypertension.* (2023) 32(2):124–33. doi: 10.1097/MNH.0000000000000870

9. Maligianni I, Yapijakis C, Nousia K, Bacopoulou F, Chrousos GP. Exosomes and exosomal non-coding RNAs throughout human gestation (Review). *Exp Ther Med* (2022) 24(3):582. doi: 10.3892/etm.2022.11518

10. Zhang T, Tang X, Zhu Y, Wang C, Jiang Z, Yang N, et al. IGF2BP2 enhances LincRNA01116 stability via m (6)A: A potential biomarker and therapeutic target for patients with pre-eclampsia. *J Cell Biochem* (2023) 124(2):239–53. doi: 10.1002/jcb.30358

11. Khazaei F, Rezakhani L, Alizadeh M, Mahdavian E, Khazaei M. Exosomes and exosome-loaded scaffolds: Characterization and application in modern regenerative medicine. *Tissue Cell* (2023) 80:102007. doi: 10.1016/j.tice.2022.102007

12. Wang Y, Liu Q, Wang F. Potential roles of exosome non-coding RNAs in cancer chemoresistance. *Oncol Rep* (2021) 45(2):439–47. doi: 10.3892/or.2020.7887

13. Théry C, Witwer KW, Aikawa E, Alcaraz MJ, Anderson JD, Andriantsitohaina R, et al. Minimal information for studies of extracellular vesicles 2018 (MISEV2018): a position statement of the International Society for Extracellular Vesicles and update of the MISEV2014 guidelines. *J Extracell Vesicles.* (2018) 7(1):1535750. doi: 10.1080/20013078.2018.1535750

14. Saheera S, Potnuri AG, Krishnamurthy P. Nano-vesicle (Mis)Communication in senescence-related pathologies. *Cells* (2020) 9(9):1974. doi: 10.3390/cells9091974

15. Kalluri R, LeBleu VS. The biology, function, and biomedical applications of exosomes. *Science* (2020) 367(6478):640–+. doi: 10.1126/science.aau6977

16. Nafar S, Nouri N, Alipour M, Fallahi J, Zare F, Tabei SMB. Exosome as a target for cancer treatment. *J Invest Med* (2022) 70(5):1212–8. doi: 10.1136/jim-2021-002194

17. Sun X, Ding T, Wang B, Chang Z, Fei H, Geng L, et al. Identification of lncRNA-miRNA-mRNA networks in circulating exosomes as potential biomarkers for systemic sclerosis. *Front Med* (2023) 10. doi: 10.3389/fmed.2023.1111812

18. Guo M, Hao Y, Feng Y, Li H, Mao Y, Dong Q, et al. Microglial exosomes in neurodegenerative disease. *Front Mol Neurosci* (2021) 14. doi: 10.3389/fnmol.2021.630808

19. Negahdaripour M, Vakili B, Nezafat N. Exosome-based vaccines and their position in next-generation vaccines. *Int Immunopharmacology.* (2022) 113(Pt A):109265. doi: 10.1016/j.intimp.2022.109265

20. Hade MD, Suire CN, Suo Z. Mesenchymal stem cell-derived exosomes: applications in regenerative medicine. *Cells* (2021) 10(8):1959. doi: 10.3390/cells10081959

21. Roy A, Girija As S, Sankar Ganesh P, Saravanan M, Sunny B. Exosome mediated cancer therapeutic approach: present status and future prospectives. *Asian Pacific J Cancer prevention: APJCP.* (2023) 24(2):363–73. doi: 10.31557/APJCP.2023.24.2.363

22. Gall AR, Amoah S, Kitase Y, Jantzie LL. Placental mediated mechanisms of perinatal brain injury: Evolving inflammation and exosomes. *Exp Neurology.* (2022) 347:113914. doi: 10.1016/j.expneurol.2021.113914

23. Ghafourian M, Mahdavi R, Akbari Jonoush Z, Sadeghi M, Ghadiri N, Farzaneh M, et al. The implications of exosomes in pregnancy: emerging as new diagnostic markers and therapeutics targets. *Cell Communication Signaling* (2022) 20(1):51. doi: 10.1186/s12964-022-00853-z

24. Shi Y, Du L, Lv D, Li Y, Zhang Z, Huang X, et al. Emerging role and therapeutic application of exosome in hepatitis virus infection and associated diseases. *J Gastroenterology.* (2021) 56(4):336–49. doi: 10.1007/s00535-021-01765-4

25. Ye Z, Wang S, Huang X, Chen P, Deng L, Li S, et al. Plasma exosomal miRNAs associated with metabolism as early predictor of gestational diabetes mellitus. *Diabetes* (2022) 71(11):2272–83. doi: 10.2337/db21-0909

26. Herman AB, Tsitsipatis D, Gorospe M. Integrated lncRNA function upon genomic and epigenomic regulation. *Mol Cell* (2022) 82(12):2252–66. doi: 10.1016/j.molcel.2022.05.027

27. Huang W, Li H, Yu Q, Xiao W, Wang DO. LncRNA-mediated DNA methylation: an emerging mechanism in cancer and beyond. *J Exp Clin Cancer Res* (2022) 41(1):100. doi: 10.1186/s13046-022-02319-z

28. Nunez-Martinez HN, Recillas-Targa F. Emerging Functions of lncRNA Loci beyond the Transcript Itself. *Int J Mol Sci* (2022) 23(11):6258. doi: 10.3390/ijms23116258

29. An B, Kameda T, Imamura T. The evolutionary acquisition and mode of functions of promoter-associated non-coding RNAs (pancRNAs) for mammalian development. In: Hon CC, editor. *Essays Biochem* 65(4):697–708. doi: 10.1042/EBC20200143

30. Sanbonmatsu K. Getting to the bottom of lncRNA mechanism: structure-function relationships. *Mamm Genome.* (2022) 33(2):343–53. doi: 10.1007/s00335-021-09924-x

31. Yang L, Li L-P, Yi H-C. DeepWalk based method to predict lncRNA-miRNA associations via lncRNA-miRNA-disease-protein-drug graph. *BMC Bioinf* (2022) 22 (SUPPL 12):621. doi: 10.1186/s12859-022-04579-0

32. Tsagakis I, Douka K, Birds I, Aspden JL. Long non-coding RNAs in development and disease: conservation to mechanisms. *J Pathology.* (2020) 250(5):480–95. doi: 10.1002/path.5405

33. Jain N, Gupta P, Sahoo S, Mallick B. Non-coding RNAs and their cross-talks impacting reproductive health of women. *Wiley Interdiscip Reviews-Rna.* (2022) 13(3): e1695. doi: 10.1002/wrna.1695

34. Farzaneh M, Najafi S, Anbiyaee O, Azizidoost S, Khoshnam SE. LncRNA MALAT1-related signaling pathways in osteosarcoma. *Clin Trans Oncol* (2023) 25 (1):21–32. doi: 10.1007/s12094-022-02876-x

35. Li C, Ni YQ, Xu H, Xiang QY, Zhao Y, Zhan JK, et al. Roles and mechanisms of exosomal non-coding RNAs in human health and diseases. *Signal Transduct Target Ther* (2021) 6(1):383. doi: 10.1038/s41392-021-00779-x

36. Yang H, Zhang H, Gu H, Wang J, Zhang J, Zen K, et al. Comparative analyses of human exosome proteomes. *Protein J* (2023) 42(4):365–73. doi: 10.1007/s10930-023-10100-0

37. Jia R, Rotenberg SA, Mirkin MV. Electrochemical resistive-pulse sensing of extracellular vesicles. *Analytical Chem* (2022) 94(37):12614–20. doi: 10.1021/acs.analchem.2c01216

38. Theodoraki M-N, Hong C-S, Donnenberg VS, Donnenberg AD, Whiteside TL. Evaluation of exosome proteins by on-bead flow cytometry. *Cytometry Part A.* (2021) 99(4):372–81. doi: 10.1002/cyto.a.24193

39. Kar R, Dhar R, Mukherjee S, Nag S, Gorai S, Mukerjee N, et al. Exosome-based smart drug delivery tool for cancer theranostics. *ACS Biomaterials Sci Engineering.* (2023) 9(2):577–94. doi: 10.1021/acsbiomaterials.2c01329

40. Peng W, Bai S, Zheng M, Chen W, Li Y, Yang Y, et al. An exosome-related lncRNA signature correlates with prognosis, immune microenvironment, and therapeutic responses in hepatocellular carcinoma. *Trans Oncol* (2023) 31:101651–. doi: 10.1016/j.tranon.2023.101651

41. Liu H, Huang X, Mor G, Liao A. Epigenetic modifications working in the decidualization and endometrial receptivity. *Cell Mol Life Sci* (2020) 77(11):2091–101. doi: 10.1007/s00018-019-03395-9

42. Liu C, Li L, Wang M, Shui S, Yao H, Sui C, et al. Endometrial extracellular vesicles of recurrent implantation failure patients inhibit the proliferation, migration, and invasion of HTR8/SVneo cells. *J Assisted Reprod Genet* (2021) 38(4):825–33. doi: 10.1007/s10815-021-02093-5

43. Hashemi M, Moosavi MS, Abed HM, Dehghani M, Aalipour M, Heydari EA, et al. Long non-coding RNA (lncRNA) H19 in human cancer: From proliferation and metastasis to therapy. *Pharmacol Res* (2022) 184:106418. doi: 10.1016/j.phrs.2022.106418

44. Kannampuzha S, Ravichandran M, Mukherjee AG, Wanjari UR, Renu K, Vellingiri B, et al. The mechanism of action of non-coding RNAs in placental disorders. *Biomedicine Pharmacotherapy* (2022) 156:113964. doi: 10.1016/j.biopha.2022.113964

45. Gurunathan S, Kang M-H, Song H, Kim NH, Kim J-H. The role of extracellular vesicles in animal reproduction and diseases. *J Anim Sci Biotechnol* (2022) 13(1):62. doi: 10.1186/s40104-022-00715-1

46. Chen F, Chen X, Cai W, Ruan H, Fang S. Mesenchymal Stem Cell-Derived Exosomal Long Noncoding RNA MALAT1-201 Regulated the Proliferation, Apoptosis and Migration of Trophoblast Cells via Targeting miR-141. *Ann Clin Lab science.* (2022) 52(5):741–52.

47. Gauster M, Moser G, Wernitznig S, Kupper N, Huppertz B. Early human trophoblast development: from morphology to function. *Cell Mol Life Sci* (2022) 79 (6):345. doi: 10.1007/s00018-022-04377-0

48. Aljubran F, Nothnick WB. Long non-coding RNAs in endometrial physiology and pathophysiology. *Mol Cell Endocrinol* (2021) 525:111190. doi: 10.1016/j.mce.2021.111190

49. Monsivais D, Nagashima T, Prunskaite-Hyyrylainen R, Nozawa K, Shimada K, Tang S, et al. Endometrial receptivity and implantation require uterine BMP signaling through an ACVR2A-SMAD1/SMAD5 axis. *Nat Commun* (2021) 12(1):3386. doi: 10.1038/s41467-021-23571-5

50. Hu L, Ma J, Cao M, Lin Y, Long W, Shi Z, et al. Exosomal mRNA and lncRNA profiles in cord blood of preeclampsia patients. *J Maternal-Fetal Neonatal Med* (2022) 35(25):8199–209. doi: 10.1080/14767058.2021.1966413

51. Ren J, Jin H, Zhu Y. The role of placental non-coding RNAs in adverse pregnancy outcomes. *Int J Mol Sci* (2023) 24(5):5030. doi: 10.3390/ijms24055030

52. Giacomini E, Vago R, Sanchez AM, Podini P, Zarovni N, Murdica V, et al. Secretome of in vitro cultured human embryos contains extracellular vesicles that are uptaken by the maternal side. *Sci Rep* (2017) 7(1):5210. doi: 10.1038/s41598-017-05549-w

53. Jin J, Menon R. Placental exosomes: A proxy to understand pregnancy complications. *Am J Reprod Immunol* (2018) 79(5):e12788. doi: 10.1111/aji.12788

54. Barbaro G, Inversetti A, Cristodoro M, Ticconi C, Scambia G, Di Simone N. HLA-G and recurrent pregnancy loss. *Int J Mol Sci* (2023) 24(3):2557. doi: 10.3390/ijms24032557

55. Chen T, Liu D. The mystery of exosomes in gestational diabetes mellitus. *Oxid Med Cell Longevity.* (2022) 2022:2169259. doi: 10.1155/2022/2169259

56. Chappell LC, Cluver CA, Kingdom J, Tong S. Pre-eclampsia. *Lancet* (2021) 398 (10297):341–54. doi: 10.1016/S0140-6736(20)32335-7

57. Gestational hypertension and preeclampsia: ACOG practice bulletin summary, number 222. *Obstet Gynecol* (2020) 135(6):1492–5. doi: 10.1097/AOG.0000000000003892

58. Mo H-Q, Tian F-J, Ma X-L, Zhang Y-C, Zhang C-X, Zeng W-H, et al. PDIA3 regulates trophoblast apoptosis and proliferation in preeclampsia via the MDM2/p53 pathway. *Reproduction* (2020) 160(2):293–305. doi: 10.1530/REP-20-0156

59. Raguema N, Moustadraf S, Bertagnolli M. Immune and apoptosis mechanisms regulating placental development and vascularization in preeclampsia. *Front Physiol* (2020) 11. doi: 10.3389/fphys.2020.00098

60. Farah O, Nguyen C, Tekkatte C, Parast MM. Trophoblast lineage-specific differentiation and associated alterations in preeclampsia and fetal growth restriction. *Placenta* (2020) 102:4–9. doi: 10.1016/j.placenta.2020.02.007

61. Peixoto-Filho FM, Costa F, Kobayashi S, Beitune PE, Garrido AG, Carmo AV, et al. Prediction and prevention of preeclampsia. *Rev Bras ginecologia e obstetricia: Rev da Federacao Bras das Sociedades Ginecologia e Obstetricia.* (2023) 45(1):49–54. doi: 10.1055/s-0043-1763495

62. Zhang T-N, Wang W, Huang X-M, Gao S-Y. Non-coding RNAs and extracellular vehicles: their role in the pathogenesis of gestational diabetes mellitus. *Front Endocrinol* (2021) 12. doi: 10.3389/fendo.2021.664287

63. Zhang Y, Chen X. lncRNA FOXD2-AS1 affects trophoblast cell proliferation, invasion and migration through targeting miRNA. *Zygote* (2020) 28(2):131–8. doi: 10.1017/S0967199419000807

64. Jing M, Chen X, Qiu H, He W, Zhou Y, Li D, et al. Insights into the immunomodulatory regulation of matrix metalloproteinase at the maternal-fetal interface during early pregnancy and pregnancy-related diseases. *Front Immunol* (2023) 13. doi: 10.3389/fimmu.2022.1067661

65. Mytareli C, Delivanis DA, Athanassouli F, Kalotychou V, Mantzourani M, Kassi E, et al. The diagnostic, prognostic and therapeutic role of miRNAs in adrenocortical carcinoma: A systematic review. *Biomedicines* (2021) 9(11):1501. doi: 10.3390/biomedicines9111501

66. Feng C, Cheng L, Jin J, Liu X, Wang F. Long non-coding RNA MALAT1 regulates trophoblast functions through VEGF/VEGFR1 signaling pathway. *Arch Gynecology Obstetrics.* (2021) 304(4):873–82. doi: 10.1007/s00404-021-05987-y

67. Chen H, Meng T, Liu X, Sun M, Tong C, Liu J, et al. Long non-coding RNA MALAT-1 is downregulated in preeclampsia and regulates proliferation, apoptosis, migration and invasion of JEG-3 trophoblast cells. *Int J Clin Exp Pathology.* (2015) 8 (10):12718–27.

68. Tao H, Liu X, Liu X, Liu W, Wu D, Wang R, et al. LncRNA MEG3 inhibits trophoblast invasion and trophoblast-mediated VSMC loss in uterine spiral artery remodeling. *Mol Reprod Dev* (2019) 86(6):686–95. doi: 10.1002/mrd.23147

69. Li X, Song Y, Liu F, Liu D, Miao H, Ren J, et al. Long non-coding RNA MALAT1 promotes proliferation, angiogenesis, and immunosuppressive properties of mesenchymal stem cells by inducing VEGF and IDO. *J Cell Biochem* (2017) 118 (9):2780–91. doi: 10.1002/jcb.25927

70. Wu H-Y, Wang X-H, Liu K, Zhang J-L. LncRNA MALAT1 regulates trophoblast cells migration and invasion via miR-206/IGF-1 axis. *Cell Cycle* (2020) 19(1):39–52. doi: 10.1080/15384101.2019.1691787

71. Liu J, Zhang X, Cheng Y, Cao X. Dendritic cell migration in inflammation and immunity. *Cell Mol Immunol* (2021) 18(11):2461–71. doi: 10.1038/s41423-021-00726-4

72. Zhang W, Zhou Y, Ding Y. Lnc-DC mediates the over-maturation of decidual dendritic cells and induces the increase in Th1 cells in preeclampsia. *Am J Reprod Immunol* (2017) 77(6). doi: 10.1111/aji.12647

73. Yang J, Qi M, Fei X, Wang X, Wang K. LncRNA H19: A novel oncogene in multiple cancers. *Int J Biol Sci* (2021) 17(12):3188–208. doi: 10.7150/ijbs.62573

74. Xu J, Xia Y, Zhang H, Guo H, Feng K, Zhang C. Overexpression of long non-coding RNA H19 promotes invasion and autophagy via the PI3K/AKT/mTOR

pathways in trophoblast cells. *Biomedicine Pharmacotherapy.* (2018) 101:691–7. doi: 10.1016/j.biopha.2018.02.134

75. Gao W-l, Liu M, Yang Y, Yang H, Liao Q, Bai Y, et al. The imprinted H19 gene regulates human placental trophoblast cell proliferation via encoding miR-675 that targets Nodal Modulator 1 (NOMO1). *RNA Biol* (2012) 9(7):1002–10. doi: 10.4161/rna.20807

76. Zheng D, Hou Y, Li Y, Bian Y, Khan M, Li F, et al. Long non-coding RNA Gas5 is associated with preeclampsia and regulates biological behaviors of trophoblast via microRNA-21 (vol 11, 188, 2020). *Front Genet* (2022) 12. doi: 10.3389/fgene.2020.00188

77. Jiang S, Chen Q, Liu H, Gao Y, Yang X, Ren Z, et al. Preeclampsia-associated lncRNA INHBA-AS1 regulates the proliferation, invasion, and migration of placental trophoblast cells. *Mol Therapy-Nucleic Acids* (2020) 22:684–95. doi: 10.1016/j.omtn.2020.09.033

78. Song X, Zhang X, Xia Q, Li C, Zhang Y, Huang Y, et al. LncRNA LINC00534 regulates cell proliferation and migration via the miR-494-3p/PTEN axis in HTR-8/SVneo cells. *J Clin Lab Anal* (2023) 37(1):e24802. doi: 10.1002/jcla.24802

79. American Diabetes Association. 2. Classification and diagnosis of diabetes: standards of medical care in diabetes-2021. *Diabetes Care* (2021) 44:S15–33. doi: 10.2337/dc21-S002

80. Tang L, Li P, Li L. Whole transcriptome expression profiles in placenta samples from women with gestational diabetes mellitus. *J Diabetes Invest* (2020) 11(5):1307–17. doi: 10.1111/jdi.13250

81. Ormazabal V, Nair S, Carrion F, McIntyre HD, Salomon C. The link between gestational diabetes and cardiovascular diseases: potential role of extracellular vesicles. *Cardiovasc Diabetology.* (2022) 21(1):174. doi: 10.1186/s12933-022-01597-3

82. Alejandro EU, Mamerto TP, Chung G, Villavieja A, Gaus NL, Morgan E, et al. Gestational diabetes mellitus: A harbinger of the vicious cycle of diabetes. *Int J Mol Sci* (2020) 21(14):5003. doi: 10.3390/ijms21145003

83. Reyes AB, Burger D. Small extracellular vesicles: a new player in GDM pathogenesis. *Clin Science.* (2022) 136(24):1873–5. doi: 10.1042/CS20220658

84. Filardi T, Catanzaro G, Mardente S, Zicari A, Santangelo C, Lenzi A, et al. Non-coding RNA: role in gestational diabetes pathophysiology and complications. *Int J Mol Sci* (2020) 21(11):4020. doi: 10.3390/ijms21114020

85. Yuan Y, Li Y, Hu L, Wen J. Exosomal RNA expression profiles and their prediction performance in patients with gestational diabetes mellitus and macrosomia. *Front Endocrinol* (2022) 13. doi: 10.3389/fendo.2022.864971

86. Mitra T, Gulati R, Uppal A, Kumari SR, Tripathy S, Ranjan P, et al. Prospecting of exosomal-miRNA signatures as prognostic marker for gestational diabetes mellitus and other adverse pregnancy outcomes. *Front Endocrinol* (2023) 14. doi: 10.3389/fendo.2023.1097337

87. Bernea EG, Suica VI, Uyy E, Cerveanu-Hogas A, Boteanu RM, Ivan L, et al. Exosome proteomics reveals the deregulation of coagulation, complement and lipid metabolism proteins in gestational diabetes mellitus. *Molecules* (2022) 27(17):5502. doi: 10.3390/molecules27175502

88. Ma L, Gao J, Zhang N, Wang J, Xu T, Lei T, et al. Long noncoding RNA SNHG17: a novel molecule in human cancers. *Cancer Cell Int* (2022) 22(1):104. doi: 10.1186/s12935-022-02529-7

89. Wang C, Qu Y, Wang D, Zhu Y. The proangiogenic roles of long nonCoding RNAs revealed by RNA-sequencing following oxygen-glucose deprivation/re-oxygenation. *Cell Physiol biochemistry: Int J Exp Cell physiology biochemistry Pharmacol* (2019) 52(4):708–27. doi: 10.33594/000000050

90. Li J, Du B, Geng X, Zhou L. lncRNA SNHG 17 is downregulated in gestational diabetes mellitus (GDM) and has predictive values. *Diabetes Metab Syndrome Obesity-Targets Ther* (2021) 14:831–8. doi: 10.2147/DMSO.S263942

91. Zhang Y, Wu H, Wang F, Ye M, Zhu H, Bu S. Long non-coding RNA MALAT1 expression in patients with gestational diabetes mellitus. *Int J Gynecol Obstet.* (2018) 140(2):164–9. doi: 10.1002/ijgo.12384

92. Liu P, Jia S-B, Shi J-M, Li W-J, Tang L-S, Zhu X-H, et al. LncRNA-MALAT1 promotes neovascularization in diabetic retinopathy through regulating miR-125b/VE-cadherin axis. *Bioscience Rep* (2019) 39(5):BSR20181469. doi: 10.1042/BSR20181469

93. Hocaoglu M, Demirer S, Loclar Karaalp I, Kaynak E, Attar E, Turgut A, et al. Identification of miR-16-5p and miR-155-5p microRNAs differentially expressed in circulating leukocytes of pregnant women with polycystic ovary syndrome and gestational diabetes. *Gynecological Endocrinology.* (2021) 37(3):216–20. doi: 10.1080/09513590.2020.1843620

94. Ye HH, Yang SH, Zhang Y. MEG3 damages fetal endothelial function induced by gestational diabetes mellitus via AKT pathway. *Eur Rev Med Pharmacol Sci* (2018) 22(24):8553–60. doi: 10.26355/eurrev_201812_16617

95. Zhang H. Mechanism associated with aberrant lncRNA MEG3 expression in gestational diabetes mellitus. *Exp Ther Med* (2019) 18(5):3699–706. doi: 10.3892/etm.2019.8062

96. Song G, Na Q, Wang R, Wang D, Chen B, Li Y, et al. LncRNA-SNX17 promotes HTR-8/SVneo proliferation and invasion through miR-517a/IGF-1 in the placenta of diabetic macrosomia. *Reprod Sci* (2022) 29(2):596–605. doi: 10.1007/s43032-021-00687-z

97. Al-Ghazali MJ, Ali HA, Al-Rufaie MM. Serum irisin levels as a potential marker for diagnosis of gestational diabetes mellitus. *Acta bio-medica: Atenei Parmensis.* (2020) 91(1):56–63. doi: 10.23750/abm.v91i1.7675

98. Fu X, Cong H, Zhao S, Li Y, Liu T, Sun Y, et al. Construction of Glycometabolism- and Hormone-Related lncRNA-Mediated Feedforward Loop Networks Reveals Global Patterns of lncRNAs and Drug Repurposing in Gestational Diabetes. *Front Endocrinol* (2020) 11. doi: 10.3389/fendo.2020.00093

99. Li Y, Li D, Cheng X. The association between expression of lncRNAs in patients with GDM. *Endocrine Connections.* (2021) 10(9):1080–90. doi: 10.1530/EC-21-0227

100. Youssef A, Vermeulen N, Lashley EELO, Goddijn M, van der Hoorn MLP. Comparison and appraisal of (inter)national recurrent pregnancy loss guidelines. *Reprod Biomedicine Online.* (2019) 39(3):497–503. doi: 10.1016/j.rbmo.2019.04.008

101. Andreescu M, Frincu F, Plotogea M, Mehedintu C. Recurrent abortion and the involvement of killer-cell immunoglobulin-like receptor (KIR) genes, activated T cells, NK abnorMalities, and cytokine profiles. *J Clin Med* (2023) 12(4):1355. doi: 10.3390/jcm12041355

102. Deng T, Liao X, Zhu S. Recent advances in treatment of recurrent spontaneous abortion. *Obstetrical Gynecological Survey.* (2022) 77(6):355–66. doi: 10.1097/OGX.0000000000001033

103. Menon R, Shahin H. Extracellular vesicles in spontaneous preterm birth. *Am J Reprod Immunol* (2021) 85(2):e13353. doi: 10.1111/aji.13353

104. Young SL. Introduction: Reproductive immunology: checkered past and bright future. *Fertility Sterility.* (2016) 106(3):497–8. doi: 10.1016/j.fertnstert.2016.07.1090

105. Gan J, Gu T, Yang H, Ao Z, Cai G, Hong L, et al. Non-coding RNAs regulate spontaneous abortion: A global network and system perspective. *Int J Mol Sci* (2022) 23(8):4214. doi: 10.3390/ijms23084214

106. Chen X, Guo D-Y, Yin T-L, Yang J. Non-coding RNAs regulate placental trophoblast function and participate in recurrent abortion. *Front Pharmacol* (2021) 12. doi: 10.3389/fphar.2021.646521

107. Jain AK, Xi Y, McCarthy R, Allton K, Akdemir KC, Patel LR, et al. LncPRESS1 is a p53-regulated lncRNA that safeguards pluripotency by disrupting SIRT6-mediated de-acetylation of histone H3K56. *Mol Cell* (2016) 64(5):967–81. doi: 10.1016/j.molcel.2016.10.039

108. Ye B, Liu B, Yang L, Zhu X, Zhang D, Wu W, et al. LncKdm2b controls self-renewal of embryonic stem cells via activating expression of transcription factor Zbtb3. *EMBO J* (2018) 37(8):e97174. doi: 10.15252/embj.201797174

109. Hamazaki N, Uesaka M, Nakashima K, Agata K, Imamura T. Gene activation-associated long noncoding RNAs function in mouse preimplantation development. *Development* (2015) 142(5):910–20. doi: 10.1242/dev.116996

110. Zhang Y, Wang S. The possible role of long non-coding RNAs in recurrent miscarriage. *Mol Biol Rep* (2022) 49(10):9687–97. doi: 10.1007/s11033-022-07427-9

111. Yang Y, Xiong Y, Pan Z. Role of ceRNAs in non-tumor female reproductive diseases(dagger). *Biol Reprod* (2022) 108(3):363–81. doi: 10.1093/biolre/ioac200

112. Fan L-j, Han H-j, Guan J, Zhang X-w, Cui Q-h, Shen H, et al. Aberrantly expressed long noncoding RNAs in recurrent implantation failure: A microarray related study. *Syst Biol Reprod Med* (2017) 63(4):269–78. doi: 10.1080/19396368.2017.1310329

113. He D, Zeng H, Chen J, Xiao L, Zhao Y, Liu N. H19 regulates trophoblastic spheroid adhesion by competitively binding to let-7. *Reproduction* (2019) 157(5):423–30. doi: 10.1530/REP-18-0339

114. Wang Y, Liu H-Z, Liu Y, Wang H-J, Pang W-W, Zhang J-J. Disordered p53-MALAT1 pathway is associated with recurrent miscarriage. *Kaohsiung J Med Sci* (2019) 35(2):87–94. doi: 10.1002/kjm2.12013

115. Wang Q, Lu X, Li C, Zhang W, Lv Y, Wang L, et al. Down-regulated long non-coding RNA PVT1 contributes to gestational diabetes mellitus and preeclampsia via regulation of human trophoblast cells. *Biomedicine Pharmacotherapy.* (2019) 120:109501. doi: 10.1016/j.biopha.2019.109501

116. Zhao H. The role of long-stranded non-coding RNA in maternal-fetal immune tolerance and recurrent miscarriage. Shandong University, Shandong, China (2021).

117. Huang Z, Du G, Huang X, Han L, Han X, Xu B, et al. The enhancer RNA lnc-SLC4A1-1 epigenetically regulates unexplained recurrent pregnancy loss (URPL) by activating CXCL8 and NF-kB pathways. *Ebiomedicine* (2018) 38:162–70. doi: 10.1016/j.ebiom.2018.11.015

118. Sawant L, Wijesekera N, Jones C. Pioneer transcription factors, progesterone receptor, and Kruppel like transcription factor 4, cooperatively stimulate the bovine herpesvirus 1 ICP0 early promoter and productive late protein expression. *Virus Res* (2020) 288:198115. doi: 10.1016/j.virusres.2020.198115

119. Huang Y, Hao J, Liao Y, Zhou L, Wang K, Zou H, et al. Transcriptome sequencing identified the ceRNA network associated with recurrent spontaneous abortion. *BMC Med Genomics* (2021) 14(1):278. doi: 10.1186/s12920-021-01125-4

120. Xiang H, Yan H, Sun B, Feng F, Chen P. Decreased expression of long non-coding RNA SNHG7 cause recurrent spontaneous abortion through suppression proliferation and invasion of trophoblast cells via miR-34a. *Am J Trans Res* (2019) 11(1):463–72.

121. Zhou H, Gao L, Yu Z-H, Hong S-J, Zhang Z-W, Qiu Z-Z. LncRNA HOTAIR promotes renal interstitial fibrosis by regulating Notch1 pathway via the modulation of miR-124. *Nephrology* (2019) 24(4):472–80. doi: 10.1111/nep.13394

122. Soltani N, Mirzaei F, Ayatollahi H. Cytogenetic studies of 608 couples with recurrent spontaneous abortions in northeastern Iran. *Iranian J pathology.* (2021) 16(4):418–25. doi: 10.30699/ijp.2021.521514.2554

123. Rezaie J, Feghhi M, Etemadi T. A review on exosomes application in clinical trials: perspective, questions, and challenges. *Cell Commun Signal* (2022) 20(1):145. doi: 10.1186/s12964-022-00959-4

124. Nikfarjam S, Rezaie J, Zolbanin NM, Jafari R. Mesenchymal stem cell derived-exosomes: a modern approach in translational medicine. *J Transl Med* (2020) 18 (1):449. doi: 10.1186/s12967-020-02622-3

125. Nemati M, Singh B, Mir RA, Nemati M, Babaei A, Ahmadi M, et al. Plant-derived extracellular vesicles: a novel nanomedicine approach with advantages and challenges. *Cell Commun Signal* (2022) 20(1):69. doi: 10.1186/s12964-022-00889-1

126. Vahabi A, Rezaie J, Hassanpour M, Panahi Y, Nemati M, Rasmi Y, et al. Tumor Cells-derived exosomal CircRNAs: Novel cancer drivers, molecular mechanisms, and clinical opportunities. *Biochem Pharmacol* (2022) 200:115038. doi: 10.1016/j.bcp.2022.115038

127. Joo HS, Suh JH, Lee HJ, Bang ES, Lee JM. Current knowledge and future perspectives on mesenchymal stem cell-derived exosomes as a new therapeutic agent. *Int J Mol Sci* (2020) 21(3):727. doi: 10.3390/ijms21030727

128. Rezaie J, Ahmadi M, Ravanbakhsh R, Mojarad B, Mahbubfam S, Shaban SA, et al. Tumor-derived extracellular vesicles: The metastatic organotropism drivers. *Life Sci* (2022) 289:120216. doi: 10.1016/j.lfs.2021.120216

129. Rezaie J, Etemadi T, Feghhi M. The distinct roles of exosomes in innate immune responses and therapeutic applications in cancer. *Eur J Pharmacol* (2022) 933:175292. doi: 10.1016/j.ejphar.2022.175292

130. Almohammai A, Rahbarghazi R, Keyhanmanesh R, Rezaie J, Ahmadi M. Asthmatic condition induced the activity of exosome secretory pathway in rat pulmonary tissues. *J Inflammation (Lond)*. (2021) 18(1):14. doi: 10.1186/s12950-021-00275-7

131. Rahbarghazi R, Jabbari N, Sani NA, Asghari R, Salimi L, Kalashani SA, et al. Tumor-derived extracellular vesicles: reliable tools for Cancer diagnosis and clinical applications. *Cell Commun Signal* (2019) 17(1):73. doi: 10.1186/s12964-019-0390-y

132. Pegtel DM, Gould SJ. Exosomes. *Annu Rev Biochem*. (2019) 88:487–514. doi: 10.1146/annurev-biochem-013118-111902

133. Shaban SA, Rezaie J, Nejati V. Exosomes derived from senescent endothelial cells contain distinct pro-angiogenic miRNAs and proteins. *Cardiovasc Toxicol* (2022) 22(6):592–601. doi: 10.1007/s12012-022-09740-y

134. Mahbubfam S, Rezaie J, Nejati V. Crosstalk between exosomes signaling pathway and autophagy flux in senescent human endothelial cells. *Tissue Cell* (2022) 76:101803. doi: 10.1016/j.tice.2022.101803

10.3389/fendo.2023.1191721

Glossary

ESE	early-sorting endosome
MVBs	multivesicular bodies
ESCRT	endosomal sorting complex required for transport
PLAP	placental-like alkaline phosphatase
PRC2	Polycomb repressive complex 2
HOTAIR	HOX antisense intergenic RNA
hnRNPA2B1	heterogeneous ribonucleoprotein A2B1
HLEC	human lymphatic vessel endothelial cells
DMR	differently methylated regions
SR	serine/arginine-rich
MALAT1	metastasis-associated lung adenocarcinoma transcript 1
PCR	polymerase chain reaction
RIF	recurrent implantation failure
ZEB2-AS1	Zinc finger E-box-binding homeobox 2 antisense RNA 1
PEXO	Placenta-derived exosome
HK2	recombinant hexokinase 2
HLAG	human leukocyte antigen G
MMP	matrix metalloproteinase
PS	phosphatidylserine
HUCMSCs	Human umbilical cord mesenchymal stem cells
VEGF	vascular endothelial growth factor
SNHG22	short nucleolar RNA host gene 22
EZH2	enhancer of zeste homolog 2
RND3	Rho family GTPase 3
DC	dendritic cell
NOMO1	nodal modulator 1
T2DM	diabetes mellitus type 2
IR	insulin resistance
NGT	normal glucose tolerance
PAPPA	pregnancy-associated plasma protein A
FBG	fasting blood glucose
HbA1c	glycosylated hemoglobin, type A1c
HOMA	homeostasis model assessment
MEG3	maternally expressed gene 3
HUVEC	human umbilical vein endothelial cells
SNX17	sorting nexin 17
HOTTIP	HOXA transcript expression at the distal tip
CDKs	cyclin-dependent kinases
URSA	unexplained recurrent spontaneous abortion
SIRT	silent information regulator
NEAT1	nuclear enriched transcript 1
PVT1	plasmacytomvariant translocation 1

frontiers | Frontiers in Endocrinology

TYPE Original Research
PUBLISHED 31 October 2023
DOI 10.3389/fendo.2023.1277873

OPEN ACCESS

EDITED BY
Fengxiang Wei,
Shenzhen Longgang District Maternal and Child Health Care Hospital, China

REVIEWED BY
Hsien-Ming Wu,
Linkou Chang Gung Memorial Hospital, Taiwan
Mehtap Polat,
Private Clinic, Ankara, Türkiye

*CORRESPONDENCE
Kazuhiro Takeuchi
y-orita@takeuchi-ladies.jp

RECEIVED 15 August 2023
ACCEPTED 10 October 2023
PUBLISHED 31 October 2023

CITATION
Takeuchi K, Orita Y, Iwakawa T, Kuwatsuru Y, Kuroki Y, Fukumoto Y, Mizobe Y, Tokudome M and Moewaki H (2023) Original delayed-start ovarian stimulation protocol with a gonadotropin-releasing hormone antagonist, medroxyprogesterone acetate, and high-dose gonadotropin for poor responders and patients with poor-quality embryos. *Front. Endocrinol.* 14:1277873. doi: 10.3389/fendo.2023.1277873

Original delayed-start ovarian stimulation protocol with a gonadotropin-releasing hormone antagonist, medroxyprogesterone acetate, and high-dose gonadotropin for poor responders and patients with poor-quality embryos

Kazuhiro Takeuchi*, Yuji Orita, Tokiko Iwakawa, Yukari Kuwatsuru, Yuko Kuroki, Yumiko Fukumoto, Yamato Mizobe, Mari Tokudome and Harue Moewaki

Takeuchi Ladies Clinic/Center for Reproductive Medicine, Kagoshima, Japan

Introduction: The delayed-start gonadotropin-releasing hormone antagonist protocol seems effective for patients who are poor ovarian responders, but there are insufficient data on whether it is also effective for patients with poor-quality embryos and low rates of good blastocyst formation. Specifically, the effectiveness of delayed-start gonadotropin-releasing hormone antagonists with progesterone has not been adequately investigated. Therefore, we compared the efficacy of the original delayed-start gonadotropin-releasing hormone antagonist protocol using medroxyprogesterone acetate (MPA) and high-dose gonadotropin in patients with poor ovarian response.

Methods: Overall, 156 patients with recurrent assisted reproductive technology failure who underwent the original protocol were included. They received cetrorelix acetate (3 mg) and MPA (10 mg) on cycle day 3, and high-dose gonadotropin was initiated on day 11. When the leading follicle reached 14 mm, ganirelix acetate (0.25 mg) was administered until the trigger day. The number of oocytes retrieved, metaphase II (MII) oocytes, two pronuclear (2PN) zygotes, and good blastocysts and live birth rates were compared between the previous (Cycle A) and original (Cycle B) cycles in three groups (Group A, all patients; Group B, poor responders; and Group C, patients with poor-quality embryos).

Results: In Group A (n=156), the number of MII oocytes (3.6 ± 3.3 versus 4.5 ± 3.6), 2PN zygotes (2.8 ± 2.9 versus 3.8 ± 3.1), good blastocysts (0.5 ± 0.9 versus 1.2 ± 1.6), and live birth rates (0.6 versus 24.4) significantly increased in Cycle B. Similar results were obtained in Group B (n=83; 2PN zygotes [1.7 ± 1.7 versus 2.3 ± 1.8], good blastocysts [0.4 ± 0.7 versus 0.9 ± 1.3], live birth rates [0 versus 18.1]) and Group C (n=73; MII oocytes [5.1 ± 3.8 versus 6.6 ± 4.0], 2PN zygotes [4.0 ±

3.4 versus 5.4 ± 3.4], good blastocysts [0.7 ± 1.1 versus 1.6 ± 1.9], and live birth rates [1.4 versus 31.5]).

Conclusion: This original protocol increased the number of MII oocytes retrieved, 2PN zygotes, good blastocysts, and live birth rates in both poor responders and in patients with poor-quality embryos.

KEYWORDS

delayed start, gonadotropin-releasing hormone antagonist, medroxyprogesterone acetate, poor responder, poor-quality embryo

1 Introduction

The main goal of controlled ovarian stimulation (COS) in assisted reproductive technology (ART), including conventional *in vitro* fertilization and intracytoplasmic sperm injection cycles, is to achieve live births in the least number of cycles. For this purpose, many COS protocols have been established to retrieve multiple mature oocytes, increase fertilized embryo count, and obtain good blastocysts according to the patients' backgrounds (1), particularly in patients with poor ovarian response (5.6–35.1% of ART patients) (2). Low COS response is a crucial concern in poor responders and patients with poor-quality embryos. To overcome this problem, several COS protocols have been reported, including delayed-start gonadotropin-releasing hormone (GnRH) antagonists (3–13), microdose GnRH agonists (14–16), and long GnRH agonists (17, 18). Among these, a current meta-analysis recommended a delayed-start GnRH antagonist protocol (13) for poor responders. In addition to the improvement in the number of mature oocytes, the clinical pregnancy rate was increased significantly (relative risk: 2.90, [95% confidence interval: 1.52–5.51], $P = 0.001$) (11). The delayed-start GnRH antagonist protocol seems effective for poor responders (3, 4, 7–13), but there are insufficient data on whether it is also effective for patients with poor-quality embryos and low rates of good blastocyst formation. The delayed-start GnRH antagonist protocol has some variations, such as the combination with estrogen or progesterone and the frequency of GnRH antagonist administration as a pretreatment. Frankfurter et al. reported the effectiveness of a delayed-start GnRH antagonist with progesterone (3). Some reports have investigated delayed-start GnRH antagonists with estrogen (7–10), but there are no additional reports investigating the effectiveness of delayed-start GnRH antagonists with progesterone. In this study, an original protocol, modified from Frankfurter's protocol, was evaluated. This study aimed to investigate the efficiency of this original delayed-start GnRH antagonist with progesterone in patients with poor ovarian response, including poor responders according to the Bologna criteria (19) and patients with poor-quality embryos.

Abbreviations: 2PN, two pronuclear; ART, assisted reproductive technology; COS, controlled ovarian stimulation; E2, estradiol; ET, embryo transfer; GnRH, gonadotropin-releasing hormone; IQR, interquartile range; LH, luteinizing hormone; MII, metaphase II; MPA, medroxyprogesterone acetate; OPU, oocyte pick-up; P4, progesterone.

2 Methods

2.1 Study design and population

Patients who underwent the original delayed-start GnRH antagonist with the progesterone protocol whose previous COS cycle resulted in poor outcomes (low rate of metaphase II [MII] oocytes, fertilization) from May 2015 to January 2021 were included. Cases with an interval >6 months between Cycle A and Cycle B, *in vitro* fertilization cycles, and without gonadotropin usage in Cycle A were excluded. Finally, 156 patients who underwent intracytoplasmic sperm injection were included in this study (Figure 1). To investigate protocol effectiveness, the previous COS cycle (Cycle A) and the delayed-start GnRH antagonist with progesterone cycle (Cycle B) were compared. In addition, patients were divided into three groups, and the outcomes were compared in each group: Group A, all patients; Group B, poor responders according to the Bologna criteria (19) and Group C, patients with poor-quality embryos who did not satisfy the Bologna criteria (Figure 1).

This study was approved by the institutional review board of Takeuchi Ladies Clinic/Center for Reproductive Medicine (Number: 23-201) and was conducted in accordance with the 2013 Declaration of Helsinki. We announced this study in displays and on the hospital's homepage and provided an opt-out option for patients.

2.2 Data collection

All data were collected from the patients' medical records. The baseline characteristics of all patients, including maternal age, number of previous oocyte pick-up (OPU) cycles and previous embryo transfer (ET) cycles including previous clinics, and anti-Müllerian hormone levels in Cycle B, were collected. The period from day 1 of the menstrual cycle to the OPU day; dose of

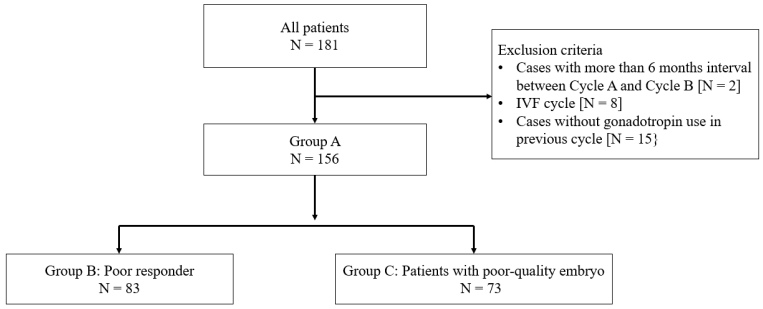

FIGURE 1
Patient selection flow chart. IVF, *in vitro* fertilization.

gonadotropin, estradiol (E2), and progesterone (P4) on the trigger day; diameter of the leading follicle on the trigger day; number of retrieved oocytes; number of MII oocytes; rate of MII oocytes; number of two pronuclear (2PN) zygotes; number of morphologically good blastocysts; implantation rate; clinical pregnancy (defined as detection of the gestational sac) rate; and live birth rate were investigated. The reasons for cancellation were also investigated and divided into the following stages: OPU=0, MII=0, and 2PN=0.

2.3 Outcome measures

The primary outcome was the efficacy of the protocol which was assessed by comparing the period from day 1 of the menstrual cycle to the OPU day; dose of gonadotropin, E2, and P4 on the trigger day; diameter of the leading follicle on the trigger day; number of retrieved oocytes; number of MII oocytes; rate of MII oocytes; number of 2PN zygotes; number of morphologically good blastocysts (defined as better than 3BB according to the Gardner blastocyst grading system); implantation rate; clinical pregnancy (defined as detection of the gestational sac) rate; and live birth rate between Cycle A and Cycle B in all patients (Group A). The rates of OPU=0, MII=0, and 2PN=0 were also compared. These parameters were also compared between Groups B and C to investigate their efficiency in poor responders and patients with poor-quality embryos.

2.4 Ovarian stimulation protocols

Cycle A: There were 87 patients with the antagonist protocol, 68 with the agonist protocol (4 patients with the long protocol and 64 patients with the short/ultrashort protocol), and 1 with progestin-primed ovarian stimulation. When the leading follicle reached 18–20 mm in diameter and more than two follicles reached 18 mm in diameter, the trigger was administered, considering the patient's background and the outcome of the past COS cycle, as appropriate (3000–10,000 IU of human chorionic gonadotropin, a GnRH agonist, and a dual trigger). Transvaginal OPU was performed 34–38 h later, as appropriate, considering the patient's outcome in the past cycle.

Cycle B: On day 3, cetrorelix acetate (3 mg) was administered subcutaneously. From days 3–10, daily oral medroxyprogesterone acetate (MPA, 5 mg twice daily) was continued. On day 11, after ovarian suppression (E2 < 50 mg/mL) was identified, daily high-dose gonadotropin (human menopausal gonadotrophin 225–450 IU, subcutaneously) was initiated. When the leading follicle measured 14 mm, ganirelix acetate (0.25 mg, subcutaneously) was initiated and continued until the trigger day. When the leading follicle reached 18–20 mm in diameter and more than two follicles reached 18 mm in diameter, the trigger was administered considering the patient's background and the outcome of the past COS cycle, as appropriate (3000–10,000 IU of human chorionic gonadotropin, a GnRH agonist, and a dual trigger). Transvaginal OPU was performed 34–38 h after, as appropriate, considering the patient's outcome in the past cycle (Figure 2).

All oocytes underwent intracytoplasmic sperm injection, and all embryos were frozen. The embryos were then thawed and transferred into the hormone replacement cycle on days 3 or 5, as appropriate, under transabdominal ultrasound guidance.

2.5 Embryo transfer protocol

All transferred embryos were frozen-thawed embryo transfers during the hormone replacement cycle. Cleavage-stage embryos were frozen on day 3, and blastocysts were frozen on day 5 or 6 as appropriate. Cleavage-stage embryos were transferred 3 days after

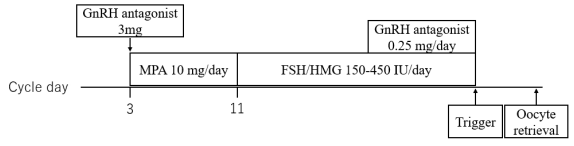

FIGURE 2
Outline of delayed-start ovarian stimulation protocol with a gonadotropin-releasing hormone antagonist, medroxyprogesterone acetate, and high-dose gonadotropin. GnRH, gonadotropin-releasing hormone; MPA, medroxyprogesterone acetate; FSH, follicle-stimulating hormone; HMG, human menopausal gonadotrophin.

progesterone administration, and blastocysts were transferred 5 days after progesterone administration.

2.6 Statistical analysis

Intergroup comparisons were performed using Student's t-test and a nonparametric test for continuous variables or Fisher's exact test for nominal variables. Statistical significance was set at $P < 0.05$. All statistical analyses were performed using EZR (Saitama Medical Center, Jichi Medical University; http://www.jichi.ac.jp/saitama-sct/SaitamaHP.files/statmedEN.html ; Kanda, 2012) (20), which is a graphical user interface for R (The R Foundation for Statistical Computing, Vienna, Austria). More precisely, it is a modified version of R Commander designed to add statistical functions frequently used in biostatistics.

3 Results

Between May 2015 and January 2021, 181 patients received a delayed GnRH antagonist according to the progesterone protocol. Eleven patients were excluded based on the exclusion criteria described above, and 156 patients were included in this study. There were 83 poor responders according to the Bologna criteria (Group B) and 73 patients with poor-quality embryos who did not meet the Bologna criteria (Group C). No surgically obtained sperms or donated sperms were used in the protocols. In Group A, the patients' median age was 40 years [interquartile range (IQR): 37–42], the median anti-Mullerian hormone level was 1.04 ng/mL [IQR: 0.48–1.83], the median number of previous OPU cycles was three [IQR: 3–5], and the median number of previous ET cycles was one [IQR: 0–3). In Group B, the patients' median age was 41 years [IQR: 38–42], the median anti-Mullerian hormone level was 0.53 ng/mL [IQR: 0.32–0.85], the median number of previous OPU cycles was three [IQR: 2–5], and the median number of previous ET cycles was one [IQR: 0–2.5]. In Group C, the patients' median age was 39 years [IQR: 35–41], the median anti-Mullerian hormone level was 1.86 ng/mL [IQR: 1.30–3.54], the median number of previous OPU cycles was three [IQR: 3–4.3], and the median number of previous ET cycles was one [IQR: 0–3] (Table 1). The rates of cleavage-stage (day 3) transfer were not different in cycles A and B (20.4% in Cycle A versus 17.9% in Cycle B, $P = 0.264$).

TABLE 1 Background of patients.

	Group A All	Group B Poor responders	Group C Poor-quality embryos
Number of patients	156	83	73
Age, years [IQR]	40 [37-42]	41 [38-42]	39 [35-41]
AMH, ng/mL [IQR]	1.04 [0.48-1.83]	0.53 [0.32-0.85]	1.86 [1.30-3.54]
Previous OPU cycles [IQR]	3 [3-5]	3 [2-5]	3 [3-4.3]
Previous ET cycles [IQR]	1 [0-3]	1 [0-2.5]	1 [0-3]

AMH, Anti-Müllerian hormone; ET, embryo transfer; IQR, interquartile range; OPU, oocyte pick-up.

In Group A, although the number of oocytes retrieved did not increase significantly between Cycles A and B (5.5 ± 5.3 versus 6.5 ± 6.3, $P = 0.120$), the number of MII oocytes (3.6 ± 3.3 versus 4.5 ± 3.6, $P = 0.015$), number of 2PN zygotes (2.8 ± 2.9 versus 3.8 ± 3.1, $P < 0.01$), and number of good blastocysts (0.5 ± 0.9 versus 1.2 ± 1.6, $P < 0.001$) increased significantly in Cycle B. Subsequent ET rates (41.0% versus 62.8%, $P < 0.001$), implantation rates/OPU cycles (11.5% versus 39.1%, $P < 0.0001$), implantation rates/the number of embryos transferred (18.4% versus 37.2%, $P < 0.01$), clinical pregnancy rates (4.5% versus 32.1%, $P < 0.0001$), and live birth rates (0.6% versus 24.4%, $P < 0.0001$) increased significantly in Cycle B. The periods up to trigger (12.8 ± 1.8 days versus 21.2 ± 2.3 days, $P < 0.001$) and gonadotropin dose (1653 ± 678 IU versus 2088 ± 819 IU, $P < 0.001$) increased significantly in Cycle B. The mean leading follicle size (21.9 ± 4.1 mm versus 21.8 ± 2.8 mm, $P = 0.764$) and E2 level (1649 ± 1231 pg/mL versus 1633 ± 1209 pg/mL, $P = 0.909$) were not different between Cycles A and B, but the P4 level was significantly lower in Cycle B (0.68 ± 0.60 ng/mL versus 0.40 ± 0.25 ng/mL, $P < 0.001$). The cancellation rates because of OPU=0 (2.6 versus 2.6, p=1) and MII=0 (5.9 versus 2.6, p=0.256) were not different, likely because the 2PN=0 was significantly lower (9.8 versus 1.4, $P < 0.01$) in Cycle B (Table 2).

Similar results were obtained for both groups B and C. In poor responders (Group B), although the number of MII oocytes (2.2 ± 1.8 versus 2.8 ± 1.9, $P = 0.053$) was not significantly increased, the number of oocytes retrieved (3.0 ± 2.2 versus 3.7 ± 2.2, $P = 0.027$), number of 2PN zygotes (1.7 ± 1.7 versus 2.3 ± 1.8, $P = 0.015$), and number of good blastocysts (0.4 ± 0.7 versus 0.9 ± 1.3, p=0.001) increased significantly in Cycle B. Subsequent ET rates (38.6 versus 59.0, $P = 0.0127$), implantation rates/OPU cycles (12.0 versus 31.3, $P < 0.01$), clinical pregnancy rates (2.4 versus 21.7, $P < 0.001$), and live birth rates (0 versus 18.1, $P < 00001$) increased significantly in Cycle B. Implantation rates/the number of embryos transferred (20.8% versus 34.7%) was higher in Cycle B; however, this was not statistically significant ($P = 0.109$). Similarly, the periods up to the trigger (12.9 ± 2.0 versus 21.3 ± 2.4, $P < 0.001$) and the gonadotropin dose (1687 ± 983 versus 2250 ± 974, $P < 0.001$) increased significantly in Cycle B. The mean leading follicle size (21.6 ± 4.1 versus 21.7 ± 2.5, $P = 0.722$) and E2 level (1093 ± 599 versus 1118 ± 557, $P = 0.783$) were not different between Cycles A and B, but the P4 level was significantly lower in Cycle B (0.62 ± 0.46 versus 0.38 ± 0.25, $P < 0.001$). The cancellation rates because of OPU=0 (4.8 versus 4.8, p=0.1) and MII=0 (8.9 versus 3.8, $P = 0.328$) were not different, but that because of 2PN=0 was significantly lower (13.9 versus 1.3, $P < 0.001$) in Cycle B (Table 3).

In Group C, although the number of oocytes retrieved did not increase significantly between Cycles A and B (8.4 ± 6.2 versus 9.8 ± 7.7, $P = 0.256$), the number of MII oocytes (5.1 ± 3.8 versus 6.6 ± 4.0, $P = 0.032$), number of 2PN zygotes (4.0 ± 3.4 versus 5.4 ± 3.4, $P = 0.015$), and number of good blastocysts (0.7 ± 1.1 versus 1.6 ± 1.9,

10.3389/fendo.2023.1277873

TABLE 2 Comparison of parameters and outcomes measured in all patients (Group A).

	Cycle A	Cycle B	P
Period up to trigger, days	12.8 ± 1.8	21.2 ± 2.3	<0.001
Duration of gonadotropin injection, days	9.6 ± 1.5	10.1 ± 2.2	0.128
Gonadotropin, IU	1653 ± 678	2088 ± 819	<0.001
Leading follicle, mm	21.9 ± 4.1	21.8 ± 2.8	0.764
Estradiol, pg/mL	1649 ± 1231	1633 ± 1209	0.909
Progesterone, ng/mL	0.68 ± 0.60	0.40 ± 0.25	<0.001
Number of oocytes	5.5 ± 5.3	6.5 ± 6.3	0.120
Number of MII oocytes	3.6 ± 3.3	4.5 ± 3.6	0.015
Number of 2PN zygote	2.8 ± 2.9	3.8 ± 3.1	<0.01
Number of good blastocysts	0.5 ± 0.9	1.2 ± 1.6	<0.001
Rate of OPU = 0, %	2.6 (4/156)	2.6 (4/156)	1
Rate of MII 0, %	5.9 (9/152)	2.6 (4/152)	0.256
Rate of 2PN = 0, %	9.8 (14/143)	1.4 (2/148)	<0.01
ET rate/OPU cycles, %	41.0 (64/156)	62.8 (98/156)	<0.001
Rate of day 3 transfer, %	20.4% (24/98)	17.9% (28/156)	0.263
Number of embryos transferred/ET cycles	1.6 ± 0.90	1.7 ± 0.86	0.578
Implantation rate/OPU cycles, %	11.5 (18/156)	39.1 (61/156)	<0.0001
Implantation rate/embryo transferred, %	18.4% (18/98)	37.2% (61/164)	<0.01
Clinical pregnancy rate/OPU cycles, %	4.5 (7/156)	32.1 (50/156)	<0.0001
Live birth/OPU cycles, %	0.6 (1/156)	24.4 (38/156)	<0.0001

ET, embryo transfer; MII, metaphase II; OPU, oocyte pickup; PN, pronuclear.

$P < 0.001$) increased significantly. Subsequent ET rates (39.7 versus 67.1, $P < 0.01$), implantation rates/OPU cycles (11.0 versus 47.9, $P < 0.001$), implantation rates/the number of embryos transferred (16.0% versus 39.3%, $P < 0.005$), clinical pregnancy rates (6.8 versus 43.8, $P < 0.0001$), and live birth rates (1.4 versus 31.5, $P < 0.0001$) increased significantly in Cycle B. The periods up to trigger (12.6 ± 1.5 versus 21.1 ± 2.2, $P < 0.001$) and gonadotropin dose (1614 ± 674 versus 1905 ± 548, $P = 0.005$) increased significantly in Cycle B. The mean leading follicle size (22.4 ± 4.2 versus 22.0 ± 3.1, $P = 0.452$) and E2 level (2281 ± 1446 versus 2220 ± 1462, $P = 0.797$) were not different between Cycles A and B, but P4 level was significantly lower in Cycle B (0.74 ± 0.73 versus 0.42 ± 0.24, $P < 0.001$). The cancellation rates because of OPU=0 (0 versus 0, p=1), MII=0 (2.7 versus 1.4, p=1), and 2PN=0 (5.6 versus 1.4, $P = 0.209$) were not different between the two cycles (Table 4).

TABLE 3 Comparison of parameters and outcomes measured in poor responders (Group B).

	Cycle A	Cycle B	P
Period up to trigger, days	12.9 ± 2.0	21.3 ± 2.4	<0.001
Gonadotropin, IU	1687 ± 983	2250 ± 974	<0.001
Leading follicle, mm	21.6 ± 4.1	21.7 ± 2.5	0.722
Estradiol, pg/mL	1093 ± 599	1118 ± 557	0.783
Progesterone, ng/mL	0.62 ± 0.46	0.38 ± 0.25	<0.001
Number of oocytes	3.0 ± 2.2	3.7 ± 2.2	0.027
Rate of MII oocyte, %	73 ± 34	75 ± 28	0.617
Number of MII oocytes	2.2 ± 1.8	2.8 ± 1.9	0.053
Number of 2PN zygote	1.7 ± 1.7	2.3 ± 1.8	0.015
Number of good blastocysts	0.4 ± 0.7	0.9 ± 1.3	0.001
Rate of OPU = 0, %	4.8 (4/83)	4.8 (4/83)	1
Rate of MII 0, %	8.9 (7/79)	3.8 (3/79)	0.328
Rate of 2PN = 0, %	13.9 (10/72)	1.3 (1/76)	< 0.001
ET rate/OPU cycles, %	38.6 (32/83)	59.0 (49/83)	0.0127
Rate of day 3 transfer, %	22.9% (11/48)	21.3% (16/75)	0.827
Implantation rate/OPU cycles, %	12.0 (10/83)	31.3 (26/83)	< 0.01
Implantation rate/embryo transferred, %	20.8% (10/48)	34.7% (26/75)	0.109
Clinical pregnancy rate/OPU cycles, %	2.4 (2/83)	21.7 (18/83)	< 0.001
Live birth/OPU cycles, %	0 (0/83)	18.1 (15/83)	<0.0001

ET, embryo transfer; MII, metaphase II; OPU, oocyte pickup; PN, pronuclear.

4 Discussion

In this study, the protocol of delayed stimulation using the GnRH antagonist with progesterone and high-dose gonadotropin was better than other conventional COS protocols in terms of the number of MII oocytes, 2PN zygotes, morphologically good blastocysts, and the live birth rates in patients with recurrent ART failure. In poor responders, although the number of MII oocytes was not significantly increased, the number of oocytes retrieved, 2PN zygotes, and number of good blastocysts increased significantly. In patients with poor-quality embryos, although the number of oocytes retrieved did not increase significantly, the number of MII oocytes, 2PN zygotes, and good blastocysts increased significantly. These results indicate that this protocol increases the number of retrieved oocyte in poor responders, and MII oocytes in patients with poor-quality embryos. In addition, the result of increasing number of good blastocyst indicates that this protocol contribute to improve the quality of the oocytes. There are many reports describing the efficiency of a delayed-start GnRH antagonist protocol in patients with a low ovarian response (3, 7–10, 12, 13). In particular, the delayed-start GnRH antagonist with an

10.3389/fendo.2023.1277873

TABLE 4 Comparison of parameters and outcomes measured in patients with poor-quality embryos (Group C).

	Cycle A	Cycle B	P
Period up to trigger, days	12.6 ± 1.5	21.1 ± 2.2	<0.001
Gonadotropin, IU	1614 ± 674	1905 ± 548	0.005
Leading follicle, mm	22.4 ± 4.2	22.0 ± 3.1	0.452
Estradiol, pg/mL	2281 ± 1446	2220 ± 1462	0.797
Progesterone, ng/mL	0.74 ± 0.73	0.42 ± 0.24	<0.001
Number of oocytes	8.4 ± 6.2	9.8 ± 7.7	0.256
Rate of MII oocyte, %	63 ± 25	74 ± 23	0.009
Number of MII oocytes	5.1 ± 3.8	6.6 ± 4.0	0.032
Number of 2PN zygote	4.0 ± 3.4	5.4 ± 3.4	0.015
Number of good blastocysts	0.7 ± 1.1	1.6 ± 1.9	<0.001
Rate of OPU=0, %	0 (0/73)	0 (0/73)	1
Rate of MII 0, %	2.7 (2/73)	1.4 (1/73)	1
Rate of 2PN=0, %	5.6 (4/71)	1.4 (1/72)	0.209
ET rate/OPU cycles, %	39.7 (29/73)	67.1 (49/73)	<0.01
Rate of day 3 transfer, %	26.0% (13/50)	13.5% (12/89)	0.106
Implantation rate/OPU cycles, %	11.0 (8/73)	47.9 (35/73)	<0.001
Implantation rate/embryo transferred, %	16.0% (8/50)	39.3% (35/89)	<0.005
Clinical pregnancy rate/OPU cycles, %	6.8 (5/73)	43.8 (32/73)	<0.0001
Live birth/OPU cycles, %	1.4 (1/73)	31.5 (23/73)	<0.0001

ET, embryo transfer; MII, metaphase II; OPU, oocyte pickup; PN, pronuclear.

estrogen priming protocol, first described by Cakmak et al. (7), seems effective based on a recent meta-analysis (13). However, the European Society of Human Reproduction and Embryology guidelines (21) considered the delayed-start GnRH protocol as a conditional low recommendation. Although the recommendation of the European Society of Human Reproduction and Embryology guidelines is low, the delayed-start GnRH protocol, compared with other conventional COS, may be effective for poor responders to increase retrieved oocytes and clinical pregnancy rate and decrease the cancellation rate (3, 4, 7–10, 12, 13), which is similar to the result in this study. Administration of GnRH antagonists in the early follicular phase is thought to suppress follicle-stimulating hormone levels, which allows growth of smaller antral follicles and halts the time for larger antral follicles (13, 22, 23). Suppression of early luteinizing hormone (LH) rise in patients with poor ovarian response may play a role in the improvement of outcomes (3). It leads to synchronized follicle growth and increased numbers of MII oocytes and good blastocysts, thereby increasing the chances of ET and live birth. Additionally, this protocol allows the use of more gonadotropin in terms of both dose and duration. Administration of GnRH antagonists in the early follicular phase suppresses the endogenous follicle-stimulating hormone and LH, which increases the requirement for gonadotropin.

A recent meta-analysis (13) has shown that a delayed-start GnRH antagonist protocol is more effective than long GnRH agonist, microdose GnRH agonist, multiple-dose GnRH agonist, GnRH antagonist, or GnRH antagonist/letrozole in patients with poor ovarian response. The main advantage is that GnRH antagonists have an early pituitary suppression and recovery from suppression compared with other protocols (4). However, the disadvantages of this protocol include a longer treatment time and a higher dose of gonadotropin. Frankfurter's protocol is an original delayed GnRH antagonist protocol combined with progesterone. Progesterone-mediated LH surge suppression is currently used as a progestin-primed ovarian stimulation protocol. This suppression is mediated by an increase in dynorphin and GABAA receptor signaling acting through kisspeptin neurons in the anteroventral periventricular nucleus of the hypothalamus (23). Therefore, we hypothesized that GnRH antagonist administration might decrease progesterone supplementation. To overcome this disadvantage, earlier and lower doses of GnRH antagonists were administered (day 3 and one administration of 3 mg cetrorelix acetate) compared with Frankfurter's protocol (days 5–8/9–12 and two administrations of 3 mg cetrorelix acetate) (3). As a result, the stimulation period was shorter (11 versus 12 days) and the gonadotropin dose was lower (2097 versus 5400 IU) than those in Frankfurter's protocol. The number of retrieved oocytes (6.3 versus 4.5), number of zygotes (3.6 versus 2.5), and live birth (ongoing pregnancy) rate (21.8% versus 25.0%) were similar in both protocols. Based on these results, our protocol is as effective as Frankfurter's protocol and addresses the disadvantage.

These findings were especially evident in poor responders but there have been few reports describing the efficiency in patients with poor-quality embryos. Younis et al. (4) investigated the efficiency of GnRH antagonist pretreatment among patients with two intact ovaries, age <39 years, body mass index 18–32 kg/m^2, and a normal uterine cavity, excluding polycystic ovary syndrome, severe endometriosis, low ovarian reserve, thyroid disease, diabetes mellitus, significant hyperprolactinemia, and hypogonadotropic-hypogonadism. They concluded that pretreatment with a GnRH antagonist improved the meiotic status of retrieved oocytes and their competence for normal fertilization by suppressing serum follicle-stimulating hormone and LH levels while COS (not significantly). Our results in patients with poor-quality embryos (Group C) are similar to those in their report. Therefore, in addition to poor responders and other patients with ART failure, including those with poor-quality embryos, early follicular-phase GnRH antagonist administration is effective in increasing the number of mature oocytes, 2PN zygotes, and good blastocysts and the chance of live birth. The most significant difference in reasons for cancellation was 2PN=0. It is difficult to explain why 2PN increased in Cycle B only because of the increased oocyte counts. This indicates that this protocol may have a positive effect on the quality of oocytes, as previously described by Younis et al. (4). Further research, including basic research, is necessary to confirm this hypothesis.

The limitations of this study are its retrospective design, the various protocols in Cycle A, and the subsequent advantage of Cycle

B. It was previously reported that a change in COS protocol for the second cycle may affect the outcome in both positive and negative ways regarding oocyte recovery and the total number of mature oocytes/embryos (7, 24, 25). In this study, the median number of previous OPU cycles was three, so personalized intervention, such as the timing of OPU after the trigger, can improve the MII rate and decrease cancellation. In fact, the size of the leading follicle on the trigger day and the cancellation rate because of OPU=0 and MII=0 were not different between Cycles A and B. In addition, an interval of more than 6 months between the two cycles was excluded to reduce the chance of improved outcomes in the latter cycle as a result of the intervention using new technology. Although the data were not shown, Frankfurter et al. (3) reported that the type of initial COS protocol used did not affect the outcomes. The limitations of this study are not completely eliminated, and the facts mentioned above support its reliability. In the future, a randomized prospective trial is desirable to evaluate the effectiveness of this protocol. To further evaluate the effectiveness of the GnRH antagonist combined with MPA, a comparison of the delayed GnRH antagonist protocol with or without MPA in the early follicular phase is desirable.

In conclusion, the original delayed-start GnRH antagonist with progesterone and high-dose gonadotropin protocol is effective and useful as an alternative protocol in patients with recurrent ART failure, both in poor responders according to the Bologna criteria and patients with poor outcomes because of poor-quality embryos. Although it has disadvantages compared with other COS protocols, such as a longer treatment period and a larger dose of gonadotropin, it has an advantage in terms of the number of oocytes retrieved, number of morphologically good blastocysts, and the live birth rate. However, further research is required to confirm this finding.

Data availability statement

The raw data supporting the conclusions of this article will be made available by the authors, without undue reservation.

Ethics statement

The studies involving humans were approved by Institutional Review Board of Takeuchi Ladies Clinic/Center for Reproductive Medicine. The studies were conducted in accordance with the local legislation and institutional requirements. Written informed consent for participation was not required from the participants or the participants' legal guardians/next of kin because this study is a retrospective study which only hundle anonymized data. So that we did not take individual written consent. But we announced this study in displays and on the hospital's homepage and provided an opt-out option for patients. No patient offered opt-out.

Author contributions

KT: Conceptualization, Data curation, Project administration, Writing – original draft, Investigation, Methodology. YO: Conceptualization, Data curation, Project administration, Writing – original draft, Formal Analysis. TI: Conceptualization, Data curation, Writing – review & editing. YKuw: Resources, Writing – review & editing. YKur: Resources, Writing – review & editing. YF: Resources, Writing – review & editing. YM: Resources, Writing – review & editing. MT: Resources, Writing – review & editing. HM: Resources, Writing – review & editing.

Funding

The author(s) declare that no financial support was received for the research, authorship, and/or publication of this article.

Acknowledgments

We would like to thank Editage (www.editage.com) for English language editing.

Conflict of interest

The authors declare that the research was conducted in the absence of any commercial or financial relationships that could be construed as a potential conflict of interest.

Publisher's note

References

1. Zhang Y, Zhang C, Shu J, Guo J, Chang HM, Leung PCK, et al. Adjuvant treatment strategies in ovarian stimulation for poor responders undergoing IVF: a systematic review and network meta-analysis. *Hum Reprod Update* (2020) 26:247–63. doi: 10.1093/humupd/dmz046

2. Abu-Musa A, Haahr T, Humaidan P. Novel physiology and definition of poor ovarian response: Clinical recommendations. *Int J Mol Sci* (2020) 21:2110. doi: 10.3390/ijms21062110

3. Frankfurter D, Dayal M, Dubey A, Peak D, Gindoff P. Novel follicular-phase gonadotropin-releasing hormone antagonist stimulation protocol for in *vitro* fertilization in the poor responder. *Fertil Steril* (2007) 88:1442–5. doi: 10.1016/j.fertnstert.2007.01.022

4. Younis JS, Soltsman S, Izhaki I, Radin O, Bar-Ami S, Ben-Ami M. Early and short follicular gonadotropin-releasing hormone antagonist supplementation improves the

meiotic status and competence of retrieved oocytes in *in vitro* fertilization-embryo transfer cycles. *Fertil Steril* (2010) 94:1350–5. doi: 10.1016/j.fertnstert.2009.08.033

5. Blockeel C, Riva A, De Vos M, Haentjens P, Devroey P. Administration of a gonadotropin-releasing hormone antagonist during the 3 days before the initiation of the in *vitro* fertilization/intracytoplasmic sperm injection treatment cycle: impact on ovarian stimulation. *A pilot study. Fertil Steril* (2011) 95:1714–9.e1. doi: 10.1016/j.fertnstert.2011.01.028

6. Di Luigi AJ, Engmann L, Schmidt DW, Benadiva CA, Nulsen JC. A randomized trial of microdose leuprolide acetate protocol versus luteal phase ganirelix protocol in predicted poor responders. *Fertil Steril* (2011) 95:2531–3. doi: 10.1016/j.fertnstert.2011.01.134

7. Cakmak H, Tran ND, Zamah AM, Cedars MI, Rosen MP. A novel "delayed start" protocol with gonadotropin-releasing hormone antagonist improves outcomes in poor responders. *Fertil Steril* (2014) 101:1308–14. doi: 10.1016/j.fertnstert.2014.01.050

8. Maged AM, Nada AM, Abohamila F, Hashem AT, Mostafa WA, Elzayat AR. Delayed start versus conventional GnRH antagonist protocol in poor responders pretreated with estradiol in luteal phase: a randomized controlled trial. *Reprod Sci* (2015) 22:1627–31. doi: 10.1177/1933719115590666

9. Aflatoonian A, Hosseinisadat A, Baradaran R, Farid Mojtahedi MM. Pregnancy outcome of "delayed start" GnRH antagonist protocol versus GnRH antagonist protocol in poor responders: a clinical trial study. *Int J Reprod BioMed* (2017) 15:231–8. doi: 10.29252/ijrm.15.4.231

10. Ashrafi M, Arabipoor A, Yahyaei A, Zolfaghari Z, Ghaffari F. Does the "delayed start" protocol with gonadotropin-releasing hormone antagonist improve the pregnancy outcome in Bologna poor responders? a randomized clinical trial. *Reprod Biol Endocrinol* (2018) 16:124. doi: 10.1186/s12958-018-0442-y

11. Cozzolino M, Franasiak J, Andrisani A, Ambrosini G, Vitagliano A. 'Delayed start' gonadotropin-releasing hormone antagonist protocol in Bologna poor-responders: A systematic review and meta-analysis of randomized controlled trials. *Eur J Obstet Gynecol Reprod Biol* (2020) 244:154–62. doi: 10.1016/j.ejogrb.2019.11.028

12. Yang S, Liu N, Li Y, Zhang L, Yue R. Efficacy of the delayed start antagonist protocol for controlled ovarian stimulation in Bologna poor ovarian responders: a systematic review and meta-analysis. *Arch Gynecol Obstet* (2021) 303:347–62. doi: 10.1007/s00404-020-05894-8

13. Di M, Wang X, Wu J, Yang H. Ovarian stimulation protocols for poor ovarian responders: a network meta-analysis of randomized controlled trials. *Arch Gynecol Obstet* (2023) 307:1713–26. doi: 10.1007/s00404-022-06565-6

14. Scott RT, Navot D. Enhancement of ovarian responsiveness with microdoses of gonadotropin-releasing hormone agonist during ovulation induction for in *vitro* fertilization. *Fertil Steril* (1994) 61:880–5. doi: 10.1016/S0015-0282(16)56700-4

15. Surrey ES, Bower J, Hill DM, Ramsey J, Surrey MW. Clinical and endocrine effects of a microdose GnRH agonist flare regimen administered to poor responders who are undergoing in *vitro* fertilization. *Fertil Steril* (1998) 69:419–24. doi: 10.1016/S0015-0282(97)00575-X

16. Ghaffari F, Jahangiri N, Madani T, Khodabakhshi S, Chehrazi M. Randomized controlled trial of gonadotropin-releasing hormone agonist microdose flare-up versus flare-up among poor responders undergoing intracytoplasmic sperm injection. *Int J Gynaecol Obstet* (2020) 148:59–64. doi: 10.1002/ijgo.12988

17. Anckaert E, Smitz J, Schiettecatte J, Klein BM, Arce JC. The value of anti-Mullerian hormone measurement in the long GnRH agonist protocol: association with ovarian response and gonadotrophin-dose adjustments. *Hum Reprod* (2012) 27:1829–39. doi: 10.1093/humrep/des101

18. Sunkara SK, Coomarasamy A, Faris R, Braude P, Khalaf Y. Long gonadotropin-releasing hormone agonist versus short agonist versus antagonist regimens in poor responders undergoing in *vitro* fertilization: a randomized controlled trial. *Fertil Steril* (2014) 101:147–53. doi: 10.1016/j.fertnstert.2013.09.035

19. Ferraretti AP, La Marca A, Fauser BC, Tarlatzis B, Nargund G, Gianaroli L, et al. ESHRE consensus on the definition of "poor response" to ovarian stimulation for in *vitro* fertilization: the Bologna criteria. *Hum Reprod* (2011) 26:1616–24. doi: 10.1093/humrep/der092

20. Kanda Y. Investigation of the freely available easy-to-use software "EZR" for medical statistics. *Bone Marrow Transplant* (2013) 48:452–8. doi: 10.1038/bmt.2012.244

21. Ovarian Stimulation TEGGO, Bosch E, Broer S, Griesinger G, Grynberg M, Humaidan P, et al. ESHRE guideline: ovarian stimulation for IVF/ICSI. *Hum Reprod Open* (2020) 2020:hoaa009. doi: 10.1093/hropen/hoaa009

22. Huirne JA, Homburg R, Lambalk CB. Are GnRH antagonists comparable to agonists for use in IVF? *Hum Reprod* (2007) 22:2805–13. doi: 10.1093/humrep/dem270

23. Liu Y, Li X, Ivanova D, Lass G, He W, Chen Q, et al. Dynorphin and GABAA receptor signaling contribute to progesterone's inhibition of the LH surge in female mice. *Endocrinology* (2020) 161:bqaa036. doi: 10.1210/endocr/bqaa036

24. Takahashi K, Mukaida T, Tomiyama T, Goto T, Oka C. GnRH antagonist improved blastocyst quality and pregnancy outcome after multiple failures of IVF/ICSI-ET with a GnRH agonist protocol. *J Assist Reprod Genet* (2004) 21:317–22. doi: 10.1023/b:jarg.0000045470.68525.a4

25. Lai Q, Zhang H, Zhu G, Li Y, Jin L, He L, et al. Comparison of the GnRH agonist and antagonist protocol on the same patients in assisted reproduction during controlled ovarian stimulation cycles. *Int J Clin Exp Pathol* (2013) 6:1903–10.

frontiers | Frontiers in Endocrinology

TYPE Mini Review
PUBLISHED 06 November 2023
DOI 10.3389/fendo.2023.1282658

OPEN ACCESS

EDITED BY
Priyadarshini Pantham,
University of California, San Diego,
United States

REVIEWED BY
Xiaowei Gu,
Cincinnati Children's Hospital Medical Center, United States
Yibao Huang,
Huazhong University of Science and Technology, China

*CORRESPONDENCE
Yuhua Shi
shiyuhua2003@126.com

†These authors have contributed equally to this work and share first authorship

RECEIVED 24 August 2023
ACCEPTED 17 October 2023
PUBLISHED 06 November 2023

CITATION
Tang M, Zhao M and Shi Y (2023) New insight into the role of macrophages in ovarian function and ovarian aging. *Front. Endocrinol.* 14:1282658. doi: 10.3389/fendo.2023.1282658

New insight into the role of macrophages in ovarian function and ovarian aging

Maoxing Tang[1†], Manzhi Zhao[2†] and Yuhua Shi[1*]

[1]Department of Reproductive Medicine, Guangdong Provincial People's Hospital (Guangdong Academy of Medical Sciences), Southern Medical University, Guangzhou, China, [2]Department of Pulmonary and Critical Care Medicine, Guangdong Provincial People's Hospital (Guangdong Academy of Medical Sciences), Southern Medical University, Guangzhou, China

Macrophages (MΦs) are the most abundant leukocytes in mammalian ovaries that have heterogeneity and plasticity. A body of evidence has indicated that these cells are important in maintaining ovarian homeostasis and they play critical roles in ovarian physiological events, such as folliculogenesis, ovulation, corpus luteum formation and regression. As females age, ovarian tissue microenvironment is typified by chronic inflammation with exacerbated ovarian fibrosis. In response to specific danger signals within aged ovaries, macrophages polarize into different M1 or M2 phenotypes, and specialize in unique functions to participate in the ovarian aging process. In this review, we will focus on the physiologic roles of MΦs in normal ovarian functions. Furthermore, we will discuss the roles of MΦs in the process of ovarian senescence, as well as the novel techniques applied in this field.

KEYWORDS

macrophages, ovarian aging, ovarian function, follicle development, inflammation, female infertility

1 Introduction

The ovary is a key organ in female reproductive system. It produces oocytes and multiple reproductive hormones including estrogen, progesterone and androgens (1). Unlike other organs in the body, the mammalian ovary is one of the first organs to undergo early senescence. Ovarian aging is characterized by ongoing reduction in follicle number and steroid hormones generation, with deterioration of oocyte quantity and quality (2–4). In humans, ovarian function usually begins to decline around age of 35 years, and deteriorates after 37 years old, ultimately leading to endocrine dysfunction, fertility loss and menopause (1, 3, 5). It is noteworthy that in recent years, a growing body of women opt to postpone childbearing to the later stage of life partially due to social factors. As a result, the decline of female fertility due to ovarian aging represents a great challenge in reproductive medicine for which there is no reliable treatment (4, 6, 7). So far, the molecular mechanisms underpinning ovarian aging remain unclear.

Macrophages (MΦs) are a central population of leukocytes in the innate immune system, with high levels of heterogeneity and plasticity in various tissues (8–11). They are the most abundant immune cells in mammalian ovaries (8). In addition to their general functions in infection, injury and inflammation, increasing evidence has suggested critical roles of MΦs in multiple aspects of ovarian physiology, including folliculogenesis, ovulation, corpus luteum formation and regression (12, 13). Notably, along with advancing maternal age, ovarian microenvironment is characterized by chronic inflammation with exacerbated stromal fibrosis (14–17). In response to tissue-derived stimuli such as inflammatory cytokines/chemokines and Th2-type cytokines, ovarian MΦs can polarize into different M1 or M2 phenotypes, and specialize in unique functions to participate in ovarian senescence (9, 14). It has become increasingly clear that during reproductive senescence, the perturbation of M1 and M2 phenotypes is closely associated with ovarian aging (8, 9, 14). Therefore, we summarize the physiologic roles of MΦs in normal ovarian functions. Moreover, we discuss the roles of MΦs in ovarian senescence, as well as novel techniques applied in this field.

2 Overview of macrophages

MΦs constitute a vital component of innate immune system, and play important roles during infections and inflammation. They are often distributed in multiple tissues/organs of the body (8, 18). Previously, MΦs are thought to solely originate from monocytes, which are derived from precursors of bone marrow. Monocytes circulate in blood for several days and ultimately migrate to specific tissues where they differentiate into MΦs. However, in addition to monocyte-derived MΦs, it has recently reported that some MΦs within tissues arise from yolk sac and fetal liver during embryogenesis (9, 11). Notably, MΦs display high levels of plasticity, as reflected by that they phenotypically and functionally adapt to diverse tissue-specific environments. These local MΦ populations are essential for maintaining tissue homeostasis (11, 19). So far, due to MΦs' complex property, the biology of MΦs is still not fully understood.

2.1 Plasticity, polarization and phenotype of macrophages

MΦs display strong heterogeneity and plasticity in their phenotypes and functions when exposed to various tissue microenvironments (20). In response to microorganism, microenvironmental stimuli/signals, MΦs switch from one phenotype to another, reflecting MΦs' plasticity (11, 14, 19). Based on surface markers and biological activities, MΦs are commonly divided into two distinct subpopulations, including classically activated (M1) and alternatively activated (M2) MΦs (19, 21). Traditionally, M1 MΦs are induced by pro-inflammatory signals, such as interferon-γ, tumor necrosis factor-α (TNF-α), granulocyte-macrophage colony stimulation factor (GM-CSF), or lipopolysaccharide. In contrast, M2 MΦs are induced by anti-inflammatory signals such as IL-4, IL-13 and IL-10. Besides, IL-21 and IL-33 can also drive M2 polarization. Under the stimulation of various stimuli, M2 MΦs can be further divided into four subsets, M2a, M2b, M2c and M2d (12, 19). Specifically, M2a subset is induced by IL-4 or IL-13, whereas M2b subset is induced by immune complexes, Toll-like receptor (TLR) ligands, or IL-1 receptor agonists (IL-1Ra). M2c subset is induced by glucocorticoids, IL-10 or TGF-β. Finally, M2d subset, also known as tumor-associated macrophages, is induced by TLR ligands, A2 adenosine receptor agonists, or IL-6 (11, 12).

2.2 Function of macrophages

Typically, activated MΦs express a variety of receptors, including co-stimulatory and antigen presenting molecules (e.g. CD80, CD86, major histocompatibility complex I/II), chemotactic/activating cytokine receptors, pattern recognition receptors, and opsonic receptors (12). MΦs perform diverse functions during inflammation, infection and injury (22–24). Firstly, they defense against microorganisms by engulfing pathogens, and removing dying cells. Secondly, they process and present antigens to helper T-cells and stimulate them. Thirdly, they produce various cytokines, chemokines, growth factors and enzymes to recruit immune cells, as well as to facilitate vasculogenesis, tissue remodeling and repair (11, 20).

With MΦs polarization into M1 and M2 phenotypes, they exhibit enormous functional heterogeneity (11, 20). Specifically, M1 MΦs have a pro-inflammatory phenotype. They generate various chemokines and pro-inflammatory cytokines, such as TNF-α, IL-1α/β, IL-6, IL-12, IL-18 and IL-23, and possess enhanced antigen-presentation capabilities to participates in adaptive immune response (11). Additionally, M1 MΦs produce lysosomal enzymes and inducible nitric oxide synthase (iNOS) to eliminate pathogens (21). By stark contrast, M2 MΦs have an anti-inflammatory phenotype. They produce anti-inflammatory cytokines including IL-10 and transforming growth factor β (TGF-β), fibroblast growth factor (FGF) and platelet-derived growth factor (PDGF), which facilitate inflammation resolution, tissue repair and fibrosis (11, 19, 21). Moreover, diverse M2 subpopulations perform differential functions (11, 12). M2a subset suppresses inflammation and promotes tissue remodeling/repair through producing IL-10 and TGF-β (21). M2b subset simultaneously secretes pro-inflammatory and anti-inflammatory cytokines including IL-1β, IL-6, TNF-α and IL-10, which are responsible for immune regulation (25, 26). In contrast, M2c subset can phagocytose apoptotic bodies and repair injured tissues (25, 27). Also, they exert a strong anti-inflammatory effect via releasing TGF-β and IL-10 (11). M2d subset produces TGF-β, IL-10, and vascular endothelial growth factor (VEGF), which promotes tumor angiogenesis and metastasis (28).

3 Macrophages and ovarian function

MΦs are the most abundant immune cells in mammalian ovaries. The number and distribution of these cells change during

ovarian cycles (8, 29). Accumulated evidence has revealed that MΦs are key players in various aspects of ovarian physiology (12, 13, 30). Table 1 summarizes the roles of MΦs subsets in normal ovarian function.

3.1 Roles of macrophages in folliculogenesis and follicular atresia

Human and animal studies have suggested an abundant presence of MΦs in thecal layer of growing follicles (9). Ovarian MΦs contribute to follicular growth via their derived cytokines and growth factors, involving VEGF, hepatocyte growth factor (HGF), FGF, epidermal growth factor (EGF), TGF-α/β, insulin-like growth factor (IGF), IL-1β and IL-6 (Figure 1). These factors promote proliferation of granulosa cells, vascular growth, follicle development and production of steroid hormones, whereas inhibit apoptosis of granulosa cells in the ovary (9, 12, 37, 38). Additionally, recent studies have identified distinct MΦs subpopulations in mouse ovaries, which play essential roles in ovarian homeostasis and functions (9, 31, 39). It is revealed that in young mouse ovaries, the proportion of $CD11c^+$ M1 MΦs increases significantly around developing follicles, while the proportion of $CD206^+$ M2 MΦs does not. Moreover, depletion of $CD11c^+$ M1 MΦs using diphtheria toxin injection in mice leads to follicular impairment, vasculature impairment and ovarian hemorrhage, whereas depletion of $CD206^+$ M2 MΦs does not (31). This implies that M1 subset plays an important role in maintenance of follicles development and ovarian physiology.

TABLE 1 Roles of macrophage subsets in normal ovarian function and ovarian aging.

Macrophage subsets	Effects on normal ovarian function	Effects on ovarian aging	References
M1	Promote vascular growth, follicle development Promote luteolysis Induce primordial follicles activation	Impair oocyte quality Increase atretic follicle number Reduce growing follicle number	Ono et al. (31) Orecchioni et al. (19) Care et al. (32) Skarzynski et al. (33) Xiao et al. (34)
M2	Promote luteinization, progesterone production Maintain follicles in a dormant status	Promote ovarian ECM deposition and fibrosis Improve growing follicle number, oocyte quality, AMH and estrogen levels Reduce atretic follicle number	Ingman et al. (35) Zhang et al. (14) Xiao et al. (34) Umehara et al. (36)

ECM, extracellular matrix; AMH, anti-mullerian hormone.

In mammalian ovaries, only a fraction of primordial follicles achieve ovulation, while more than 99% of follicles undergo atresia (40). Studies have revealed that ovarian MΦs increasingly infiltrate granulosa cell layers surrounding atretic follicles (9, 41). This migration/recruitment event is mediated by IL-33, which is mostly generated by endothelial cells adjacent to atretic follicles (42, 43). The infiltrated MΦs facilitate granulosa cell apoptosis and follicle atresia by secretion of TNF-α (44) (Figure 1). Subsequently, these cells are responsible for removing apoptotic cells and degrading atretic follicles through production of matrix metalloproteinases (MMPs) like MMP-3[9] (Figure 1).

3.2 Roles of macrophages in ovulation, corpus luteum formation and regression

A surge of luteinizing hormone (LH) secreted by pituitary gland initiates ovulation, which involves preovulatory follicles rupture at the apex and extrude cumulus cell-oocyte complex (45). Animal studies have revealed that ovarian MΦs actively participate in ovulation (12), as colony stimulation factor-1 knockout female mice with elimination of MΦs demonstrate compromised ovulation (46). During ovulatory process, LH surge facilitates production of multiple chemoattractants by granulosa cells, such as chemokine (C-X-C motif) ligand 10, C-C-motif ligand-20, monocyte chemoattractant protein-1 (MCP-1), IL-1 and IL-6. As a result, a large number of ovarian MΦs are recruited to preovulatory follicles by the chemoattractants (34, 47). These cells promote ovulation through secreting MCP-1 and pro-inflammatory cytokines like IL-1β, IL-6 and TNF-α, which simultaneously amplify recruitment effects (Figure 1). Besides, recruited MΦs produce MMPs like MMP-1 and MMP-19 contributing to extracellular matrix (ECM) breakdown, which facilitates follicle rupture and oocyte extrusion (9, 45) (Figure 1).

Following ovulation, the remains of ovarian follicles undergo tissue remodeling, involving luteinization of follicular theca cells and granulosa cells, and vascularization, to develop a corpus luteum (CL) (48). The CL functions as a temporary endocrine structure through generation of high levels of progesterone and moderate levels of estradiol and inhibin A (9, 48). Evidence from human and animal models has suggested a close relationship between ovarian MΦs and CL development and function (9, 32, 49, 50). Upon stimulation of chemokine MCP-1 and C-C-motif ligand-2 (CCL-2), and GM-CSF, MΦs accumulate and exhibit an activation status in theca-lutein layer of CL (49, 50). They support vascularization of luteal cells and synthesis of progesterone through releasing of FGF, VEGF and MMPs (9, 51) (Figure 1). It is worth noting that disruption of M2 phenotype polarization in TGF-β-deficient female mice leads to impaired luteinization and reduced progesterone production in CL, implying that M2 subset is a key player in developing CL (9, 35). If the oocyte is not fertilized, the CL subsequently undergoes degeneration. This process is also called luteolysis, which is set off by prostaglandin F2α (PGF2α) (32). Ovarian MΦs are found to polarize towards M1 phenotype that facilitate PGF2α production through secretion of TNF-α, thereby promoting luteolysis, indicative of importance of M1 subset in CL

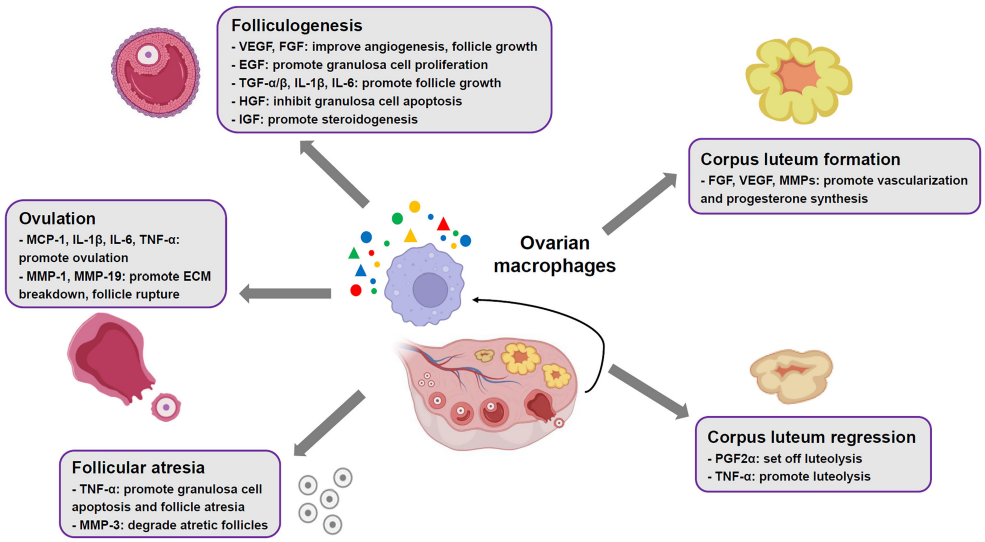

FIGURE 1
Roles of ovarian macrophages in normal ovarian functions. In mammalian ovaries, the macrophages contribute to ovarian physiological events, such as folliculogenesis, ovulation, corpus luteum formation and regression, through production of multiple cytokines and mediators.

regression (19, 32, 33) (Figure 1). Conversely, if the oocyte is fertilized and implantation occurs, human chorionic gonadotropin produced by syncytiotrophoblast prevents MΦs accumulation, resulting in the CL maintenance (12).

4 Macrophages and ovarian aging

As a key reproductive organ in females, the ovary, however, ages early in life (2, 3, 39). Until now, the mechanisms underlying ovarian aging have not been fully elucidated. The studies of ovarian MΦs in both mice and humans are constrained, as their number is very small and they display high heterogeneities in phenotypes (9, 34). Recently, the advance of high-throughput sequencing techniques has made it possible to investigate ovarian MΦs at the single-cell level. Using these novel technologies, emerging studies highlight critical roles of MΦs in ovarian aging (9, 39). Table 1 summarizes the roles of MΦs subsets in ovarian aging process.

4.1 Macrophages dictates the inflammatory milieu within the aging ovary

Mounting evidence suggests that ovarian aging in mammals is associated with a sterile chronic inflammation in ovaries, which adversely affects ovarian function and oocyte quality (14, 16, 17, 52, 53). Recent studies have revealed that as female C57BL/6 mice age (from two to eighteen months old), levels of pro-inflammatory cytokines, including TNF-α, IL-1α/β and IL-6, were significantly elevated in serum and ovary (53). Furthermore, similar alterations were seen in levels of inflammasome genes, involving nucleotide-binding domain and leucine rich repeat containing family, pyrin domain containing 3 (NLRP3) and apoptosis-associated speck-like protein containing a CARD (ASC). They are capable of boosting production of pro-inflammatory cytokines IL-1β and IL-18 (53). Notably, the increased levels of these pro-inflammatory cytokines and inflammasome genes are found to be closely related to declined follicle reserve along with reproductive senescence (53, 54) (Figure 2). Nonetheless, the mechanisms underlying persistent inflammatory condition in aged ovaries remain elusive.

Recently, it has been proposed that MΦs are responsible for age-associated inflammation within the ovary (9, 14, 39). In comparison with reproductively young mice (2-month-old), there is a conspicuous increase in the MΦs proportion within ovaries from reproductively aged mice (12-month-old), which were driven by CCL-2 and chemokine ligand-5 (16, 53). These cells showed an activation status reflected by secreting high levels of pro-inflammatory cytokines including IL-1, IL-6 and TNF-α, exacerbating granulosa cell apoptosis and follicular depletion (9, 53) (Figure 2). In addition, other mouse studies demonstrated the presence of a hyperactivated form of MΦs, multinucleated giant cells, in ovarian stroma over the course of reproductive ageing (15, 16). However, the mechanisms underlying activation status of ovarian MΦs as females age remain poorly understood. Several studies in mouse models have revealed that excessive accumulation of incompletely digested cell debris like lipofuscin, and low molecular weight hyaluronan fragments from ECM, might be the drivers of intensive activation status of MΦs during ovarian aging (54–56).

4.2 Macrophages contribute to ovarian fibrosis during reproductive aging

In addition to chronic inflammation, stromal fibrosis within ovaries is another hallmark of mammalian ovarian senescence (16,

10.3389/fendo.2023.1282658

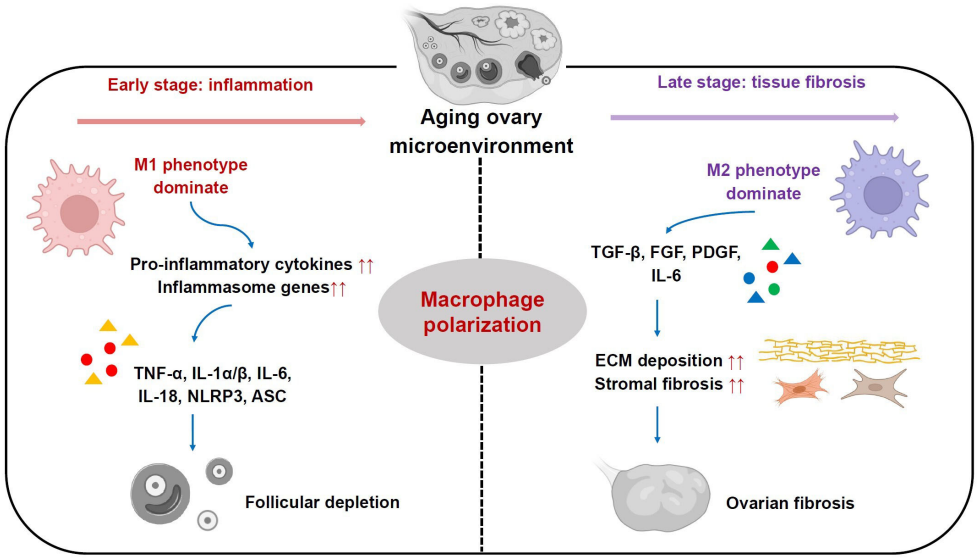

FIGURE 2
Roles of ovarian macrophages and their subsets in ovarian aging process. In the early stage, M1 phenotype subset is dominant and plays a pro-inflammatory role by secreting pro-inflammatory cytokines, including TNF-α, IL-1α/β, IL-6, IL-18, which in turn boost elevated expression of inflammasome genes like NLRP3 and ASC. In the late stage, M2 phenotype subset is more predominant and participates in ECM deposition and stromal fibrosis, ultimately leading to ovarian fibrosis.

57). Ovarian stroma is broadly considered as non-follicular components of the ovary, including immune cells, blood vessels, nerves, and ovary-specific components like spindle-shaped stromal cells, stem cells and ECM (39, 57–59). It serves as an essential supporting tissue for maintaining ovarian homeostasis and functions (9). Previous works in mice and humans have shown an increase in stromal fibrosis and an excessive deposition of ECM components in reproductively old ovaries, which are associated with reduced follicle number, impaired follicle development and ovarian dysfunction (16, 60). Besides aging-related increase of fibrosis, a marked increase in monocyte recruitment and a shift in MΦs phenotype towards M2 were found within ovaries from reproductively aged mice (18 months) relative to young mice (3 months). Subsequently, the monocyte-derived MΦs and M2 subpopulation become more predominant with reproductive aging. They promote ovarian ECM deposition and fibrosis by secreting high levels of TGF-β, FGF, PDGF as well as pro-inflammatory cytokines like IL-6 (9, 14) (Figure 2). Moreover, recent transcriptomics data from ovarian aging models of cynomolgus monkey has further confirmed these findings (61).

4.3 Macrophage polarization is associated with ovarian aging

Recent animal studies have revealed that shifted MΦs subpopulations with different phenotypes resulting from their polarization play critical roles in ovarian senescence (17, 62, 63) (Figure 2). It has been found that in ovaries of young female ICR mice at 8 weeks old, M1 phenotype mainly functions in primordial follicles activation, while M2 phenotype functions in maintenance of follicles in a dormant status (34). They perform differential functions through MΦs-derived distinct extracellular vesicles (EVs) (34). Notably, with female ICR mice aged at 10 months old, the percentage of M1 phenotype within ovaries was increased relative to young females, which is accompanied by an elevated expression of several pro-inflammatory genes including *IL-6*, *TNF-α*, *IL-17*, *iNOS*, *ASC* and *NLRP3*. By contrast, M2 phenotype did not show significant changes (34). Furthermore, the addition of M2-derived EVs into these old mice could enhance M2 phenotype proportion, which ultimately rescued growing follicle number, oocyte quality, serum anti-mullerian hormone and estrogen levels. Meanwhile, it could reduce atretic follicle number, and levels of pro-inflammatory genes expression involving *IL-1β*, *IL-6*, *iNOS* and *TNF-α*. This implies that the perturbed dynamics of M1 and M2 subpopulations are actively involved in ovarian functional decay with reproductive senescence (34) (Figure 2). However, another recent study showed inconsistent results using C57BL mouse models with advanced reproductive age at 12-16 months old. This work revealed high expression levels of inflammatory chemokines (CCL-2, CCL-3, and CXCL-2), pro-inflammatory cytokines TNF-α and IL-6, and Th2-type cytokines IL-4 and IL-13 in the aged ovarian stroma, which drove MΦs polarization. As a result, there were increase numbers of both M1 and M2 subpopulations, while M2 number was more predominant within ovarian stroma of old mice. These cells promoted ovarian fibrosis by stimulating fibrotic collagen deposition (Figure 2). Following suppression of the M2 subpopulation by antifibrosis drug (BGP-15), it was observed that ovarian fibrosis was reversed, and ovarian function and female fertility were finally improved (36). The discrepancy of these findings may be due to dynamic changes of M1/M2 phenotype in different stages of ovarian aging. In early phase, M1 phenotype is dominant and plays a pro-inflammatory role, whereas in late phase, M2 phenotype is more predominant and

participates in inflammation resolution, tissue remodeling and repair in aging ovaries (9, 14, 64) (Figure 2). Thus, regulation of the balance of MΦs polarization may be a potential therapeutic strategy for reproductively aged women to restore ovarian function and fertility.

Until now, most studies on ovarian MΦs during aging are focused on animals, while human studies are still scarce, probably due to difficulties in obtaining human samples (17, 65). A recent human study has shown that in comparison to premenopausal women (30-50 years old), MΦs number was remarkably higher in ovarian stroma in women at early (55-59 years old) and late menopausal (60-85 years old) stages. These MΦs produce high levels of interleukin 16 (IL-16), a pro-inflammatory and chemotactic cytokine, indicative of an inflammatory role of ovarian MΦs during female aging (66). Therefore, more investigations in human models are still required to elaborate the roles of different MΦs phenotypes during ovarian aging.

Remarkably, recent studies have successfully applied single-cell RNA sequencing (ScRNA-seq) technology to transcriptomic analysis of ovaries, follicles as well as MΦs subpopulations (61, 67). Diverse methods have been further derived from ScRNA-seq, involving massively parallel single-cell RNA sequencing (MARS-seq), CEL-seq, Drop-seq, and Slide-seq (68–71). Additionally, *in vivo* imaging techniques, like intravital two-photon imaging and multichannel spinning-disk confocal intravital microscopy, will allow researchers to track ovarian MΦs subpopulations and investigate their polarization behaviors in real time within aging ovaries (72–74). Hence, these advanced technologies may assist an in-depth understanding of the roles of different MΦs subsets in ovarian senescence.

5 Conclusion and perspectives

Ovarian MΦs play pivotal roles in normal ovarian functions and ovarian aging. During reproductive senescence, danger signals within aged ovaries induce MΦs polarization into different M1/M2 phenotypes. Perturbation of balance of M1/M2 phenotypes in aged ovaries dictates chronic inflammatory milieu concurrent with stromal fibrosis, leading to follicular loss and ovarian dysfunction. To regulate the balance between M1 and M2 subsets might be a promising therapeutic strategy for women with advanced reproductive age. Future studies are still needed to further unravel the roles of MΦs in ovarian aging and develop a new approach to ameliorate ovarian decay.

Author contributions

MT: Writing – original draft. MZ: Writing – review & editing. YS: Supervision, Writing – review & editing.

Funding

The author(s) declare financial support was received for the research, authorship, and/or publication of this article. This work was supported by grants from National Natural Science Foundation of China (82201735), Basic and Applied Basic Research Foundation of Guangdong Province of China (2023A1515010352, 2023A1515010192), Medical Scientific Research Foundation of Guangdong Province of China (A2022376) and Science and Technology Planning Project of Guangzhou city of China (2023A04J0494).

Conflict of interest

The authors declare that the research was conducted in the absence of any commercial or financial relationships that could be construed as a potential conflict of interest.

Publisher's note

References

1. Wu JC, Liu Y, Song YH, Wang LJ, Ai JH, Li KZ. Aging conundrum: a perspective for ovarian aging. *Front Endocrinol (Lausanne)* (2022) 13:952471. doi: 10.3389/fendo.2022.952471

2. Tang M, Popovic M, Stamatiadis P, van der Jeught M, Van Coster R, Deforce D, et al. Germline nuclear transfer in mice may rescue poor embryo development associated with advanced maternal age and early embryo arrest. *Hum Reprod* (2020) 35:1562–77. doi: 10.1093/humrep/deaa112

3. Secomandi L, Borghesan M, Velarde M, Demaria M. The role of cellular senescence in female reproductive aging and the potential for senotherapeutic interventions. *Hum Reprod Update* (2022) 28(2):172–89. doi: 10.1093/humupd/dmab038

4. Sang Q, Ray PF, Wang L. Understanding the genetics of human infertility. *Science* (2023) 380(6641):158–63. doi: 10.1126/science.adf7760

5. American College of Obstetricians and Gynecologists Committee on Gynecologic Practice and Practice Committee. Female age-related fertility decline. Committee Opinion No. 589. *Fertil Steril* (2014) 101(3):633–4. doi: 10.1016/j.fertnstert.2013.12.032

6. Magnus MC, Wilcox AJ, Morken NH, Weinberg CR, Haberg SE. Role of maternal age and pregnancy history in risk of miscarriage: prospective register based study. *BMJ* (2019) 364:l869. doi: 10.1136/bmj.l869

7. Tesarik J, Galan-Lazaro M, Mendoza-Tesarik R. Ovarian aging: molecular mechanisms and medical management. *Int J Mol Sci* (2021) 22(3):1371. doi: 10.3390/ijms22031371

8. Li NY, Li ZQ, Fang F, Zhu CD, Zhang WZ, Lu YS. Two distinct resident macrophage populations coexist in the ovary. *Front Immunol* (2022) 13:1007711. doi: 10.3389/fimmu.2022.1007711

9. Zhang ZJ, Huang L, Brayboy L. Macrophages: an indispensable piece of ovarian health. *Biol Reprod* (2021) 104(3):527–38. doi: 10.1093/biolre/ioaa219

10. Carlock C, Wu J, Zhou C, Ross A, Adams H, Lou YH. Ovarian phagocyte subsets and their distinct tissue distribution patterns. *Reproduction* (2013) 146(5):491–500. doi: 10.1530/REP-13-0134

11. Kadomoto S, Izumi K, Mizokami A. Macrophage polarity and disease control. *Int J Mol Sci* (2021) 23(1):144. doi: 10.3390/ijms23010144

12. Rehman A, Pacher P, Hasko G. Role of macrophages in the endocrine system. *Trends Endocrinol Metab* (2021) 32(4):238–56. doi: 10.1016/j.tem.2020.12.001

13. Wu RJ, van der Hoek KH, Ryan NK, Norman RJ, Robker RL. Macrophage contributions to ovarian function. *Hum Reprod Update* (2004) 10(2):119–33. doi: 10.1093/humupd/dmh011

14. Zhang ZJ, Schlamp F, Huang L, Clark H, Brayboy L. Inflammaging is associated with shifted macrophage ontogeny and polarization in the aging mouse ovary. *Reproduction* (2020) 159(3):325–37. doi: 10.1530/REP-19-0330

15. Foley KG, Pritchard MT, Duncan FE. Macrophage-derived multinucleated giant cells: hallmarks of the aging ovary. *Reproduction* (2021) 161(2):V5–9. doi: 10.1530/REP-20-0489

16. Briley SM, Jasti S, McCracken JM, Hornick JE, Fegley B, Pritchard MT. Reproductive age-associated fibrosis in the stroma of the mammalian ovary. *Reproduction* (2016) 152(3):245–60. doi: 10.1530/REP-16-0129

17. Zavatta A, Parisi F, Mando C, Scaccabarozzi C, Savasi VM, Cetin I. Role of inflammaging on the reproductive function and pregnancy. *Clin Rev Allergy Immunol* (2023) 64(2):145–60. doi: 10.1007/s12016-021-08907-9

18. Cui CY, Ferrucci LG, Gorospe M. Macrophage involvement in aging-associated skeletal muscle regeneration. *Cells 12* (2023) 12(9):1214. doi: 10.3390/cells12091214

19. Orecchioni M, Ghosheh Y, Pramod AB, Ley K. Macrophage Polarization: Different Gene Signatures in M1(LPS+) vs. Classically and M2(LPS-) vs. Alternatively Activated Macrophages. *Front Immunol* (2019) 10:1084. doi: 10.3389/fimmu.2019.01084

20. Murray PJ. Macrophage polarization. *Annu Rev Physiol* (2017) 79:541–66. doi: 10.1146/annurev-physiol-022516-034339

21. Shapouri-Moghaddam A, Mohammadian S, Vazini H, Taghadosi M, Esmaeili SA, Mardani F. Macrophage plasticity, polarization, and function in health and disease. *J Cell Physiol* (2018) 233(9):6425–40. doi: 10.1002/jcp.26429

22. Laskin DL, Sunil VR, Gardner CR, Laskin JD. Macrophages and tissue injury: agents of defense or destruction? *Annu Rev Pharmacol Toxicol* (2011) 51:267–88. doi: 10.1146/annurev.pharmtox.010909.105812

23. Watanabe S, Alexander M, Misharin AV, Budinger GRS. The role of macrophages in the resolution of inflammation. *J Clin Invest* (2019) 129(7):2619–28. doi: 10.1172/JCI124615

24. Liu YC, Zou XB, Chai YF, Yao YM. Macrophage polarization in inflammatory diseases. *Int J Biol Sci* (2014) 10(5):520–9. doi: 10.7150/ijbs.8879

25. Yao Y, Xu XH, Jin L. Macrophage polarization in physiological and pathological pregnancy. *Front Immunol* (2019) 10:792. doi: 10.3389/fimmu.2019.00792

26. Wang LX, Zhang SX, Wu HJ, Rong XL, Guo J. M2b macrophage polarization and its roles in diseases. *J Leukoc Biol* (2019) 106(2):345–58. doi: 10.1002/JLB.3RU1018-378RR

27. Zizzo G, Hilliard BA, Monestier M, Cohen PL. Efficient clearance of early apoptotic cells by human macrophages requires M2c polarization and MerTK induction. *J Immunol* (2012) 189(7):3508–20. doi: 10.4049/jimmunol.1200662

28. Wu KY, Lin KJ, Li XY, Yuan XL, Xu PQ, Ni PH. Redefining tumor-associated macrophage subpopulations and functions in the tumor microenvironment. *Front Immunol* (2020) 11:1731. doi: 10.3389/fimmu.2020.01731

29. Jokela H, Lokka E, Kiviranta M, Tyystjarvi S, Gerke H, Elima K. Fetal-derived macrophages persist and sequentially maturate in ovaries after birth in mice. *Eur J Immunol* (2020) 50(10):1500–14. doi: 10.1002/eji.202048531

30. Pepe G, Locati M, Della Torre S, Mornata F, Cignarella A, Maggi A. The estrogen-macrophage interplay in the homeostasis of the female reproductive tract. *Hum Reprod Update* (2018) 24(6):652–72. doi: 10.1093/humupd/dmy026

31. Ono Y, Nagai M, Yoshino O, Koga K, Nawaz A, Hatta H. CD11c+ M1-like macrophages (MPhis) but not CD206+ M2-like MPhi are involved in folliculogenesis in mice ovary. *Sci Rep* (2018) 8(1):8171. doi: 10.1038/s41598-018-25837-3

32. Care AS, Diener KR, Jasper MJ, Brown HM, Ingman WV, Robertson SA. Macrophages regulate corpus luteum development during embryo implantation in mice. *J Clin Invest* (2013) 123(8):3472–87. doi: 10.1172/JCI60561

33. Skarzynski DJ, Jaroszewski JJ, Okuda K. Role of tumor necrosis factor-alpha and nitric oxide in luteolysis in cattle. *Domest Anim Endocrinol* (2005) 29(2):340–6. doi: 10.1016/j.domaniend.2005.02.005

34. Xiao Y, Peng XX, Peng Y, Zhang C, Liu W, Yang WJ. Macrophage-derived extracellular vesicles regulate follicular activation and improve ovarian function in old mice by modulating local environment. *Clin Transl Med* (2022) 12(10):e1071. doi: 10.1002/ctm2.1071

35. Ingman WV, Robker RL, Woittiez K, Robertson SA. Null mutation in transforming growth factor beta1 disrupts ovarian function and causes oocyte incompetence and early embryo arrest. *Endocrinology* (2006) 147(2):835–45. doi: 10.1210/en.2005-1189

36. Umehara T, Winstanley YE, Andreas E, Morimoto A, Williams EJ, Smith KM. Female reproductive life span is extended by targeted removal of fibrotic collagen from the mouse ovary. *Sci Adv* (2022) 8(24):eabn4564. doi: 10.1126/sciadv.abn4564

37. Tamanini C, De Ambrogi M. Angiogenesis in developing follicle and corpus luteum. *Reprod Domest Anim* (2004) 39(4):206–16. doi: 10.1111/j.1439-0531.2004.00505.x

38. Fraser HM. Regulation of the ovarian follicular vasculature. *Reprod Biol Endocrinol* (2006) 4:18. doi: 10.1186/1477-7827-4-18

39. Camaioni A, Ucci MA, Campagnolo L, De Felici M, Klinger FG. Italian Society of Embryology, Reproduction and Research (SIERR). The process of ovarian aging: it is not just about oocytes and granulosa cells. *J Assist Reprod Genet* (2022) 39(4):783–92. doi: 10.1007/s10815-022-02478-0

40. Zhou J, Peng X, Mei S. Autophagy in ovarian follicular development and atresia. *Int J Biol Sci* (2019) 15(4):726–37. doi: 10.7150/ijbs.30369

41. Irving-Rodgers HF, van Wezel IL, Mussard ML, Kinder JE, Rodgers RJ. Atresia revisited: two basic patterns of atresia of bovine antral follicles. *Reproduction* (2001) 122(5):761–75. doi: 10.1530/rep.0.1220761

42. Carlock CI, Wu J, Zhou C, Tatum K, Adams HP, Tan F. Unique temporal and spatial expression patterns of IL-33 in ovaries during ovulation and estrous cycle are associated with ovarian tissue homeostasis. *J Immunol* (2014) 193(1):161–9. doi: 10.4049/jimmunol.1400381

43. Wu J, Carlock C, Zhou C, Nakae S, Hicks J, Adams HP. IL-33 is required for disposal of unnecessary cells during ovarian atresia through regulation of autophagy and macrophage migration. *J Immunol* (2015) 194(5):2140–7. doi: 10.4049/jimmunol.1402503

44. Cui LL, Yang GW, Pan J, Zhang C. Tumor necrosis factor alpha knockout increases fertility of mice. *Theriogenology* (2011) 75(5):867–76. doi: 10.1016/j.theriogenology.2010.10.029

45. Duffy DM, Ko C, Jo M, Brannstrom M, Curry TE. Ovulation: parallels with inflammatory processes. *Endocr Rev* (2019) 40(2):369–416. doi: 10.1210/er.2018-00075

46. Cohen PE, Zhu L, Pollard JW. Absence of colony stimulating factor-1 in osteopetrotic (csfmop/csfmop) mice disrupts estrous cycles and ovulation. *Biol Reprod* (1997) 56(1):110–8. doi: 10.1095/biolreprod56.1.110

47. Al-Alem L, Puttabyatappa M, Rosewell K, Brannstrom M, Akin J, Boldt J. Chemokine ligand 20: A signal for leukocyte recruitment during human ovulation? *Endocrinology* (2015) 156(9):3358–69. doi: 10.1210/en.2014-1874

48. Devoto L, Fuentes A, Kohen P, Cespedes P, Palomino A, Pommer R, et al. The human corpus luteum: life cycle and function in natural cycles. *Fertil Steril* (2009) 92(3):1067–79. doi: 10.1016/j.fertnstert.2008.07.1745

49. Townson DH, O'Connor CL, Pru JK. Expression of monocyte chemoattractant protein-1 and distribution of immune cell populations in the bovine corpus luteum throughout the estrous cycle. *Biol Reprod* (2002) 66(2):361–6. doi: 10.1095/biolreprod66.2.361

50. Nio-Kobayashi J, Kudo M, Sakuragi N, Kimura S, Iwanaga T, Duncan WC. Regulated C-C motif ligand 2 (CCL2) in luteal cells contributes to macrophage infiltration into the human corpus luteum during luteolysis. *Mol Hum Reprod* (2015) 21(8):645–54. doi: 10.1093/molehr/gav028

51. Turner EC, Hughes J, Wilson H, Clay M, Mylonas KJ, Kipari T. Conditional ablation of macrophages disrupts ovarian vasculature. *Reproduction* (2011) 141(6):821–31. doi: 10.1530/REP-10-0327

52. Rea IM, Gibson DS, McGilligan V, McNerlan SE, Alexander HD, Ross OA. Age and age-related diseases: role of inflammation triggers and cytokines. *Front Immunol* (2018) 9:586. doi: 10.3389/fimmu.2018.00586

53. Lliberos C, Liew SH, Zareie P, La Gruta NL, Mansell A, Hutt K. Evaluation of inflammation and follicle depletion during ovarian ageing in mice. *Sci Rep* (2021) 11(1):278. doi: 10.1038/s41598-020-79488-4

54. Lliberos C, Liew SH, Mansell A, Hutt KJ. The inflammasome contributes to depletion of the ovarian reserve during aging in mice. *Front Cell Dev Biol* (2020) 8:628473. doi: 10.3389/fcell.2020.628473

55. Rowley JE, Amargant F, Zhou LT, Galligos A, Simon LE, Pritchard MT. Low molecular weight hyaluronan induces an inflammatory response in ovarian stromal cells and impairs gamete development. *In Vitro. Int J Mol Sci* (2020) 21(3):1036. doi: 10.3390/ijms21031036

56. Urzua U, Chacon C, Espinoza R, Martinez S, Hernandez N. Parity-dependent hemosiderin and lipofuscin accumulation in the reproductively aged mouse ovary. *Anal Cell Pathol (Amst)* (2018) 2018:1289103. doi: 10.1155/2018/1289103

57. Kinnear HM, Tomaszewski CE, Chang FL, Moravek MB, Xu M, Padmanabhan V. The ovarian stroma as a new frontier. *Reproduction* (2020) 160(3):R25–39. doi: 10.1530/REP-19-0501

58. Hummitzsch K, Hatzirodos N, Macpherson AM, Schwartz J, Rodgers RJ, Irving-Rodgers HF. Transcriptome analyses of ovarian stroma: tunica albuginea, interstitium and theca interna. *Reproduction* (2019) 157(6):545–65. doi: 10.1530/REP-18-0323

59. Cui L, Bao H, Liu Z, Man X, Liu H, Hou Y, et al. hUMSCs regulate the differentiation of ovarian stromal cells via TGF-beta(1)/Smad3 signaling pathway to inhibit ovarian fibrosis to repair ovarian function in POI rats. *Stem Cell Res Ther* (2020) 11(1):386. doi: 10.1186/s13287-020-01904-3

60. Amargant F, Manuel SL, Tu Q, Parkes WS, Rivas F, Zhou LT. Ovarian stiffness increases with age in the mammalian ovary and depends on collagen and hyaluronan matrices. *Aging Cell* (2020) 19(11):e13259. doi: 10.1111/acel.13259

61. Wang S, Zheng YX, Li JY, Yu Y, Zhang WQ, Song MS. Single-cell transcriptomic atlas of primate ovarian aging. *Cell* (2020) 180(3):585–600 e19. doi: 10.1016/j.cell.2020.01.009

62. Zheng K, Hong WL, Ye HF, Zhou ZQ, Ling SY, Li Y. Chito-oligosaccharides and macrophages have synergistic effects on improving ovarian stem cells function by regulating inflammatory factors. *J Ovarian Res* (2023) 16(1):76. doi: 10.1186/s13048-023-01143-z

63. Wu M, Huang Y, Zhu Q, Zhu X, Xue L, Xiong J, et al. Adipose tissue and ovarian aging: Potential mechanism and protective strategies. *Ageing Res Rev* (2022) 80:101683. doi: 10.1016/j.arr.2022.101683

64. Vasse GF, Nizamoglu M, Heijink IH, Schleputz M, van Rijn P, Thomas MJ. Macrophage-stroma interactions in fibrosis: biochemical, biophysical, and cellular perspectives. *J Pathol* (2021) 254(4):344–57. doi: 10.1002/path.5632

65. Huang YQ, Hu C, Ye HF, Luo RC, Fu XX, Li XY. Inflamm-aging: A new mechanism affecting premature ovarian insufficiency. *J Immunol Res* (2019) 2019:8069898. doi: 10.1155/2019/8069898

66. Ramirez J, Bitterman P, Basu S, Barua A. Changes in IL-16 expression in the ovary during aging and its potential consequences to ovarian pathology. *J Immunol Res* (2022) 2022:2870389. doi: 10.1155/2022/2870389

67. Fan X, Bialecka M, Moustakas I, Lam E, Torrens-Juaneda V, Borggreven NV. Single-cell reconstruction of follicular remodeling in the human adult ovary. *Nat Commun* (2019) 10(1):3164. doi: 10.1038/s41467-019-11036-9

68. Macosko EZ, Basu A, Satija R, Nemesh J, Shekhar K, Goldman M. Highly parallel genome-wide expression profiling of individual cells using nanoliter droplets. *Cell* (2015) 161(5):1202–14. doi: 10.1016/j.cell.2015.05.002

69. Hashimshony T, Senderovich N, Avital G, Klochendler A, de Leeuw Y, Anavy L. CEL-Seq2: sensitive highly-multiplexed single-cell RNA-Seq. *Genome Biol* (2016) 17:77. doi: 10.1186/s13059-016-0938-8

70. Rodriques SG, Stickels RR, Goeva A, Martin CA, Murray E, Vanderburg CR. Slide-seq: A scalable technology for measuring genome-wide expression at high spatial resolution. *Science* (2019) 363(6434):1463–67. doi: 10.1126/science.aaw1219

71. Keren-Shaul H, Kenigsberg E, Jaitin DA, David E, Paul F, Tanay A. MARS-seq2.0: an experimental and analytical pipeline for indexed sorting combined with single-cell RNA sequencing. *Nat Protoc* (2019) 14(6):1841–62. doi: 10.1038/s41596-019-0164-4

72. Li Y, Liu TM. Discovering macrophage functions using *in vivo* optical imaging techniques. *Front Immunol* (2018) 9:502. doi: 10.3389/fimmu.2018.00502

73. Zhang N, Czepielewski RS, Jarjour NN, Erlich EC, Esaulova E, Saunders BT. Expression of factor V by resident macrophages boosts host defense in the peritoneal cavity. *J Exp Med* (2019) 216(6):1291–300. doi: 10.1084/jem.20182024

74. Neupane AS, Willson M, Chojnacki AK, Vargas ESCF, Morehouse C, Carestia A. Patrolling alveolar macrophages conceal bacteria from the immune system to maintain homeostasis. *Cell* (2020) 183(1):110–25 e11. doi: 10.1016/j.cell.2020.08.020

frontiers | Frontiers in Medicine

TYPE Case Report
PUBLISHED 07 December 2023
DOI 10.3389/fmed.2023.1274303

OPEN ACCESS

EDITED BY
Bin Liu,
Baoan Women's and Children's Hospital, China

REVIEWED BY
Ariel Berlinski,
University of Arkansas for Medical Sciences, United States
Janelle Noel-MacDonnell,
Children's Mercy Kansas City, United States

*CORRESPONDENCE
Pietro Ripani
✉ pietro.ripani@aslteramo.it
Antonio Recchiuti
✉ antonio.recchiuti@unich.it

†These authors share first authorship

RECEIVED 08 August 2023
ACCEPTED 07 November 2023
PUBLISHED 07 December 2023

CITATION
Ripani P, Mucci M, Pantano S, Di Sabatino M, Collini F, Ferri G, Romano M and Recchiuti A (2023) Maternal, newborn and breast milk concentrations of elexacaftor/tezacaftor/ivacaftor in a F508del heterozygous woman with cystic fibrosis following successful pregnancy.
Front. Med. 10:1274303.
doi: 10.3389/fmed.2023.1274303

Maternal, newborn and breast milk concentrations of elexacaftor/tezacaftor/ivacaftor in a F508del heterozygous woman with cystic fibrosis following successful pregnancy

Pietro Ripani[1*†], Matteo Mucci[2†], Stefano Pantano[1], Maria Di Sabatino[1], Francesca Collini[1], Giulia Ferri[2], Mario Romano[2] and Antonio Recchiuti[2*]

[1]Unità Operativa Semplice a valenza Dipartimentale Centro Regionale di Riferimento per la Fibrosi Cistica, Teramo, Italy, [2]Department of Medical, Oral, and Biotechnology Science (DSMOB), Center of Advanced Studies and Technology, Università "G. d'Annunzio", Chieti, Italy

With the introduction of elexacaftor/tezacaftor/ivacaftor (ETI), more women with cystic fibrosis (CF) are likely to grow families. Hence, an understanding long-term safety and effects of CFTR modulators on fertile women and children while monitoring their concentrations is crucial. Here, we report on the development of an improved LC–MS/MS methodology to measure ETI concentrations in maternal and child blood and breastmilk, applied in one case of successful pregnancy of a 30-year-old woman with CF (F508del/R334W). We observed that ETI remains stable in breastmilk, is absorbed by the infant and can be detected in child plasma. Our results confirm accumulating evidence of a successful pregnancy in women treated with CFTR modulators without significant side effects on the child and provide valuable analytical procedures suitable for the post-marketing evaluation of CFTR modulators in pregnant and lactating women, as well as in their infants.

KEYWORDS

novel therapies, pregnancy, drug monitoring, F508del CFTR, CFTR modulator therapy, R334W CFTR, mass spectrometry

1 Introduction

Highly effective CFTR modulator therapies, such as the triple combination of elexacaftor/tezacaftor/ivacaftor (ETI), have brought about a transformative treatment for people with cystic fibrosis (CF), significantly improving the quality and length of their lives (1, 2). Consequently, an increasing number of women living with CF are expressing the desire for pregnancy and the number of pregnancies among adults with CF is increasing. ETI and other modulators may enhance female fertility by improving physical and psychological status as well as by normalizing the cervical micro-environment (3). Although teratogenicity has not been observed in animals treated with ETI at doses routinely administered to humans (4) and accruing clinical data show no alarming signals (3), there are though concerns on the effects of chronic exposure of a fetus or an infant who may not have CF to ETI. Given the absence of clear data or guidelines, the decision to discontinue ETI during pregnancy and lactation (increasing the risk of maternal

health decline) or to continue it (with uncertain fetal/newborn outcomes) remains a dilemma for both women and caregivers.

Here, we report on the development of a pioneering method for measuring the concentration of these compounds in maternal and newborn biological fluids, which we tested in one case of pregnancy of a patient with CF treated with ETI.

2 Results

2.1 Case

The proband was diagnosed at 18 years of age with CF-causing mutations (F508del/R334W), pancreatic sufficiency, and 115 mmol/L sweat Cl-concentration. Besides chronic lung colonization by *Staphylococcus aureus*, she had atopy and cholestasis requiring treatment with ursodeoxycholic acid (450 mg/die). She was treated at the Abruzzo regional CF center in Atri, Teramo (TE), Italy.

At the age of 31, she was prescribed ETI (Elexacaftor 100 mg/die, Tezacaftor, 50 mg/die, Ivacaftor 75 mg/die) in combination with Ivacaftor (150 mg/die) as standard of care (Kaftrio + Kalydeco, Vertex Pharmaceuticals) in association with flunisolide (Fluspiral) 125 μg 1 puff × 2/day and salbutamol 3 puff × 2/day. Anthropometric characteristics of the patient were as follows: weight = 60 kg; height = 163 cm; BMI = 22 kg/m^2. Prior to ETI + Iva therapy, the sweat Cl-was 82 mmol/L and the respiratory function was moderately reduced, with a forced expiratory volume percent of predicted (FEV1pp) of 61–66, and multiple diffuse chest bronchiectasis and bronchiolectasis were deduced. She had an average of two episodes of hemoptysis/year and five infection reacutizations/year. Ultrasound scan revealed liver within normal limits with mild echogenicity. The mean total score in the Cystic Fibrosis Questionnaire Revised (CFQ-R) was 66. The six-minute walking test (6MWT) was 500 m (normal range 400–700 m).

The proband initiated ETI + Iva therapy in December 2021 had no relevant adverse side effects, with normal blood tests and negative eye exams (carried out to exclude cataract, which is reported as a side effect of ETI + Iva). Normal blood tests included the following evaluations: total blood cell count, glycemia, liver function tests (albumin, total protein, alkaline phosphatase, alanine transaminase, aspartate aminotransferase, gamma-glutamyl transferase, bilirubin, lactate dehydrogenase), prothrombin time, and pancreatic enzymes.

One month post ETI + Iva, sweat Cl-was 89 mEq/L and FEV1pp raised up to 83. Vital parameters were normal. Body weight was 62 kg, height 163 cm, BMI 23.3, CFQ-R 87, 6MWT 600 m, blood pressure (BP) 116/64 mmHg.

The proband reported had unprotected sexual intercourse with her partner for 9 years without conceiving. However, in March 2022, 3 months after the initiation of ETI + Iva therapy, she announced her pregnancy. Body weight was 64 kg, BMI 24, CFQ-R 83, 6MWT 575 m. FEV1pp was 85. Vital parameters were normal (sO_2 100%, respiratory rate 88 bpm/r, BP 112/64 mmHg). Urinary pregnancy exams tested positive (serum beta hCG 14,042 mIU/mL). Gynecological examination confirmed the pregnancy, the correct embryo implant, and the presence of the gestational sac. A fibromatous uterus was reported.

Since safety data on ETI + Iva during human pregnancy were limited to few case reports (5, 6) with only a single large study on 45 pregnant American women (7) and the general recommendation was still to avoid the administration of ETI during pregnancy, we discontinued the therapy with ETI + Iva, with disclosed gravidity in accordance with the proband, and continued the general clinical evaluation regarding the patient's respiratory and infectious state. However, her symptoms started to deteriorate as early as 1 week after discontinuation: pulmonary function declined (FEV1pp 64), cough increased, and she had a reactivation of pulmonary infection at 1 month post discontinuation (treated with cefuroxime 500 mg/every 8 h for 14 days, os). This worsening of symptoms prompted us to reinitiate therapy with ETI + Ivacaftor in May 2022 (12 weeks of gestation). CFQ-R was 74, BP 103/56 mmHg. The patient tested positive for SARS-COV-2 virus prior to the re-initiation of therapy with CFTR modulators, with generic symptoms, fever, and cough. No specific therapies were given. Echograpic exams showed a normal fetus. In July 2022, FEV1pp had raised up to 86, BP was 100/60 mmHg, and weight 63.7 kg. In January 2023, sweat Cl-was 77 mmol/L.

Pregnancy was regular. From May to July 2022, the proband underwent morphometric echography who did not show any fetal abnormality. Amniotic fluid, auxological parameters, and growth percentiles were normal. No gynecological concerns existed. The oral glucose tolerance test was negative, and the fetal growth followed the normal path. A mild hydronephrosis was suspected upon close prenatal fetal sonoanatomy (resolved at birth).

The proband completed the pregnancy regularly at week 37 + 6 by a Cesarean section. She gave birth to a healthy boy of 3.625 kg (50th percentile), 50 cm of body length (75th percentile), and 37 cm of cranial circumference (>97th percentile). Patent foramen ovale was observed for the newborn at birth. APGAR score was 9–10, and sO_2 was 100%. The newborn underwent total cell count, alanine transaminase, aspartate aminotransferase, and hemogas blood test in addition to eye exam, otoemission exam, clinical exam, and renal ecograph (all negative). Sweet Cl-was 11 mEq/L and genetic screening revealed that the newborn was carrier of one F508del Cftr allele. The mother continued to breastfeed her child while continuing ETI + Iva therapy, and no significant side effects related to ETI + Iva have been observed in the child thus far.

2.2 ETI measurements

In order to assess the presence of ETI in both maternal and fetal biological fluids and mother–child passage, given the limited number of reported analytical methods (8), we developed a new rapid, sensitive, and robust quantification methodology using LC/MS–MS.

Fasting EDTA-plasma and breast milk were collected at 8 a.m., 12 h after the last Iva dose (in the evening) and before the morning administration of ETI + Iva.

The baby was 3 months old and was not breastfed 2 h prior to milk and blood collection. The mother was breastfeeding exclusively.

Samples (100 μL) were mixed with four volumes of methanol containing an internal standard (IS), consisting of 10 pg/μL (final concentration) VX 770 d-19 (Cayman Chemical Company), and precipitated by centrifugation (14,000 × g 10 min at 4°C). Ten μL of supernatants were injected into a Ultivo LC–MS–MS system (Agilent Technologies, United States) equipped with LC-1260 Infinity II HPLC (Agilent Technologies, United States). An Agilent Eclipse Plus C18 (50 × 2.1 mm, 1.8 μm) was used with a gradient of water/formic acid/acetonitrile from 55:0.1:45 to 65:0.1:35 vol/vol at 0.3 mL/min flow rate for 8 min of run. The chromatographic separation and MS/MS spectra of each compound are illustrated in Figure 1.

10.3389/fmed.2023.1274303

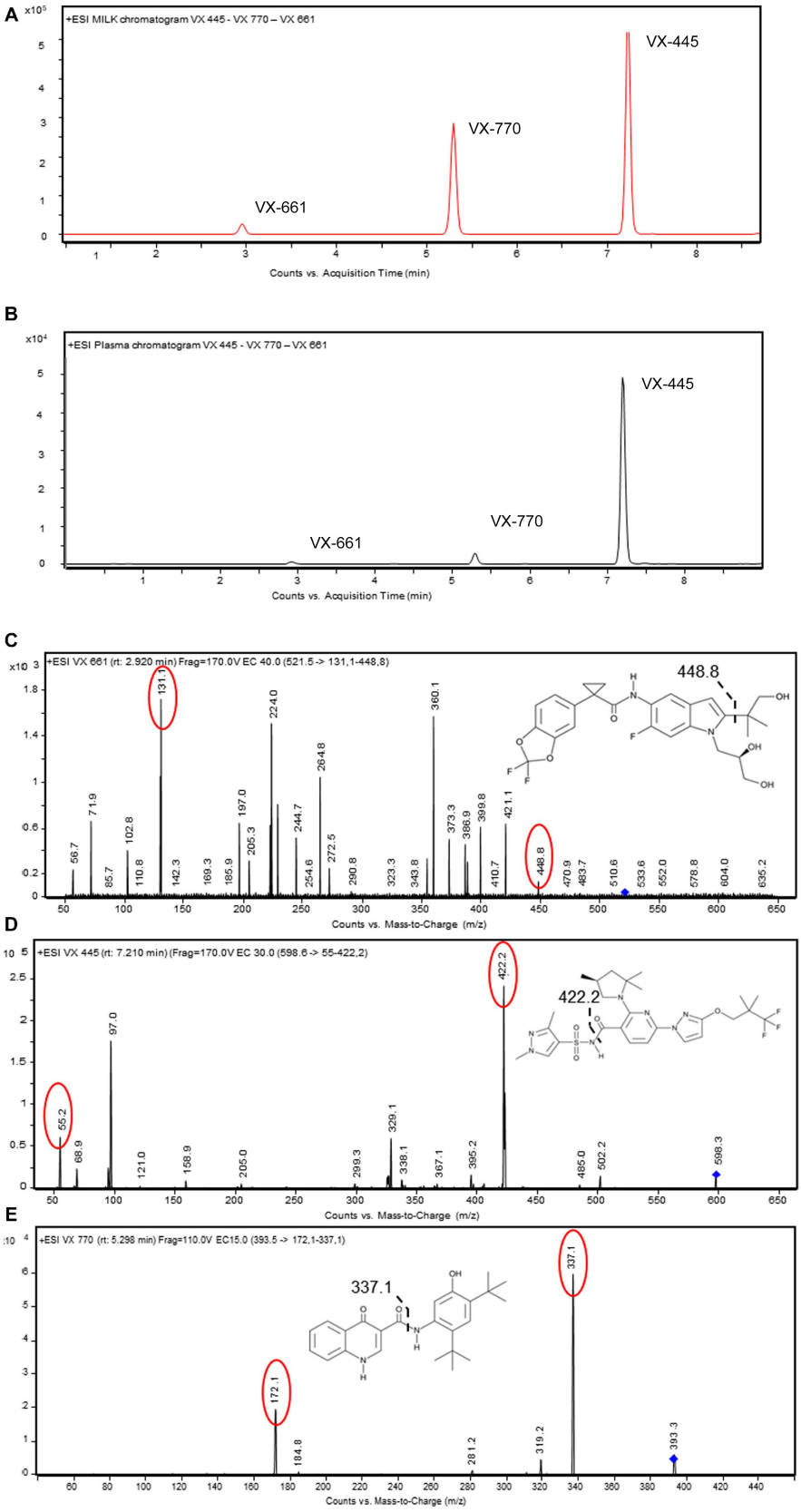

FIGURE 1
LC–MS/MS method development for measuring ETI in biological samples. **(A,B)** HPLC chromatograms of VX-445, VX-661, and VX-770 spiked (0.05ng/μL) in pooled blank human plasma or breastmilk. Proteins were removed by precipitation and samples injected (10μL) into the C18-HPLC system. **(C–E)** Full product ion scan plots of VX-455, VX-661, and VX-770 obtained with MS/MS. Main transitions for each target molecules are in red. Bond cleavage sites are represented by dashed lines. Data are representative from *n*=20 LC–MS/MS separate injections.

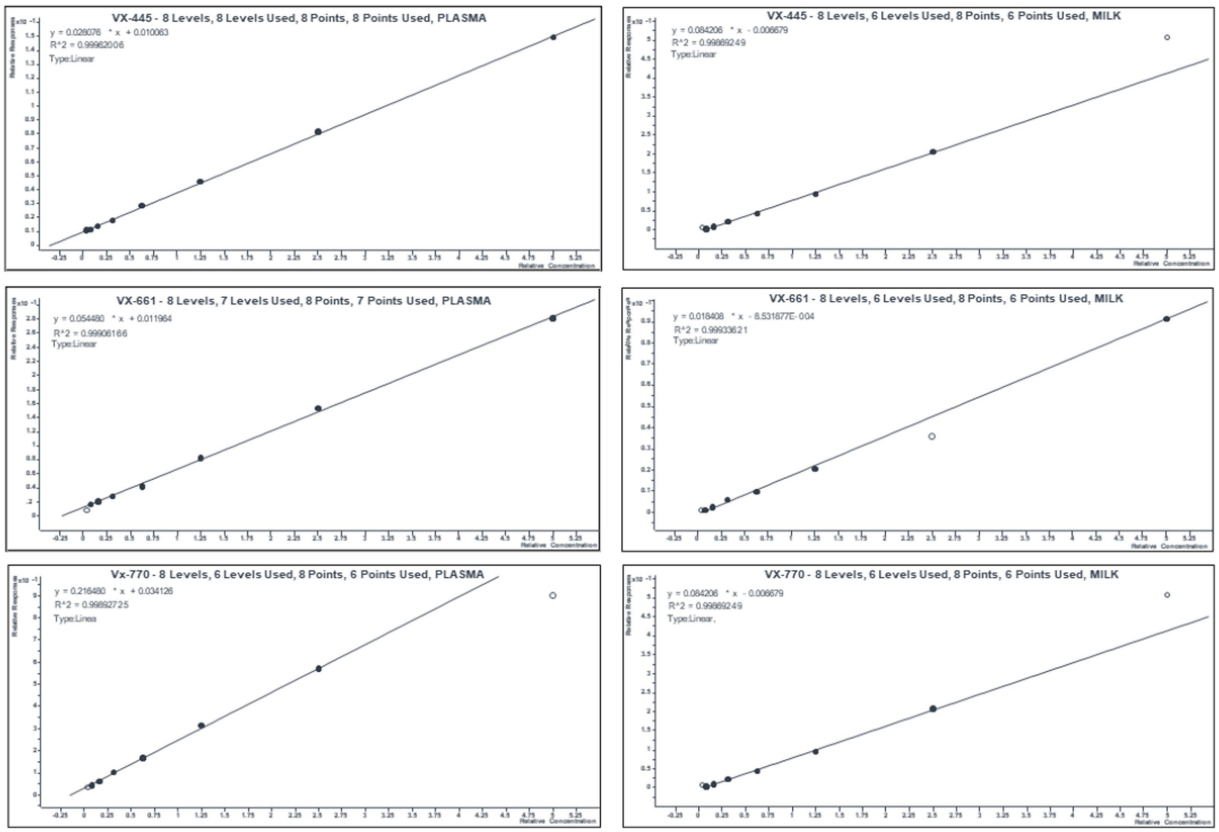

FIGURE 2
Mean calibration curves of ETI in human plasma and breast milk. Eight-point calibration curves were obtained for each an-analyte with a pool of blank plasma and/ milk spiked with 0.39–50 pg./μL of working solutions of VX-445, VX-661, and VX-770. Relative responses were calculated as ratio between area of the standard (n = 5 replicate/concentration) over that of IS.

TABLE 1 Analytical performance parameters of the ETI quantification methods.

Name	RT (min)	Transition	Avg. Conc. (ng/mL)	Std. Dev. (ng/mL)	Avg. Conc./SD	MDL (ng/mL)	LOQ (ng/mL)	LOD (ng/mL)	S/N (ng/mL)
Plasma									
VX-445	7.279	598.6 → 55.0	5.5450	0.2266	24.67	0.7624	0.6797	2.0345	100.67
VX-661	3.058	521.5 → 449.1	5.2789	0.4159	12.69	1.3995	1.2477	2.6182	∞
VX-770	5.351	393.5 → 172.1	5.6461	0.3112	18.14	1.0471	0.9336	2.5899	∞
Breastmilk									
VX-445	7.279	598.6 → 55.0	5.6948	0.1331	42.78	0.4479	1.3311	0.3993	354.03
VX-661	3.058	521.5 → 449.1	5.6850	0.1512	37.59	0.5089	1.5125	0.4537	147.46
VX-770	5.351	393.5 → 172.1	5.3919	0.0648	83.19	0.1944	0.6481	0.1944	402.51

Average concentration, SD, method detection limit (MDL), limit of quantification (LOQ), limit of detection (LOD), and signal-to-noise (SN) were determined in human plasma and breastmilk from 3 separate determinations. MDL, LOQ, and LOD were calculated using 6 replicates of the 0.0625 ng/μL standard.

Standard curves and quality controls were obtained by spiking a pool of blank plasma and/o milk and with analytes from different batches of working solutions of VX-770, VX-661, and VX-445 (from Cayman Chemical Company). The 8-point calibration curve, ranging from 0.39 to 50 pg/μL, which included limit of quantitation, limit of detection, and method detection limit, are shown in Figure 2 and Table 1. Concentrations of VX 661, VX 770, VX 445 in mother's plasma, breast milk, and child's plasma are reported in Table 2.

3 Discussion

Here, we report a case of a woman with CF who delivered a healthy, term infant while remaining on ETI therapy for most of her pregnancy. We quantified ETI in breast milk and in the child plasma.

Expression of CFTR in female reproductive organs has been established ~30 years ago by Tizzano and colleagues (9). Although the reproductive anatomy of women with CF is generally similar to that

TABLE 2 Concentrations of VX-661, VX-770, and VX-445 measured in plasma and breastmilk (mean ± SD from $n = 3$ separate determinations).

Drug (ng/mL)	VX-661	VX-445	VX-770
Maternal plasma	1017.57 ± 80.02	1185.2 ± 114.01	1071.5 ± 80.12
Breast milk	761.3 ± 22.62	1049.07 ± 68.77	1794.50 ± 4.95
Child plasma	13.91 ± 2.25	4.66 ± 1.15	23.93 ± 2.95

of women without CF, abnormal CFTR function can lead to increased mucus viscosity, pH imbalances, dysbiosis, and chronic inflammation that can reduce fertility. Suboptimal nutrition status and overall health conditions may also decrease the chances of becoming pregnant for some women with CF (10). With the advent of CFTR modulators, fertility of women with CF is expected to increase. Consistent with this, few cases of pregnancies shortly after the initiation of CFTR modulator therapy have been reported, and in phase 3 clinical trials with ivacaftor, ~2% of the participating women disclosed pregnancy during the study. ETI was approved by the Italian Medicine Agency (AIFA), the government's regulatory authority, for patients with CF older than 12 years with two or a single F508del allele in July 2021 (AIFA DG. 784 and 786 07/1/2021). Hence, our case represents one of the earliest reporting a successful pregnancy in women with CF upon therapy with ETI in Italy. Given that 90% of women with CF eligible for CFTR modulators are in their childbearing age (11, 12), our results demonstrate further the timeliness of properly designed clinical studies aimed at ascertaining the basic effects of CFTR modulators on fertility, which is likely to be a growing desire for people with CF.

Our results show that ETI can pass and remain chemically stable in breast milk for a long time after intake and into infant plasma in high ng/mL ranges, confirming preclinical studies and other reports on Ivacaftor, Ivacaftor/Lumacaftor, and Tezacaftor/Ivacaftor (8), or ETI (5). Even if accruing evidence from sparse case reports and preclinical toxicity studies are reassuring on the safety of CFTR modulators, there have been cases of congenital cataracts in babies exposed to ETI *in utero* and during breast feeding (12). In keeping with other case reports from real-life experience, our results indicate that growth, eye, and blood tests were normal in the child exposed to ETI + Iva *in utero* and after birth.

The fact that CFTR modulators can pass into breast milk and be absorbed by infants can be advantageous for treating children with CF, similarly to the case in which ETI + Iva was used to intentionally treat CF-associated meconium ileus (13). Considering the concentrations measured in breast milk and the average daily intake of milk [~720 mL/day at 1 month, ~750 mL/day at 3 months, ~850 mL/day at 6 months (14)] by healthy babies, the following milk-delivered doses can be estimated: VX-661 ~ 800 μg/day, VX-445 ~ 1,000 μg/day, VX-770 ~ 700 μg/day in the first month of age; VX-661 ~ 830 μg/day, VX-4451100 μg/day, VX-770 ~ 740 μg/day at 3 months; VX-661 ~ 940 μg/day, VX-4451270 μg/day, VX-770 ~ 830 μg/day at 6 months. These data deserve clinical consideration. On the contrary, further medical aspects should be considered in the case of heterozygous children, for whom the risks of long-term side effects of CFTR modulators may outweigh the benefits associated with improved CFTR function. These aspects impose an accurate clinical monitoring of the baby's health over the breastfeeding period. The different concentrations of VX-661 between maternal plasma and breast milk could be explained by physiologic changes in pregnancy that may alter the pharmacokinetics of this molecule. Additionally, increases in maternal body fat during pregnancy can change VX-661 distribution between plasma and breast milk. Moreover, VX-661 may undergo a more rapid metabolism compared to other compounds. Furthermore, the different ratio or percentage between child plasma and breastmilk concentrations for the three molecules could depend upon solubility and pharmacokinetics aspects.

Further studies on ETI pharmacokinetics in pregnancy will be useful to clarify these points.

The methodology, developed and employed here, represents a step forward over previous published methods (15, 16) since it allows quantification of ETI from a small amount of biological fluids, thus minimizing the impact of withdrawal procedures. It also has a linear dynamic range of pg./mL [1,000 times lower than the one reported in (16)], which enables a more precise and sensitive ETI monitoring. A detailed description of the methodology will be published separately. Thus, the present procedure can be useful for post-marketing evaluation of CFTR modulators in patients with CF, including pregnant/lactating women and their babies. At the time this report was released, the Maternal and Fetal Outcomes in the Era of Modulators (MAYFLOWER) study sponsored by the CF Foundation and CF Therapeutics Development Network is ongoing (17).

Our work has some limitations: it reports a single case and lacks a study of ETI kinetics following administration.

In conclusion, here we present one of the few cases registered in Italy of successful delivery upon therapy with ETI without adverse pregnancy outcomes and post birth abnormalities, thus contributing to the continuous data on the use of ETI in pregnant and breast-feeding women, which adds a crucial wealth of knowledge in the absence of large clinical studies. We also present the development and use of a LC–MS/MS method for quantifying ETI in human biological fluids, which can be valuable in clinical laboratories for directing medical decisions.

4 Patient perspective

From the patient and CF community perspective, this case highlights that spontaneous conception and pregnancy are possible in female with CF treated with ETI, and urges more women to participate in a large clinical trial to better understand the long-term effects of ETI on the health of the newborn.

Data availability statement

The datasets presented in this article are not readily available because of ethical/privacy restrictions. Requests to access the datasets should be directed to the corresponding authors.

Ethics statement

Written informed consent was obtained from the individual for the publication of any potentially identifiable images or data included in this article.

Author contributions

PR: Data curation, Supervision, Writing – original draft, Investigation, Validation. MM: Data curation, Investigation, Methodology, Writing – original draft, Writing – review & editing. SP: Investigation, Writing – original draft. MD: Investigation, Writing – original draft. FC: Investigation, Writing – original draft. GF: Investigation, Writing – original draft. MR: Writing – original draft. AR: Writing – original draft, Conceptualization, Data curation, Funding acquisition, Supervision, Writing – review & editing.

Funding

The author(s) declare financial support was received for the research, authorship, and/or publication of this article. This work was supported in part by grants from the US Cystic Fibrosis Foundation (CFF grant RECCHI22I0 to AR).

Acknowledgments

The technical support of Marco Fagioni (Agilent Field Service Engineer LC–MS) is gratefully acknowledged.

Conflict of interest

The authors declare that the research was conducted in the absence of any commercial or financial relationships that could be construed as a potential conflict of interest.

The author(s) declared that they were an editorial board member of Frontiers, at the time of submission. This had no impact on the peer review process and the final decision.

Publisher's note

References

1. Saluzzo F, Riberi L, Messore B, Loré NI, Esposito I, Bignamini E, et al. CFTR modulator therapies: potential impact on airway infections in cystic fibrosis. *Cells*. (2022) 11:1243. doi: 10.3390/cells11071243

2. Nichols DP, Paynter AC, Heltshe SL, Donaldson SH, Frederick CA, Freedman SD, et al. Clinical effectiveness of elexacaftor/tezacftor/ivacaftor in people with cystic fibrosis. *Am J Respir Crit Care Med [Internet]*. (2021) 205:529–39. doi: 10.1164/rccm.202108-1986OC

3. Taylor-Cousar JL. CFTR modulators: impact on fertility, pregnancy, and lactation in women with cystic fibrosis. *J Clin Med*. (2020) 9:2706. doi: 10.3390/jcm9092706

4. Smith S, Borchardt M. Analyzing the use and impact of elexacaftor/tezacaftor/ivacaftor on total cost of care and other health care resource utilization in a commercially insured population. *JMCP*. (2022) 28:721–31. doi: 10.18553/jmcp.2022.28.7.721

5. Collins B, Fortner C, Cotey A, Esther CRJ, Trimble A. Drug exposure to infants born to mothers taking Elexacaftor, Tezacaftor, and Ivacaftor. *J Cyst Fibros*. (2022) 21:725–7. doi: 10.1016/j.jcf.2021.12.004

6. Goodwin J, Quon BS, Wilcox PG. Experience to date with CFTR modulators during pregnancy and breastfeeding in the British Columbia cystic fibrosis clinic. *Respir Med Case Rep*. (2022) 40:101778. doi: 10.1016/j.rmcr.2022.101778

7. Taylor-Cousar JL, Jain R. Maternal and fetal outcomes following elexacaftor-tezacaftor-ivacaftor use during preg-nancy and lactation. *J Cyst Fibros*. (2021) 20:402–6. doi: 10.1016/j.jcf.2021.03.006

8. Trimble A, McKinzie C, Terrell M, Stringer E, Esther CR. Measured fetal and neonatal exposure to Lumacaftor and Ivacaftor during pregnancy and while breastfeeding. *J Cyst Fibros*. (2018) 17:779–82. doi: 10.1016/j.jcf.2018.05.009

9. Tizzano EF, Silver MM, Chitayat D, Benichou JC, Buchwald M. Differential cellular expression of cystic fibrosis transmembrane regulator in human reproductive tissues. Clues for the infertility in patients with cystic fibrosis. *Am J Pathol*. (1994) 144:906–14.

10. Ahmad A, Ahmed A, Patrizio P. Cystic fibrosis and fertility. *Curr Opin Obstet Gynecol*. (2013) 25:167–72. doi: 10.1097/GCO.0b013e32835f1745

11. Campagna G, Amato A, Majo F, Ferrari G, Quattrucci S, Padoan R, et al. Registro italiano Fibrosi Cistica (RIFC). Rap-porto 2019-2020. *Ee&P*. (2021) 46:1–38. doi: 10.19191/EP22.4S2.060

12. Jain R, Wolf A, Molad M, Taylor-Cousar J, Esther CR, Shteinberg M. Congenital bilateral cataracts in newborns ex-posed to elexacaftor-tezacaftor-ivacaftor in utero and while breast feeding. *J Cyst Fibros*. (2022) 21:1074–6. doi: 10.1016/j.jcf.2022.10.004

13. Szentpetery S, Foil K, Hendrix S, Gray S, Mingora C, Head B, et al. A case report of CFTR modulator administration via carrier mother to treat meconium ileus in a F508del homozygous fetus. *J Cyst Fibros*. (2022) 21:721–4. doi: 10.1016/j.jcf.2022.04.005

14. Butte NF, Lopez-Alarcon MG. *Nutrient adequacy of exclusive breastfeeding for the term infant during the first six months of life*. (Geneva, Switzerland): World Health Organization (2002).

15. Habler K, Kalla AS, Rychlik M, Bruegel M, Teupser D, Nährig S, et al. Isotope dilution LC-MS/MS quantification of the cystic fibrosis transmembrane conductance regulator (CFTR) modulators ivacaftor, lumacaftor, tezacaftor, elexacaftor, and their major metabolites in human serum. *Clin Chem Lab Med*. (2022) 60:82–91. doi: 10.1515/cclm-2021-0724

16. Pigliasco F, Cafaro A, Stella M, Baiardi G, Barco S, Pedemonte N, et al. Simultaneous quantification of Ivacaftor, Te-zacaftor, and Elexacaftor in cystic fibrosis patients' plasma by a novel LC–MS/MS method. *Biomedicine*. (2023) 11:628. doi: 10.3390/biomedicines11020628

17. Jain R, Magaret A, Vu PT, Van Dalfsen JM, Keller A, Wilson A, et al. Prospectively evaluating maternal and fetal out-comes in the era of CFTR modulators: the MAYFLOWERS observational clinical trial study design. *BMJ Open Resp Res*. (2022) 9:e001289. doi: 10.1136/bmjresp-2022-001289

frontiers | Frontiers in Physiology

TYPE Original Research
PUBLISHED 21 March 2024
DOI 10.3389/fphys.2024.1304513

OPEN ACCESS

EDITED BY
Gendie Lash,
Guangzhou Medical University, China

REVIEWED BY
Zhongxian Yang,
Southern Medical University, China
Zhuozhi Dai,
Shantou Central Hospital, China

*CORRESPONDENCE
Hongkui Yu,
yhk20@163.com

RECEIVED 29 September 2023
ACCEPTED 26 February 2024
PUBLISHED 21 March 2024

CITATION
Zhang M, Li S, Tian C, Li M, Zhang B and Yu H (2024), Changes of uterocervical angle and cervical length in early and mid-pregnancy and their value in predicting spontaneous preterm birth.
Front. Physiol. 15:1304513.
doi: 10.3389/fphys.2024.1304513

Changes of uterocervical angle and cervical length in early and mid-pregnancy and their value in predicting spontaneous preterm birth

Miaomiao Zhang, Shuilan Li, Chao Tian, Min Li, Baofang Zhang and Hongkui Yu*

Department of Sonography, Shenzhen Baoan Women's and Children's Hospital, Shenzhen, China

Objective: To explore the feasibility of transvaginal ultrasound measurement of uterocervical angle (UCA) and cervical length (CL) in early and mid-pregnancy and evaluate their combined prediction of spontaneous preterm birth (sPTB) in singleton pregnancies.

Patients and Methods: This retrospective study comprised 274 pregnant women who underwent transvaginal ultrasound measurement of CL in mid-pregnancy (15–23+6 weeks); in 75 among them, CL also had been measured in early-pregnancy (<14 weeks). These 274 pregnant women were further divided into a preterm group (n = 149, <37 weeks gestation) and a control group (n = 125, >37 weeks gestation) according to delivery before or after 37 weeks, respectively. In the preterm group, 35 patients delivered before 34 weeks and the remaining 114 delivered between 34 and 37 weeks.

Results: The optimal threshold of CL to predict preterm birth risk in women with <37 weeks gestation was 3.38 cm, and the optimal threshold of the UCA to predict preterm birth risk in the same group of women was 96°. The optimal threshold of CL to predict preterm birth risk in women with <34 weeks gestation was 2.54 cm, while that of the UCA in the same group of patients was 106°. The area under the curve for predicting preterm birth by combining the UCA and CL measurements was greater than that by using the UCA or CL alone ($p < 0.01$). The sensitivity and specificity for predicting preterm birth at <34 weeks gestation was 71.7% and 86.4%, respectively; and the sensitivity and specificity for predicting preterm birth at <37 weeks gestation was 87.6% and 80.6%, respectively. The difference between the two groups in CL and UCA were not significant in early pregnancy ($p > 0.01$), but only in mid-pregnancy ($p < 0.01$). There was a negative correlation between UCA and gestational week at delivery ($r = -0.361$, $p < 0.001$) and a positive correlation between CL and gestational week at delivery ($r = 0.346$, $p < 0.001$) in mid-pregnancy. The proportion of deliveries at <34 weeks was highest when the UCA was >105°, and the proportion of deliveries between 35 and 37 weeks was highest when the UCA was between 95° and 105°. The proportion of deliveries at <34 weeks was highest when the CL was <2.5 cm.

Conclusion: The combination of UCA and CL has a better ability to predict preterm birth than either measurement alone. A more obtuse UCA or a shorter CL is associated with an earlier spontaneous preterm birth. The UCA increases from early to mid-pregnancy, while the CL decreases from early to mid-pregnancy.

KEYWORDS

cervical length, uterocervical angle, spontaneous preterm birth, transvaginal ultrasound examination, early and mid-pregnancy

1 Introduction

According to global statistics, more than one-tenth (15 million) of infants are born prematurely every year (Blencowe et al., 2012), and about 1 million infants die from complications of preterm birth (Perin et al., 2022). It is reported that approximately 75% of these deaths could be avoided by timely intervention measures (Iams et al., 2008). According to the gestational week of preterm birth, it can be divided into the following types: extremely preterm birth occurring before 28 weeks, accounting for about 5%, severe preterm birth occurring between 28 and 31 weeks, accounting for about 15%, moderate preterm birth occurring between 32 and 33 weeks, accounting for about 20%, and near-term birth occurring between 34 and 36 weeks, accounting for 60%–70% (Goldenberg et al., 2008). Therefore, early identification of pregnant women at risk of preterm birth is critical, which can provide them with timely follow-up and treatment (Cunningham et al., 2014).

Currently, the techniques for diagnosing risk of preterm birth include the patient's history of preterm birth; transvaginal ultrasound; clinical signs including uterine contractions, vaginal bleeding, uterocervical angle (UCA) and cervical length (CL) (McCarty-Singleton and Sciscione, 2012). During pregnancy and delivery, the cervical tissue undergoes a series of cervical remodeling behaviors such as softening and increased compliance, which enables the cervix to better adapt to the gravity of pregnancy tissue and fetal delivery (Myers et al., 2015). Therefore, the cervix is considered an anatomical marker of the potential pathological process leading to spontaneous preterm birth (Wendy and Katherine, 2011), and transvaginal ultrasound measurement of CL or UCA has been applied in the clinical prediction of preterm birth (Dziadosz et al., 2016). However, Hiersch et al. (2016) analyzed 1,068 pregnant women at high risk of preterm birth in mid-pregnancy and found that a simple CL measurement of <3 cm could not really predict preterm birth with good specificity. Given that the measurement of UCA is closely related to factors such as gestational week, patient ethnicity, and medical history, which leads to differences in the optimal cut-off point judgment among various studies, the international range of UCA for predicting preterm birth is between 95° and 115°(Dziadosz et al., 2016; Farràs Llobet et al., 2017). There are only few studies on the optimal cut-off segment of UCA for Chinese people (Shi et al., 2018). At present, limited literature exists on the analysis of spontaneous preterm birth prediction by combining CL and UCA in a multivariate regression model in mid-pregnancy and the relationship between gestational period (early pregnancy vs. mid-pregnancy) and preterm birth. We hope that our research data can further supplement this field of study.

2 Materials and methods

2.1 Subjects

A retrospective study was conducted among 30,039 pregnant women who delivered at Shenzhen Baoan Women's and Children's Hospital from January 2021 to March 2023. Of these, 1,865 were born prematurely with a rate of 6.2%. Out of 1865, 149 persons who had mid-trimester CL measurements were selected as the experimental group. Age and height and weight matched 125 full term deliveries were used as controls. The study was approved by the ethical review board of our hospital.

Inclusion criteria: (1) clear and excellent cervical images; (2) complete clinical data.

Exclusion criteria: (1) multiple pregnancies; (2) congenital fetal malformations; (3) premature rupture of membranes; (4) uterine malformations.

2.2 Measurement of CL and UCA

In this retrospective study, the sample measurement was performed by several attending ultrasound physicians with >5 years' relevant work experience, who measured the CL. Patients were examined using a GE Voluson E8 color Doppler ultrasound diagnostic instrument with RIC5-9-D probe. The Frequency range is 4.55MHz–8.33 MHz. The patients were placed in the lithotomy position after emptying the bladder, and the CL were measured. The specific operation method was as follows: The vaginal ultrasound probe was covered with a medical disposable condom. To minimize acoustic impedance, the inner and outer layers of the condom are coated with medical sterile coupling agent. The probe was slowly moved to the vault of the vagina, and images of the lower segment of the uterus and the internal and external ora of the cervix were obtained. The cervical image occupied two-thirds of the whole image. The CL was measured by the internal and external ora of the cervix on the sagittal plane of the cervix (Kagan and Sonek, 2015) (Figure 1). ImageJ software was used by an attending ultrasound physician with more than 5 years of work experience to measure the UCA on the previously stored cervical image again, and repeated 3 times to obtain the average value. The angle between the lower segment of the uterus and the

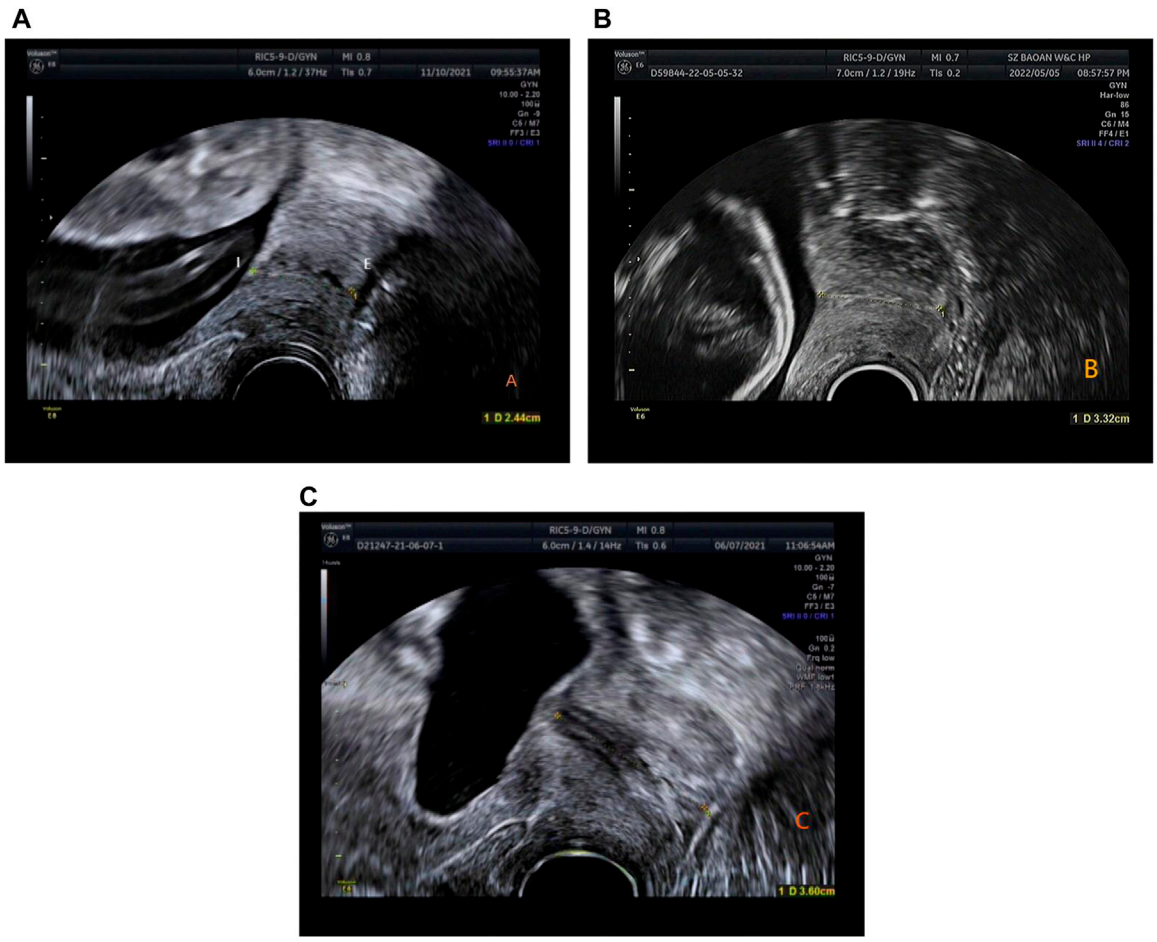

FIGURE 1
(A) Time of delivery <34 weeks, CL is 2.44 cm (gestation time: 23 weeks 5 days). **(B)** Time of delivery between 34 and 37 weeks, CL is 3.32 cm (gestation time: 23 weeks). **(C)** Time of delivery >37 weeks, CL is 3.6 cm (gestation time: 20 weeks 2 days).

internal and external os of the cervix was considered the UCA (Sawaddisan et al., 2020) (Figure 2).

2.3 Statistical analysis

Data analysis was performed using R version 4.2.3 (Shortstop Beagle), count data were expressed as frequency (percentage), comparison between groups was performed by chi-square test, If the theoretical frequency was relatively small, Fisher's exact test was used. Measurement data were tested for normality and homogeneity of variance. If variables showed normal distribution and homogeneity, they were expressed as mean ± standard deviation, and *t*-test was used for intergroup comparison. Otherwise, they were expressed as the median (interquartile range), and independent sample Wilcoxon rank sum test was used for intergroup comparison. In this study, we used linear regression to analyze the relationship between cervical angle, cervical length and weeks of labor, and logistic regression to develop a predictive model for the risk of preterm birth. The area under the receiver operating characteristic (ROC) curve (AUC) and its 95% Confidence interval (CI) were calculated. Comparisons of AUC were made using the delong test. If the AUC was >0.5 and the difference was significant compared with 0.5, the diagnostic index was considered to have some diagnostic value. The point on the ROC curve where the Jordon index (sensitivity + specificity-1) was greatest was used as the cut-off point. $p < 0.05$ was considered statistically significant, and all tests were two-sided.

3 Results

3.1 General data

There was no statistical significance in the comparison of pre-pregnancy BMI, prenatal BMI, female fetus, prior artificial abortion, hypertensive disorder, prior ectopic, anemia, thyroid disease and prior spontaneous abortion between the two groups. However, there were significant differences with respect to age, delivery week, fetal weight, *in vitro* fertilizer, diabetes, cesarean delivery repeat ($p < 0.05$) (Table 1)

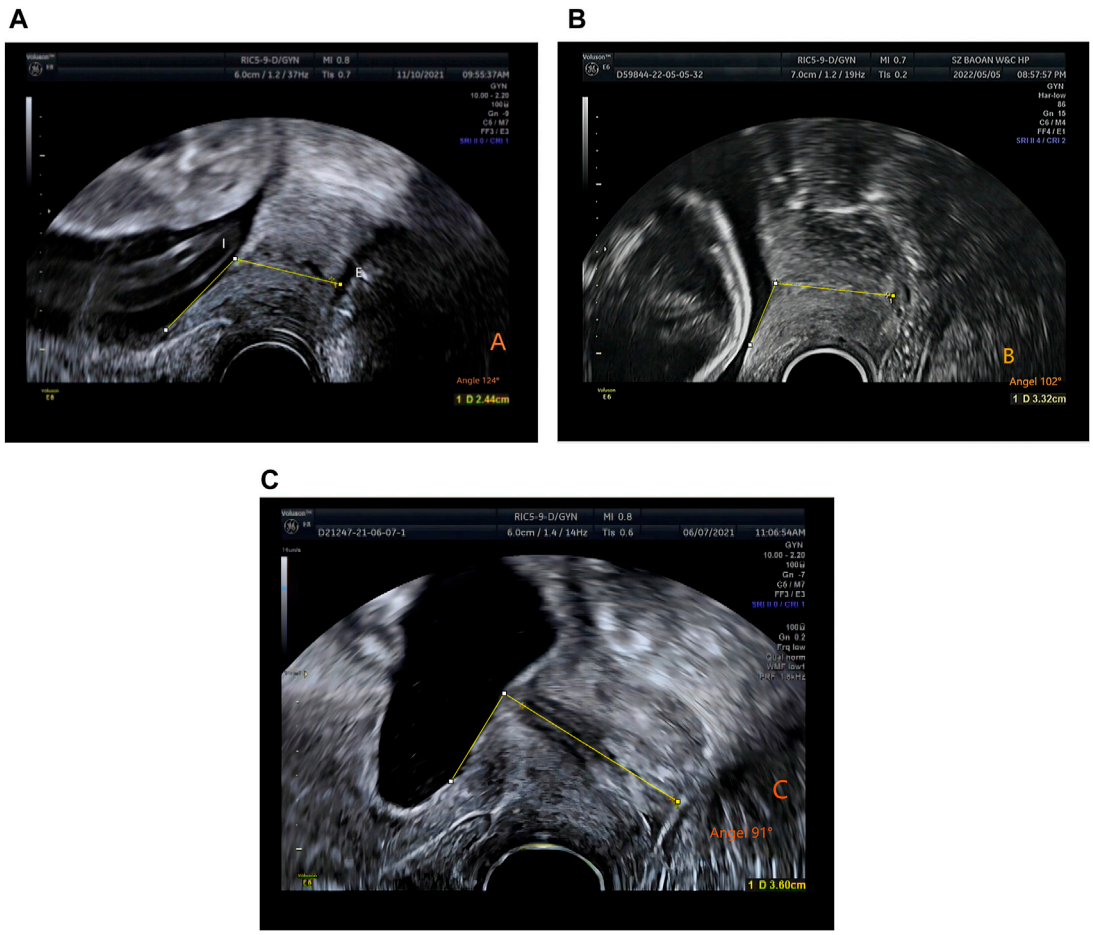

FIGURE 2
The measurement of uterocervical angle (UCA). UCA was calculated as the angle between two lines. The first line was drawn between the internal **(I)** and external ostium (os) **(E)**. The second line was drawn 3 cm parallel to the lower aspect of the anterior inner uterine wall passing through the end of the first line at the internal os. **(A)** Time of delivery <34 weeks, UCA 124° (gestation time: 23 weeks and 5 days). **(B)** Time of delivery between 34 and 37 weeks, UCA 102° (gestation time: 17 weeks). **(C)** Time of delivery >37 weeks, UCA 91° (gestation time: 17 weeks 1 day).

3.2 Changes of UCA and CL in early and mid-pregnancy

From early to mid-pregnancy, the UCA increased and the CL shortened. There was no significant statistical difference in the CL and UCA between the two groups in early pregnancy. Spearman' correlation coefficient between the UCA and CL in early pregnancy was 0.06 (p = 0.608), and there was no correlation between the changes of the two variables. However, the CL was shorter and the UCA was larger in the preterm group in mid-pregnancy. Spearman's correlation coefficient between the UCA and CL was −0.517 (p < 0.001) (Table 2).

3.3 The relationship between UCA and CL in mid-pregnancy and gestational week at delivery

There was a negative correlation between UCA in mid-pregnancy and gestational week at delivery (r = −0.361, p < 0.001) (Figure 3A), and a positive correlation between CL in mid-pregnancy and gestational week at delivery (r = 0.346, p < 0.001) (Figure 3B).

3.4 Distribution of UCA and CL in different delivery gestational weeks

In Tables 3, 4, it can be seen that the proportion of deliveries that happened <34 weeks was highest when the UCA was greater than 105°, and the proportion of deliveries between 35 and 37 weeks was highest when the UCA was between 95° and 105°. The proportion of deliveries <34 weeks was highest when the CL was <2.5 cm.

3.5 Analysis of the efficacy graph of CL and UCA for predicting spontaneous preterm birth

In Figure 4A of the efficacy graph of CL and UCA for predicting spontaneous preterm birth, it can be seen that the area under the ROC curve (AUC) for predicting preterm birth (<34 weeks) by CL

TABLE 1 Demographic data.

Demographic data	Overall	Birth at term (>37wk)	Birth at term (<37wk)	Z/t/χ2	*p*-value[b]
	N = 274[a]	N = 125 (45%)[a]	N = 149 (55%)[a]		
Age,yr	31.63 ± 3.94	32.29 ± 3.66	31.09 ± 4.09	2.429	0.015
Pre-pregnancy BMI	22.49 (19.52, 25.61)	23.04 (19.99, 25.92)	22.15 (19.28, 25.05)	1.540	0.124
Prenatal BMI	24.16 (21.29, 27.01)	24.60 (21.60, 27.51)	23.57 (21.19, 26.85)	1.473	0.141
Delivery week	36.71 (35.57, 39.00)	39.14 (38.43, 39.86)	35.71 (33.86, 36.43)	14.156	<0.001
fetal weight	2,840.00 (2,400.00, 3,250.00)	3,260.00 (3,000.00, 3,500.00)	2,430.00 (2,115.00, 2,700.00)	12.411	<0.001
Female fetas	106 (39.4%)	50 (40.7%)	56 (38.4%)	0.147	0.701
in vitro fertilizer	24 (8.7%)	18 (14.4%)	6 (4.0%)	9.258	0.002
Prior artificial abortion	68 (24.7%)	37 (29.6%)	31 (20.7%)	2.923	0.087
Diabetes	73 (26.5%)	25 (20.0%)	48 (32.0%)	5.035	0.025
Prior spontaneous preterm birth	33 (12.0%)	14 (11.2%)	19 (12.7%)	0.139	0.709
Hypertensive disorder	17 (6.2%)	6 (4.8%)	11 (7.3%)	0.754	0.385
Cesarean delivery repeat	32 (11.6%)	21 (16.8%)	11 (7.3%)	5.943	0.015
prior ectopic pregnancy	7 (2.5%)	5 (4.0%)	2 (1.3%)	1.027	0.311
anemia	43 (15.6%)	23 (18.4%)	20 (13.3%)	1.327	0.249
Thyroid Diseases	25 (9.1%)	15 (12.0%)	10 (6.7%)	2.347	0.126
Prior spontaneous abortion	39 (14.2%)	16 (12.8%)	23 (15.3%)	0.360	0.549

[a]Mean ± SD; median (IQR); n (%).
[b]Wilcoxon–Mann-Whitney test; Two Sample *t*-test; Pearson's chi-squared test; Pearson's chi-squared test with Yates' continuity correction; Fisher's Exact Test for Count Data.

TABLE 2 Test characteristics of the UCA and CL for the prediction of sPTB.

Parameters	Overall	Birth at term (>37wk)	Birth at term (<37wk)	Z/t/χ2	*p*-value[2]
	N = 274[1]	N = 125 (45%)[1]	N = 149 (55%)[1]		
Early-pregnancy CL	3.50 ± 0.37	3.57 ± 0.40	3.37 ± 0.26	2.267	0.026
	(n = 75)	(n = 49)	(n = 26)		
Early-pregnancy UCA	75.67 ± 15.05 (n = 75)	76.43 ± 15.63	74.16 ± 14.01 (n = 26)	0.615	0.541
		(n = 49)			
mid-pregnancy CL	3.19 (2.82,3.60)	3.61 (3.30,3.96)	2.90 (2.67,3.15)	10.996	<0.001
	(n = 274)	(n = 125)	(n = 149)		
mid-pregnancy UCA	96.73 (85.40,105.67)	85.34 (75.28, 93.30)	102.51 (97.10,111.36)	−10.793	<0.001
	(n = 274)	(n = 125)	(n = 149)		

was 0.726 (0.633–0.819). The threshold value was 2.54 cm, corresponding to a sensitivity, specificity, positive predictive value, and negative predictive value of 42.9%, 91.7%, 42.9%,91.7%, respectively. The AUC for predicting preterm birth (<34 weeks) by UCA was 0.837 (95% confidence interval [CI]: 0.757–0.917), and the threshold value was 106°, corresponding to a sensitivity, specificity, positive predictive value, and negative predictive value of 71.4%, 83.1%, 37.9%, and 95.3%, respectively. The AUC for predicting preterm birth (<34 weeks) by combining the CL and UCA was 0.85 (0.773–0.927), and the sensitivity, specificity, positive predictive value, and negative predictive value were 71.4%, 86.4%, 43.1%, and 95.4%, respectively.

In Figure 4B of the efficacy graph of CL and UCA for predicting spontaneous preterm birth, it could be observed that the optimal threshold for predicting preterm birth risk (<37 weeks) by CL was 3.38 cm, with an AUC of 0.892 (0.851–0.932), and the sensitivity, specificity, positive predictive value, and negative predictive value were 93.5%, 75%, 82.2%, and 90.3%, respectively. The optimal threshold for predicting preterm birth risk (<37 weeks) by UCA was 96°, with an AUC of 0.883 (0.843–0.922). The sensitivity,

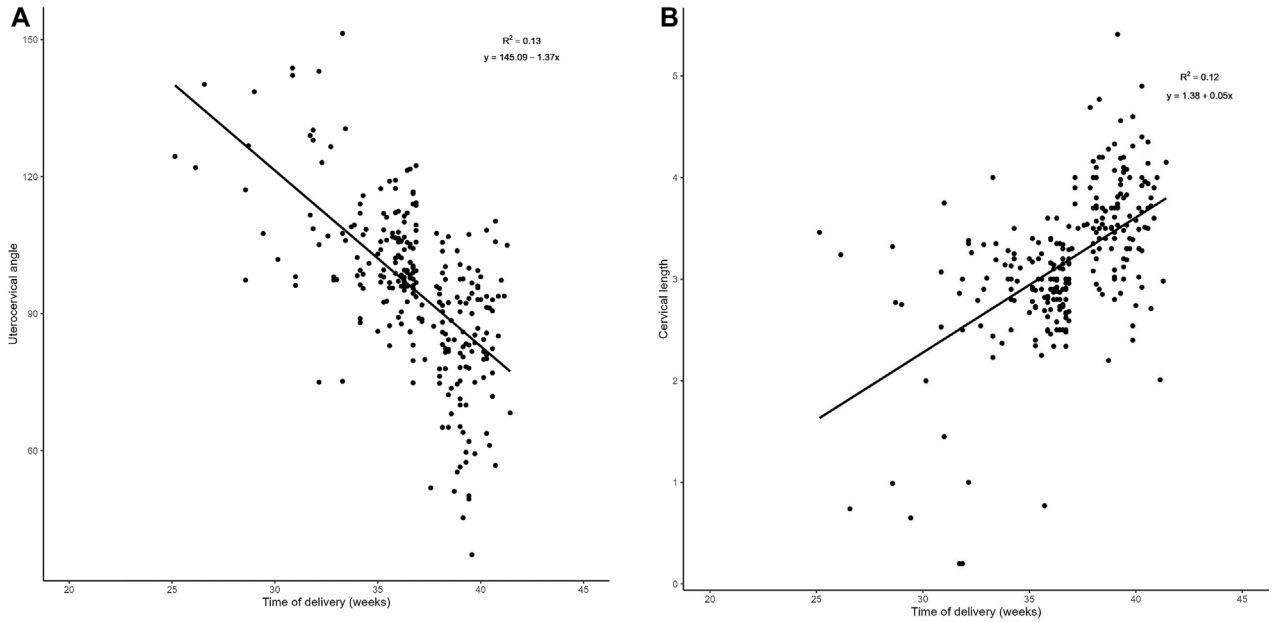

FIGURE 3
Regression analysis: **(A)**. Plot of UCA in relation to the week of labor in the middle trimester There was a negative correlation between the UCA in mid-pregnancy and gestational week at delivery (r = −0.361, $p < 0.001$).

TABLE 3 Distribution of sPTB (at < 37 weeks) and term births in women according to uterocervical angle (UCA).

UCA	Delivery at < 34weeks N = 35	Delivery at 34–36+6 weeks N = 114	Delivery at ≥37 weeks N = 125
≥105	26 (74.29%)	42 (36.84%)	6 (4.80%)
95–105	7 (20.00%)	54 (47.37%)	19 (15.20%)
<95	2 (5.71%)	18 (15.79%)	100 (80.00%)

Kendall's correlation coefficient is −0.634, $p < 0.001$.

TABLE 4 Distribution of sPTB (at < 37 weeks) and term births in women according to cervical length (CL).

CL (cm)	Delivery at <34 weeks	Delivery at 34–37 weeks	Delivery at ≥37 weeks
≤2.5 (CM)	13 (37. 14%)	16 (13.56%)	3 (2.42%)
>2.5 (CM)	22 (62.86%)	102 (86.44%)	121 (97.58%)

specificity, positive predictive value, and negative predictive value were 87.6%, 80.6%, 84.8% and, 80.4%, respectively. The AUC for predicting preterm birth risk (<37 weeks) by combining the UCA and CL was 0.942 (0.914–0.969), and the sensitivity, specificity, positive predictive value, and negative predictive value were 85%, 91.1%, 92.2%, and 83.1%,respectively.

3.5.1 Statistical analysis of AUC

For preterm birth occurring <34 weeks of gestation, the combination of UCA and CL predicted preterm birth better than CL alone, with a statistically significant difference ($p < 0.01$). The UCA predicted preterm birth better than CL, with a statistically significant difference ($p < 0.01$). The efficacy of predicting preterm birth by combining UCA and CL was the same as that by UCA alone, with no statistical significance ($p > 0.01$) (Figure 4A; Table 5).

For preterm birth occurring <34 weeks of gestation, a combination of UCA and CL predicted preterm birth better than either of these two indicators alone, with a statistically significant difference ($p < 0.01$). The efficacy of predicting preterm birth by UCA and CL was the same, with no statistical significance ($p > 0.01$) (Figure 4B; Table 5).

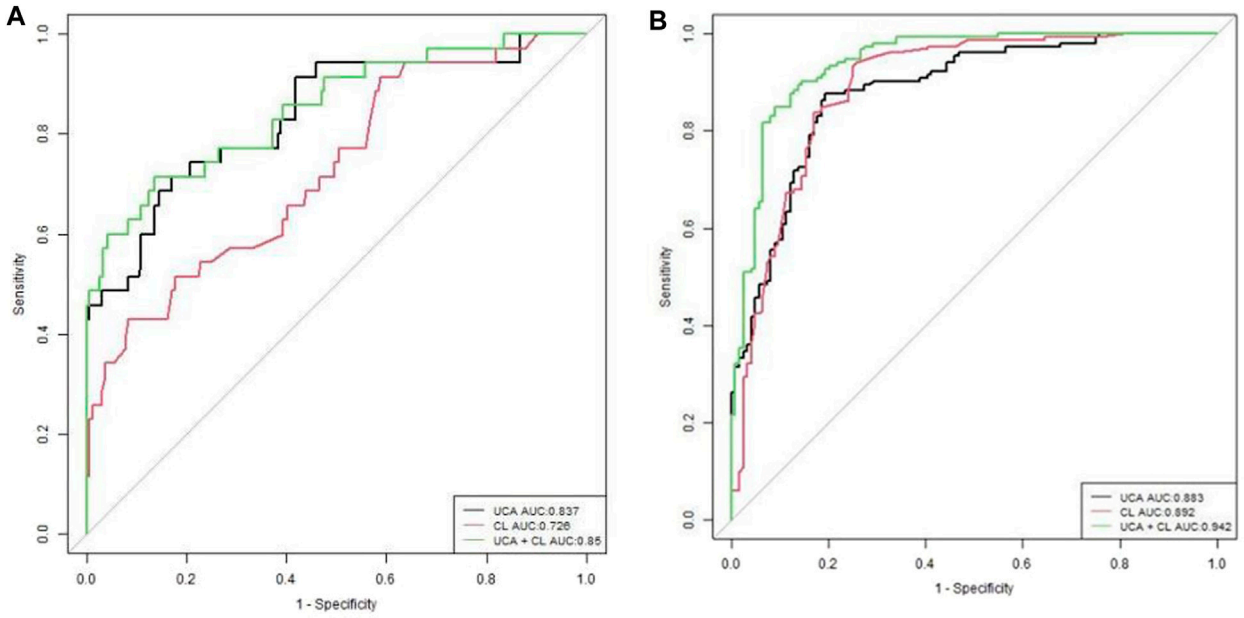

FIGURE 4
Receiver operating characteristic curves of evaluating UCA, CL, and gestational age at delivery **(A)**. UCA and CL for sPTB <34 weeks, **(B)**. UCA and CL for sPTB <37 weeks.

TABLE 5 Statistical analysis of area under the curve (AUC) in Figure 3A, B.

Delivery at <34 weeks	*p*-value	Delivery at <37 weeks	*p*-value
UCA (0.837)vs. CL (0.726)	0.046	UCA (0.883) vs. CL (0.892)	0.746
UCA(0.837)vs. UCA + CL (0.85)	0.395	UCA(0.883) vs.UCA + CL (0.942)	<0.001
CL (0.726) vs. UCA + CL	0.005	CL vs. UCA + CL (0.942)	<0.001

The equation using the joint diagnostic model is: Log (p/1−p) = −9.189 + 0.095*UCA−0.904 ×CL.

4 Discussion

This study showed that the combination of UCA and CL had the best effect in predicting preterm birth according to the efficacy graph. As pregnancy progressed from early to mid-stages, the UCA increased significantly and the CL shortened significantly in the preterm group. A more obtuse UCA or shorter CL was associated with a more premature spontaneous preterm birth.

Previous studies by Dziadosz et al. (Dziadosz et al., 2016) showed that the optimal threshold for CL was 2.5 cm with a specificity and negative predictive value of 98% and 96%, respectively, when preterm birth occurred<34 weeks. Comparing only single indicators, they also shows UCA was a better predictor of preterm labor than CL in predicting spontaneous preterm birth <34 weeks. Our conclusion was consistent with theirs. We found that the efficacy of UCA was greater than that of CL in predicting preterm birth <34 weeks, which was consistent with Rasha E. Khamees (Khamees et al., 2022) and Dziadosz et al.'s (Dziadosz et al., 2016) studies. This suggests that our results are reproducible. Our optimal threshold for predicting preterm birth by UCA was consistent with the studies of Dziadosz et al. (2016) and Kumar et al. (Kumar et al., 2022), but our specificity was the highest. The specificity was 83.1% and the specificity was 80.6%, which indicates that our research results had the greatest ability to screen out patients who were not preterm, and strengthened the previous research results of Dziadosz et al. (Dziadosz et al., 2016) and Kumar et al. (Kumar et al., 2022).

The optimal threshold for CL was 3.38 cm, which was the same as that obtained by Luechathananonr et al. (2021), When preterm birth occurred<37 weeks. This is likely because our population was a predominantly Asian population, and the literature suggests that the CL of pregnant Asian women was different from that of Western women, which may be related to body mass index (BMI), height, and/or ethnicity. However, comparing single indicator alone, Luechathananonr et al. (2021) reported CL had more advantages than UCA in predicting spontaneous preterm birth<37 weeks.Our research shows UCA has no advantage over CLfor predicting spontaneous preterm labor <37 weeks. Either one of them is a good predictor of preterm labor <37 weeks.This result conflicts with Luechathananonr et al., which we will investigate further later.

In addition to drawing the above conclusions, our study also showed that the combination of UCA and CL had application and promotion value in screening our pregnant women who may have preterm birth.

Dziadosz et al. (Dziadosz et al., 2016) also concluded that the efficacy of predicting preterm birth by combining UCA and CL

(including <37 weeks and <34 weeks) was higher than that by single indicators. However, their study did not provide the specific AUC value, rather they only calculated the specificity and negative predictive value. In our study, we calculated not only the sensitivity, specificity, positive predictive value, and negative predictive value but also the specific AUC value of the ROC curve. Hence, we believe our results are more complete and clinically meaningful.

We analyzed that as the pregnancy progressed from early to mid-stages, the UCA increased significantly and the CL shortened significantly in the preterm group. Spearman's correlation coefficient between the UCA and CL in mid-pregnancy was −0.517 ($p < 0.001$), which was similar to Dziadosz et al.'s study (Dziadosz et al., 2016) (correlation coefficient: −0.05 [$p < 0.05$]) and Kumar et al.'s study (correlation coefficient: −0.264 [$p < 0.001$]), (Kumar et al., 2022),suggesting that the UCA increased significantly while the CL decreased significantly. According to Sochacki-Wojcicka et al. (2015) and House et al. (House et al., 2013), the cervix bears pressure from the surrounding pelvic organs and increased uterine gravity and load during pregnancy. An acute angle of the cervix can buffer these loads transmitted to the cervix, maintaining normal morphology of the cervix. An obtuse UCA may transmit these loads to the cervix, causing dilation of the cervical canal, leading to preterm birth. At the same time, Dziadosz et al. (Dziadosz et al., 2016) also pointed out that the same force acting on a blunt cervical canal may more likely cause the cervical canal to open. Therefore, the UCA changes from an acute angle in early pregnancy to an obtuse angle in mid-pregnancy, leading to preterm birth. However, the UCA of pregnant women who delivered at term remained acute from early to mid-pregnancy. This is because the acute angle forms a "inverted triangle support" in the lower segment of the uterus to support the pressure from the top, thus reducing the pressure and maintaining its normal shape (Yao et al., 2014; Yoshida et al., 2014). In this study, the change of CL length in early pregnancy was consistent with that of Thain et al. (2020), who found that there was no statistical significance in the change of CL in early pregnancy in the Asian population. However, in mid-pregnancy (18–22 weeks), the CL of the preterm group was lower than that of the control group, which was also similar to the study by Shi et al. (Shi et al., 2018). The CL of the preterm group was relatively shorter than that of the term group (3.09 cm vs.3.78 cm). There was no significant statistical difference in the UCA in early pregnancy. We speculate that the underlying mechanism is that in early pregnancy, the weight of the uterus is not large, and the cervix bears relatively less load, so the cervical function remains normal. With fetal growth, the load on the uterus increases, and at the same time, the smooth muscle or elastic fiber of the cervix reduces that, in turn, reduces cervical compliance, and resists deformation caused by collagen fiber disorder and a 5% increase in the water content. The cervix of preterm patients softens prematurely, leading to cervical shortening (Myers et al., 2009; House et al., 2013).

Our study reviewed not only the previous studies on UCA and CL in mid-pregnancy but also studies on UCA and CL in early pregnancy and compared the changes in these two stages. By studying these two stages of UCA and CL, we found that when pregnant women's UCA changed from acute angle in early pregnancy to obtuse angle in mid-pregnancy, we should be alert to preterm birth. We observed that there was no significant statistical difference in CL and UCA between the two groups in early pregnancy. The UCA of pregnant women at this stage was acute and the CL was greater than 3.37 cm. Spearman's correlation coefficient between the UCA and CL in early pregnancy was 0.06, $p = 0.608$, indicating that there was no correlation between the changes of these two variables. T here was no regularity in early pregnancy, and cervical softening started from mid-pregnancy (Iams et al., 1996). Therefore, we speculate that there is no difference in the softness and toughness of the cervix among all pregnant women at this stage, and there is no deformation and remodeling. This conclusion is partly consistent with Conoscenti et al. (2003), whose study showed that measuring CL in early pregnancy had no significance for predicting preterm birth. We think that measuring CL alone in early pregnancy has no significance, rather it needs to be analyzed together with CL in mid-pregnancy.

This study has some limitations. First, this was a retrospective study, and the subjects were singleton pregnant women with gestational age <25 weeks, which may have led to selection bias. Second, there were very few samples of patients who had both CL and UCA measurements in both early and mid-pregnancy. In the future, we plan to conduct prospective studies and increase the sample size of patients who have both cervical examinations in both stages of pregnancy. Finally, this study was a single-center study, and the optimal cut-off value selected may not be representative enough.

In summary, measuring the UCA combined with CL is more accurate than measuring the CL or UCA alone for predicting preterm birth risk, which is worthy of further investigation and clinical application. If transvaginal ultrasound shows that CL is short especially less than 2.48 cm or the UCA is obtuse, especially larger than 106° in mid-pregnancy, clinicians should be alerted to a high risk of preterm birth less than 34 weeks.

5 Scope statement

We believe that our study is a significant contribution because we identified the combination of uterocervical angle (UCA) and cervical length (CL) has a better ability to predict preterm birth than cervical length or uterocervical angle alone. A more obtuse uterocervical angle or a shorter cervical length is associated with an earlier spontaneous preterm birth. The uterocervical angle increases from early to mid-pregnancy, while the cervical length decreases from early to mid-pregnancy. Further, we believe that this paper will be of interest to the readership of your journal because it matches your researches topics about aging in female infertility and pathologic pregnancy.

Data availability statement

The original contributions presented in the study are included in the article/Supplementary material, further inquiries can be directed to the corresponding author.

Ethics statement

The studies involving humans were approved by the Ethics Committee of Shenzhen Baoan Women's and Children's Hospital. The studies were conducted in accordance with the local legislation and institutional requirements. The participants provided their written informed consent to participate in this study.

Author contributions

MZ: Conceptualization, Methodology, Investigation, Data curation, Writing–review and editing, Writing–original draft. SL: Writing–review and editing, Formal Analysis. CT: Writing–original draft, Data curation. HY: Software, Writing–review and editing, Supervision, Methodology. ML: Writing–review and editing. BZ: Writing–review and editing, Methodology.

Funding

The author(s) declare that no financial support was received for the research, authorship, and/or publication of this article.

Conflict of interest

The authors declare that the research was conducted in the absence of any commercial or financial relationships that could be construed as a potential conflict of interest.

Publisher's note

All claims expressed in this article are solely those of the authors and do not necessarily represent those of their affiliated organizations, or those of the publisher, the editors and the reviewers. Any product that may be evaluated in this article, or claim that may be made by its manufacturer, is not guaranteed or endorsed by the publisher.

References

Blencowe, H., Cousens, S., Oestergaard, M. Z., Chou, D., Moller, A. B., Narwal, R., et al. (2012). National, regional, and worldwide estimates of preterm birth rates in the year 2010 with time trends since 1990 for selected countries: a systematic analysis and implications. *Lancet* 379, 2162–2172. doi:10.1016/S0140-6736(12)60820-4

Cunningham, F. G., Leveno, K. G., Bloom, S. L., and Spong, C. Y. (2014). "Preterm labor," in *William obstetrics, twenty-fourth*. Editors F. Cunningham, K. G. Leveno, S. L. Bloom, and C. Y. Spong (New York: McGraw-Hill Education/Medical), 829–830.

Dziadosz, M., Bennett, T. A., Dolin, C., Honart, A. W., Pham, A., Lee, S. S., et al. (2016). Uterocervical angle: a novel ultrasound screening tool to predict spontaneous preterm birth. *J. Obstet. Gynecol.* 215, 376.e1–376.e7. doi:10.1016/j.ajog.2016.03.033

Farràs Llobet, A., Martí, L. R., Higueras, T., Calero Fernández, I. Z., Gascón Portalés, A., Goya Canino, M. M., et al. (2017). The uterocervical angle and its relationship with preterm birth. *J. Matern. Fetal Neonatal Med.* 31, 1881–1884. doi:10.1080/14767058.2017.1331427

Goldenberg, R. L., Culhane, J. F., Iams, J. D., and Romero, R. (2008). Epidemiology and causes of preterm birth. *Lancet* 371, 75–84. doi:10.1016/S0140-6736(08)60074-4

Hiersch, L., Ashwal, E., Melamed, N., Bardin, R., Aviram, A., Meizner, I., et al. (2016). Role of cervical length measurement for preterm delivery prediction in women with threatened preterm labor and cervical dilatation. *J. Ultrasound Med.* 35, 2631–2640. doi:10.7863/ultra.15.12007

House, M., McCabe, R., and Socrate, S. (2013). Using imaging-based, three-dimensional models of the cervix and uterus for studies of cervical changes during pregnancy. *Clin. Anat.* 26, 97–104. doi:10.1002/ca.22183

Iams, J. D., Goldenberg, R. L., Meis, P. J., Mercer, B. M., Moawad, A., Das, A., et al. (1996). The length of the cervix and the risk of spontaneous premature delivery. National Institute of Child Health and Human Development maternal Fetal Medicine Unit network. *N. Engl. J. Med.* 334, 567–572. doi:10.1056/NEJM199602293340904

Iams, J. D., Romero, R., Culhane, J. F., and Goldenberg, R. L. (2008). Primary, secondary, and tertiary interventions to reduce the morbidity and mortality of preterm birth. *Lancet* 371, 164–175. doi:10.1016/S0140-6736(08)60108-7

Kagan, K. O., and Sonek, J. (2015). How to measure cervical length. *Ultrasound Obstet. Gynecol.* 45, 358–362. doi:10.1002/uog.14742

Khamees, R. E., Khattab, B. M., Elshahat, A. M., Taha, O. T., and Aboelroose, A. A. (2022). Uterocervical angle versus cervical length in the prediction of spontaneous preterm birth in singleton pregnancy. *Int. J. Gynecol. Obstet.* 156, 304–308. doi:10.1002/ijgo.13629

Kumar, P., Resham, S., Kumar, S. I., Rai, S., Pandey, S., Ram, C., et al. (2022). Evaluation of uterocervical angle and cervical length as predictors of spontaneous preterm birth. *Indian J. Radiol. Imaging* 32, 10–15. doi:10.1055/s-0041-1741411

Luechathananon, S., Songthamwat, M., and Chaiyarach, S. (2021). Uterocervical angle and cervical length as a tool to predict preterm birth in threatened preterm labor. *Int. J. Womens Health* 13, 153–159. doi:10.2147/IJWH.S283132

McCarty-Singleton, S., and Sciscione, A. (2012). Committee on Practice Bulletins—obstetrics, the American College of Obstetricians and Gynecologists, Kilpatrick Practice Bulletin no. 130:prediction and prevention of preterm birth.Practice bulletin no. 130: prediction and prevention of preterm birth. *Pract. Bull.* 120, 964–973. doi:10.1097/AOG.0b013e3182723b1b

Meir, Y. J., D'Ottavio, G., Rustico, M. A., Pinzano, R., Fischer-Tamaro, L., Stampalija, T., et al. (2003). Does cervical length at 13- 15 weeks ' gestation predict preterm delivery in an unselected population? Ultrasound Obstet. *Gynecol* 21, 128–134. doi:10.1002/uog.4

Myers, K., Socrate, S., Tzeranis, D., and House, M. (2009). Changes in the biochemical constituents and morphologic appearance of the human cervical stroma during pregnancy. *Eur. J. Obstet. Gynecol.Reprod. Biol.* 144, S82–S89. doi:10.1016/j.ejogrb.2009.02.008

Myers, K. M., Feltovich, H., Mazza, E., Vink, J., Bajka, M., Wapner, R. J., et al. (2015). The mechanical role of the cervix in pregnancy. *J. Biomech.* 48, 1511–1523. doi:10.1016/j.jbiomech.2015.02.065

Perin, J., Mulick, A., Yeung, D., Villavicencio, F., Lopez, G., Strong, K. L., et al. (2022). Global,regional, and national causes of under-5 mortality in 2000- 19: an updated systematic analysis with implications for the Sustainable Development Goals. *Lancet Child. Adolesc. Health* 6, 106–115. doi:10.1016/S2352-4642(21)00311-4

Rumack, C. M., Wilson, S. R., Charboneau, J. W., and Levine, D. (2011). *Diagnostic ultrasound*. Philadelphia: Elsevier Mosby, 1527–1528.

Sawaddisan, R., Kor-Anantakul, O., Pruksanusak, N., and Geater, A. (2021). Distribution of uterocervical angles in the second trimester of pregnant women at low risk for preterm delivery. *J. Obstet. Gynaecol.* 41, 77–82. doi:10.1080/01443615.2020.1718622

Shi, W., Qin, J., Ding, Y., Zhao, X., Chen, L., Wu, C., et al. (2018). The prediction role of transperineal ultrasound measuring anterior utericervical angle and cervical length on preterm birth. *Int. J. Clin. Exp. Med.* 11, 5980–5985.

Sochacki-Wojcicka, N., Wojcicki, J., Bomba-Opon, D., and Wielgos, M. (2015). Anterior angle as a new biophysical ultrasound marker for prediction of spontaneous preterm birth Ultrasound. *Obstet. Gynecol.* 46, 376–379. doi:10.1002/uog.1480

Thain, S., Yeo, G. S. H., Kwek, K., Chern, B., and Tan, K. H. (2020). Spontaneous preterm birth and cervical length in a pregnant Asian population. *PLOS ONE* 15, e0230125. doi:10.1371/journal.pone.0230125

Wendy, L. W., and Katherine, W. F. (2011), *Cervical ultrasound and preterm birth*, Mosby, Maryland.

Yao, W., Yoshida, K., Fernandez, M., Vink, J., Wapner, R. J., Ananth, C. V., et al. (2014). Measuring the compressive viscoelastic mechanical properties of human cervical tissue using indentation. *J.Mech. Behav. Biomed. Mater.* 34, 18–26. doi:10.1016/j.jmbbm.2014.01.016

Yoshida, K., Jiang, H., Kim, M., Vink, J., Cremers, S., Paik, D., et al. (2014). Quantitative evaluation of collagen crosslinks and corresponding tensile mechanical properties in mouse cervical tissue during normal pregnancy. *PLOS ONE* 9, e112391. doi:10.1371/journal.pone.0112391

frontiers | Frontiers in Endocrinology

TYPE Original Research
PUBLISHED 28 March 2024
DOI 10.3389/fendo.2024.1309082

OPEN ACCESS

EDITED BY
Fengxiang Wei,
Shenzhen Longgang District Maternal and Child Health Care Hospital, China

REVIEWED BY
Yuan Han,
Fudan University, China
Jia-feng Wang,
Second Military Medical University, China
Keyi Wang,
Tongji University, China

*CORRESPONDENCE
Lize Xiong
mzkxlz@126.com
Xiya Yu
yuxiyash@163.com

†These authors have contributed equally to this work

RECEIVED 07 October 2023
ACCEPTED 18 March 2024
PUBLISHED 28 March 2024

CITATION
Hong D, Zhang H, Yu Y, Qian H, Yu X and Xiong L (2024) Total muscle-to-fat ratio influences urinary incontinence in United States adult women: a population-based study.
Front. Endocrinol. 15:1309082.
doi: 10.3389/fendo.2024.1309082

Total muscle-to-fat ratio influences urinary incontinence in United States adult women: a population-based study

Dongmei Hong†, Hui Zhang†, Yong Yu, Huijie Qian, Xiya Yu* and Lize Xiong*

Department of Anesthesiology and Perioperative Medicine, Shanghai Key Laboratory of Anesthesiology and Brain Functional Modulation, Clinical Research Center for Anesthesiology and Perioperative Medicine, Translational Research Institute of Brain and Brain-Like Intelligence, Shanghai Fourth People's Hospital, School of Medicine, Tongji University, Shanghai, China

Purpose: This study aims to investigate the relationship between the total muscle-to-fat ratio (tMFR) and female urinary incontinence (UI), determine whether tMFR can serve as a useful index for predicting UI, and identify factors that may influence this relationship.

Methods: We retrospectively analyzed data from 4391 adult women participating in the National Health and Nutrition Examination Survey (NHANES) conducted between 2011 and 2018. The correlation between tMFR and UI was examined using a dose-response curve generated through a restricted cubic spline (RCS) function, LASSO and multivariate logistic regression. Furthermore, predictive models were constructed incorporating factors such as age, race, hypertension, diabetes, cotinine levels, and tMFR. The performance of these predictive models was evaluated using training and test datasets, employing calibration curves, receiver operating characteristic curves, and clinical decision curves. Mediation effects were also analyzed to explore potential relationships between tMFR and female UI.

Results: In a sample of 4391 adult women, 1073 (24.4%) self-reported experiencing UI, while 3318 (75.6%) reported not having UI. Based on the analyses involving LASSO regression and multivariate logistic regression, it was found that tMFR exhibited a negative association with UI (OR = 0.599, 95% CI: 0.497-0.719, P < 0.001). The results from the restricted cubic spline chart indicated a decreasing risk of UI in women as tMFR increased. Furthermore, the model constructed based on logistic regression analysis demonstrated a certain level of accuracy (in the training dataset: area under the curve (AUC) = 0.663; in the test dataset: AUC = 0.662) and clinical applicability. The mediation

analysis revealed that the influence of tMFR on the occurrence of UI in women might potentially occur through the blood index lymphocyte count (P = 0.040).

Conclusion: A high tMFR serves as a protective factor against UI in women. Furthermore, lymphocyte might be involved in the relationship between tMFR and female UI.

KEYWORDS

total muscle-to-fat ratio, urinary incontinence, logistic regression analysis, predictive model, lymphocyte count

Introduction

An individual experiencing urinary incontinence (UI) involuntarily leaks urine for various reasons (1). It is more prevalent in women (2) and has adverse effects on the female population (3), including their careers and family life. UI can be categorized into three types: stress urinary incontinence (SUI), urge urinary incontinence (UUI), and mixed urinary incontinence (MUI) (4). An illustrative instance is SUI, which refers to involuntary urine leakage during physical activities, sneezing, or coughing. UI is linked to age, obesity, and childbirth (5, 6). According to surveys, the incidence of SUI in the female population can be as high as 24.8% (7), significantly impacting social engagements, mental well-being, and sexual function (3, 8), and adding to the economic and medical burdens for patients to a certain extent (9).

As individuals age and their physical activity decreases, sarcopenia becomes more prevalent. Sarcopenia entails both functional and mass loss in skeletal muscles (10). There's evidence indicating that obesity escalates the risk of urinary incontinence (11), and the body mass index (BMI) stands as the primary measure of obesity. However, BMI fails to identify a substantial portion of individuals with high body fat content (12) as it doesn't differentiate between abdominal obesity and age-related obesity. More critically, BMI doesn't distinguish between the relative quantities of muscle and fat. Research indicates that the muscle-to-fat ratio (MFR) can serve as a biomarker for chronic kidney disease (13). While managing weight and achieving weight loss can effectively decrease the frequency and severity of urinary incontinence in women (14), diminishing body fat and augmenting muscle mass are pivotal for UI prevention. Nonetheless, it remains uncertain whether the MFR can be employed as a predictor of UI in women.

No previous study has explored the correlation between the prevalence of UI in women and the total muscle mass divided by the total body fat mass (tMFR), as assessed by dual-energy x-ray absorptiometry (DXA). Hence, we utilized data from participants within the National Health and Nutrition Examination Survey (NHANES) database to investigate whether tMFR could serve as an indirect radiological predictor for the prevalence of UI in women. Our objective is to offer novel insights into female UI prevention strategies.

Materials and methods

Study population

NHANES is a research program designed to assess the health and nutritional status of adults and children in the United States. It integrates interviews and physical examinations, with a focus on various populations and health topics. The diseases investigated by NHANES are diverse and encompass various systems. The program primarily relies on health interviews. The research team includes physicians, medical and health technicians, as well as diet and health interviewers. NHANES is structured to facilitate and incentivize participation, and all participants receive compensation and medical outcome reports. All data collected during the survey are held in strict confidentiality. NHANES obtains informed consent and ethical approval from all participants. The NHANES survey utilized a computer-assisted personal interview system conducted by trained medical personnel. Information on age, race, education, and disease status was obtained through a professional home questionnaire. Body measurements were taken during medical examinations at mobile medical screening centers. Blood samples were collected and quality controlled for all participants except for the very young. For more information about the database, please visit the website https://www.cdc.gov/nchs/nhanes.

In this study, we utilized questionnaire and survey data from NHANES for four consecutive periods (2011-2012, 2013-2014, 2015-2016, and 2017-2018) in a retrospective analysis. Throughout this eight-year timeframe, a cumulative total of 39,196 individuals took part in the NHANES survey, out of which 34,765 were excluded from our study. The inclusion and exclusion criteria for this study were: i) exclusion of male participants, 19,308; ii) exclusion of participants missing information on the UI questionnaire, 9,877; iii) exclusion of participants missing information on total body fat weight, 4,916; iv) exclusion of

participants missing information on educational level and family income to poverty ratio, 381; and v) exclusion of participants missing information on history of hypertension, history of diabetes mellitus and blood urea nitrogen, 283. Supplementary Figure 1 illustrates our screening process. Following the screening criteria, a total of 4,391 women were included in this study.

Definition of the tMFR

In this study, our aim was to investigate whether tMFR could serve as a physical measurement for predicting UI in women. tMFR is computed by dividing the total body muscle mass by the total body fat mass. Both total body muscle mass and total body fat mass can be quantified using DXA. DXA's quality control measures include equipment calibration and field inspection observations. Site visits by NCHS staff, subject matter experts from collaborating agencies, and component-specific contract technical consultants were done throughout the year to monitor staff performance as part of quality assurance. Periodic retraining sessions were conducted with the MEC staff. The rigorous schedule of quality control scans provided continuous monitoring of machine performance. The expert review procedures helped to ensure that scan analysis was accurate and consistent. In accordance with the NHANES measurement protocol, the exclusion criteria for DXA are as follows: 1) Pregnancy (confirmed through a positive urine pregnancy test and/or self-report); 2) Self-reported history of recent use of radiographic contrast media (such as barium) within the past 7 days; 3) Self-reported weight exceeding 450 lb or height surpassing 1.75 m.

Assessment of UI

The outcome variable in this study was female UI, diagnosed by the Kidney Conditions-Urology section of the NHANES database. Participants who responded "yes" to any of the following three questions were categorized as having UI: "In the past 12 months, have you experienced any leakage or loss of control of even a small amount of urine during activities such as coughing, lifting, or exercising?"; "In the past 12 months, have you experienced any leakage or loss of control of even a small amount of urine when experiencing an urge or pressure to urinate and were unable to reach a toilet quickly enough?"; "In the past 12 months, have you experienced any leakage or loss of control of even a small amount of urine without engaging in activities such as coughing, lifting, or exercising, or without experiencing an urge to urinate?".

Other covariates

The study also included the following confounding factors, including age, race (Spanish white, non-Hispanic black, Mexican United States, other Hispanic, and other), education (less than 9th grade, 9-11th grade, high school graduate/GED or equivalent, some college or AA degree, and college graduate or higher), marital status (married, widowed, divorced, separated, never married, and living with a partner), family income-to-poverty ratio, history of hypertension, history of diabetes mellitus, vigorous leisure activities, moderate leisure activities, blood urea nitrogen, creatinine, and cotinine. Hypertension and diabetes were diagnosed based on tests performed by a professional physician or self-reported history of hypertension/diabetes. "Do you do any vigorous-intensity sports, fitness, or recreational activities that cause a large increase in breathing or heart rate, such as running or basketball for at least 10 minutes continuously?", "Do you do any moderate-intensity sports, fitness, or recreational activities that cause a small increase in breathing or heart rate, such as brisk walking, bicycling, swimming, or golf for at least 10 minutes continuously? Serum cotinine levels are a measure of the prevalence and extent of tobacco use, and blood concentrations can be used as markers of active smoking and exposure to second-hand smoke.

Statistical analysis

To further assess the predictive value of tMFR for the risk of UI in women, we first used LASSO regression (15) to screen for relevant variables and then constructed a nomogram (16) predictive model using $P < 0.05$ indicators in multivariate logistic regression. We randomly selected 50% of the participants to form a training dataset, and receiver operating characteristic (ROC) curves (17), calibration curves, and decision curve analysis (DCA) curves (18) were used to evaluate the nomograms predictive model. The remaining 50% of participants form an internal validation set to validate the model. In addition, mediation effect was applied to explore the internal mechanism between tMFR and female UI.

The variables used in this study include both continuous and categorical variables. The mean ± standard deviation (SD) is used for continuous variables that follow a normal distribution, the median (upper and lower quartiles) is used for continuous variables that do not follow a normal distribution, and proportions are used for categorical variables. In this study, the chi-squared test is used for statistical difference analysis of categorical variables. We used logistic regression to estimate the odds ratio (OR) and 95% confidence interval (CI) between tMFR and the risk of UI in women and visualized using the 'forester' package. In addition, dose curves were used to show the dose-response relationship between tMFR and UI in women. Statistical analyses were performed using SPSS (version 24.0) and R (version 4.2.3) software, and graphs were created using R (version 4.2.3) and Adobe Illustrator (version 26.0) software. $P<0.05$ (two-sided) was considered statistically significant.

Results

Participant characteristics

The study included 4391 women who met the criteria in the NHANES database from 2011 to 2018. The baseline clinical

characteristics of all participants are shown in Supplementary Table 1, with 1073 (24.4%) self-reporting UI and 3318 (75.6%) without UI. We then assessed the clinical characteristics of all women using chi-squared tests, including variables such as age ($P < 0.001$), race ($P < 0.001$), education level ($P < 0.001$), marital status ($P < 0.001$), household income ($P < 0.001$), hypertension ($P < 0.001$), diabetes mellitus ($P < 0.001$), vigorous leisure time activity ($P < 0.001$), moderate leisure time activity ($P = 0.002$), blood urea nitrogen ($P < 0.001$), creatinine ($P = 0.006$), cotinine ($P = 0.001$) and tMFR ($P < 0.001$). We found that the average age of UI patients was 46 years, and women who did not engage in leisure activities were more likely to develop UI.

Relationship between tMFR and female UI

We further analyzed the relationship between tMFR and UI. We used LASSO regression to screen 4391 participants for variables. According to Figure 1, age, marital status, household income and poverty ratio, hypertension, diabetes, intensive leisure time activity, moderate leisure time activity, blood urea nitrogen, cotinine and tMFR were the variables screened by LASSO regression. Multivariate logistic regression analysis (Figure 2A) was performed using the above indicators to obtain age (OR = 1.037, 95%CI = 1.029-1.045, $P < 0.001$), marital status (OR = 1.087, 95%CI = 1.044-1.131, $P < 0.001$), household income and poverty ratio (OR= 0.937, 95% CI, 0.893-0.983, P= 0. 008), diabetes mellitus (OR = 1.378, 95%CI = 1.079-1.755, P = 0.010), blood urea nitrogen (OR = 1.017, 95%CI = 1.000-1.034, P = 0.047), cotinine (OR= 1. 001, 95%CI, 1.000-1.002, P= 0.003) and tMFR (OR = 0.599, 95%CI: 0.497-0.719, $P < 0.001$) were strongly associated with the prevalence of UI in women. In addition, we used the dose curve in the restricted cubic spline (RCS) plot (19) to analyze the dose-response relationship between tMFR and UI in women. Figure 2B showed that the risk of UI in women decreased with increasing tMFR, which was inversely related.

Model development and validation

According to the results of multivariate logistic regression, we randomly selected 50% of the participants as the training dataset and the remaining 50% as the internal test dataset. We constructed a nomogram to predict the risk of UI in women based on the training dataset (Figure 3). To verify the predictive performance of the nomogram model in the test dataset, we used the calibration curve as a calibration tool to evaluate the accuracy of the nomogram model. Figures 4A, D showed the calibration of the training and test datasets. The predicted risk of UI in women is highly consistent with the actual observed results, indicating that the calibration effect of the nomogram is significant. Figures 4B, E showed the ROC results for the training and test datasets, with an area under the curve (AUC) of 0.663 (0.636-0.690) and 0.662 (0.636-0.689), respectively. Those indicated that the constructed model is highly accurate in predicting the UI in women. Finally, we evaluated the clinical value of the nomogram in predicting the risk of UI in women using DCA curves. Figures 4C, F showed that patients could benefit from the predicting model.

Mediation effect analysis

The above results lead to the conclusion that tMFR is negatively associated with female UI, so we analyzed the potential mechanism between them by using mediation effects. A community health study found a significant association between C-reactive protein levels and UI in women (20). Additionally, several clinical studies have demonstrated a potential role for inflammation in female overactive bladders (21, 22). It is likely that inflammatory cytokines play a key role in the regulation of connexin expression and the pathogenesis of bladder dysfunction (23, 24). Therefore, blood white blood cells (WBC), the most common indicator of inflammatory conditions, were used to mediate the effect. The mediating variables included blood WBC, lymphocytes (LYM),

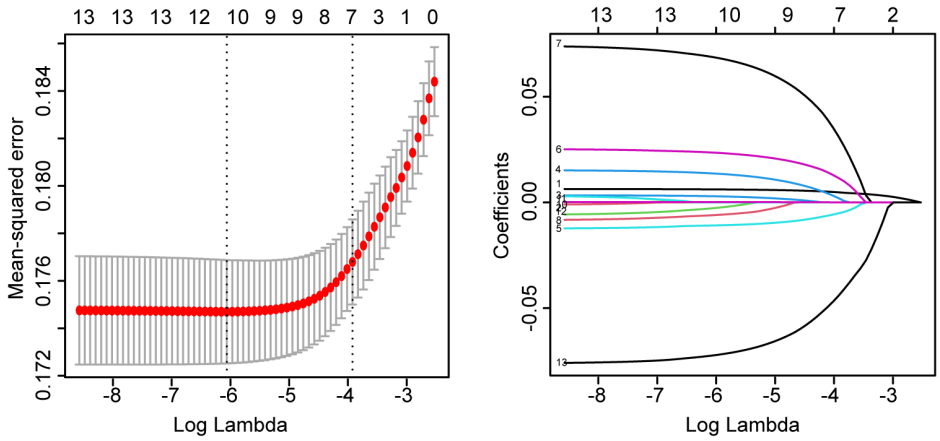

FIGURE 1
LASSO regression results for age, race, education level, marital status, ratio of family income to poverty, hypertension, diabetes, vigorous recreational activity, moderate recreational activity, blood urea nitrogen, creatinine, cotinine levels, and tMFR versus female UI for all participants.

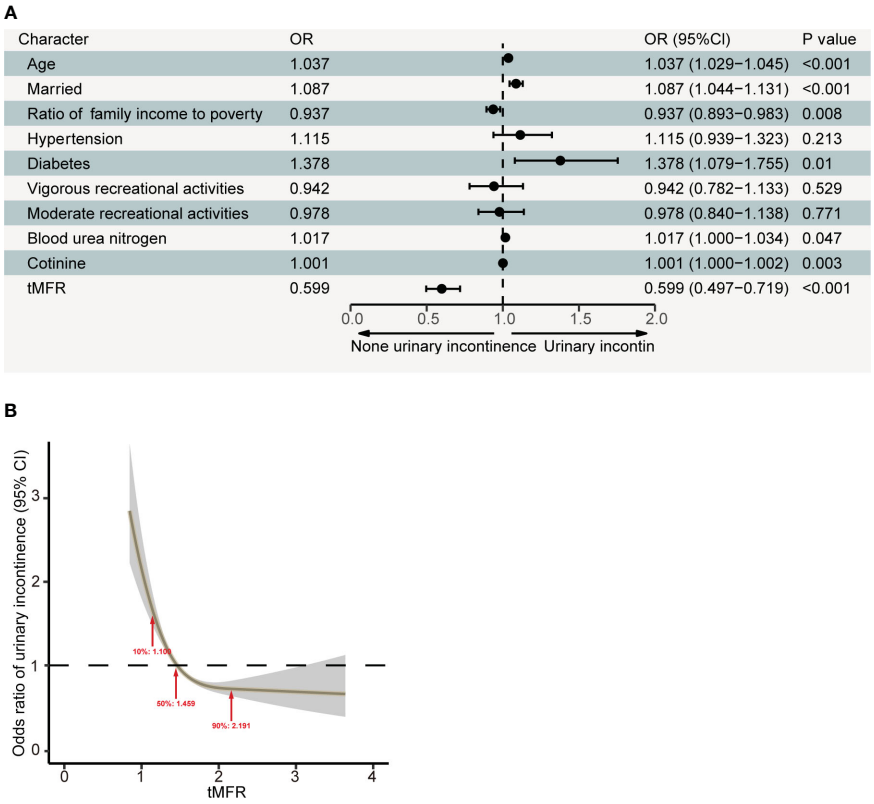

FIGURE 2
(A) Results of a multivariate logistic regression analysis of age, marital status, household income to poverty ratio, hypertension, diabetes, vigorous recreational activity, moderate recreational activity, blood urea nitrogen, cotinine levels, and tMFR in all participants and prevalence of UI in women; **(B)** Dose-response relationship between tMFR and female UI.

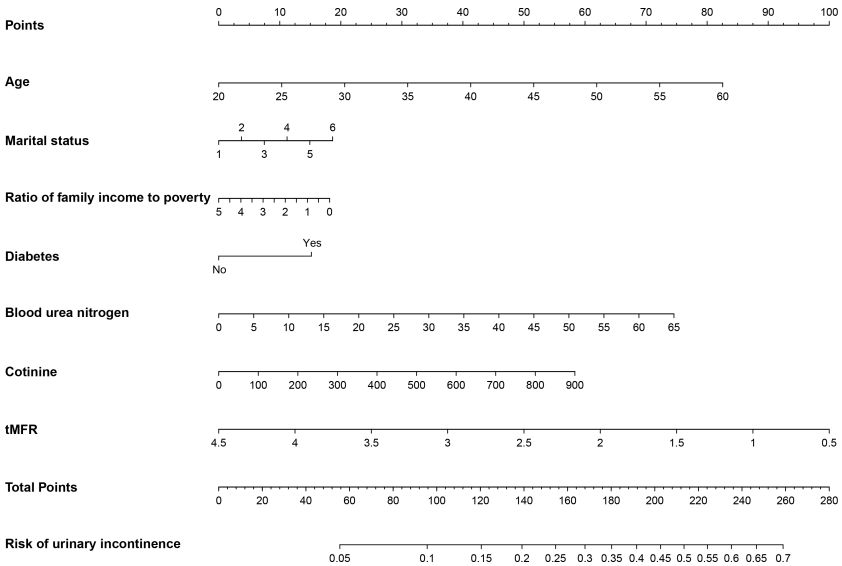

FIGURE 3
Nongram predicting the risk of UI in women were calculated by scoring each numerical level for age, marital status, household income to poverty ratio, diabetes, blood urea nitrogen, cotinine levels, and tMFR for all participants.

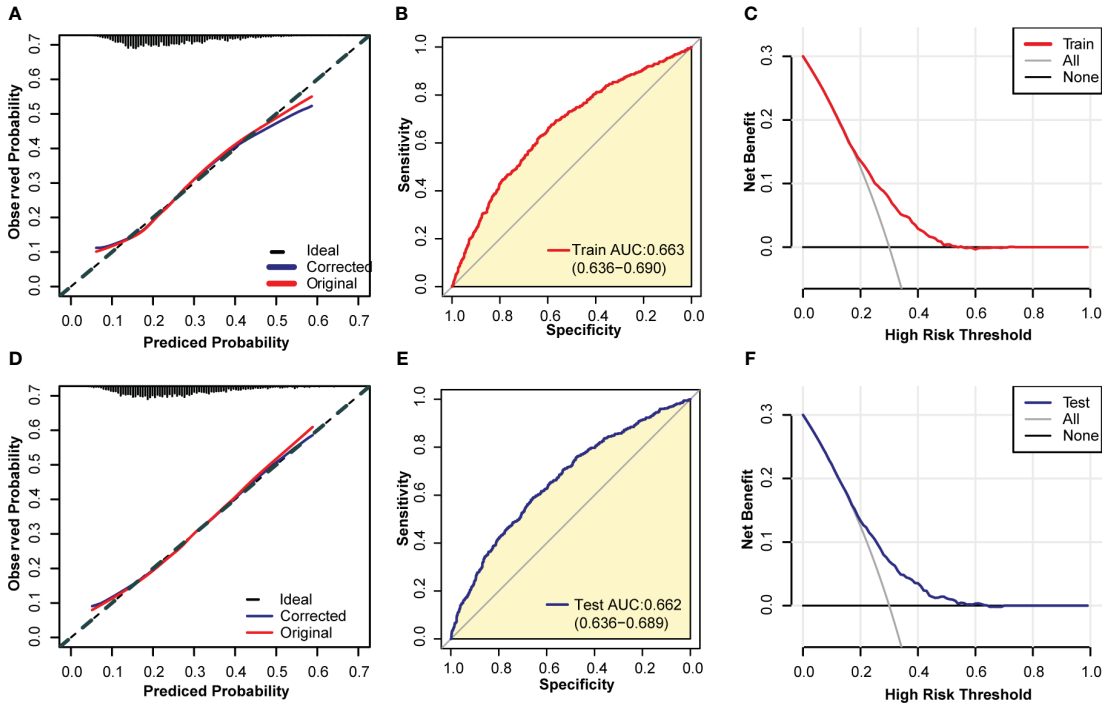

FIGURE 4
Evaluation of the model. **(A)** a calibration curve of the model constructed from the training set; **(B)** ROC curve of the model constructed from the training set; **(C)** DCA curve of the model constructed from the training set; **(D)** Calibration curve of the model constructed from the internal test set; **(E)** ROC curve of the model constructed from the internal test set; **(F)** DCA curve of the model built from the internal test set.

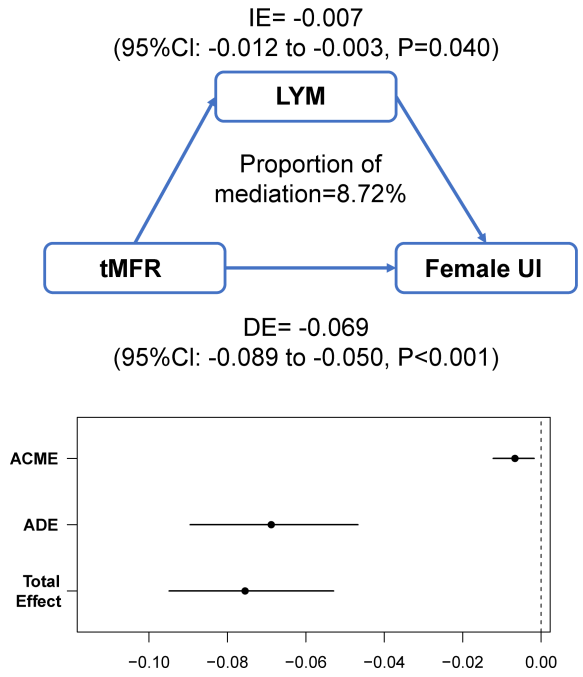

FIGURE 5
Analysis of the mediating effect between tMFR and female UI. Peripheral blood lymphocytes mediated the association between tMFR and UI in women (IE= -0.007; 95%CI: -0.012 to -0.003; P=0.040).

monocytes (PBMC), neutrophils (GRAN), and eosinophils (E). The results of the mediation analysis are shown in Figure 5 and Supplementary Figure 2. It is concluded that tMFR may affect female UI through the mediating variable LYM (P=0.040).

Discussion

UI is a prevalent condition in women, significantly impacting their quality of life and mental well-being. In severe cases, it can also elevate the risk of falls and fractures (25, 26). Research has highlighted the close connection between UI and disruptions in homeostasis, making health-related indicators potential predictors of UI risk (27). The tMFR serves as an indirect marker of human health. However, it remains uncertain whether it correlates with female UI within a domestic context and whether it can anticipate the risk of female UI. In light of this uncertainty, the present study conducted a comprehensive analysis using a large sample derived from nationally representative NHANES data. The findings revealed a negative correlation between tMFR and female UI. Moreover, the model constructed based on tMFR demonstrated some predictive efficacy. Consequently, tMFR emerges as a crucial factor in both the prevention of female UI and the enhancement of the quality of life for individuals affected by UI.

Recent research has highlighted that cannabis use heightens the risk of UI in women (28). A potential mechanism behind this association could be that cannabis smoking leads to muscle weakness and fatigue (29), which, in turn, strongly correlates with UI in women.

Obesity is recognized as a contributor to the heightened risk of urinary incontinence, particularly when it comes to abdominal obesity. This type of obesity augments the likelihood of urinary incontinence in women by elevating intra-abdominal and bladder pressure (30, 31). The prolonged elevation in intra-abdominal pressure results in varying degrees of damage to the pelvic muscles and nerves, culminating in pelvic floor muscle weakness and dysfunction (32). Consequently, this reduction in support for the pelvic organs transpires (33). Moreover, obese individuals often experience endocrine-metabolic system dysregulation, which fosters the secretion of pro-inflammatory factors within the body (34). This condition subsequently leads to bladder dysfunction (23) and eventually culminates in UI. Weakness or loss of elasticity in the bladder muscles can affect the storage and discharge of urine. Maintaining the health and strength of bladder muscles can reduce the risk of UI. Bladder control is dependent on the function of the muscles. Pelvic floor muscles play a crucial role in preventing UI, as greater muscle mass leads to better urine control. Muscle strength is also closely linked to the nervous system. Impairment of nerve conduction can affect bladder and urethral function. Therefore, maintaining neural health and normal neural conduction is crucial in preventing UI. The principal variable under scrutiny in this paper, tMFR, might amplify the risk of UI in women by virtue of the loss of total body muscle and concurrent increase in fat.

LYM is a type of WBC that play a crucial role in the immune system by fighting infections, clearing pathogens, and maintaining immune balance. Inflammation and infection can cause an increase in LYM, particularly in the urinary tract and bladder regions, which can lead to urinary issues. Abnormal increases in LYM due to urinary inflammation can affect the function of the urethra and bladder, resulting in UI.

This paper's primary research highlights are centered around the following aspects. Firstly, it presents the inaugural analysis of tMFR as a predictive measure for the risk of UI in women, contributing value to the domain of female UI prevention. Secondly, we identified LYM as a potential mediating variable between tMFR and female UI. Lastly, in comparison to conventional computed tomography and magnetic resonance imaging methods, DXA offers a convenient, non-invasive (35), and cost-effective approach for assessing tMFR in women. Despite the aforementioned advantages, this study also encounters certain limitations. Initially, cross-sectional studies are unable to establish unequivocal causal relationships. Second, the data utilized in this study stem from participants' self-reported responses, potentially introducing recall and reporting biases. Furthermore, this study solely analyzed correlations using the public NHANES database, which lacks external validation. Prospective studies using clinical data are required to validate the findings.

Conclusion

Our analysis indicates that tMFR is linked to the risk of UI in women in the United States. Enhancing tMFR may lead to a reduction in the likelihood of UI occurrence. These findings offer fresh insights into UI prevention. Furthermore, the study also unveils the potential involvement of LYM in the pathogenesis of UI among women with low tMFR.

Data availability statement

The original contributions presented in the study are included in the article/Supplementary Material. Further inquiries can be directed to the corresponding authors.

Ethics statement

We are accountable for all aspects of this study.

Author contributions

DH: Conceptualization, Data curation, Investigation, Methodology, Software, Supervision, Writing – original draft, Writing – review & editing. HZ: Conceptualization, Data curation, Formal analysis, Methodology, Supervision, Writing – original draft, Writing – review & editing. YY: Data curation, Methodology, Project administration, Validation, Writing – original draft, Writing – review & editing. HQ: Formal analysis, Project administration, Resources, Validation, Writing – original draft, Writing – review & editing. XY: Conceptualization, Data curation, Investigation, Methodology, Project administration, Resources, Software, Writing – original draft. LX: Conceptualization, Funding acquisition, Investigation, Methodology, Project administration, Resources, Software, Supervision, Visualization, Writing – original draft, Writing – review & editing.

Funding

The author(s) declare financial support was received for the research, authorship, and/or publication of this article. We acknowledge the Major Program of National Natural Science Foundation of China [grant number: 82293640], and Shanghai Fourth People's Hospital, School of Medicine, Tongji University [grant numbers: sykyqd05901 and SY-XKZT-2022-1003] for providing funding support to the current work.

Conflict of interest

The authors declare that the research was conducted in the absence of any commercial or financial relationships that could be construed as a potential conflict of interest.

Publisher's note

All claims expressed in this article are solely those of the authors and do not necessarily represent those of their affiliated organizations, or those of the publisher, the editors and the reviewers. Any product that may be evaluated in this article, or claim that may be made by its manufacturer, is not guaranteed or endorsed by the publisher.

Supplementary material

The Supplementary Material for this article can be found online at: https://www.frontiersin.org/articles/10.3389/fendo.2024.1309082/full#supplementary-material

SUPPLEMENTARY FIGURE 1
Inclusion criteria for all participants in this paper.

SUPPLEMENTARY FIGURE 2
WBC, PBMC, GRAN, and E did not mediate the association of tMFR with UI in women (P >0.05).

References

1. Haylen BT, de Ridder D, Freeman RM, Swift SE, Berghmans B, Lee J, et al. An International Urogynecological Association (IUGA)/International Continence Society (ICS) joint report on the terminology for female pelvic floor dysfunction. *Int Urogynecol J*. (2010) 21:5–26. doi: 10.1007/s00192-009-0976-9

2. Vaughan CP, Markland AD. Urinary incontinence in women. *Ann Intern Med*. (2020) 172:ITC17–32. doi: 10.7326/AITC202002040

3. Kwon BE, Kim GY, Son YJ, Roh YS, You MA. Quality of life of women with urinary incontinence: a systematic literature review. *Int Neurourol J*. (2010) 14:133–8. doi: 10.5213/inj.2010.14.3.133

4. Abrams P, Cardozo L, Fall M, Griffiths D, Rosier P, Ulmsten U, et al. The standardisation of terminology of lower urinary tract function: report from the Standardisation Sub-committee of the International Continence Society. *Neurourol Urodyn*. (2002) 21:167–78. doi: 10.1002/nau.10052

5. Abufaraj M, Xu T, Cao C, Siyam A, Isleem U, Massad A, et al. : Prevalence and trends in urinary incontinence among women in the United States, 2005-2018. *Am J Obstet Gynecol*. (2021) 225:166.e1–166.e12. doi: 10.1016/j.ajog.2021.03.016

6. Pang H, Lv J, Xu T, Li Z, Gong J, Liu Q, et al. Incidence and risk factors of female urinary incontinence: a 4-year longitudinal study among 24 985 adult women in China. *BJOG*. (2022) 129:580–9. doi: 10.1111/1471-0528.16936

7. Zhu L, Lang J, Liu C, Han S, Huang J, Li X. The epidemiological study of women with urinary incontinence and risk factors for stress urinary incontinence in China. *Menopause*. (2009) 16:831–6. doi: 10.1097/gme.0b013e3181967b5d

8. Felde G, Bjelland I, Hunskaar S. Anxiety and depression associated with incontinence in middle-aged women: a large Norwegian cross-sectional study. *Int Urogynecol J*. (2012) 23:299–306. doi: 10.1007/s00192-011-1564-3

9. Krhut J, Gartner M, Mokris J, Horcicka L, Svabik K, Zachoval R, et al. : Effect of severity of urinary incontinence on quality of life in women. *Neurourol Urodyn*. (2018) 37:1925–30. doi: 10.1002/nau.23568

10. Chen LK, Woo J, Assantachai P, Auyeung TW, Chou MY, Iijima K, et al. Asian working group for sarcopenia: 2019 consensus update on sarcopenia diagnosis and treatment. *J Am Med Dir Assoc*. (2020) 21:300–307.e2. doi: 10.1016/j.jamda.2019.12.012

11. Doumouchtsis SK, Loganathan J, Pergialiotis V. The role of obesity on urinary incontinence and anal incontinence in women: a review. *BJOG*. (2022) 129:162–70. doi: 10.1111/1471-0528.16848

12. Okorodudu DO, Jumean MF, Montori VM, Romero-Corral A, Somers VK, Erwin PJ, et al. Diagnostic performance of body mass index to identify obesity as defined by body adiposity: a systematic review and meta-analysis. *Int J Obes (Lond)*. (2010) 34:791–9. doi: 10.1038/ijo.2010.5

13. Jhee JH, Joo YS, Han SH, Yoo TH, Kang SW, Park JT. High muscle-to-fat ratio is associated with lower risk of chronic kidney disease development. *J Cachexia Sarcopenia Muscle*. (2020) 11:726–34. doi: 10.1002/jcsm.12549

14. Vissers D, Neels H, Vermandel A, De Wachter S, Tjalma WA, Wyndaele JJ, et al. The effect of non-surgical weight loss interventions on urinary incontinence in overweight women: a systematic review and meta-analysis. *Obes Rev*. (2014) 15:610–7. doi: 10.1111/obr.12170

15. Frosch Z, Hasler J, Handorf E, DuBois T, Bleicher RJ, Edelman MJ, et al. Development of a multilevel model to identify patients at risk for delay in starting cancer treatment. *JAMA Netw Open*. (2023) 6:e2328712. doi: 10.1001/jamanetworkopen.2023.28712

16. Iasonos A, Schrag D, Raj GV, Panageas KS. How to build and interpret a nomogram for cancer prognosis. *J Clin Oncol*. (2008) 26:1364–70. doi: 10.1200/JCO.2007.12.9791

17. Zhang H, Cao S, Xu Y, Sun X, Fei M, Jing Q, et al. Landscape of immune infiltration in entorhinal cortex of patients with Alzheimer's disease. *Front Pharmacol*. (2022) 13:941656. doi: 10.3389/fphar.2022.941656

18. Vickers AJ, Van Calster B, Steyerberg E. Decision curves, calibration, and subgroups. *J Clin Oncol*. (2017) 35:472–3. doi: 10.1200/JCO.2016.69.1576

19. Mao W, Wang K, Zhang H, Lu H, Sun S, Tian C, et al. Sarcopenia as a poor prognostic indicator for renal cell carcinoma patients undergoing nephrectomy in China: A multicenter study. *Clin Transl Med*. (2021) 11:e270. doi: 10.1002/ctm2.270

20. Kupelian V, McVary KT, Barry MJ, Link CL, Rosen RC, Aiyer LP, et al. Association of C-reactive protein and lower urinary tract symptoms in men and women: results from Boston Area Community Health survey. *Urology*. (2009) 73:950–7. doi: 10.1016/j.urology.2008.12.012

21. Comperat E, Reitz A, Delcourt A, Capron F, Denys P, Chartier-Kastler E. Histologic features in the urinary bladder wall affected from neurogenic overactivity–a comparison of inflammation, oedema and fibrosis with and without injection of botulinum toxin type A. *Eur Urol*. (2006) 50:1058–64. doi: 10.1016/j.eururo.2006.01.025

22. Tyagi P, Barclay D, Zamora R, Yoshimura N, Peters K, Vodovotz Y, et al. Urine cytokines suggest an inflammatory response in the overactive bladder: a pilot study. *Int Urol Nephrol*. (2010) 42:629–35. doi: 10.1007/s11255-009-9647-5

23. Wang Z, Cheng Z, Cristofaro V, Li J, Xiao X, Gomez P, et al. Inhibition of TNF-alpha improves the bladder dysfunction that is associated with type 2 diabetes. *Diabetes*. (2012) 61:2134–45. doi: 10.2337/db11-1763

24. Heinrich M, Oberbach A, Schlichting N, Stolzenburg JU, Neuhaus J. Cytokine effects on gap junction communication and connexin expression in human bladder smooth muscle cells and suburothelial myofibroblasts. *PloS One*. (2011) 6:e20792. doi: 10.1371/journal.pone.0020792

25. Brown JS, Vittinghoff E, Wyman JF, Stone KL, Nevitt MC, Ensrud KE, et al. Urinary incontinence: does it increase risk for falls and fractures? Study of Osteoporotic Fractures Research Group. *J Am Geriatr Soc*. (2000) 48:721–5. doi: 10.1111/j.1532-5415.2000.tb04744.x

26. Yang E, Lisha NE, Walter L, Obedin-Maliver J, Huang AJ. Urinary incontinence in a national cohort of older women: implications for caregiving and care dependence. *J Womens Health (Larchmt)*. (2018) 27:1097–103. doi: 10.1089/jwh.2017.6891

27. Chughtai B, Thomas D, Russell D, Bowles K, Prigerson H. Prevalence of and risk factors for urinary incontinence in home hospice patients. *Eur Urol*. (2019) 75:268–71. doi: 10.1016/j.eururo.2018.10.027

28. Xie L, Yu Z, Gao F. The association between recent cannabis use and urinary incontinence in women: a population-based analysis of the NHANES from 2009 to 2018. *World J Urol*. (2022) 40:3099–105. doi: 10.1007/s00345-022-04193-y

29. Olah T, Bodnar D, Toth A, Vincze J, Fodor J, Reischl B, et al. Cannabinoid signalling inhibits sarcoplasmic Ca(2+) release and regulates excitation-contraction coupling in mammalian skeletal muscle. *J Physiol*. (2016) 594:7381–98. doi: 10.1113/JP272449

30. Cummings JM, Rodning CB. Urinary stress incontinence among obese women: review of pathophysiology therapy. *Int Urogynecol J Pelvic Floor Dysfunct*. (2000) 11:41–4. doi: 10.1007/s001920050008

31. Stroher R, Sartori M, Takano CC, de Araujo MP, Girao M. Metabolic syndrome in women with and without stress urinary incontinence. *Int Urogynecol J*. (2020) 31:173–9. doi: 10.1007/s00192-019-03880-6

32. Ramalingam K, Monga A. Obesity and pelvic floor dysfunction. *Best Pract Res Clin Obstet Gynaecol*. (2015) 29:541–7. doi: 10.1016/j.bpobgyn.2015.02.002

33. Bart S, Ciangura C, Thibault F, Cardot V, Richard F, Basdevant A, et al. [Stress urinary incontinence and obesity]. *Prog Urol*. (2008) 18:493–8. doi: 10.1016/j.purol.2008.04.015

34. Marcelissen T, Anding R, Averbeck M, Hanna-Mitchell A, Rahnama'I S, Cardozo L. Exploring the relation between obesity and urinary incontinence: Pathophysiology, clinical implications, and the effect of weight reduction, ICI-RS 2018. *Neurourol Urodyn*. (2019) 38 Suppl 5:S18–24. doi: 10.1002/nau.24072

35. Njeh CF, Fuerst T, Hans D, Blake GM, Genant HK. Radiation exposure in bone mineral density assessment. *Appl Radiat Isot*. (1999) 50:215–36. doi: 10.1016/s0969-8043(98)00026-8

Frontiers in Physiology

Understanding how an organism's components work together to maintain a healthy state

The second most-cited physiology journal, promoting a multidisciplinary approach to the physiology of living systems - from the subcellular and molecular domains to the intact organism and its interaction with the environment.

Discover the latest Research Topics

See more →

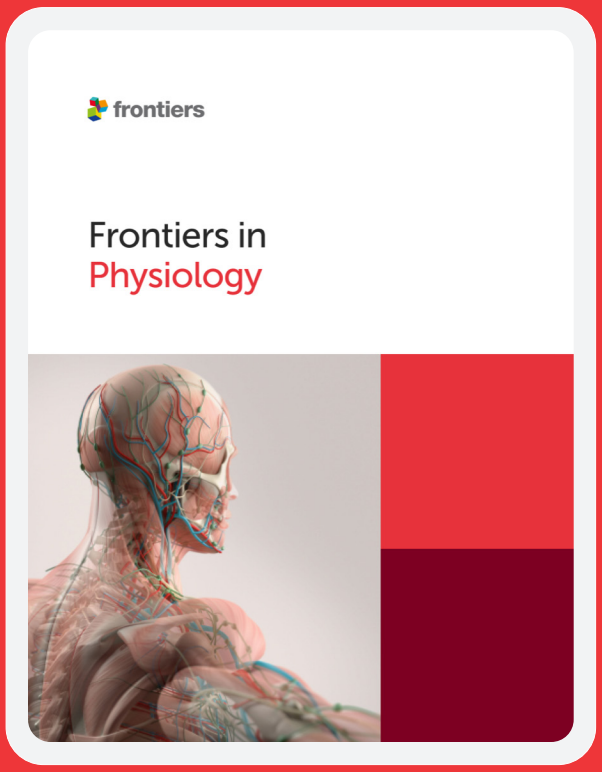

Frontiers

Avenue du Tribunal-Fédéral 34
1005 Lausanne, Switzerland
frontiersin.org

Contact us

+41 (0)21 510 17 00
frontiersin.org/about/contact